

Cranfield University

Cranfield Health

PhD Thesis

**Development of Life Marker Chip
Technology for *in-situ* Life Detection on Mars**

Paul Kerr Wilson

Supervisors: Dr. David Cullen

Prof. Naresh Magan

Submitted: April 2007

Abstract

The European Space Agency (ESA) is currently developing its flagship Life Detection Mission, ExoMars, which is scheduled to fly to Mars in 2013. The primary goal of this mission is to compliment the Phoenix NASA mission in confirming the presence of organic material on Mars, and, for the first time, analyse this organic material to determine the presence of organic species indicative of presence of past or present Life. One of the proposed Life detection technologies is the Life Marker Chip (LMC), which uses immunoassays with fluorescent readout to detect small organics and proteins in a microarray format within microfluidic channel structures. This PhD thesis encompasses the work done by the author on the development of the SMILE LMC during the period prior to, and during part of the first phase of, the Life Marker Chip Technology Readiness Level Upgrade Study funded by ESA from 2005 to 2007.

The work carried out is split into three key areas. The first of these is the radiation environment and requirements to fly biological materials in space. The likely radiation and sterilisation environments are discussed and a series of experiments carried out to determine the effects of such environments on antibodies and fluorescent dyes. Dry heat sterilisation was found to be incompatible with biological immunoassay reagents. However, both antibodies and fluorescent dyes were shown to maintain some activity after exposure to several different relevant radiation environments, including in the case of fluorescent dyes a sterilisation gamma radiation exposure, thus validating the continued development of an antibody-based detection system with fluorescent readout.

The second key area is development of a breadboard instrument platform and assay protocols. A breadboard system representative of the core design for the Life Marker chip was assembled and a series of experiments performed towards establishing assay protocols, imaging techniques, and functionalisation of surfaces, advancing the development of the Life Marker Chip technology and practical knowledge and experience within the SMILE consortium. Although the assay protocol has not been fully optimised, this work demonstrates an immunoassay in a microarray format on surfaces representative of those currently proposed for the LMC instrument.

The final area explored was the likely effects of Martian Regolith salts and sample processing reagents on immunoassays. This research identified the potential problem of salts in the Martian samples forming insoluble precipitates by reacting with buffer salts, although this reaction appears to be prevented by the addition of an antioxidant (ascorbate). The presence of highly a-polar organic solvents and high concentration of Guanidine-HCl in assay buffers was not compatible with immunoassays, however less polar solvents e.g. methanol / water mixtures and lower concentrations of Guanidine-HCl may be tolerated by the assay. This knowledge is an important input into the design of the LMC sample processing system.

In summary, although the development of the LMC continues beyond the period of this PhD thesis, significant progress has been made in three key areas, and this has contributed towards the continuing potential inclusion of the SMILE LMC on board the ExoMars mission, as well as advancing scientific knowledge in these areas.

Acknowledgements

There are many people who I would like to thank for their support and contributions to my work on this project, both from the viewpoint of academic support and making my time working on this project interesting and enjoyable.

Firstly I thank Professor Seamus Higson for giving me the opportunity to come to Cranfield University to work on a PhD. While unfortunate circumstances resulted in discontinuation of this work, this experience gave me early training in the qualities required to succeed in a research environment and a platform from which to pursue my future career.

I am grateful to Dr. David Cullen for a great many reasons, including for taking me on as a research student at a time when others may not have, creating an opportunity for me to work on a project of interest to the general public as well as a scientific challenge with a diverse range of activities, and for continued advice and support throughout this project.

I thank Professor Naresh Magan, primarily for facilitating and supporting my change in project direction and supervision, but also for his input during my initial project and continued support throughout this work.

I am also grateful to Dr. Mark Sims (University of Leicester) for welcoming me into the SMILE Life Marker Chip consortium, and for his continued effort and contributions both to the design and development of the Life Marker Chip and to the management of the overall project.

It has been a pleasure to work alongside Mr Daniel Thompson (University of Leicester) throughout this project, particularly on the radiation testing of antibodies and fluorescent dyes, and I have enjoyed both his practical contributions and company throughout this work.

I also thank all other members of the SMILE consortium not mentioned here for welcoming me into the group and making our meetings constructive, interesting and informative while maintaining a positive work ethic and great team spirit. I hope all projects I am involved in in the future can work as well as this one!

To Mr Derek Annan, it has been a pleasure to work with and alongside you since you began your work here, your positive attitude makes everything seem so much easier!

For and colleagues working within IBST / IBSAT / IBST / Cranfield Health during this time I am grateful to all particularly, to name but a few, Judith Taylor, Marjorie Allen, Allen Hilton, and many others for your contributions and advice on my work, and for your enjoyable company throughout.

Last, but by no means least, I thank my friends and current and former student colleagues within Cranfield Health over the past 3 years, for their friendship and support during this time.

Abstract	i
Acknowledgements	iii
Table of Contents	v
List of Figures	xi
List of Tables	xv
List of Abbreviations	xvi
Chapter 1: Introduction, Aims and Objectives	1
1.1 Introduction	2
1.2 Thesis objectives and structure.....	4
1.2.1 Theme 1: Radiation and flight environment conditions.....	4
1.2.2 Theme 2: Development of optical breadboard and microarray assay system.....	5
1.2.3 Theme 3: Effects of Mars environment and sample processing reagents on antibody-based assays.....	6
Chapter 2: Literature Review	7
2.1 The Effect of Extreme Environments on Biological Materials	7
2.1.1 Introduction and space mission environments.....	7
2.1.1.1 Space mission environments.....	8
2.1.1.2 Life Marker Chip instruments.....	9
2.1.1.3 The space and planetary radiation environment.....	10
2.1.1.4 Planetary protection.....	10
2.1.1.5 Radiation and its effects on organic and biological materials.....	11
2.1.1.6 Effects of radiation on Life Marker Chip and related instruments.....	13
2.1.2 Expected radiation levels during a Mars mission.....	14
2.1.2.1 Radiation during a Mars mission.....	14
2.1.2.2 Measured radiation environment at Mars.....	14
2.1.2.3 Summary of information about the radiation environment from NASA MARIE.....	18
2.1.2.4 Predictions of the radiation environment and the radiation dose and testing problem.....	18
2.1.3 Effects of radiation on whole cells and cellular components.....	19
2.1.3.1 Introduction: viral and bacterial exposure to radiation.....	19
2.1.3.2 Cellular component exposure to radiation.....	20
2.1.3.3 Causes of aggregation.....	22
2.1.3.4 Fragmentation mechanisms.....	23

2.1.3.5	Structural changes caused by radiation damage.....	23
2.1.3.6	Effect of radiation on dried biological materials.....	25
2.1.3.7	Tests involving biological materials in space environments.....	26
2.1.3.8	Results from tests on Life Marker Chip components.....	27
2.1.3.9	Planetary protection and effects of sterilisation on Life Marker Chip instruments.....	27
2.1.3.10	The likely effects of temperature.....	28
2.1.3.11	Other effects	30
2.1.3.12	Conclusions and implications.....	30
2.1.4	Summary.....	31
2.2	The Analytical Problem and Likely Biomarker Targets for the LMC.....	32
2.2.1	Introduction and background to this review.....	32
2.2.2	Types of Life and strategy for Life detection.....	33
2.2.3	The advantages of antibody-based assay systems.....	35
2.2.4	Effects of the Martian environment on biomarker preservation and stability.....	35
2.2.5	Sample site selection and the advantages of sub-surface drilling.....	36
2.2.6	Potential biomarker targets.....	37
2.2.6.1	Indicators of extant Life.....	37
2.2.6.2	Indicators of extinct Life.....	38
2.2.6.3	Indicators of the presence of organic material of meteoritic origin.....	38
2.2.6.4	Indicators of spacecraft contamination.....	39
2.2.7	Biomarker Workshop target list.....	39
2.2.8	Implications of the biomarker target list for the LMC sample processing system..	46
2.2.9	Summary of the analytical problem.....	46
2.3	Multianalyte Sensor Technologies for Microlitre-Scale Sample Volumes,.....	47
2.3.1	The SMILE solution and evolution of the instrument design concept.....	47
2.3.2	Introduction to relevant analytical methods and technologies.....	48
2.3.3	Surface refractive index based sensors	51
2.3.4	Detection systems utilising fluorescently labelled components	51
2.3.5	Multi-mode (bulk) waveguides.....	52
2.3.6	Mono-Mode (thin film) waveguides.....	54
2.3.7	Methods of Creating multi-analyte sensors.....	56
2.3.8	Surface functionalisation.....	57
2.3.9	Imaging Systems.....	57

2.3.10 Gas chromatography mass spectrometry	58
2.3.11 Summary of Literature Review on technologies for the simultaneous detection of a number of different analytes using microlitre-scale sample volumes.....	58
2.4 Mars Geological Environments and Sample Related Media.....	60
2.4.1 Review of the geological characteristics of the Martian surface relevant to Life detection, and reagents commonly used in sample processing and extraction.....	60
2.4.1.1 Introduction.....	60
2.4.1.2 Martian surface geology.....	60
2.4.1.3 Sample processing system methods, reagents and solvents.....	62
2.4.1.4 Additional considerations.....	63
2.4.1.5 Summary of possible environmental and sample processing reagents that may have an effect on antibody assays.....	64
2.5 Literature Review Summary.....	65
Chapter 3: Exposure of Fluorescent Dyes and Antibodies to simulated Radiation and Sterilisation protocols.....	67
3.1 Introduction.....	67
3.2 Proton and helium ion exposures – introduction.....	69
3.2.1 Preliminary particle radiation testing.....	70
3.2.2 Fluorimeter analysis of Fluorescein and Alexa Fluor® 633 samples.....	74
3.2.3 ELISA method.....	75
3.2.4 Development of sample preparation procedure for ion beam exposures.....	81
3.2.5 Particle radiation testing with modified sample preparation and exposure procedures.....	88
3.2.6 Summary and discussion of particle radiation testing results.....	97
3.3 Gamma irradiation exposure of fluorescent dyes and antibodies.....	98
3.3.1 Preliminary gamma irradiation experiment.....	99
3.3.2 Gamma irradiation method development and reproducibility study.....	101
3.3.3 Investigating the potential for sterilisation of the Life Marker Chip by gamma irradiation.....	104
3.3.4 Determination of the maximum tolerated gamma radiation dose for fluorescein	107
3.3.5 Summary of gamma irradiation experiments.....	111
3.3.6 Particle and gamma radiation testing summary.....	112
3.4 Heat sterilisation tests on antibodies and fluorescent dyes.....	114

3.4.1 Preliminary heat sterilisation test – materials and methods.....	114
3.4.2 Preliminary heat sterilisation testing - results and discussion.....	116
3.4.3 Modified protocol for heat sterilisation testing.....	117
3.4.4 Improved reproducibility heat sterilisation test.....	121
3.5 Summary and conclusions from radiation and sterilisation experiments.....	124
Chapter 4: Development of the Life Marker Chip Microarray Readout Breadboard System.....	126
4.1 Introduction.....	126
4.2 Development of a breadboard imaging system and adaptation of assay protocols to use representative Life Marker Chip biomarker targets and Alexa Fluor® 633 dye.....	127
4.2.1 LMC readout design consideration and development of the breadboard imaging system – introduction.....	127
4.2.2 Breadboard imaging system development - specifications and assembly.....	128
4.3 Determining the detection limits of the new breadboard imaging system – introduction.....	129
4.3.1 Determining the detection limits of the new breadboard imaging system – materials and methods.....	131
4.3.2 Determining the detection limits of the new breadboard imaging system – results and discussion.....	132
4.4 Optimising immunoassays in a microarray format using fluorescent readout..	135
4.5 Initial assays using Alexa Fluor® 633 labelled reagents in the optical breadboard.....	135
4.5.1 Initial assay using Alexa Fluor® 633 labelled reagents in the optical breadboard – materials and methods.....	135
4.5.2 Initial assay using Alexa Fluor® 633 labelled reagents in the optical breadboard – results and discussion.....	137
4.5.3 Preliminary immunoassay in microarray format – materials and methods.....	138
4.5.4 Preliminary immunoassay in microarray format – results and discussion.....	138
4.6 Optimisation of blocking and washing protocols.....	140
4.6.1 Optimisation of blocking and washing protocols – materials and methods.....	140
4.6.2 Optimisation of blocking and washing protocols – results and discussion.....	141
4.7 Development of immunoassay on epoxy coated slides	144
4.7.1 Validation of epoxy coated slides – materials and methods.....	145

4.7.2	Validation of epoxy coated slides – results and discussion.....	145
4.8	Selection of an assay system directly relevant to Martian samples.....	146
4.9	Initial <i>in-situ</i> labelling protocol for GroEL protein.....	146
4.9.1	Initial <i>in-situ</i> labelling protocol for GroEL protein – materials and method.....	147
4.9.2	Initial <i>in-situ</i> labelling protocol for GroEL Protein – results and discussion.....	148
4.10	(3-glycidoxypropyl)trimethoxysilane (GOPS) functionalisation protocol.....	149
4.10.1	(3-glycidoxypropyl)trimethoxysilane (GOPS) functionalisation protocol – materials and methods.....	150
4.10.2	Silane (GOPS) functionalisation of glass – results and discussion.....	154
4.11	Silane (GOPS) functionalisation of silicon.....	156
4.11.1	Silane (GOPS) functionalisation of silicon – materials and methods.....	154
4.11.2	Silane (GOPS) functionalisation of silicon – results and discussion.....	155
4.12	Use of <i>in-situ</i> labelled GroEL in microarray assays on in-house GOPS functionalised surfaces.....	156
4.12.1	Initial assay using <i>in-situ</i> labelled GroEL in microarray assays – materials and methods.....	157
4.12.2	Initial assay using <i>in-situ</i> labelled GroEL in microarray assays – results and discussion.....	158
4.12.3	Modification of <i>in-situ</i> labelling protocol to include ethanolamine as a quenching reagent for un-reacted dye – materials and methods.....	159
4.12.4	Modification of <i>in-situ</i> labelling protocol to include ethanolamine as a quenching reagent for un-reacted dye – results and discussion.....	160
4.12.5	Assay including test with inactivated dye filtrate – materials and methods.....	162
4.12.6	Assay including test with inactivated dye filtrate – results and discussion.....	162
4.13	Calibration curve for an immunoassay in a microarray format.....	164
4.13.1	Calibration curve for an immunoassay in a microarray format - materials and methods.....	164
4.13.2	Calibration curve for an immunoassay in a microarray format – results and discussion.....	165
4.14	Summary and conclusions from instrument platform development experiments.....	168
	Chapter 5: Effect of Martian Regolith Salts and Sample Extraction Solvents on Antibody-based Assays.....	170
5.1	Introduction.....	170

5.2 Effect of representative Martian regolith salts on antibody assays.....	171
5.2.1 Effect of calcium sulphate (CaSO ₄) on anti-atrazine binding ELISA – materials and methods.....	172
5.2.2 Effect of calcium sulphate (CaSO ₄) on anti-atrazine binding ELISA – results and discussion.....	173
5.2.3 Effect of magnesium sulphate (MgSO ₄) on anti-atrazine ELISA – materials and methods.....	174
5.2.4 Effect of magnesium sulphate (MgSO ₄) on anti-atrazine ELISA – results and discussion.....	174
5.2.5 Effect of iron II sulphate (FeSO ₄) on anti-atrazine ELISA – materials and methods.....	175
5.2.6 Effect of iron II sulphate (FeSO ₄) on anti-atrazine ELISA – results and discussion.....	176
5.3 Investigation of buffer compatibility with Martian regolith salts.....	177
5.3.1 Preliminary experiment to determine compatibility of biological buffers with iron (II) sulphate – materials and methods.....	177
5.3.2 Preliminary experiment to determine compatibility of biological buffers with iron (II) sulphate – results and discussion.....	177
5.3.3 Controlled experiment to characterise precipitation in different buffers – materials and methods.....	178
5.3.4 Controlled experiment to characterise precipitation in different buffers – results and discussion.....	179
5.3.5 Controlled experiment with buffer salts and antioxidant (ascorbic acid) – materials and methods.....	180
5.3.5 Controlled experiment with buffer salts and antioxidant (ascorbic acid) – results and discussion.....	180
5.4 Sample extraction reagents and organic solvents.....	183
5.4.1 Effect of guanidine-HCl on antibody-antigen interaction – materials and methods.....	184
5.4.2 Effect of guanidine-HCl on antibody-antigen interaction – results and discussion.....	185
5.4.3 Effect of sample extraction organic solvents on antibody assays – materials and methods.....	186

5.4.4 Effect of sample extraction organic solvents on antibody assays – results and discussion.....	187
5.5 Summary and discussion of the effects of Martian regolith salts and sample extraction solvents on antibody-based assays.....	189
Chapter 6: Discussion and Future Work.....	191
6.1 Discussion of developments in Life Marker Chip Technology for <i>in-situ</i> Life Detection on Mars Made During this Work.....	191
6.2 Future Work.....	194
References.....	197
Appendix A: Initial Development of Microarray Spotting Equipment and Immunoassay Readout Protocols.....	A-1

List of Figures

Figure 2.1: Provisional data from the MARIE: absorbed dose rate vs. HZETRN model calculations during flight, as presented on the NASA MARIE website in 2002-3.....	15
Figure 2.2: Provisional figure showing MARIE Measurements vs. HZETRN model calculations during Martian orbit as presented on the NASA MARIE website in 2002-3	16
Figure 2.4: Provisional MARIE measurements of the average charge of non-stopping particles (low Z) as presented on the NASA MARIE website in 2002-3.....	17
Figure 2.5: Provisional MARIE measurements of average charge of non-stopping particles (High Z) as presented on the NASA MARIE website in 2002-3.....	17
Figure 3.1: Cyclotron beam port attachment used to mount samples in front of the 1cm x 1cm particle radiation beam.....	72
Figure 3.2: Customised 864 well microtitre plate with 9-well sample and control areas marked.....	73
Figure 3.3: Modified 864 well microtitre plate mounted on the cyclotron beam port.....	77
Figure 3.4: Effect of proton irradiation on fluorescent properties of fluorescein.....	78
Figure 3.5: Effect of initial proton exposures on anti-atrazine scAb antibody, compared to samples outside the beam line and a stock antibody sample that was not included in the cyclotron tests.....	79
Figure 3.6: A petri dish used as a baffle to protect sample clocks during the freeze-drying process.....	83
Figure 3.7: Petri-dish and sample blocks wrapped in aluminium foil.....	84
Figure 3.8: Immersion of Sample Blocks in Liquid Nitrogen.....	85
Figure 3.9: The foil coated lid of a petri-dish after a freeze-drying cycle, clearly showing material escaping the sample block wells and building up on the surface of the aluminium foil.....	87
Figure 3.10: Effect of proton radiation (10, 100 and 10,000 times the mission fluence) on the fluorescent properties of fluorescein.....	89
Figure 3.11: Effect of proton radiation (10, 100 and 10,000 times the expected mission fluence) on the fluorescent emission properties of Alexa Fluor [®] 633.....	90
Figure 3.12: Effect of proton radiation (10, 100 and 10,000 the mission fluence) on the binding properties of a representative recombinant antibody (anti-atrazine scAb).....	91
Figure 3.13: Sample blocks after proton and helium ion exposures. Note the surface appearance of block no. 3 (bottom right) is different from the other sample blocks.....	93

Figure 3.14: Effect of helium ion radiation (10 and 100 times the mission fluence) on the fluorescent properties of fluorescein.....	94
Figure 3.15: Effect of helium ion radiation (10 and 100 times the mission fluence) on the fluorescent properties of Alexa Fluor® 633.....	95
Figure 3.16: Effect of helium ion radiation (10 and 100 times the mission fluence) on the binding properties of a representative recombinant antibody (anti-atrazine scAb).....	96
Figure 3.17: Effect of proton and helium ion radiation on the fluorescent properties of fluorescein samples in Figure 3.1.10 and Figure 3.1.14, showing the intensities of each sample.....	97
Figure 3.18: Effect of preliminary Gamma radiation exposure on peak emission wavelength and intensity of fluorescein.....	100
Figure 3.19: Effect of 30 and 300kRad of gamma irradiation on the fluorescent emission properties of fluorescein.....	102
Figure 3.20: Effect of 30 and 300kRad of gamma irradiation on the fluorescent emission properties of Alexa Fluor® 633.....	103
Figure 3.21: Effect of mission and sterilisation doses of gamma irradiation on the fluorescent emission properties of fluorescein.....	105
Figure 3.22: Effect of mission and sterilisation doses of gamma irradiation on the fluorescent emission properties of Alexa Fluor® 633.....	106
Figure 3.23: Effect of Gamma irradiation on fluorescent emission intensity of dried down and liquid fluorescein.....	108
Figure 3.24: Effect of Gamma irradiation on fluorescent emission intensity of dried down and liquid fluorescein.....	109
Figure 3.25: Effect of a heat sterilisation run consisting of 125°C for 3 hours on the fluorescent properties of fluorescein.....	116
Figure 3.26: Second design of the heat sterilisation sample block.....	117
Figure 3.27: Effect of modified heat sterilisation on the fluorescent emission properties of fluorescein.....	119
Figure 3.28: Effect of modified heat sterilisation on the fluorescent emission properties of Alexa Fluor® 633.....	120
Figure 3.29: Effect of optimised heat sterilisation on the fluorescent emission properties of fluorescein.....	123
Figure 3.30: Effect of optimised heat sterilisation on the fluorescent emission properties of Alexa Fluor® 633.....	123

Figure 3.31: Effect of heat sterilisation on the antigen binding properties of anti-atrazine scAb assessed by ELISA.....	124
Figure 4.1 Schematic layout of the breadboard imaging system.....	129
Figure 4.2: A 60 second exposure image of an array of different concentrations of Alexa Flour [®] 633 dye taken with the Starlight Express CCD camera with a 60 second exposure time.....	132
Figure 4.3: A 60 second exposure image of an array of different concentrations of Alexa Flour [®] 633 dye taken with the Starlight Express CCD camera and enhanced with the software filters.....	133
Figure 4.4: Analysis of the 60-second exposure image of Alexa Flour [®] 633 spots at different concentrations (Figure 4.2).....	134
Figure 4.5: 60 second exposures of the assay area of a microfluidic channel on which a binding immunoassay was carried out.....	137
Figure 4.6: An ELISA in which 110µm diameter spots of anti-atrazine scAb were deposited onto an activated amine surface and exposed to Alexa Flour [®] 633 labelled secondary antibody.....	138
Figure 4.7: An immunoassay in which 110µm diameter spots of anti-atrazine scAb were deposited onto an activated amine surface and exposed to Alexa Flour [®] 633 labelled secondary antibody.....	140
Figure 4.8: An immunoassay in which a 4 x 20 array of 110µm diameter spots of anti-atrazine scAb were deposited onto an epoxy coated slide (Genetix) and exposed to Alexa Flour [®] 633 labelled secondary antibody.....	145
Figure 4.9: Photograph of labelled GroEL protein under different conditions.....	148
Figure 4.10: 300 second exposure image of an assay area in which a 5 x 5 array of anti-GroEL was printed and exposed to Alexa Flour [®] 633 labelled GroEL protein after addition of ethanolamine.....	160
Figure 4.11: 300 second exposure image of an assay area in which a 5 x 5 array of anti-GroEL was printed and exposed to Alexa Flour [®] 633 labelled GroEL protein after addition of ethanolamine.....	161
Figure 4.12: A 60 second exposure image of an assay area in which a 5 x 5 array of anti-GroEL was printed and exposed to Alexa Flour [®] 633 labelled GroEL protein after addition of ethanolamine.	162

Figure 4.13: A 60 second exposure image of an assay area in which a 5 x 5 array of anti-GroEL was printed and exposed to filtrate produced from the GroEL reaction mixture after the addition of ethanolamine.	163
Figure 4.14: GroEL calibration results including a fitted curve.....	167
Figure 5.1: Comparison of anti-atrazine scAb binding ELISA run in PBS, HEPES and HEPES saturated with CaSO ₄	172
Figure 5.2: Comparison of Anti-Atrazine scAb binding ELISA run in HEPES containing MgSO ₄ at 3.6 and 17.3mg.ml ⁻¹	174
Figure 5.3: Comparison of Anti-Atrazine scAb binding ELISA run in HEPES containing FeSO ₄ at 2.6, 13.3 and 26.6mg.ml ⁻¹	176
Figure 5.4: Photograph of iron (II) sulphate in different solutions.....	178
Figure 5.5: Photograph of iron (II) sulphate in different solutions.....	178
Figure 5.6: Photograph showing different buffers immediately after the addition of 26.6mg.ml ⁻¹ iron (II) sulphate.	179
Figure 5.7: Photograph showing different buffers 1 hour after the addition of 26.6mg.ml ⁻¹ iron (II) sulphate. From left to right the solutions are RO water, 10mM HEPES, 10mM TRIS, and 10mM MOPS all pH 7.4.	179
Figure 5.8: Buffer solutions after the addition of ascorbic acid at a concentration 20.6mg.ml ⁻¹ . From left to right the buffers are: RO water, 10mM HEPES, 10mM MOPS, 10mM TRIS all pH 7.4.....	180
Figure 5.9: Buffer solutions containing ascorbic acid immediately after the addition of iron (II) sulphate at a concentration of 26.6mg.ml ⁻¹	181
Figure 5.10: Buffer solutions containing ascorbic acid 1 hour after the addition of iron (II) sulphate at a concentration of 26.6mg.ml ⁻¹	181
Figure 5.11: Effect of the presence of different dilutions of guanidine-HCl on anti-atrazine scAb in a binding ELISA format.....	185
Figure 5.12: Effect of the presence of different concentrations of methanol in HEPES Buffer on the binding properties of anti-atrazine scAb recombinant antibody fragment.....	187
Figure 5.13: Effect of the presence of hexane, methanol and a hexane / methanol mixture on the binding properties of anti-atrazine scAb recombinant antibody fragment.....	188

List of Tables

Table 2.1: Types of radiation present in the space environment and their RBE values...	11
Table 2.2: List of Biomarkers (and their properties) Identified during the Biomarker Workshop, grouped into categories of indicators of Extant Life, Extinct Life, Spacecraft Contamination and Meteoritic organics.....	40
Table 3.1: Calculation of the resulting number of dye molecules per protein for a series of Alexa Fluor® 633 dye concentrations after the spotting solution was evaporated away from the surface.....	130
Table 4.1: Results of a number of different blocking and washing experiments on epoxy coated slides.....	142
Table 4.2: Results of contact angle measurements at different stages of GOPS functionalisation.....	154
Table 4.3: Contact angle measurement of silicon nitride and silicon oxide surfaces before and after GOPS functionalisation.....	156
Table 4.4: Images showing the results of the experiments described in section 4.11.1.....	158
Table 4.5: Results and observations from initial assays on commercial and in-house GOPS coated slides.....	158
Table 4.6: Images used to form a calibration curve for the GroEL Assay system.....	165

List of Abbreviations

CCD – Charge-coupled device

ESA – European Space Agency

GCR – Galactic cosmic rays

GOPS – (3-glycidoxy)trimethoxysilane

HZETRN – High-charge-and energy transport computer program

LMC – Life Marker Chip

MARIE – Mars radiation environment experiment

MASSE – Microarray Assay for Solar System Exploration instrument

MOBILD – Molecular Biology for Life Detection instrument

PDMS – poly(dimethylsiloxane)

SMILE – Specific molecular indications of life experiment

SPENVIS – Space environment information systems modelling program

TRL – Technology readiness level

Chapter 1: Introduction, Aims and Objectives

1.1 Introduction

All of the work reported in this document was carried out in the context of developing the Specific Molecular Identification of Life Experiment (SMILE). SMILE is a Life Marker Chip (LMC) which was proposed as a potential instrument on board ExoMars, the European Space Agency's (ESA) next planned mission to Mars. ExoMars is one of the flagship missions of ESA's AURORA programme (the European programme for exploration of the solar system), and aims to characterise the potential of the surface environment of Mars to support Life, and this includes a surface rover carrying astrobiological experiments aiming to determine the presence of Life (Vago *et al.*, 2003). Life detection is to be achieved through a specific complementary package of instruments in the Pasteur Payload. The Pasteur Payload is proposed to include a gas-chromatography mass-spectrometer, which will detect and identify small organic molecules, the Urey instrument, which can identify certain types of organic molecules and detect differences in the chiral ratios of for example amino acids, and the Life Marker Chip (LMC), which would use antibody based assays to detect a range of organic molecules e.g. membrane breakdown products and complete proteins (Vago *et al.*, 2003, Sims *et al.*, 2005). The SMILE LMC is being developed by a consortium led by the University of Leicester and Cranfield University, which includes European partners and input from the MASSE group (Steele *et al.*, 2004).

There are a number of types of evidence supporting the possibility that Life may have evolved on Mars, including the fact that Mars was once within the 'habitable zone' of the Solar System (the region of temperatures within which liquid water can exist), the similarity of early Mars and early Earth geochemistry, the discovery of dried river valleys, seas and sedimentary rocks on the Martian surface, and the discovery of structures within Martian meteorites which resemble fossilised terrestrial micro-organisms. There are also arguments against such a possibility, including a lack of sufficient geological activity on Mars to support life chemistry and other theoretical studies. This area will be discussed in more detail in the literature review (Chapter 2), but in summary there is sufficient evidence for the possibility of life to warrant further investigation either by analysing samples on the Martian surface or, in the future, to

attempt to transport samples from Mars back to Earth for detailed laboratory analysis (Vago *et al.*, 2003, Sims *et al.*, 2005).

The SMILE Life Marker Chip proposed for the Pasteur Payoad is to utilise protein chip technology within a microfluidic channel, in order that a large number of relevant target molecules can be detected simultaneously within a single sample of low volume. The current concept of the SMILE LMC is a multiplexed antibody-based assay for the detection of molecular biomarkers. These biomarkers can be split into two broad categories, namely polar biomarkers (of which most are indicators of extant Life), and a-polar biomarkers (of which most are indicators of preserved, and normally altered, biomarkers i.e. extinct Life). In addition to the detection of biomarkers related to past and present Life on the Martian Surface, molecules associated with spacecraft contamination and characteristic of organics from meteoritic infall will be considered. The assay readout was proposed to utilise fluorescent detection of labelled components, since optical fluorescent biosensors can achieve very low limits of detection. To support this fluorescent readout, the assay system will either utilise fluorescently labelled analytes or antibodies in a competitive or inhibition assay with pre-labelled reagents, or include *in-situ* labelling of the biomarkers in the sample. The fluorescent excitation and readout will be achieved by carrying out the immunoassay on an optical waveguide and passing light down the waveguide to generate an evanescent field at the surface. The evanescent field would excite any fluorescent dye on a labelled reagent that had bound (specifically by antibody-antigen interaction) to the surface and generate fluorescence, which could be detected by a cooled CCD imaging system. The technology being developed for SMILE is also being considered for applications in the detection of Life in subglacial Antarctic lakes, specifically Lake Ellsworth, but these other applications will not be discussed in this thesis (Vago *et al.*, 2003, Sims *et al.*, 2005).

In order for the Life Marker Chip instrument to be confirmed for flight on Pasteur Payload, a number of factors have to be defined. These include:

- the identification of suitable stable molecular targets which may indicate the presence of extinct or extant life.
- the development of specific antibodies to these targets.

- ensuring that these antibodies survive the operational conditions required i.e. high resistance to gamma and particle radiation, extreme high and low temperatures and stability over long periods of time.
- determining the effects of radiation on the properties of fluorescent dyes required for readout of the proposed SMILE LMC.
- the development of a multiplexed assay system which can detect low concentrations of many target analytes using very low sample volumes.
- developing a breadboard imaging system to develop the flight instrument design concept and demonstrate fluorescent readout of immunoassays in a microarray format.
- establishing any limitations the assay system would impose upon the sample extraction and processing system, including investigating the effects of Martian regolith salts, and solvents that may be used in the sample processing, on representative assays.
- the development of an extraction system capable of extracting low concentrations of target molecules from a variety of mineral rocks.
- the development of suitable microfluidic devices for transporting small volumes of liquid to the sensing area.
- the identification of areas on the surface of Mars which may be/have been suitable for the evolution of life, and within these areas identification of appropriate samples to take for analysis.

All of the factors listed above were considered in the same time frame as the work reported in this document, although this author was not solely responsible for all of the objectives. The work was carried out initially with a view to securing funding from the European Space Agency (ESA) to carry out a 2 year LMC Technology Readiness Level (TRL) Upgrade Study. When this funding was received, the work was continued within this TRL upgrade study, developing the design of the instrument and sample processing system. A further phase of work is planned to develop the breadboard system that is to be produced as an outcome of the Technology Readiness Level Upgrade Study into a flight instrument, and some of the work reported here contributes to the design of the

flight instrument in addition to breadboard development (Vago *et al.*, 2003, Sims *et al.*, 2005).

1.2 Thesis Objectives and Structure

The work reported here focuses on three key areas of the LMC development. The first of these was testing the resistance of biological recognition elements and fluorescent dyes to the environmental conditions encountered during a nominal mission, including pre-flight sterilisation and radiation exposure during flight. The second area involved developing the multiplexed assay system and a prototype breadboard system, and the third area was a series of studies to determine the effect of Martian regolith salts and potential solvents used in sample processing and extraction of biological assays. While these activities were carried out, other aspects of the LMC were being developed by partners in the project.

This document, therefore, will be presented in the form of three streams of work carried out in these different key areas of work. The approach adopted throughout the project was to establish methodology using reagents and protocols that were available when work began, representative of the proposed design for the flight instrument, and allowed simple verification of whether a protocol was successful. As the project became more advanced the protocols were refined and new equipment became available through the ESA funding, enabling the final experiments to become closely related to the design concept at the conclusion of this thesis. The streams of work were carried out in overlapping timescales, but are reported here in distinct sections.

1.2.1 Theme 1: Radiation and Flight Environment conditions

The first priority in terms of the timing of this work was to determine whether there was any fundamental reason why antibody-based assays with a fluorescent readout could not survive in space. The processes of spacecraft assembly and flight to Mars involve a large number of environmental conditions which biological materials e.g. antibodies and fluorescent dyes are not routinely exposed to. These conditions include long term storage at room temperature, exposure to high levels of acoustic energy, exposure to particle and gamma radiation from different sources (both solar and galactic cosmic

rays, and possibly during spacecraft sterilisation) and of various types (gamma, particle radiation and UV), landing shock and vibrations, low atmospheric pressure, and temperature cycling in extreme cold on the Martian surface. Many of these factors had not been fully evaluated when proposing the LMC for the Pasteur package (Sims *et al.*, 2005). At that time it was considered feasible to overcome engineering issues such as withstanding vibration and impact tests, and the biological materials were known to be compatible with extremes of cold as this is how they are stored routinely. The effects of radiation on antibodies and fluorescent dyes, however, was unknown and of critical importance to the feasibility of the proposed instrument, since both of these types of reagent are required for the proposed assay system. The objectives of this section of work, therefore, were to determine any effect of radiation on the properties of fluorescent dyes and antibodies in an immunoassay, to test the feasibility of using a gamma radiation treatment to sterilise the flight instrument, and determine the effects of dry heat sterilisation on antibodies and fluorescent dyes.

1.2.2 Theme 2: Development of optical breadboard and microarray assay system

After performing a number of radiation and heat sterilisation tests on antibodies and fluorescent dyes, and securing funding for the Technology Readiness Level (TRL) Upgrade Study, the focus of the project moved to development of the instrumentation platform. The basic components and methods used in the proposed SMILE instrument were already well established in the biotechnology sector, but the combination of antibody assays and fluorescent readout assays had not been carried out in such a small scale as was proposed, and using these assay systems in microfluidic channels had rarely been carried out. In addition, some of the techniques used had not been done previously in the laboratories at Cranfield University, where the assay development work was carried out, so some work was required to develop suitable protocols for microarray spot deposition before attempting to deposit arrays of antibody spots. The key objectives of this section of work were to assemble and test a breadboard imaging system representative of the flight LMC design, to develop immunoassays in a microarray format using fluorescently labelled reagents, to develop and optimise an immunoassay protocol based on a representative biomarker target, to establish protocols for *in-situ* fluorescent labelling of proteins and to demonstrate in-house functionalisation of surfaces representing those used in the LMC design.

1.2.3 Theme 3: Effects of Mars environment and sample processing reagents on antibody-based assays

Part of the work of the TRL upgrade study was to develop a specific sample processing and extraction system for the LMC. An important consideration in this was to determine the tolerance of the antibody assay to sample components that may pass through the sample processing system, since this is fundamental in the selection of the extraction method and solvents used. For example, if salts were found to present a large problem for the assay, a demineralisation step in the sample processing system would have to be considered. Similarly if organic solvents were not tolerated above certain levels, the solvents selected may have to be diluted or removed by evaporation or solid phase extraction. To develop this input to the sample processing system design, experiments were carried out to determine whether, and how much, antibody assays are affected by the presence of salts found to be common on the Martian surface and organic solvents that may be present in the sample processing and extraction system. The objectives of this section of work were to determine the effect of Martian regolith salts and solvents that may be used in the LMC sample processing system on immunoassays, and to use this information to provide input into the design of the LMC sample processing system.

Chapter 2: Literature review

The literature review in this document will be divided into four main sections. The first section will review the current state of knowledge of the relevant radiation and pre-flight sterilisation requirements and the possible effects on biological materials, and is presented in the form of a draft publication which the author of this thesis contributed significantly to¹. The second section is a brief review of the targets for the Life Marker Chip, and is included to explain the decision to base the LMC instrument on optical biosensing technology. The third section will review the existing optical biosensing technologies that may form components of the SMILE LMC instrument, and the final section will describe the expected conditions and sample types on the Martian surface, and possible effects that regolith materials and sample processing reagents may have on the biological assay.

2.1 The effect of extreme environments on biological materials

2.1.1 Introduction and space mission environments

One of the key targets for the SMILE LMC is the planet Mars and consequently the following sections and discussion concentrate almost exclusively on this environment as the example mission environment and in particular on the effects of radiation. Although as an aside it should be noted that LMC technology has applications in crewed missions in near-Earth orbit e.g. the International Space Station or on missions to other targets e.g. Europa, where the radiation environment may differ significantly.

The review will initially focus on the expected levels of radiation during a Mars mission. This will be followed by the likely and measured effects of planetary protection as relevant to Life Marker Chips, and then a discussion of the basic effects of radiation on biological materials and its possible effects on components within a LMC instrument. The measured effects of radiation on biological and biologically based materials will then be described. Finally some additional effects and factors will be briefly discussed. A summary of the environmental considerations for the LMC will be presented, along with the areas where further testing and development were required prior to this work.

1. This publication, provisionally titled "Review of Radiation Effects on Biologically Based Experiments" is pending submission to the journal *Astrobiology* in the near future. The author of this thesis was responsible for the major content of the review of radiation effects on biological materials, the NASA MARIE data, and the review of Planetary Protection requirements, and is a named author on this paper. The publication will be submitted when the authors receive permission for the use of figures from the NASA MARIE experiment and final corrections. The MARIE figures included here were prepared from preliminary data and indicate the trends of the final results, but may not be true representations of the actual amount of radiation encountered. The full author list currently is as follows:

M.R. Sims^{1*}, P.K. Wilson², D.P. Thompson¹ and D.C. Cullen²

1. Space Research Centre, Department of Physics and Astronomy, University of Leicester, Leicester LE1 7RH, UK

2. Cranfield Biotechnology Centre, Cranfield Health, Cranfield University, Silsoe, Bedfordshire MK45 4DT

Corresponding author e-mail mrs@star.le.ac.uk, tel: 00 44 116 2523513, fax: 00 44 116 2522464

2.1.1.1 Space mission environments

A key science goal of many space missions and in particular those in astrobiology is detection of organic molecules that can be directly associated with present or past Life, namely polar and a-polar biomarkers. Life detection instruments must also detect organic targets characteristic of meteoritic organic chemistry and spacecraft contamination. Current target planetary bodies within the Solar System include Mars, Europa and Titan. All have radically different environments, and, in the case of Titan, perhaps different potential life chemistries associated with them. All targets have common extreme environment challenges that need to be dealt with, the only difference between them being the exact values of the extremes. These target environmental challenges combine with those of the mission itself and are namely

- Temperature
- Chemical Environment
- Radiation including particles radiation, gamma and UV
- Pressure (or low pressure)
- Planetary Protection i.e. the need to sterilise and clean the instrument to avoid contaminating the target. This is to be achieved either by thermal sterilisation or potentially gamma irradiation

The environmental challenges at all stages of the mission must be considered in any space instrument design and development programme, including final assembly, integration and testing, pre-launch storage, launch, cruise to the target (Mars), and operation *in-situ*.

The three key environments, are considered by the author to be, namely, pre-launch sterilisation, the flight through inter-planetary space during which the craft will be exposed to galactic cosmic radiation and solar radiation including gamma rays, protons and heavy ion radiation, and the operational conditions on the planet/moon, which may include high radiation dose and extremely cold temperatures. Temperatures in turn could vary considerably on a daily, seasonal, and landing location basis.

2.1.1.2 Life Marker Chip instruments

Although a number of instrumentation technologies are highly sensitive in the detection of organics, for example gas-chromatography mass-spectrometers (GCMS), there has been a move towards confirmation of particular targets by multiple instruments, and highly specific molecular detection. One method of detection involves use of sensors based on antibodies or other specific molecular receptors e.g. Molecular Imprinted Polymers (MIPs), where high sensitivities and, more importantly, low limits of detection can be achieved in small compact instruments. One such example is the so-called Life Marker Chip (LMC) instrument for example the SMILE (Sims *et al.* 2005), MASSE (Steele *et al.*, 2004) or MOBILD (Gómez-Elvira *et al.*, 2004) all of which are based on similar concepts. MIPs offer a potentially higher environment robustness, but require considerable developments so “first generation” LMC instruments will utilise antibody based detection methods. Such instruments may utilise fluorescence, refractive index or electrochemical readout or even a combination to provide information rich and confirmatory data. First generation instrumentation will most likely use a fluorescent readout as it is relatively simple and well-known technique extensively utilised in biotechnology.

Life Marker Chip (LMC) instruments e.g. SMILE, MASSE, MOBILD, although having a strong biotechnology heritage, have not been flown in space. The biological materials used in these LMC instrument designs, and their compatibility with the space environment and likely ground Assembly, Integration and Verification (AIV) requirements are at best poorly known. One key mission effect is space radiation particularly as relatively complex organic molecules i.e. proteins are used within the devices. Consequently compatibility with the mission radiation specification is a key test to be performed early within any space LMC development.

2.1.1.3 The space and planetary radiation environment

Radiation in space and on the surface of another planet consists of the following inputs:

- Electrons
- Protons
- Neutrons
- Ions i.e. Cosmic rays
- X-rays and Gamma-rays
- UV radiation

Each radiation type listed is, in principle, capable of producing secondary radiation from interaction with the instrument or material surrounding the instrument and modifying the radiation spectra seen by any LMC. In addition environmental challenges induced by design of the spacecraft need to be taken into account for example in an Radioactive Thermal Generator (RTG) powered rover there may be a considerable flux of neutrons resulting from the RTG power source, see section 2.1.2.4.

2.1.1.4 Planetary protection

Planetary Protection is a specific term used to describe the international effort to prevent terrestrial life being introduced to other planetary bodies by the transfer of living biological organisms between worlds through spacecraft contamination. The classifications of spacecraft and the requirements for each type are controlled and regulated by the Committee of Space Research (COSPAR), and are described as a series of pre-flight and operational requirements for each mission type (DeVincenzi *et al.*, 1984). The regulations state that appropriate sterilisation procedures must be carried out on all entities that may come into contact with a planetary surface where there is interest in the process of chemical evolution. The specific requirements and procedures to achieve sterilisation are dependent on the type of mission and the instrumentation on board. In the case of landers or other spacecraft which may come into contact with planetary surfaces procedures must be carried out to quantify and reduce microbial contamination and overall bioload, calculate the probability of contamination of the target environment, and document all organics on board and the procedures and results of pre-flight sterilisation (Divincenzi *et al.*, 1984). In the case of

Mars missions, this has been further defined such that all Mars landers must be sterilised to at least the levels used for the Viking landers i.e. a total spore count of $\leq 300 \text{ m}^{-2}$ and a total spore burden not exceeding 3.0×10^5 (Mahaffy *et al.*, 2004, DeVincenzi *et al.*, 1996). Thus any molecular or biological components of an instrument must therefore survive at least one of the approved procedures used to reach this level of sterilisation, namely gamma irradiation, ultraviolet (UV) irradiation, heat sterilisation - a minimum of 111.7°C for 30 hours (DeVincenzi *et al.*, 1996), or precision cleaning (Mahaffy *et al.*, 2004). In addition the materials will be exposed to additional sterilisation via the electromagnetic and particle radiation encountered during the flight to Mars and on the Martian surface.

2.1.1.5 Radiation and its effects on organic and biological materials

It is assumed that the antibodies and other biological type molecule components within LMC type instruments will be affected by radiation as per other biological systems. The various types of radiation are classified in terms of their effect by the so called biological quality factors which are used to derive a biological dose which has the unit of a Sievert (see for example Holmes-Seidle and Adams 2002). The relative biological effectiveness or quality factors for the various types of radiation are as follows (Table 2.1):

Table 2.1: Types of radiation present in the space environment and their RBE values.

Type of Radiation	Relative Biological Effectiveness (RBE)
X-ray, UV, Gamma, Beta particles (electrons)	1
Slow neutrons	5
Fast neutrons/protons	10
Alpha particles	20
High Z particles	20

Consequently the “most” damage is expected by ions as they have the highest RBE value.

Electrons interact at the atomic level, causing excitation and ionisation that can cause them to be scattered and produce Bremsstrahlung radiation. Protons and heavier ions can produce excitation and ionisation but can also react directly with the atomic nucleus causing fragmentation of the nucleus and emission of secondary neutrons and protons. Neutrons having no charge are difficult to stop but interact strongly with water, which can produce an effective shield. Neutrons can interact directly with the nucleus.

Biological materials are however exposed to radiation treatments for a number of reasons, including the sterilisation of food and medical supplies (including diagnostic reagents) and for the immobilisation of bioactive materials such as enzymes, (Kume & Matsada, 1995, White *et al.*, 1990). The primary reason for most treatments is to achieve inactivation of any bacteria present, although some studies have investigated the feasibility of radiation-inactivation of proteins to reduce their antigenicity and therefore prevent allergic reactions to specific proteins (Kume & Matsada, 1995).

The effect of radiation on polymers, including biological ones, is the conversion of particles into much lower energy radiation and the formation of short-lived intermediate compounds, usually free radicals (see for example Yamaguchi *et al.* 2005). Radiolytic hydrogen gas can be generated from ruptured C-H bonds and any intermediates can react with water and oxygen to produce OH radicals that may produce further chemical damage. Consequently freeze-drying may be a very effective way to reduce radiation damage, (see section 2.1.3.6). As short-lived intermediate compounds are produced, any radiation effects may unfortunately be rate dependant (see section 3.1 regarding implications for radiation testing). In general, for biological and chemical materials, radiation causes damage by two methods, producing cross-linking and via scission or bond breaking, with the resulting production of new compounds and a consequent change in properties.

There are number of commonly used terms in the description of radiation exposure (see for example Holmes-Seidle and Adams 2002). The radiation dose is refined as the amount of energy absorbed by the target. The units used to describe this are the Rad (1Rad = 0.00001 Joules of energy absorbed per gram of substance), Grays (Gy - 1 Gy = 100Rads), and the Roentgen Equivalent Mean (REM). The REM is a much more complicated unit as it describes the amount of biological damage produced and is

dependent on a large number of factors including the type and energy of radiation. The REM is related to the Rad by the following equation:

$$\text{REM Dose Equivalent} = \text{Relative Biological Effectiveness (RBE)} \times \text{Rads}$$

where the relative biological effectiveness (RBE) is a proportionality constant as given in Table 2.1. By convention the damage done to a human by a whole body irradiation of 250keV X-Rays is considered to be equivalent to 1 rad, and the RBE under these conditions is unity. Space mission doses are normally quoted in rads.

2.1.1.6 Effects of radiation on the Life Marker Chip and related instruments

One of the major unknown factors in the potential application of biological recognition elements e.g. antibodies in an LMC-type experiment is the effect of the different types of radiation that would be encountered during the mission. Since very few experiments involving the irradiation of antibodies or other molecular receptors have been carried out, particularly those involving freeze-dried antibodies and particle radiation, the majority of literature included in the review below is based on the effect of gamma radiation on proteins and enzymes in both liquid and freeze dried states, as these provide a basis for determining the possible effects of radiation on antibodies and other molecular receptors. Similarly there have been very few experiments on the resistance of freeze-dried biological materials to extreme temperatures and temperature cycling.

A variety of different potential damage mechanisms might be expected within an instrument, as given below.

- Damage to fluorophore / fluorescent molecules would lead to a change in quantum efficiency, peak emission or excitation fluorescent wavelength or even complete loss of fluorescence.
- Damage to the antibodies would cause a loss of affinity to their antigen, or stronger binding to other (non-target) compounds, i.e. loss of specificity.
- Radiation may damage the binding of materials to surfaces or change the surface free energy, therefore affecting the ability to move fluids through a system and non-specific binding.

As the biologically based elements will be housed inside the instrument it is assumed in what follows that UV radiation is not a factor that is likely to affect such instruments, due to the effect of shielding offered by the spacecraft and rover structure. Therefore, UV radiation will not be considered in the following sections.

2.1.2 Expected radiation levels during a Mars Mission

2.1.2.1 Radiation during a Mars mission

During transfer to Mars, a spacecraft will be exposed to a wide range of radiation types and energies including gamma rays, protons, neutrons and heavy ions (e.g. Adams (1992), Petrov (2004)) at energies ranging from a few MeV to thousands of GeV and beyond, peaking at around 1 GeV (see for example Benton and Benton (2001)).

Additional contributions may come from any on-board radio-active sources (Butcher *et al.*, 2006) or radio-active heater units or radio-active thermal generators (RTGs). For example in the case of the Mars Science Laboratory Mars Rover mission expected to fly in 2009 which will carry an Radioactive Power Supply (RPS) based on RTGs the radiation dose on the surface of Mars is dominated by the RPS with a expected dose of 76 Rads compared to 28 Rads of the natural environment. The RPS results in a total mission fluence of 3.2×10^{10} equivalent 1 MeV neutron fluence through the analytical laboratory during the nominal mission consisting of 300 days cruise to Mars and 670 Sols (Martian days) (approximately 645 Earth days) on the Martian surface (MSL PIP 2004).

2.1.2.2 Measured radiation environment at Mars

The Mars Radiation Environment Experiment (MARIE) on board the 2001 Mars Odyssey orbiter was designed to record the radiation environment during flight to and in orbit around Mars (see <http://marie.jsc.nasa.gov/Data/Index.cfm>). This includes data on the galactic cosmic ray energy spectra and solar energetic particles, and changes occurring during solar events e.g. solar flares. Solar energetic particle events occur sporadically during the 3 year prior to and 4 years following a solar maximum, and lead to sharp, short-term increases in radiation dose and dose rate. MARIE can measure

particle energies between 15MeV and 500MeV per nucleon, a range encompassing most radiation particles which are harmful to humans and that can damage DNA.

A basic calculation of the expected radiation dose is given by the HZETRN model (Wilson *et al.*, 1995), which uses the daily solar deceleration parameter (ϕ) to determine the galactic cosmic radiation spectra. **Error! Reference source not found.** shows a plot of the dose predicted by this model against the actual data recorded by MARIE during flight to Mars, and Figure 2.2 shows the same plot for radiation dose at Mars orbit.

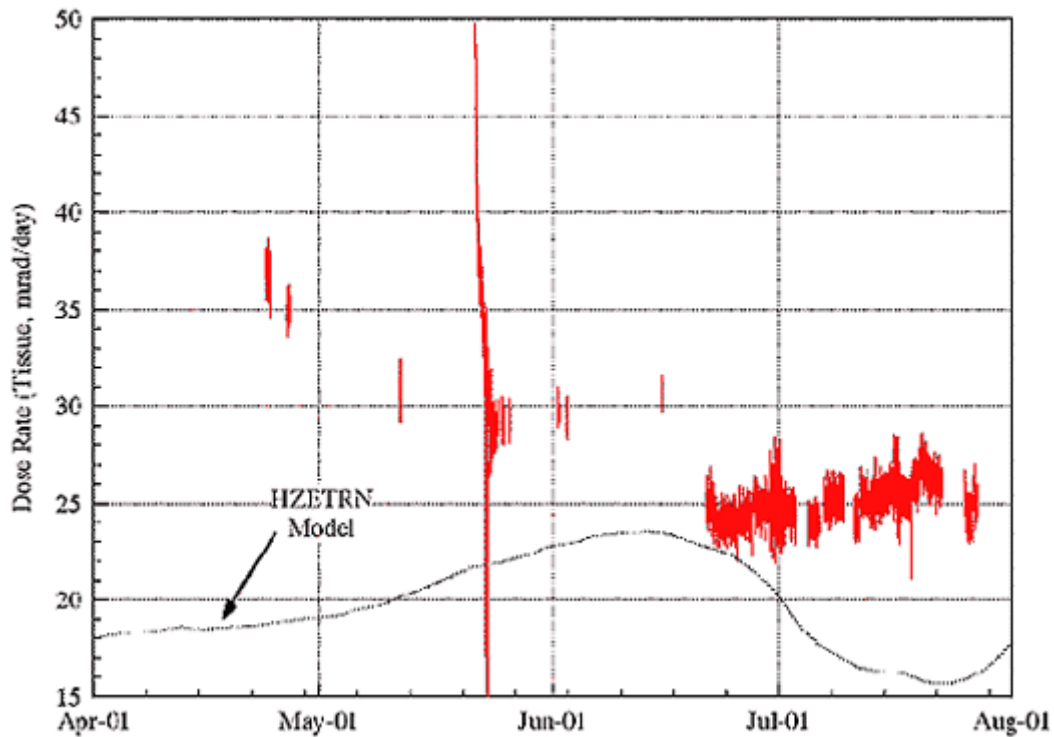


Figure 2.1: Provisional data from the MARIE: Absorbed Dose Rate vs HZETRN Model Calculations During Flight, as presented on the NASA MARIE website in 2002-3. NOTE: This provisional figure is no longer available, but revised versions that compensate for some calibration issues have been prepared and will be published in the near future by the NASA MARIE group (Personal Communication, Cary Zeitlin (2006)).

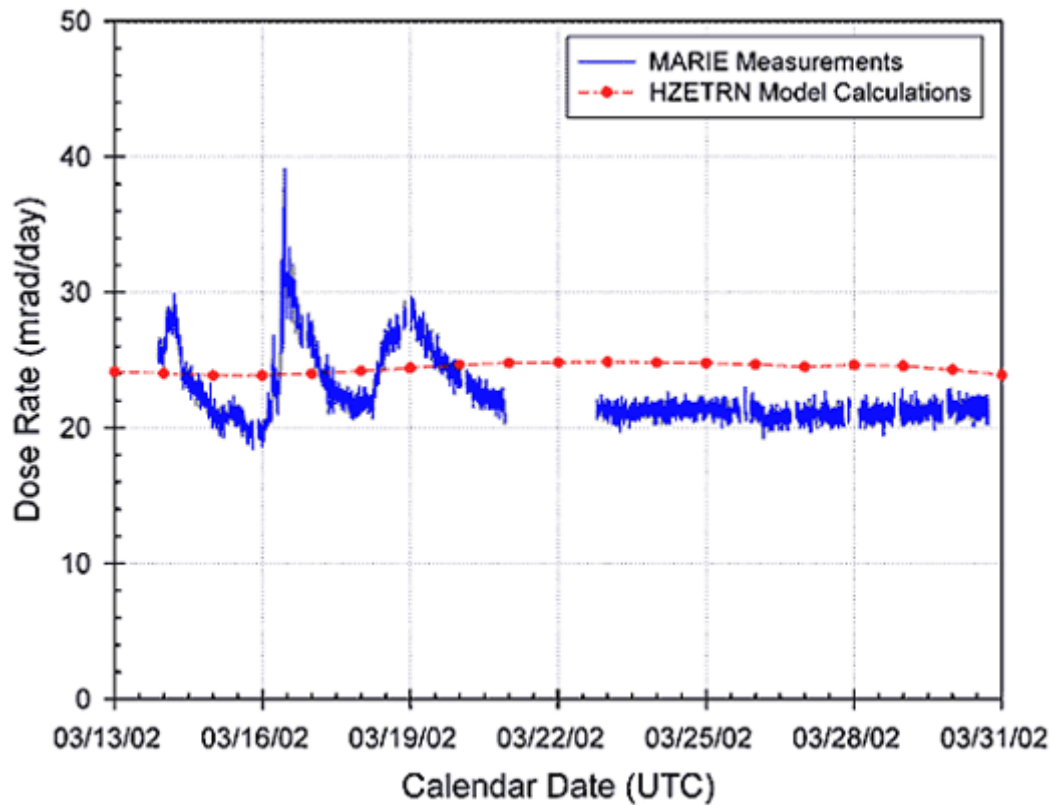


Figure 2.2: Provisional figure showing MARIE measurements vs. HZETRN model calculations during Martian orbit as presented on the NASA MARIE website in 2002-3. NOTE: This provisional figure is no longer available, but revised versions that compensate for some calibration issues have been prepared and will be published in the near future by the NASA MARIE group (Personal Communication, Cary Zeitlin (2006)).

The gaps in data in Figure 2.1 and Figure 2.2 are due to alterations to the instrument and downloading of data. The HZETRN model predicts a basic dose rate of $\sim 25 \text{ mRad.day}^{-1}$ due to galactic cosmic radiation alone in both cases, although in Figure 2.2 there is some variation due to solar modulation during this period. Figure 2.1 includes a large peak in dose rate (nearly 50 mrad.day^{-1}) on May 22nd 2002, due to a solar particle event (SPE). There are also some smaller peaks in dose rate in Figure 2.2, which are also likely to be due to SPEs. The basic dose rate in Martian orbit appears to be slightly below that predicted by the HZETRN model, possibly due to the limited range of angles in which radiation is recorded by the MARIE instrument.

The distribution of charged particles detected by the MARIE instrument is shown in Figure 2.3 and Figure 2.4 (<http://marie.jsc.nasa.gov/Data/Index.cfm>). These show that the vast majority of particle radiation encountered by MARIE has been protons ($z = 1$) and helium nuclei ($z = 2$). However, significant numbers of carbon nuclei ($Z = 6$), nitrogen nuclei ($Z = 7$), and oxygen nuclei ($Z = 8$) can be clearly seen in Figure 4, and

some indications of boron nuclei ($Z = 5$) and a slight Neon nuclei ($Z = 10$) peak may also be present.

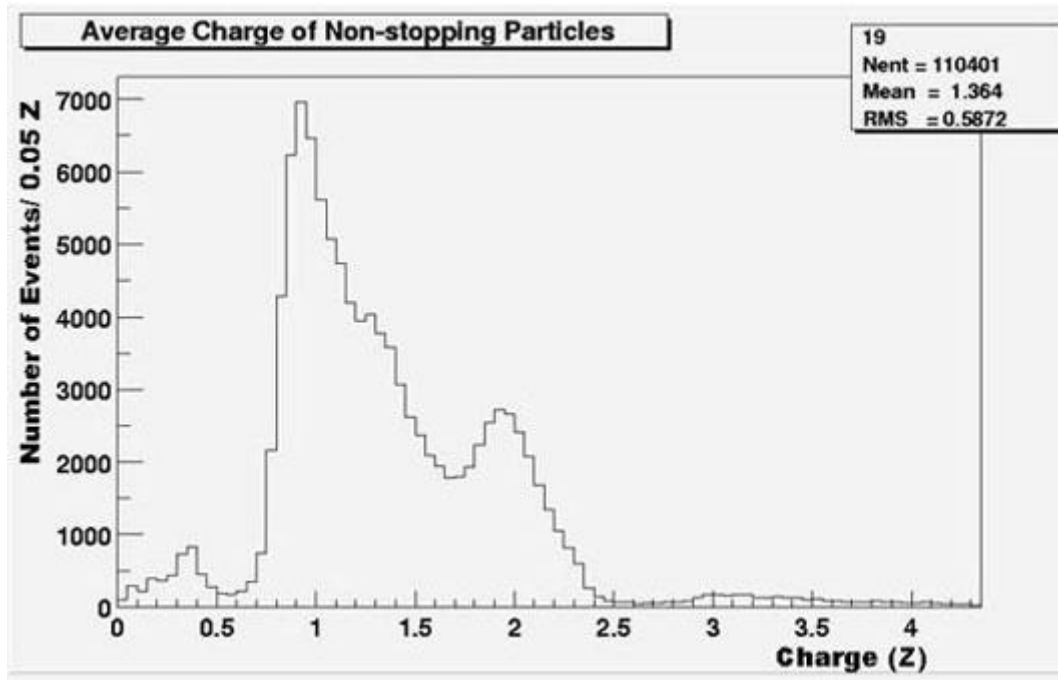


Figure 2.3: Provisional MARIE measurements of the Average Charge of Non-Stopping Particles (low Z) as presented on the NASA MARIE website in 2002-3. NOTE: This provisional figure is no longer available, but revised versions that compensate for some calibration issues have been prepared and will be published in the near future by the NASA MARIE group (Personal Communication, Cary Zeitlin (2006)).

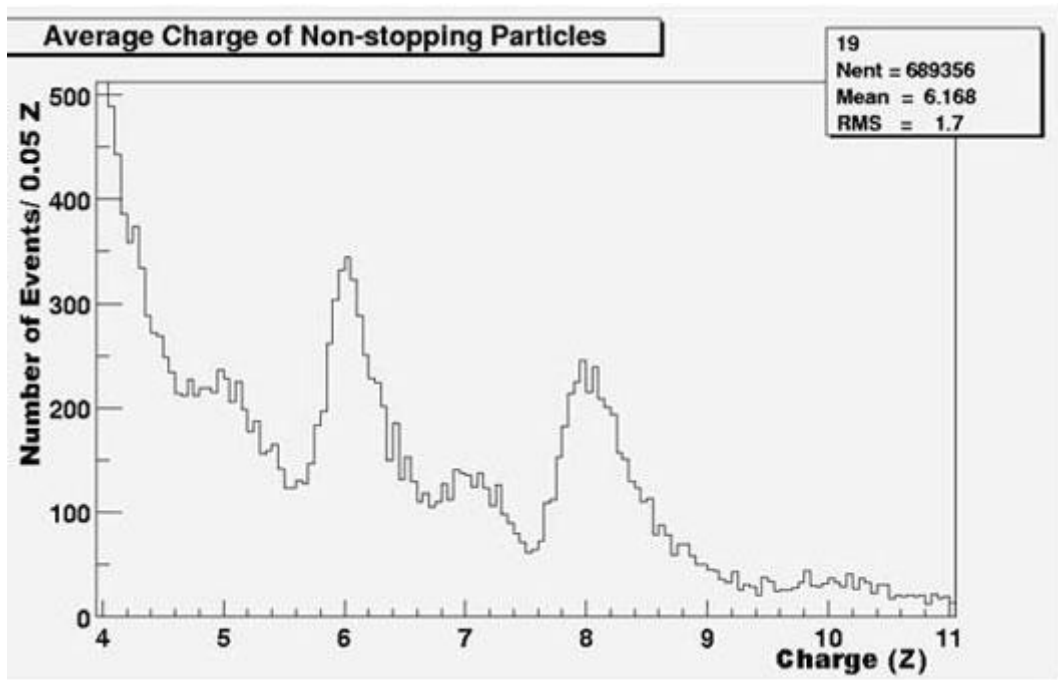


Figure 2.4: Provisional MARIE Measurements of Average Charge of Non-Stopping Particles (High Z) as presented on the NASA MARIE website in 2002-3. NOTE: This provisional figure is no longer available, but revised versions that compensate for some calibration issues have been prepared and will be published in the near future by the NASA MARIE group (Personal Communication, Cary Zeitlin (2006)).

Since Mars, unlike Earth, is not protected from radiation by a magnetic shield (NASA MARIE) and its atmosphere is less than 1% as thick as Earth's, it can be assumed that radiation on the planetary surface will be similar to that in orbit around the planet. This gives an indication of the dose that all the biological molecules involved in the Life Marker Chip must withstand in order to be suitable for this application.

2.1.2.3 Summary of information about the radiation environment from NASA MARIE

While the MARIE experiment does not give a fixed radiation dose for any given mission to Mars (due to the variation in duration, flight path and solar activity between missions), the correlation of the measured radiation dose with that predicted by modelling techniques (Figure 2.2), within at least an order of magnitude, validates the use of the HZETRN model to calculate approximate expected radiation environment for any given mission. The basis of this model and other similar models and predictions of the radiation environment for ExoMars will be discussed in section 2.1.2.4.

2.1.2.4 Predictions of the radiation environment and the radiation dose and testing problem

It is possible to model the expected radiation environment during a space mission. Such tools as the High-charge-and Energy TRANsport computer program (HZETRN) model and SPace ENVIRONMENT Information System (SPENVIS) (European Space Agency General Support Technologies Programme – see www.spennis.oma.be) can be used. Many mission design specifications however give the integrated radiation dose (equivalent to the absorbed by silicon) in rads. There therefore remains a “calibration” problem when biological materials are used, unless a standard silicon detector is utilized in any tests.

Alternatively using such tools as SPENVIS the fluence vs. energy of a particular radiation type can be calculated allowing for the shielding of the spacecraft/probe and instrumentation. This fluence can then be used to provide inputs for testing components for space flight for a given mission, such as testing LMC components and biological materials to determine whether they will survive the mission radiation environment of ExoMars. The radiation is normally described in terms of total ionising dose and total non-ionising dose.

At the time that the radiation studies reported in this document were performed, the minimum radiation environment for instruments on board the ExoMars Mission to survive had been calculated to consist of a total ionising radiation dose of 2.5 krad (assuming 4mm Aluminum shielding), and a non-ionising energy loss of 5×10^7 MeV/g(Si) (assuming 4mm Aluminum shielding) (ESA, 2005). For Mars Science Laboratory, a NASA mission comparable to ExoMars in that it will also fly to Mars carrying a rover with a payload of instruments for the detection of organics, the expected ionising radiation dose is expected to be 3.0krad, and non-ionising dose equivalent to 3.2×10^{10} 1MeV neutrons for the analytical instruments (MSL PIP, 2004). The experiments reported in section 3.1 of this thesis were based on these figures. However, more recently, a study has been carried out within the Technology Readiness Level Upgrade Study (Alex Hands and David Rodgers, QinetiQ, Personal Communication), which indicates that in fact the total ionising radiation dose for ExoMars will be 6.6kRads and total non ionising dose of 1.4×10^8 MeV/g. These slightly higher figures do not invalidate the work carried out in section 3.1, due to the large over-testing philosophy adopted at the time of these experiments, and exposures many orders of magnitude greater than the minimum requirement for the mission.

The problem in testing is however that normally either one single energy or a limited range of energies of particular radiation types are present and can only be applied at higher rates than during the mission. The former has the problem that not all energies can be run simultaneously and consequently multiple tests and limited energy range tests must be conducted. The latter has the advantage that tests can be conducted in a reasonable and limited time, however its does not allow for any decay-type processes that may occur in a real material during a mission e.g. decay of excited states etc. Some combined testing is possible with exposures of targets to mixed radiation for example via reactors, however undesirable radiation components (from a test point of view) cannot be excluded from use of such test apparatus.

2.1.3 Effects of radiation on whole cells and cellular components

2.1.3.1 Introduction: viral and bacterial exposure to radiation

The results of exposure of whole cells and cellular components to different types of radiation are reviewed below, and the overall results and relevance to the current application discussed. The primary aim of exposing viruses or bacteria to radiation is to

achieve sterilisation, either for food or medical products. The main goal is to achieve inactivation of these pathogens, and studies therefore focus on the minimum radiation dose required to achieve this.

Gamma photons are by far the most widely used radiation treatment of biological materials (Lowy *et al.*, 2001). In this review, only two studies were found in which biological materials were exposed to neutrons (Lowy *et al.*, 2001, Singh, S. *et al.*, 1990). Lowy *et al.* (2001) found that neutrons were less effective at inactivating bacteria than gamma radiation, with relative biological effectiveness (RBE) value of approximately 0.5. They showed this using two different methods and different bacterial strains (Lowy *et al.*, 2001). In contrast Singh, S. *et al.* (1990) had previously reported that neutrons were more effective than gamma photons at inactivating bacteria. During this review no publications were found in which biological materials of any type were exposed to proton radiation.

It has been found in a number of studies that viral replication is inactivated at a lower radiation dose than protein-dependent activities, such as antigenicity (Deflora and Badolati, 1973, Gamble *et al.*, 1980, White *et al.*, 1990, Elliott *et al.*, 1992, Pang *et al.*, 1992, Lowy *et al.*, 2001). Lowy *et al.* (2001) were not able to associate inactivation of a virus with structural damage to any particular type of cellular component nor did they find that gross structural changes occurred in the majority of viruses (Lowy *et al.*, 2001). The specific type of radiation damage to viruses could not be identified for either neutrons or gamma radiation (Lowy *et al.*, 2001). They also observed that if viral inactivation plateaus exist at a certain dose this would be very difficult to demonstrate, as it would require very accurate measurement and an extremely high radiation dose (Lowy *et al.*, 2001). These results suggest that proteins and other viral components may retain their functionality at higher radiation dose than is required for inactivation of the pathogen itself (Lowy *et al.*, 2001).

2.1.3.2 Cellular component exposure to radiation

The effects of gamma radiation on proteins has been extensively studied under a number of different conditions, although the effects of other radiation types have not been investigated. There are a number of common effects to all proteins exposed to

gamma radiation. These include conformational changes, oxidation of amino acids, rupture of covalent bonds leading to fragmentation, and the formation of protein free radicals which can lead to cross-linking and aggregation of proteins (Lee *et al.*, 2004, Lee *et al.*, 2003, Lee and Song, 2002, Cho and Song, 2000, Cho *et al.*, 1999, Filali-Mouhim *et al.*, 1997, Kume and Matsuda, 1995, Puchala & Schuessler, 1993, Davies and Delsignore, 1987, Garrisson, 1987, Cheftel *et al.*, 1985, Schuessler and Schilling, 1984, Yamamoto, 1977). The dominant effect(s), and hence the resulting characteristics of the protein, appears to be dependent on a number of factors. These include the radiation dose, the presence of water, oxygen and free-radical scavengers, protein concentration, and protein-specific factors such as the primary amino acid sequence, local conformation of amino acids, and accessibility to water radiolysis products or other free radicals (Lee *et al.*, 2004, Lee *et al.*, 2003, Lee and Song, 2002, Cho and Song, 2000, Filali-Mouhim *et al.*, 1997, Kume & Matsuda, 1995, Woods and Pickaev, 1994, Davies and Delsignore, 1987, Garrisson, 1987, Cheftel *et al.*, 1985, Schuessler and Schilling, 1984).

In proteins, a large number of studies on different proteins in solution have demonstrated that a low radiation dose e.g. 100krad, results in fragmentation, observable by a decrease in the intensity of the major band in electrophoretic gels, and the corresponding appearance of new bands below the major band. At higher radiation doses e.g. 500, - 1600krad, aggregation becomes the dominant effect and cross-linked products are formed, which are not able to penetrate electrophoretic gels. At a given radiation dose, whichever effect is dominant (either fragmentation or aggregation), occurs more rapidly at lower protein concentrations i.e. lowering the protein concentration increases the rate of these radiation effects (Stevens *et al.*, 1967, Schuessler and Schilling, 1984, Krumhar and Berry, 1990, Le Maire *et al.*, 1990, Puchala and Schuessler, 1993, Kume and Matsuda, 1995, Cho and Song, 2000, Moon and Song, 2001, Lee and Song, 2002, Lee *et al.*, 2003, Lee *et al.*, 2004).

Davies and co-workers produced a series of papers on protein damage and degradation by oxygen radicals (Davies, 1987, Davies and Delsignore, 1987, Davies *et al.*, 1987ab) (Cho and Song, 2000). Hydroxyl radical and super-oxide anion radical generated by the radiation could modify the primary structure of proteins, which would result in distortions

of the secondary and tertiary structures (Cho and Song, 2000, Davies and Delsignore, 1987ab)

2.1.3.3 Causes of aggregation

The formation of protein aggregates during radiation exposure can be explained by the creation of protein radicals, which can cause cross-linking reactions to occur including the formation of disulphide bonds, and the stimulation of additional hydrophobic and electrostatic interactions e.g. by the exposure of new protein surfaces exposed by fragmentation or protein structure alteration (Lee *et al.*, 2004, Lee *et al.*, 2003, Lee and Song, 2002, Cho and Song, 2000, Cho *et al.*, 1999, Davies and Delsignore, 1987, Le Maire *et al.*, 1990, Garrison, 1987, Kato *et al.*, 1981). The exposure of new protein surfaces was shown in studies on myoglobin, in which UV spectra revealed that radiation disrupted the haem group and caused tryptophanyl residues usually present in a hydrophobic pocket of the haem group to be exposed to the protein surface (Lee and Song, 2002). In a previous study the hydrophobicity of ovalbumin (OVA) was found to increase rapidly with radiation dose, reaching a maximum after a dose of 800krad. This may contribute to protein aggregation at higher radiation doses (Kume and Matsuda, 1995). In contrast BSA, which is a hydrophobic protein, showed a significant decrease in hydrophobicity over the same range of radiation dose (Kume and Matsuda, 1995).

Kume and Matsuda (1995) found that protein radiation products, i.e. fragments and aggregates, retain a significant proportion of their antigenicity, although the reactivity is reduced. They concluded that this is because while radiation can alter the secondary structure of a protein and reduce the specificity of antibody binding, antigenicity relying primarily on the sequence of amino acids may remain even if the conformation is altered (Kume and Matsuda, 1995). This is in general agreement with the work of Yang *et al.* (1996), who found that irradiated enzymes (which also rely on a specific binding site in their structure to bind to their target molecule) retain a proportion of their activity.

Kume and Matsuda (1995) found that radiation dose required to reduce the antigenicity of 0.1% OVA in solution was 800kRad in a nitrogen atmosphere and 400kRad in oxygen. In contrast the radiation-induced reduction of antigenicity of BSA in solution was independent of the atmosphere. They also observed that aggregation of OVA and BSA was greater at high dose in a nitrogen atmosphere than in oxygen, indicating that

while oxygen appears to enhance fragmentation it also reduces aggregation effects. This effect was much greater on BSA than OVA, emphasising the effect of local protein structure on the effect of radiation. The effect of radiation on hydrophobicity was less pronounced in the presence of oxygen, possibly because fragmentation of proteins by oxygen radicals prevented the detection of changes in hydrophobicity. This shows that oxygen has a role in the damage of some proteins by radiation, and the atmosphere must therefore be considered when determining the effect of radiation on proteins.

These effects of oxygen are well known, and a number of studies have demonstrated that the fragmentation damage and aggregation caused by radiation can be significantly reduced by the addition of free radical scavengers such as ascorbic acid (Singh, A. *et al.*, 1990, Cho *et al.*, 1999, Moon and Song, 2001, Lee and Song, 2002).

2.1.3.4 Fragmentation mechanisms

The fragmentation of proteins has been found to produce both random and non-random products, depending on the experimental conditions (Lee *et al.*, 2003, Lee and Song, 2002, Cho and Song, 2000, Cho *et al.*, 1999, Kempler, 1993). Some specific mechanisms of radiation-induced protein fragmentation have been proposed. These include the formation of peroxy radicals at the α -carbon by the reaction of α -carbon radicals with oxygen, followed by decomposition of these radicals which causes fragmentation of the polypeptide chain at the α -carbon (Cho and Song, 2000). It has also been suggested that fragmentation occurs by the specific breakage of 'fragile bonds' within a polypeptide chain (possibly linked to transfer of radiation energy within a protein to these specific points (Cho and Song, 2000, Le Maire *et al.*, 1990), and by the oxidative destruction of proline residues (Lee *et al.*, 2003, Cho and Song, 2000, Wolff *et al.* 1986, Schuessler and Schilling, 1984).

2.1.3.5 Structural changes caused by radiation damage

Radiation-induced changes in structure have been shown by studies of the far-UV CD spectra of irradiated proteins in solution (Lee *et al.*, 2003, Lee and Song, 2002). This technique has revealed increasing changes in the proportion of α -helices, β -sheets and random structures at higher radiation dose, which indicates that radiation disrupts the

secondary structure of proteins (Lee *et al.*, 2003, Lee and Song, 2002). A study on myoglobin (an α -helical protein) in solution found that a 1000kRad gamma radiation exposure caused the α -helix content to be reduced from 67% to 12%, with a corresponding increase in random coil structure from 23% to 44% (Lee and Song, 2002). The same trend of secondary structure breakdown was also found in other studies on BSA, another α -helical protein, and β -lactoglobulin, a typical β -sheet structure protein (Cho and Song, 2000). In the case of β -lactoglobulin the absorption minimum was moved to a lower wavelength with increasing radiation dose (Cho & Song, 2000). In these studies the alteration in secondary structure was associated with damage by water radiolytic products (Davies and Delsingnore, 1987, Cho *et al.*, 1999, Cho and Song, 2000, Lee and Song, 2002, Lee *et al.*, 2003), but it is not clear if such changes would occur in the absence of water.

Changes in the tertiary structure of proteins can be studied by the measurement of fluorescence emission intensity (Lee and Song, 2002). Excitation at 280nm can reveal the tertiary structure through the excitation of tryptophan and tyrosine residues, for example changes in the emission intensity or peak wavelength can indicate a change in the local environment of these residues (Cho and Song, 2000, Lee and Song, 2002). This technique has been applied to the detection of tertiary structure changes in irradiation of myoglobin, BSA, and β -lactoglobulin in which different changes were observed. Irradiated myoglobin was found to have an increased emission intensity, whereas BSA and β -lactoglobulin had reduced emission intensities. The peak intensity of irradiated BSA was at a slightly higher wavelength (blue shift) than unirradiated BSA, whereas the peak intensity of irradiated β -lactoglobulin reduced (red shift) (Lee and Song, 2002, Cho and Song, 2000). These changes and difference in results with different proteins may reflect differences in the effect of radiation on proteins with different structures (Lee and Song, 2002, Cho and Song, 2000).

The changes in the secondary structure caused by radiation can be clearly seen by comparing ellipticity values (measured by circular dichroism) of irradiated and control proteins (Lee and Song, 2002). The spectrum of native myoglobin has a typical α -helical structure, which has a negative minimum ellipticity values at 207 and 221nm, and a positive maximum at 193 nm (Cho and Song, 2000, Lee and Song, 2002). Myoglobin consists of eight helices that surround the haem group (Lee and Song,

2002). However, gamma-irradiation clearly affected the CD-spectrum and disrupted the globin fold (Lee and Song, 2002). The ellipticity values at 207 and 221nm increased with increasing radiation dose (Cho and Song, 2000, Lee and Song, 2002). This indicates that gamma-irradiation at the level of 1000krad can alter the native function of a protein (Cho and Song, 2000, Lee and Song, 2002).

2.1.3.6 Effect of radiation on dried biological materials

There have been far fewer experiments carried out on dried biological materials than with materials in solution, and for this reason the effects are less well understood. In all of the studies found during the preparation of this review it has been found that dried materials are much more resistant to damage by radiation than material in solution. For example, studies on bovine and porcine powders, soy isolate and whey protein concentrate have found no significant change in the molecular weight profile or CD-spectra of these materials after they were irradiated at doses above 1000krad (Lee *et al.*, 2003, Cho and Song, 1999). This indicates that while water is present the generation of oxygen and peroxide radicals is responsible for almost all radiation damage to proteins, and that when water is removed there is no other mechanism which causes large amounts of damage (Lee *et al.*, 2003).

Two studies have been carried out on the effect of gamma radiation on freeze-dried antibodies. Caballero *et al.* (2004) and Grieb *et al.* (2002) both exposed freeze-dried antibodies to gamma radiation sources both alone and in the presence of a free radical scavenger. Caballero *et al.* (2004) found that while no changes in the antibody could be observed by chromatography or UV-Spectroscopy, only 5% fragmentation of antibodies could be detected by high performance liquid chromatography at a dose of 500kRad. In addition, free radicals could be detected in the antibody samples by electron paramagnetic resonance, and these were found to be stable for periods exceeding nine months. However they did not carry out standard biological techniques such as an immunoassay or gel electrophoresis on the samples.

Grieb *et al.* (2002) irradiated freeze-dried antibodies at 1.5Mrad and 4.5Mrad, and then carried out immunoassays on the samples. They found that without a free radical scavenger a 1.5Mrad dose reduced the binding affinity of the antibody by three orders

of magnitude, and no binding activity remained after a 4.5MRad exposure (Grieb *et al.* 2002). In contrast, when ascorbate was present at an initial concentration of 200mM, no significant difference in the binding affinity of the antibody could be detected at either 1.5Mrad or 4.5Mrad. Furthermore, a detailed analysis of the structure of the antibody before and after radiation indicated that there was no alteration in the proportion or structure of the heavy and light chains, and that no changes in secondary structure could be detected after irradiation (Grieb *et al.*, 2002). This is a key observation for the potential inclusion of an LMC on the ExoMars mission, since it demonstrated not only that the antibodies can survive the mission radiation environment, but also that Gamma radiation could be used to sterilise the antibodies to meet the planetary protection requirements provided an antioxidant e.g. ascorbate is present.

2.1.3.7 Tests involving biological materials in space environments

In addition to the testing of biological materials for sterilisation purposes, some experiments have been carried to determine whether active Life or bacterial spores can survive the radiation environment in space, to provide evidence for or against the possibility of lithopanspermia, see for example Horneck *et al.* (2001) and references within. This is because bacterial spores are one of the hardiest known forms of life, with samples of genus *Bacillus* spores having been shown to survive extreme desiccation, extremes of temperature and high vacuum environments including up to 6 years in space on the LDEF mission (Horneck *et al.* 2001). However, when bacterial spores are exposed to the full spectrum of solar UV radiation in the laboratory (>170nm) 99% of the spores are killed within seconds (Horneck *et al.*, 1984 as cited in Horneck *et al.*, 2001). This was confirmed in an experiment on one of the ESA BIOPAN missions (BIOPAN-5) by spore samples which were exposed to the space environment with no shielding; in samples which initially contained 7×10^7 viable spores, less than 120 spores remained viable after exposure to approximately 7500rad.

The lithopanspermia hypothesis is based on the transfer of meteorites between planetary surfaces. In order to determine whether the meteorite material could provide radiation shielding from the solar UV radiation and therefore enable the survival of bacterial spores in space, Horneck *et al.* (2001) exposed bacterial spores either

shielded by or mixed with Mars analogue soils, ground meteorites and ground terrestrial rocks. It was found that bacterial spores mixed with these materials had far greater survival rate than spores exposed directly to the solar UV flux, with up to 10^5 times more spores remaining viable after exposure (~80% of the original spore count). This was comparable with the results for ground control samples, and provides strong evidence that bacterial spores within meteorites could be sufficiently shielded from the solar UV flux to allow transfer of Life between Earth and Mars (or vice-versa) by lithopanspermia (Horneck *et al.*, 2001).

2.1.3.8 Results from tests on Life Marker Chip components

Testing of the basic components of a LMC assay was carried out during the work reported in this thesis. Fluorophores have been exposed to a proton beam (Thompson *et al.*, 2006) (see Chapter 3). These tests showed that these basic components (antibodies and fluorescent dyes) in freeze-dried form are capable of surviving radiation doses from protons in excess of those expected during a mission, verifying the design approach of using reagents in freeze dried form. Tests exposing antibodies and fluorophores to Gamma-rays exposure were carried out and are also reported in Chapter 3. Testing these components under neutron sources is planned for the near future but is not reported in this document.

2.1.3.9 Planetary protection and effects of sterilisation on Life Marker Chip instruments

As described in section 2.1.1.4, the Life Marker Chip must be sterilised to a level such that total spore count is $\leq 300 \text{ m}^{-2}$ and the total spore burden does not exceed 3.0×10^5 . Therefore any molecular or biological components of an instrument must therefore survive at least one of the approved procedures used to reach this level of sterilisation. The standard methods used to achieve this sterilisation (Mahaffy *et al.*, 2004, DeVincenzi *et al.*, 1996, DeVincenzi *et al.*, 1984) include:

- Dry Heat (125°C for 5 hours or 110°C for 50 hours)
- UV
- Gamma-ray
- Chemical cleaning with hydrogen peroxide plasma
- Precision cleaning with sterile wipes.

All the above methods are likely to be incompatible with the use of biologically based receptors as all techniques will damage or destroy biological material. It is not just the molecular receptors or fluorophores (if used) that may be affected but the bonding of any compounds to surfaces, or even the surfaces themselves where their surface properties may be changed (as described in section 2.1.1.6). The incompatibility of antibodies with dry heat sterilisation has been tested and verified within this thesis in the context of freeze dried reagents, as it was hoped that these may have proved more robust to heating than reagents in liquid form. These experiments are reported in section 3.1.

One is left with the problem of how such a device may be sterilised. The only viable route is sterilisation of optics, micro-fluidics, and LMC detectors by one of the above methods, with sterilisation of reagents and solvents via ultra-filtration (or possibly gamma irradiation), followed by assembly in an aseptic environment. These limitations and approach requires any such instrument being integrated into the spacecraft rover only after any spacecraft terminal sterilisation procedure such as dry heat. This approach has been taken as the baseline approach for the future LMC development programme.

2.1.3.10 The likely effects of temperature

Temperatures experienced during a mission fall into five areas:

- Temperatures during pre-launch integration into the ExoMars Rover and final testing and storage
- Temperatures during the time that the payload is under the rocket fairing immediately prior to and during launch
- Temperatures during cruise to the target
- Temperatures during entry, descent and landing
- Temperatures on the surface.

All the above temperature regions need to be taken into account.

Temperatures during pre-launch integration and testing are unlikely to exceed normal laboratory conditions except in the case of qualification tests, which will be dealt with under surface temperatures. Care must be taken to allow for temperatures under a

rocket fairing, as most launch sites are in regions of high ($\sim 40^{\circ}\text{C}$) or low temperature. The potentially high temperature must be considered in the LMC design unless the fairing temperature is controlled by air conditioning.

Temperatures during cruise are likely to be relatively benign depending on the thermal design of the spacecraft and may be slowly varying. It should however be noted that if an RTG/RPS is used that locally high temperatures may exist close to the unit unless care is taken with design of any cooling loops which are required to dissipate excess heat during the cruise. Typically temperature limits during cruise are not expected to exceed the surface constraints e.g. Mars Science Laboratory (MSL) (see MSL PIP 2004).

Any instrument designer and mission planner should allow for possible heat soak-back into a probe during its entry, descent and landing stage of the mission. High temperatures incompatible with the instrument could be generated for a limited time.

The largest temperature challenge to the instrument will be the temperature regime on the target planet / moon, so for example on Mars a large number of repeated freeze thaw cycles (perhaps hundreds in terms of a long lived (RPS powered) mission) will be encountered with temperatures cycling from sub-zero $\sim -40^{\circ}\text{C}$ to small or even large positive temperatures. MSL expects temperature cycling of between limits of -40°C to $+50^{\circ}\text{C}$ with a diurnal cycle of $\pm 20^{\circ}\text{C}$ at the payload interface over a Martian year (MSL PIP, 2004).

Allowance must be made for these cycles both in terms of design i.e. containers for reagents that have sufficient volume to allow for freezing of reagents including water to the effects on the biologically based components themselves. Tests of the effects of the freeze-thaw are currently planned in the near future, however given the positive effects of freeze drying highlighted in terms of radiation sensitivity it is expected and hoped that this will not be a problem where freeze-dried reagents are utilised.

Operation of any LMC instrument will require temperatures to be raised to such a level that liquid solvents can flow which requires careful thermal design of the instrument,

such temperatures will however be within typical laboratory levels and are not expected to be a design driver.

2.1.3.11 Other Effects

Any instrument will need to be delivered several months prior to launch and then must survive the cruise to the target which may be several years, even in the case of a Mars mission e.g. two years for ExoMars (Vago et al, 2003). The effects of long-term storage of reagents will also need to be addressed prior to flight of any instrument. On-going tests (Steele, 2005, private communication) indicate that long-term storage may not be an issue.

2.1.3.12 Conclusions and Implications

In this section the studies carried out on the potential to utilise biological materials for astrobiology missions involving extreme radiation environments has been reviewed. The radiation environment for a mission to Mars as proposed for the LMC instrument on board ExoMars has been characterised, both by *in-situ* measurements of the flight radiation dose by the NASA MARIE group, and by predictions using models as HZETRN and SPENVIS. Both ExoMars and Mars Science Laboratory indicated at the time of these experiments that the minimum requirement for instruments to survive was a total ionising radiation dose of approximately 3krad, and a non-ionizing energy loss of between 5×10^7 MeV/g and 3.2×10^{10} 1MeV neutrons (equivalent to between 0.80 to 512.6rad in air) (ESA, 2005, MSL PIP, 2004). For comparison, the typical gamma radiation dose to achieve sterilisation is 1.5 – 4.5MRad (Grieb *et al.*, 2002), illustrating that a gamma radiation sterilisation protocol would involve a significantly greater exposure to ionising radiation than the mission itself. Later figures indicate a slightly greater ionising and non-ionising radiation exposure during the mission (Alex Hands and David Rodgers, QinetiQ, Personal Communication), but this does not invalidate the experiments carried out in this document due to the large over-tests and sterilisation dose exposures.

The majority of studies on biological materials in radiation environments to date have been carried out on proteins in solution using gamma radiation; little research has been carried out using UV and particle radiation, extreme temperatures or freeze-dried

materials. It is found that proteins in solution are significantly affected by gamma radiation, depending on a number of factors: exposure can result in specific or non-specific fragmentation, aggregation and structural changes down to the secondary structure level. Even though these effects can be reduced by the presence of free radical scavengers, active material in a sample is still lost and antigenicity may not be retained, rendering the materials unsuitable for biological assays in conditions resembling those required for astrobiology applications.

The few studies that have been carried out on freeze-dried antibodies and proteins in the presence of free radical scavengers have shown that these effects are considerably reduced, an effect ascribed to the removal of damage caused by the ionisation products of water. The possibility that antibodies survive gamma radiation exposure is a strong indication that the use of biological materials in astrobiology missions such as ExoMars may be possible. Although some material may be rendered inactive and some radicals can remain stable under freeze-dried conditions for considerable periods of time, further investigation is required to determine more precisely the conditions they can be tolerated while maintaining a functional biological assay. Some of this work has been carried out in the work reported in this document, and is described in chapter 3.

2.1.4 Summary

This section has focussed on describing the radiation and sterilisation environments the reagents proposed for use in the SMILE Life Marker Chip must tolerate, and literature relating to the effects of these environments on proteins, antibodies and fluorescent dyes. Further research into previous work on the effect of these environments on other reagents such as any solvents or buffers that may be required or surface immobilisation chemistry has not been reviewed as yet, though there are expected to be few studies and few if any effects observed. The materials selected for the optical waveguide and supporting microfluidic structures must also be tolerant to these environments. In section 2.2 and 2.3 the requirements of the detection system and technologies capable of meeting those requirements will be reviewed.

2.2 The analytical problem and likely biomarker targets for the LMC

2.2.1 Introduction and background to this review

To outline the requirements of the detection system, this section is a brief discussion of the target molecules of interest to indicate the range and types of molecules that are relevant for detection by the LMC. The next key area for the LMC to discuss the potential target molecules that such an instrument could detect. Since the focus of the work reported in this document is the development of the instrumentation platform and not the individual assays for each target, the purpose of this section is to illustrate that there are a range of potential astrobiology targets relevant for detection by the LMC and describe the process by which the final range of targets will be selected, rather than to produce a final list of targets for the flight instrument and a detailed discussion of each target and its relevance to astrobiology.

Although many members of the astrobiology scientific community have published opinions on what type of Life may exist on Mars, and how one might go about detecting it, prior to the work of the SMILE LMC consortium there was no single reference source discussing all approaches to the detection of Life on Mars or listing suitable targets, especially for antibody-based assays (Parnell *et al.* 2006). Parnell *et al.* (2006) state that, "Numerous publications list, in general terms, the compound classes that should be sought. These place emphasis on amino acids, carboxylic acids, fatty acids, sugars, pigments, and cell membrane constituents/derivatives as a whole. However they do not conclude a list of specific molecules or prioritize them." Examples include publications by Mahaffey *et al.* (2004), Buch *et al.* (2003), Schweitzer *et al.* (2000), Westall *et al.* (2000), and Simoneit *et al.* (1998). This was the reason that the Biomarker Workshop (Leicester, May 24-26th, 2006) was held, i.e. to take these potential target molecules and classes and prioritise them in terms of relevance not only to the LMC but to other Life detection instrumentation on the Pasteur payload.

One of the core early objectives of the TRL Upgrade Study was to identify a range of astrobiology target molecules and class of molecules of scientific relevance and suitable for an instrument based on an antibody-based assay. This was achieved through the two-day Biomarker Workshop, during which leading members of the astrobiology

scientific community, representatives from the European Space Agency and members of the SMILE consortium (including the author of this thesis) discussed the range of organisms that could potentially exist or have existed on Mars, classes of molecular marker both ubiquitous to Life and representative of specific classes of organisms, the effect of the environment and oxidative / radiation environment on these targets and the likely classes of breakdown products, and availability or likelihood of being able to produce antibodies to detect these molecular markers. In addition, molecular markers suitable for control assays, molecular indicators of spacecraft contamination and meteoritic organic material were discussed, and linking some targets to those that could be detected by other instruments in the Pasteur Payload were also discussed. The principal aim of the workshop was to generate a priority list of potential targets for the Life Marker Chip based on scientific relevance and feasibility to include in the flight instrument.

The results of this Biomarker Workshop are pending publication (Parnell *et al.*, 2006). While the author of this thesis was present at the workshop, he is not named on this publication due to not achieving full academic status at the time of publication. Since this publication is by far the most useful and relevant reference source for this section of the literature review and this author was involved in the Biomarker Workshop on which it is based, the pending publication will be the main reference source in this section. Non-referenced statements not present in the draft publication are either the consensus of opinion of the astrobiology community or the authors own views.

2.2.2 Types of Life and Strategy for Life Detection

Although Life may potentially exist based on a wide range of different chemistries, the current strategy for Life detection is based primarily on water and carbon-based chemistry. This is appropriate particularly to the Life Marker Chip, since in order to raise antibodies against a specific target, the target must be of known structure, have suitable chemistry to bind to proteins and be soluble in aqueous solutions at suitable concentrations. In addition, recent evidence from the NASA Mars Exploration Rovers suggests that at one time in the history of Mars large areas of the surface were covered by liquid water, for a sufficient timescale that all rocks studied in areas where this

occurred have been altered by water in some way and that the depth of water-altered rocks extends for several tens of metres below the surface (Parnell *et al.*, 2006, Harland, 2005). Indeed, very recent observations indicate that there may be periodic flows of water in craters on the Martian surface even to the present day (Malin *et al.*, 2006).

There are four possible scenarios that can be considered in the search for Life on Mars (Parnell *et al.*, 2006):

- Life never evolved on Mars, so any organic molecules present are simply accumulated from meteoritic in-fall and altered by the radiation and geological environment on the surface.
- Life originated at a common point in the solar system, and was transferred between Earth and Mars by a meteoritic impact of sufficient magnitude that ejecta (containing early life forms) from one planetary surface was transported to the other planet – a process known as lithopanspermia (Mileikowsky *et al.* 2000). In this case the basic biochemistry of Martian and terrestrial life would be expected to be similar, since Life on both planets would have evolved from a common ancestor.
- Life evolved independently on Earth and Mars. In this case since it is known that the two planets had similar characteristics in their early history, organisms with similar biochemistry may have evolved independently – a theory known as convergionism (Parnell *et al.*, 2006, Malin & Edgett 2000, Westall *et al.*, 2002, Morris, 2003). Alternatively, Life on other planets including Mars could have evolved with a completely different biochemistry, perhaps not even carbon-based. This alternative theory is known as divergionism (Darling, 2002).
- Terrestrial contamination e.g. from spacecraft surfaces could prevent or cast doubt upon results indicating the detection of any Martian Life by providing false positive signals.

In all of these cases, particularly to test for contamination of the spacecraft and the possibility that lithopanspermia has occurred, it appears that the initial approach of Life detection with the LMC should be to attempt to detect molecular targets similar to those that would indicate the presence of Life on Earth (Parnell *et al.*, 2006, Schweitzer *et al.*,

2005). This is a key finding for this work, since it validates the approach of using antibodies to specific molecular targets based on terrestrial Life for the ExoMars LMC.

The range of environments in which terrestrial life is known to exist is continually expanding. Organisms have been found to survive and grow in high radiation environments, temperatures ranging from -7° to 115°C and at extremes of pH. The discovery of these 'extremophile' organisms raises the possibility that if Life did evolve on Mars, it could potentially survive to the present day by similar adaptations to those of existing organisms on Earth (Parnell *et al.*, 2006, Malin & Edgett 2000). This is also a key finding, since if this is the case there may be active Life on Mars today, and therefore indicators of extant Life are required for the LMC.

2.2.3 The advantages of antibody-based assay systems

Antibodies are capable of binding to a specific target, which may be either an entire molecule or a particular area of a molecule (epitope). This property of antibodies can be utilised in the selection of biomarker targets for the LMC, by in some cases selecting an antibody that only binds to a specific molecules within one class, and in other cases selecting the antibody to bind to an epitope common to an entire class of targets of interest (Schweitzer *et al.*, 2005). The Viking mission indicated that oxidation reactions take place in the Martian regolith. Such oxidation reactions may have degraded any molecular biomarkers, from past Life in particular. There are a number of features which are common degradation products of biomarkers of particular types, for example a single common end-product or a structure common to a class of biomarker that is preserved throughout the degradation reactions (Parnell *et al.*, 2006). The selection of appropriate antibody epitopes could enable such common structures to be used to identify classes of molecule present, or to identify a specific molecule within a class. The particular antibody epitopes chosen for certain biomarkers is therefore important for the LMC. Therefore, some of the targets selected in the pending publication by Parnell *et al.* (2006), are classes of molecular biomarker with similar or common elements in their structure, rather than individual specific molecules (Parnell *et al.*, 2006).

2.2.4 Effects of the Martian environment on Biomarker preservation and stability

The cold dry environment of present-day Mars is conducive to the preservation of molecular fossil remains of extinct Life, since degradation by oxidation reactions cannot

occur at a high rate. However, once the regolith sample is dissolved in an aqueous solution and raised to a higher temperature, oxidation may occur due to the presence of oxidising agents. This may be overcome by the addition of an antioxidant, e.g. ascorbate, to the buffer, which would prevent oxidation reactions and is compatible with antibody-based assays (Parnell *et al.*, 2006, Grieb *et al.*, 2002, Simoneit *et al.*, 1998).

Another major factor affecting the preservation and possible presence of Life on or near the Martian surface is the radiation environment. The radiation arises from a number of sources and has different penetration depths below the surface. UV radiation and Solar Energetic Particles (SEP) only penetrate to a depth of ~30cm. Galactic Cosmic Rays penetrate to a depth of approximately 300cm. There may also be radioactive minerals within the Martian regolith, which would create a background level of radiation. In terms of the effect of this radiation environment on the possibility of extant Life being present on Mars, the key conclusion drawn by Parnell *et al.* (2006) was that the UV radiation flux is the only environmental factor that would render active Life at the surface unviable. This UV flux and resulting damage to organic materials would also be expected to degrade many potential biomarkers within the uppermost 10cm of aeolian dust / regolith, although stable degradation products such as organic acids and salts may be present and large meteorites may provide sheltered sites at some locations (Parnell *et al.*, 2006).

2.2.5 Sample site selection and the advantages of sub-surface drilling

An important feature of the Mars surface environment is that at depths greater than 10cm UV radiation is no longer present. In addition, some localised sites may have surface coating of evaporite minerals that can absorb UV radiation, and would provide an environment with increased preservation of organic biomarkers and possibly supportive of extant life (Amaral, Martinez-Frias & Vázquez, 2005). Therefore, the radiation environment at depths greater than 10cm are more suitable than the surface environment for the preservation of some organic species of interest for the Life Marker Chip. Since the ExoMars rover is to be equipped with a drill capable of extracting samples at depths up to 200cm below the surface, by direct drilling and selection of samples sites in appropriate locations it appears possible to extract samples that have

not been damaged by UV radiation (Parnell *et al.*, 2006, Vago *et al.*, 2003). It is true that a 200cm drill would not reach material below the penetration depth of GCR unless an eroded area was discovered. The level of GCR radiation may be sufficient to have inactivated any micro-organisms at a depth of 200cm if they have been dormant and exposed to the GCR flux for over 450,000 years, although more recently exposed areas may allow viable organisms to be found (Dartnell *et al.*, 2007). Martian surface erosion rates are currently unknown but are estimated to be within the range 1 – 20nm.yr⁻¹ (Parnell *et al.*, 2006). Importantly, active cratering due to meteoritic impact has been observed on Mars in the present day (Malin *et al.*, 2006), exposing new surfaces and potentially allowing access to regolith material not exposed to GCR radiation for long periods of time (and therefore possibly containing viable organisms), should ExoMars be fortunate enough to land near enough to a location where this has occurred.

While there are a range of local environments that are believed to be of interest for life detection, the molecular targets for the Life Marker Chip remain very similar for all sample sites due to the degradation of molecular targets by the environment particularly the radiation environment at the surface of Mars (Parnell *et al.*, 2006, Simoneit *et al.*, 1998).

2.2.6 Potential Biomarker targets

The complete list of Biomarker Targets produced by the Biomarker Workshop is included in section 2.2.7. The principles behind the selection of these targets and typical examples will be given below.

2.2.6.1 Indicators of extant Life

Since there are environmental factors that would contribute to the rapid breakdown of amino acids, proteins and many other cellular components, if any of these were detected particularly in the upper layers of the surface this would indicate the presence of extant Life as they would have to be replaced by active Life. To maximise the range of organisms that could be detected very general targets have been identified, such as adenosine tri-phosphate (ATP) and the molecular chaperone protein GroEL (chaperonin-60) (Parnell *et al.*, 2006).

2.2.6.2 Indicators of extinct Life

Indicators of extinct Life will only be found in the subsurface, where they may have been present for more than 3 billion years. Over this length of time, the GCR radiation may have degraded the organic materials through the formation of free radicals and contributing to oxidation reactions. The detection of extinct Life would therefore be indicated by the detection of radiolytic / oxidation degradation products of proteins, fatty acids or other cellular components. If these were detected in the absence of any indications of current Life, that would suggest that Life had once evolved on Mars but was no longer active. As for indicators of extant Life, indicators of extinct Life have been selected for biological ubiquity but additionally with stable degradation products that are common to the degradation products of many biomarkers. Typical molecules in this class of targets include hopanes and isoprenoids (Parnell *et al.*, 2006),

2.2.6.3 Indicators of the presence of organic material of meteoritic origin

Since meteoritic in-fall is the original source of most organics unaltered by the Martian environment, it would be prudent to include some target molecules specific to unaltered meteorites to verify the detection of material from this source. Since organics present of meteorites are not of biological origin, many more structural variations have been detected – for example on the Murchison meteorite over seventy-five types of amino acids have been detected of which only eight are used by Life on Earth. This range of structural variation occurs because where Life is present the synthesis of specific amino acids is catalysed by the biochemistry of the organism(s), whereas in meteoritic organic chemistry no biological catalysis has taken place so all possible structural variations of amino acids are produced according to their energy requirements alone. Typical examples in the biomarker list include isovaline and aminoisobutyric acid. There are also variations of polyaromatic hydrocarbons (PAHs) that are specific to meteorites and could be used by the Life Marker Chip for the purpose of confirming the presence of meteoritic organic material (Parnell *et al.*, 2006).

2.2.6.4 Indicators of spacecraft contamination

Spacecraft contamination has to be considered for planetary protection as described in section 2.1.1.4, but also for the LMC some of the target biomarkers, particularly for current Life, may originate from contamination and cast doubt upon other results. A key implication of this is that it would be difficult to differentiate between the detection of spacecraft contamination and Life with a common ancestor i.e. originating from lithopanspermia, because the basic biochemistry of these organisms would be expected to be similar. To ensure that false positives can be identified, it is proposed to include antibodies corresponding to the most common species of bacteria in terrestrial environments, and those specifically associated with spacecraft / clean room. This will be achieved using either antibodies against specific species or some highly specific targets indicative of these species. The specific example species cited by Parnell *et al.* (2006) are *Staphylococcus* (57, A), *Streptococcus* (58, A), *Bacillus* (59, A), *Micrococcus* (60, A) and *Pseudomonas* (61, A). In addition a fuel marker such as hydrazine will be included, dependent on the type of fuel used by the spacecraft (Parnell *et al.*, 2006).

2.2.7 Biomarker Workshop target list

The biomarker target list (Table 2.2) produced by the Biomarker Workshop is included below in a tabular form (Parnell *et al.*, 2006). The table includes data on the name, type and biological significance of the target molecule, whether it is polar or a-polar (i.e. which mode of extraction is appropriate for this target – see section 2.2.7 for a description of the possible sample extraction methods), molecular mass, oldest occurrence on Earth (to give an indication of whether this target indicates past or present Life, or both), whether this molecule is known to form abiotically i.e. in the absence of Life, and the radiation sensitivity of the target where known, to indicate whether breakdown products may be found and the lifetime of the molecule in the Martian environment.

Table 2.2.2: List of Biomarkers (and their properties) Identified during the Biomarker Workshop, grouped into categories of indicators of Extant Life, Extinct Life, Spacecraft Contamination and Meteoritic organics.

Target Category	No.	Priority	Biomarker	Molecular type	Polar Molecule	Molecular Mass No. of daltons	Biological Significance	Oldest Occurrence (where known)	Abiotic Origin Known?	Radiation Sensitivity
Extant	1	A	ATP	Phosphate	Yes	505	energy	extant only		moderate
	2	A	Phosphoenolpyruvate	Phosphate	Yes	185	energy	extant only		moderate
	3	B	Acetyl phosphate	Phosphate	Yes	162	energy	extant only		moderate
	4	C	cyclic AMP	Phosphate	Yes	323	signalling	extant only		moderate
	5	A	Generic pyrimidine base	Nucleobase	Yes	thy 124	Information		yes?	moderate
	6	A	Generic purine base	Nucleobase	Yes	ad 135	Information		yes?	moderate
	7	A	DNA	Nucleobase	Yes	macromolecule	Information	>100000 years		moderate
	8	A	Nicotinamide (generic NAD, NADP)	Vitamin	Yes	122 NAD 685	electron transfer electron transfer		Yes	moderate
	9	C	Flavin (isoalloxazine ring)	Vitamin	Yes	239	electron transfer			moderate

10	C	Fe-S centres	redox centre	Yes	176-352	electron transfer		Yes	moderate
11	C	Quinones	electron transport	No	generic ~200	electron transfer		Yes	lower
12	B	Generic carotenoid	Pigment	No	~ 150(chain), 200 (chain plus cyclic), B carotene 536	light harvest	>million years		higher
13	C	Phycocyanin	Pigment	No	~150 (ring), whole 525	light harvest	million years?		moderate
14	C	Thiol Esters	Ester	Yes	CoA 786	energy			moderate
15	A	Generic porphyrin	Porphyrin	No	310	electron transfer			lower
16	B	Chaperons	Protein	Yes	E.coli GroEL 65000	stress protein	extant only?		moderate
17	A	ATP Synthase	Protein	Yes	52000	Enzyme	extant only?		moderate
18	B	Phytane	lhydrocarbon	No	282	archaeal lipid	2.7Ga		higher
19	A	Fatty acids (1 or 2)	Carboxylic acid	Weakly	stearic 284	bacterial lipid (18 bio, 19 not)	>million years	Yes	higher
20	A	Teichoic Acid	Amino acid + phosphate polymer	Yes	ribitol P ~ 612	Gram +ve wall			lower
21	A	LPS	Macromolecule	Yes	macromolecule	Gram -ve wall			lower

22	B	Ectoine	Compatible solute	Yes	142	osmotic protectant			moderate
23	C	Trehalose	Compatible solute	Yes	342	osmotic protectant			moderate
24	B	Squalene	Hydrocarbon	No	410	lipid biosynthesis (isoprenoid precursor)			higher
25	C	Diploptene	Hopanoid	No	~ 370?	bacterial membrane			moderate
26	B	Melanoidins	Macromolecule	No	macromolecule				moderate
		Sediment/cell extracts:							
27	C	1. Acid mine drainage	Multiple	Some	N/A	whole cells			lower
28	C	2. Methanogens	Multiple	Some	N/A	whole cells			lower
29	C	3. Cyanobacteria	Multiple	Some	N/A	whole cells			lower
30	C	4. Mars Energy Users	Multiple	Some	N/A	whole cells			lower
31	C	5. Extract/abiotic mix	Multiple	Some	N/A	whole cells			lower
Extinct									
32	A	Generic isoprenoid	Hydrocarbon	No	142-563	Chlorophyll,	2.7Ga		moderate

33	A	Pristane	Hydrocarbon	No	270	quinones, archeal membranes	2.7Ga		higher
18	B	Phytane	Hydrocarbon	No	284		2.7Ga		higher
34	A	B-carotane	Hydrocarbon	No	559	Fossil carotenoids	1.7Ga		higher
35	C	Tetramethyl benzenes	Hydrocarbon	No	>204	Fossil carotenoids	1.7Ga	If <C15	lower
36	C	Tetramethyl cyclohexanes	Hydrocarbon	No	>210	Fossil carotenoids	1.7Ga	If <C15	moderate
37	C	Squalane	Hydrocarbon	No	422	Membranes (prokaryotes)	1.7Ga		higher
38	A	Generic ABC terpane	Hydrocarbon	No			2.7Ga		lower
39	A	Generic hopane	Hydrocarbon	No	>370		2.7Ga		lower
40	C	Gammacerane	Hydrocarbon	No	412		1.7Ga		moderate
41	B	Generic diasterane	Hydrocarbon	No	>372	Membranes (euks & prokaryotes)	2.7, not 1.7Ga		lower
42	C	Generic sterane	Hydrocarbon	No	>372		2.7, not 1.7Ga		lower
43	A	Generic porphyrin (ancient)	Porphyrin	No	460-500+		?		lower
44	A	Generic Straight-chain Fatty Acid	Carboxylic acid	Weakly	256-300+	Membrane	100s Ma	Yes	higher
19a,b	A	2 individual Fatty Acids	Carboxylic acid	Weakly	256-300+	18 bio, 19 not	100s Ma	Yes	higher
45	A	Generic amino acid	Amino acid	Yes				Yes	higher

Meteoritic	46	B	Quaternary carbon alkane	Hydrocarbon	No		Origin unclear	2.2Ga		higher
	47	A	Napthalene	Hydrocarbon	No	128	N/A		Yes	higher
	48	A	Coronene	Hydrocarbon	No	300	N/A		Yes	lower
	49	B	Pyrene	Hydrocarbon	No	202	N/A		Yes	moderate
	50	A	1,3 Dimethylbenzene	Hydrocarbon	No	106	N/A		Yes	higher
	51	A	1,4 Dimethylbenzene	Hydrocarbon	No	106	N/A		Yes	higher
	45	A	Generic amino acid	Amino acid	Yes		N/A		Yes	higher
	52	A	OR isovaline AND	Amino acid	Yes	117	N/A		Yes	higher
	53	A	a-aminoisobutyric acid	Amino acid	Yes	103	N/A		Yes	higher
	54	B	Generic aromatic carboxylic acid	Carboxylic acid	Yes		N/A		Yes	lower
Contaminants	55	A	Experimental abiotic	Complex			N/A		Yes	lower
	56	A	Generic fungal			N/A	Fungal			higher
	20	A	Teichoic Acid	Amino acid + phosphate polymer	Yes	ribitol P ~612-	Cell wall Gram +ve			higher

21	A	LPS	Macromolecule	Yes	macromolecule	Cell wall Gram - ve			higher
57	A	Staphylococcus	Bacterium genus		N/A	whole bacterium			higher
58	A	Streptococcus	Bacterium genus		N/A	whole bacterium			higher
59	A	Bacillus	Bacterium genus		N/A	whole bacterium			higher
60	A	Micrococcus	Bacterium genus		N/A	whole bacterium			higher
61	A	Pseudomonas	Bacterium genus		N/A	whole bacterium			higher
62	A	Dipicolinic acid	Carboxylic acid	Weakly	168	spores			lower
63	A	Hydrazine (or equivalent)	Base	Yes	<110	(Fuel)			moderate

2.2.8 Implications of the biomarkers target list for the LMC sample processing system

Since the range of target molecules of interest extends from the very polar to to very a-polar, including hydrocarbons with extremely low solubilities in water e.g. PAHs, hopanes, the optimum sample processing and extraction system could be to split the sample in two and perform both aqueous and a-polar extractions. In this case the sample processing system may become very complex, and considerations of the effects of solvents from the sample processing system being carried through into the biological assay chamber would need to be considered (Parnell *et al.*, 2006).

2.2.9 Summary of the analytical problem

All of the evidence suggests that large areas of the Martian surface were once covered by liquid water. The similarities in environment of the early Earth and early Mars, coupled with the possibility that Life could have been transported to or from Mars via panspermia indicate that aqueous based organic biomarker targets are the most appropriate molecular indicators for the Life Marker Chip to target as the initial approach to Life detection. It has been established that the Life Marker Chip would be an appropriate instrument to detect a range of targets in many sampling environments, and a priority list of which target classes could be included in the flight instrument has been generated. The important points arising from this is that due to differences in the chemical properties of the classes of target molecules, it is apparent that each Martian sample will require two assay channels; one dedicated to the detection of water-soluble targets (largely indicators of extant life) and one for a-polar molecules (largely indicative of past life or meteoritic organic material). There are a number of target molecules of very high priority interest in each class, and the final sample volume will be low, so the proposed micro-array assay format in a microfluidic channel appears to be the most efficient way to detect all the targets of interest simultaneously. In the following section, the current state of instrumentation technology on which the Life Marker Chip design is based will be reviewed.

2.3 Multianalyte sensor technologies for microlitre-scale sample volumes

2.3.1 The SMILE solution and evolution of the instrument design concept

In order to meet the requirements for detecting at least some of the wide range of molecular indicators of Life described in sections 2.2.6 and listed in Table 2.2.2, the proposed SMILE detection system will be capable of simultaneous detection of approximately 25 specific target biomarker molecules that could indicate the presence of extinct or extant life on planetary surfaces. This will be carried out by the extraction and subsequent analysis of any organics within rocks on the Martian surface and at varying depths down to 2m below the surface. At the current time, the Life Marker Chip Sample Processing System design is based on receiving ~1g of material the form of a dried powder with a maximum particle size of 40µm. This sample will be split equally into two sample processing chambers, one for water-soluble biomarker targets and one for a-polar targets. Each of these processing lines will incorporate a concentration step such that all of the target molecules available for extraction from the 0.5g of material will be concentrated into a volume of a few microlitres. The two sample types will then pass into single use assay channels dedicated to the targets relevant to the extraction method, and the protein microarray assay format used to detect a number of relevant targets in each sample simultaneously.

During the course of the work reported in this document the proposed design for the LMC instrument has been continuously evolving. The initial concept proposed for the Pasteur Payload was outlined in a publication by Sims *et al.* (2005), but the design has subsequently become more refined. The initial broad concept was a fluorescence / surface plasmon resonance dual readout system that utilised the specific molecular recognition properties of both antibodies and molecular imprinted polymers. This was to be achieved by creating a microarray of approximately 100 spots of molecular receptors, each approximately 100µm in diameter, within a microfluidic channel system on a gold-coated optical waveguide (Sims *et al.*, 2005). Later developments have included removing molecular imprinted polymers from the design concept for two reasons, namely their relatively poor lower limits of detection compared to antibodies, and the wider range of well established immunoassay formats and labelling techniques available for antibody assays. In addition, later work has focussed primarily on fluorescent readout alone rather than a dual readout system, due to the increased complexity and mass requirements of the dual readout design. The current design is

therefore an antibody microarray within a microfluidic channel system mounted onto an optical waveguide with a fluorescent readout. The readout is proposed to be based on a low light level CCD chip due to the potentially low levels of fluorescence and high signal/noise ratio of these devices. In the final device it is proposed to use thin film optical waveguides rather than bulk waveguides since thin film waveguides have a more intense evanescent field than a bulk waveguide if the same amount of light passes through them, and therefore they would yield a higher signal.

This section is a review of the different technologies used in multi-analyte detection systems that demonstrate the current state of technology in carrying out antibody or protein binding assays within microfluidic channels, in order to highlight the areas of established technology and those which required further development during the ongoing SMILE Technology Readiness Level Upgrade study, and the preceding and overlapping PhD study.

2.3.2 Introduction to relevant analytical methods and technologies

The growing pressure to increase throughput, reduce sample volumes and lower the price per test while maintaining high sensitivity and throughput has led to considerable effort towards, and some success in, the miniaturisation of classical immunological binding assays and chromatographic and electrophoretic separation methods (Weinberger *et al.*, 2000, Duveneck *et al.*, 1997). However, these methods are limited in flexibility by their analytical speed, the requirement for serial throughput, moderate sensitivity and difficulties in coupling the separation methods with the detection systems. These newer methods which enable multiple analytes to be tested simultaneously are becoming increasingly more important (Weinberger *et al.*, 2000).

While a number of targets have been detected simultaneously in ELISA format, the principal technologies being developed in multianalyte sensing are solid-phase based, fabricated by the immobilisation of a range of capture molecules at a distinct location on the sensing surface, and simultaneous analysis of all of these regions (Joos *et al.*, 2001, Weinberger *et al.*, 2000). Highly sensitive multispot and multianalyte immunoassays were demonstrated over ten years ago, and the huge potential to address these needs

in diagnostic applications was recognised (Joos *et al.*, 2001, Etkins *et al.*, 1990, Etkins, 1989).

One of the most promising developments in multianalyte sensing is microarray technology, which has been applied mainly in DNA chips, and more recently protein chips (Song *et al.*, 2004, Joos *et al.*, 2001, Weinberger *et al.*, 2000, Duveneck *et al.*, 1997). The equipment use for both the preparation and reading of microarrays is now commonplace, with products available from over 100 companies, and can be used to fabricate both DNA and protein microarrays (Joos *et al.*, 2001).

Multianalyte sensing is the simultaneous detection of a number of different target molecules from the same sample and thus inherently involves the analysis of complex sample media. This in turn requires both recognition elements with very high specificity and binding affinity for their targets and a detection system with a very high signal to noise ratio (Duveneck *et al.*, 1997). The most commonly used recognition elements used in ligand binding assays are monoclonal antibodies immobilised on the sensor surface. Monoclonal antibodies are preferred over polyclonal antibodies in these applications due to their higher specificity. This is true for a number of different types of analytes including proteins, peptides and low-molecular weight molecules. Alternative methods such as phage-display techniques are being developed to rapidly produce synthetic binder molecules with high affinities for their targets, but these have not yet reached the stage of replacing antibodies in most applications (Joos *et al.*, 2001, Lecerf *et al.*, 2001, Ryu & Nam, 2000). This is principally because while a number of readout techniques such as fluorophores, radioisotope and enzyme labelling are well established with antibodies, this is not the case with other binding molecules (Joos *et al.*, 2001).

Since there is a wide range of potential target molecules for the LMC (see section 2.2.7), different assay methods may be more effective for certain targets. In addition to the advantage that more advanced labelling methods available with antibody assays, the range of assay formats that can be used is more advanced. A number of competitive and non-competitive immunoassay methods have been developed and are commonly used to increase the specificity and sensitivity of immunoassays for specific

applications (Joos *et al.*, 2001). Therefore, in order to have greater flexibility in the assay system to optimise the assay for all targets, antibodies are currently preferred to molecular imprinted polymers for the SMILE LMC.

The readout systems of choice for multianalyte sensing are optical sensors of various types, because these have the potential for easier fabrication, higher chemical stability and lower risk of exterior interferences than sensors based on electrical or piezoelectric transducers (Benini *et al.*, 2006, Duveneck *et al.*, 1997). Techniques based on evanescent field analysis are highly suited to microarray spot analysis because they inherently analyse only processes occurring at the sensor surface. This is because the strength of the evanescent field exponentially decreases with distance from the surface, limiting the penetration depth into the target solution to 100-150nm (Joos *et al.*, 2001, Weinberger *et al.*, 2000, Duveneck *et al.*, 1997). This surface-specific analysis is a major advantage of evanescent field sensing, as it means that species interaction in the bulk solution is not included in the analysis (Benini *et al.*, 2006, Joos *et al.*, 2001). Once again, the advantages of evanescent field sensing over other transducer systems were considered in incorporating this method into the proposed LMC design.

There are many optical readout systems that have been applied to waveguide or near-field sensing, and therefore could be applied to the analysis of fluorescent microarray spots on a waveguide (Duveneck *et al.*, 1997). The most successful methods thus far are surface plasmon resonance (SPR), direct measurement of fluorescence by CCD imaging, fibre-optic evanescent field sensors, and optical waveguides utilising evanescent field excitation of fluorophores coupled to a CCD imaging system (Joos *et al.*, 2001, Weinberger *et al.*, 2000). The final method is said to have greater sensitivity than other evanescent field sensing systems (Joos *et al.*, 2001, Rowe *et al.*, 2000, Rowe *et al.*, 1999), consequently the most recent work on the SMILE LMC has focussed on evanescent field sensing of fluorescently labelled targets bound to the surface by antibody-antigen interaction.

While the selection of methodology was made in the proposed LMC design before the work in this thesis began, it is of interest to discuss the reasons behind this selection. The evanescent field sensing methods can be divided broadly into two groups, those

based on fluorescence (using labels) and those which do not use fluorescence (label-free) (Duveneck *et al.*, 1997). The principals and advantages of each of these approaches will be discussed below.

2.3.3 Surface refractive index based sensors

The principal advantage of using surface bulk property detectors such as surface plasmon resonance or grating couplers over fluorescence-based sensors is that they detect the target molecule directly, and do not require labels. The signal obtained is related to the mass of material adsorbed to the sensor surface, and therefore can be affected by non-specific binding. This can be a significant problem in multi-analyte sensors, as some biomolecules have multivalent binding characteristics i.e. they can bind non-specifically to unrelated array positions, and in doing so reduce the sensitivity of the device below the desired operating concentration level. Consequently the development of array sensors based on label-free surface affinity methods has proved to be problematic (Weinberger *et al.*, 2000, Duveneck *et al.*, 1997).

2.3.4 Detection systems utilising fluorescently labelled components

The driving force behind the development of miniaturised fluorescence-based sensors had been the increasing demand for multiplexed bioanalytical technologies, including but not limited to genomic and proteomic microarrays. The principle advantage of fluorescence-based detection schemes over refractive index based sensors is specific analysis of any given target and extremely high sensitivity, regardless of the size of the target molecule (since the readout is based on detection of a fluorescent label) (Weinberger *et al.*, 2000, Rowe-Taitt *et al.*, 2000, Duveneck *et al.*, 1997). The principle disadvantage of an immunoassay with a label-based readout is that only target molecules which can bind to the specific antibodies used, i.e. only known target molecules, can be detected, whereas other methods can identify organic species that would not be expected to be present in a given sample (Weinberger *et al.*, 2000). The high specificity and sensitivity still make fluorescence-based detection systems the method of choice for the Life Marker Chip, due to the likelihood of any target molecules present to be at very low concentrations, in the parts per billion range (Vago *et al.*, 2003).

As fluorescent-based detection based on optical evanescent field sensing has been selected for the design of the proposed SMILE Life Marker Chip, the development and principles of the different methods and applications will be described below. The most fundamental component is an optical waveguide, so the discussion will be split into two sections according to the two basic waveguide types.

2.3.5 Multi-mode (bulk) Waveguides

The term 'waveguide' encompasses a number of types of waveguide, but in this review it will be used in reference to either multi-mode (bulk) waveguides, a typical example of which is a commercial quality microscope slide, or mono-mode (thin film) waveguides. Both of these types of waveguide are described in this section. Optical waveguides allow light to travel along them provided that the light is contained within the waveguide by total internal reflection (TIR) at the surface of the waveguide. TIR occurring at the waveguide surface generates an evanescent field, which can be utilised to excite fluorophores bound to the sensor surface by specific receptors, and the light emitted can be recorded by a detection system in order to analyse binding events at the surface (Weinberger *et al.*, 2000, Feldstein *et al.*, 1999). Use of the evanescent field method ensures that the signal obtained is specific to the surface of the sensor and not the bulk properties of the sample, and when optimised can give excitation intensities up to a hundred times greater than that of other techniques such as confocal excitation (Joos *et al.*, 2001, Weinberger *et al.*, 2000). However, with a bulk waveguide this high excitation intensity is difficult to achieve since most of the light is contained within the waveguide and only a small proportion of light is present in the evanescent field (Feldstein *et al.*, 1999).

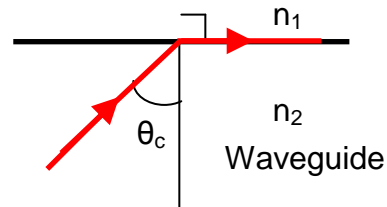
Creating a set of conditions which enable a high evanescent field strength (and therefore high sensitivity) to be produced while keeping the optical parameters within the range required for total internal reflection is not straightforward (Feldstein *et al.*, 1999, Benini *et al.*, 2006). The difficulty is created because the conditions required for TIR are limited and dependent on many parameters, including the wavelength and incidence angle of the excitation light and the refractive index of both the waveguide material and the surrounding medium. In addition, the refractive index of the waveguide must be higher than that of the surrounding media (Feldstein *et al.*, 1999, Benini *et al.*,

2006). For a given waveguide and medium, the critical angle below which TIR will not occur is given by a special case of Snell's Law, which states that $\sin\theta_1 n_1 = \sin\theta_2 n_2$ where θ is the angle measured from the surface normal and n_1 and n_2 are the refractive indices of the surrounding medium (low refractive index) and the waveguide material (high refractive index) respectively (i.e. $n_1 < n_2$) (Feldstein *et al.*, 1999).

For the case shown on the right, $\sin\theta_c n_1 = \sin 90 n_2$

Therefore $\sin\theta_c n_1 = n_2$

and $\sin\theta_{\text{critical}} = n_1/n_2$



However there is also an inverse relationship between evanescent field penetration depth (d_p) and the optical incidence angle (θ):

$$d_p = 1 / ((n_2/n_1)^2 \sin^2\theta - 1)^2$$

This means that while the evanescent field penetration depth increases with reducing angle of incident light the angle cannot be reduced below a critical value otherwise TIR will no longer occur. For an air-glass interface this angle is $\sim 40^\circ$ and for a water-glass interface it is $\sim 67^\circ$. Both the penetration depth and the critical angle are dependent on the refractive indices of both the waveguide and the surrounding medium (Feldstein *et al.*, 1999, Benini *et al.*, 2006).

There are a number of possible solutions to this. One is to optimise sensitivity with a bulk waveguide and suitable detection system, as while this is not ideal it still has advantages over other methods. Rowe *et al.* have demonstrated this in the form of an array immunosensor for both clinical analytes and biohazardous reagents in a sandwich immunoassay format. In this case discrete regions of biotinylated antibodies were deposited onto avidin-coated waveguides to form specifically orientated immobilised capture molecules, which were then exposed to fluorescent-labelled targets and visualised using a 635nm diode laser with a CCD based imaging system (Joos *et al.*, 2001, Rowe *et al.*, 2000, Rowe *et al.*, 1999).

Methods used to further enhance the sensitivity of waveguide based optical readout methods, and overcome the difficulties described above, include the application of

tapered waveguides and mono-mode waveguides (which are described in the next section), both of which are designed to increase the penetration depth of the evanescent field while maintaining the incident light within the waveguide (Feldstein *et al.*, 1999).

2.3.6 Mono-Mode (thin film) Waveguides

The development of mono-mode waveguide technology enabled a further increase in the sensitivity and lower limits of detection of this method (Duveneck *et al.*, 1997). This is because for the same amount of light transmitted, a mono-mode waveguide has a greater amount of light in the evanescent field, and therefore a greater amount of fluorescence is generated from fluorescent labels at the surface. The disadvantage of mono-mode waveguides is that they are very thin and it is more difficult to achieve efficient coupling of light in to the waveguide (Duveneck *et al.*, 1997). Additionally, in a multi-mode waveguide the distribution of optical power between optical modes, and therefore amount of fluorescence at the surface, can vary. This cannot happen in a mono-mode waveguide, so fluorescence intensity is more reproducible (Benini *et al.*, 2006)

A mono-mode waveguide is fabricated by the deposition of a thin film (typically 150-300nm) of high-refractive index material such as Ta₂O or TiO₂ onto a transparent base material with a lower refractive index, typically glass or plastic. The precision required for this deposition process makes mono-mode waveguides relatively expensive. In addition optical coupling of the light from the surface into the waveguide is more difficult in a thin-film waveguide than a conventional (multi-mode) waveguide. Light will enter a multi-mode (bulk) waveguide if it is directed towards the edge face of the waveguide at an angle within the waveguides numerical aperture, making bulk waveguides fairly tolerant to slight misalignment. However a thin film waveguide normally requires a diffraction grating or prism to efficiently couple light into the waveguide, necessitating much more precise construction (since the light source must be accurately aligned with the diffraction grating). A diffraction grating allows areas of over a square centimetre to be homogeneously illuminated. This area is ideally suited to analysis by imaging, which is typically achieved by the use of CCD camera arrays which provide high sensitivity and readout times of less than a second (Joos *et al.*, 2001, Weinberger *et al.*, 2000, Feldstein *et al.*, 1999). In this way, highly sensitive miniaturised immunoassays can be

performed on a large number of analytes simultaneously using a very small sample volume, which is precisely the type of assay that is required and proposed for the SMILE Life Marker Chip.

However, in order to make the best use of space for the LMC, it will be necessary to perform several assays on each waveguide, which will involve the attachment of a microfluidic system to the waveguide surface. The addition of separate flow cells to waveguide surfaces complicates the development of these sensors, as any object in contact with the waveguide surface reduces the magnitude of the signals and therefore reduces the sensitivity. There are two main causes of this reduction in performance, firstly the flow cell would be in optical contact with the waveguide so light would be coupled out of the waveguide and into the flow cell material, so the intensity of incident light is reduced. Secondly light that entered the flow cell would be scattered in all directions including towards the detector array, so the level of system noise would be greater (Feldstein *et al.*, 1999). There are two possible solutions to such a problem. The most common is to use the low refractive index material covering as one surface of the microfluidic system. An alternative is to use a reflective cladding layer to contain light within the waveguide until it reaches the area with the immobilised reagents (as described by Feldstein *et al.*, 1999). The former is the approach adopted in the design of the Life Marker Chip; specifically the waveguide is to be fabricated into a silicon chip, and a protective silicon layer covers the waveguide and forms the surface of the microfluidic channel until the area that will contain the microarray of immobilised assay reagents. A window will be cut into the protective layer over this assay area, allowing the evanescent field to excite any labelled assay reagents that bind to the microarray spots.

Normally microfluidic channel structures for use with optical waveguides are fabricated using polymer structures, as shown by Rowe *et al.* (1999, 2000). However, for biological applications there are many advantages to the use of silicon microfluidics based on photolithography fabrication methods (Whitesides, 2006, Mitchell *et al.*, 2004), including ease of attachment of the microfluidic structure to the waveguide and more reliable adhesion in aqueous environments within the temperature range compatible with surfaces coated with a functional protein (Rowe-Taitt *et al.*, 2000). Such microfluidic devices in silicon can be fabricated such that the microfluidic structure and

optical waveguide are a single unit in direct contact with one another, so have very similar refractive indices (Mitchell, 2004). The Life Marker Chip design is based on mono-mode waveguides with integrated microfluidics in order to utilise all of these advantages over polymer based systems, namely increased compatibility with biological assays, improved adhesion and better optical properties due to the similar refractive indices of the materials. In addition, very few polymeric materials are acceptable for space flight missions due to the potential for out-gassing of trapped gaseous polymerisation products.

With the SMILE Life Marker Chip design therefore being primarily based on silicon mono-mode waveguide microfluidic devices, the next consideration is methods of producing the multianalyte sensing region and reviewing the current state of development of multianalyte sensors in microfluidic channels.

2.3.7 Methods of Creating Multi-Analyte Sensors

In addition to the well-established and accepted method of photolithography, there are two methods used to create multi-analyte sensors; physically isolated patterning (PIP) and the use of microarray spotting robots (Feldstein *et al.*, 1999).

PIP is based on the deposition of antibodies or antigens onto the waveguide surface using a poly(dimethylsiloxane) (PDMS) multiple flow cell template, which contains channels of 0.75-1.5mm width. This template can be used to immobilise lines of substrate across the waveguide, and as PDMS forms a watertight seal with the waveguide surface the lines can be clearly separated without applying large pressure to the template or the waveguide. However the pressure applied must be tightly controlled as PDMS deforms under pressure, and this must be a uniform deformation if a uniform batch of sensors is to be produced (Feldstein *et al.*, 1999). This method is not applicable to the production of high density arrays, since it requires a mask that physically separates the reagents for each spot and this is not established technology for spot sizes of the order of 100µm, as proposed for the LMC (see section 2.3.1). The method will therefore not be expanded upon in this document.

2.3.8 Surface functionalisation

In order to take full advantage of a highly sensitive detection system, the target analyte must be stably immobilised to the sensor surface in a functional state and accessible to the binding molecule. There are a number of methods that have been used to achieve this, including surface modification with silanes, photo-immobilised polymers and self-assembled monolayers (Weinberger *et al.*, 2000 Brovelli *et al.*, 1999, Pawlack *et al.*, 1999), and immobilisation to native surfaces by physical adsorption. Having selected a silicon-based waveguide and microfluidics system i.e. silicon oxide surfaces, the first surface functionalisation protocols considered for the LMC were based on silanes (see chapter 5), since these are routinely carried out on glass surfaces with similar chemical properties to silicon oxide. This has the advantage of creating a covalent attachment as well as being well established in the literature and a relatively straightforward laboratory procedure.

2.3.9 Imaging Systems

There are a number of variations in the imaging systems used to capture and analyse signals obtained from fluorescent planar waveguides, and these will be discussed briefly. The most important component of these imaging systems is an imaging detector, typically in the form of an array of charge-couple devices (CCDs) which may or may not be thermoelectrically (Peltier) cooled. Peltier cooling reduces the background noise and interference in the image at the cost of making the device more complex (Feldstein *et al.*, 1999, Rowe *et al.*, 1999, Ligler *et al.*, 1998). Filters are placed over the CCD array to block out any scattered excitation light. In some systems a lens array is included to focus the image onto the CCD array, enhance fluorescence capture efficiency and minimise the size of the sensor (Feldstein *et al.*, 1999, Golden, 1998). The images produced are then analysed by averaging the fluorescent intensity over each spot and using this average to determine the level of binding that has occurred. Very low concentrations of analyte are typically distinguished from noise by the use of an intensity cutoff value (Feldstein *et al.*, 1999).

2.3.10 Gas-chromatography-mass spectrometry

Gas-chromatography-mass-spectrometry (GCMS) is the gold standard for multianalyte sensing and trace organic detection with large sample volumes, and is becoming increasingly developed for low volume applications. It is therefore extremely well suited to applications in Life detection such as the analytical problem for biomarkers described in section 2.2. Indeed, there will be a mass spectrometer on board the ExoMars Rover alongside the LMC and Urey instruments. However, mass spectrometry cannot detect entire proteins or larger organic biomarkers, so although there will be some shared targets with the LMC for the purposes of multiple confirmations of particular biomarkers, the antibody assay format allows the detection of additional higher mass targets.

2.3.11 Summary of Literature Review on technologies for the simultaneous detection of a number of different analytes using microlitre-scale sample volumes

A number of methods and technologies have been developed for multianalyte sensing using small sample volumes, which are the requirements of the technology platform on which the SMILE Life Marker Chip must be based. The three main technologies that are most commonly used for this purpose are gas chromatography mass spectrometry, surface plasmon resonance and optical waveguides. The most developed of these technologies are fluorescence-based detection of analytes on thin film (mono-mode) optical waveguides. GCMS is also well developed and will be included on board the ExoMars mission.

Channel systems have been used on mono-mode waveguides, and this does not significantly affect the sensitivity provided an appropriate cladding layer is used to prevent loss of light from within the waveguide. The detection system is usually based on charge-couple device (CCD) imaging system, as these have a number of advantages over alternative imagines system, including greater sensitivity, lower limits of detection and ease of miniaturisation.

The SMILE LMC is currently proposed to be based on a biological receptor assay for detection of analytes on thin film mono-mode silicon wafer optical waveguide, utilising evanescent field excitation and imaging of the emitted fluorescence with a cooled CCD

chip. This design combines the advantages of the most relevant, sensitive and specific approaches to multianalyte sensing found in the literature, but the combination of the proposed technologies and methods has not been demonstrated in existing work. A number of elements of the proposed LMC instrument design have also been shown to have been used in microfluidic devices to assay very small sample volumes. Fluorescent optical biosensor devices are known to be capable of achieving high sensitivity, so the requirements of performing a multiplexed assay on microlitre-scale sample volume may be met with the proposed Life Marker Chip technology.

Since the proposed Life Marker Chip design appears to be a logical development from current analytical technology in this area, it appears feasible to produce an instrument capable of space-flight with the required analytical capability for Life detection. In the final section of this literature review, the environments in which the Life Marker Chip must function, and salts and solvents that may consequently be carried into the biological assay chamber, will be discussed.

2.4 Mars Geological Environments and Sample Related Media

2.4.1 Review of the geological characteristics of the Martian surface relevant to Life detection, and reagents commonly used in sample processing and extraction.

2.4.1.1 Introduction

This section focuses on the chemistry of the Martian surface and reagents that may be considered in the sample processing and extraction system. Since the design of the sample processing system is currently at a very early stage of development, this chapter does not describe in detail the system to be used, but briefly describes appropriate sample extraction methods and the types of reagent that may pass through into the Life Marker Chip assay area with these potential methods. This literature review was used as the basis for developing experimental procedures to determine the effect(s) of Martian regolith salts on antibody assays, as while the potential environments are known no work has been done to determine whether antibody assays will function in the presence of these salts. The results of these experiments are presented in chapter 5.

2.4.1.2 Martian surface geology

The first point to consider in this section is the geology of the areas that the ExoMars rover is likely to explore. Observations from the Mars Express orbiter indicated the presence of hydrated magnesium and calcium sulphates on the Martian surface (Bibring *et al.*, 2005), confirming the previous detection of sulphates during the Mariner 9 mission (Clarke & Van Hart, 1981).

Of greater relevance to the ExoMars Mission, the NASA MER Rover Opportunity has revealed that significant areas of the Martian surface and near-subsurface rocks accessible to ExoMars have been affected by water (Clarke *et al.*, 2005). This has been established due to the strong indications that the Meridiani Planum region contains substantial deposits of evaporite minerals formed only in the presence of water, particularly sulphates such as the epsomite form of magnesium sulphate ($\text{MgSO}_4 \cdot 7\text{H}_2\text{O}$), Iron (III) sulphate in the form of jarosite ($\text{KFe}_3(\text{SO}_4)_2(\text{OH})_6$), and calcium sulphate in the form of gypsum ($\text{CaSO}_4 \cdot 2\text{H}_2\text{O}$) (Harland, 2005, Amaral, Martinez-Frias &

Vázquez, 2005, Clarke *et al.*, 2005, Peterson & Wang, 2006). The presence of these water-altered minerals is direct evidence that there was once a warmer, wetter period in the history of Mars during which life could have evolved (Clarke *et al.*, 2005, Squyres *et al.*, 2004).

In addition to the formation of these minerals by water, there is also evidence that Martian salts have undergone paragenesis (mineral change over time) (Marion *et al.*, 2006, Clark *et al.*, 2005). Paragenetic processes of iron minerals, which are widespread on the surface of Mars, follow the following sequence on Earth:

rock → ferrous sulfates → ferrous/ferric sulfates → ferric sulfates → ferric hydroxides → ferric oxides. (Marion *et al.*, 2006).

This oxidation cannot be explained by the presence of sulphuric acid, which has previously been suggested as an oxidation source, since jarosite is stable in the presence of sulphuric acid (Marion *et al.*, 2006). It has been proposed that this oxidation of iron occurred in liquid water that was present for long periods of time, providing support for the case for Life having evolved on Mars (Squyres *et al.*, 2004). An alternative explanation for the oxidation of iron (III) jarosite minerals has also been proposed, based on the deposition of a volcanic ash and subsequent oxidation by gaseous sulphuric acid. This gaseous sulphuric acid is formed by the reaction of water and sulphur dioxide emitted from fumaroles. This could have occurred without the presence of standing water and at higher temperatures (McCollom & Hynek, 2005). In either case, iron (II) minerals must be considered as a possible mineral constituent of ExoMars samples reaching the LMC.

Jarosite is of particular significance for the Life Marker Chip since it has been proposed that it could function as an iron source for chemolithotrophic microorganisms on Mars, following the discovery of such organisms in the Rio Tinto river system, a site proposed to be an analogue for early Mars (Amaral, Martinez-Frias & Vázquez, 2005, Schweitzer *et al.*, 2005). In addition, it has been shown that even a 500µm layer of jarosite on the surface could shield microorganisms from UV radiation (Amaral, Martinez-Frias & Vázquez, 2005), which is critical for the preservation of Life since direct exposure to solar UV radiation is extremely harmful to even the most resilient of terrestrial organisms (Horneck *et al.*, 2001).

Given the abundance of these minerals on the Martian surface and interest in Life detection associated with them, it is important for the development of the sample processing system to understand if the presence of these materials in the assay reaction chamber would have an adverse effect on the assay. An adverse effect would not necessarily invalidate the Life Marker Chip approach, but may necessitate a demineralisation step in the sample processing system to remove mineral ions before they reach the assay chamber. At the start of this work, the effects of these mineral salts on antibody assays were unknown.

2.4.1.3 Sample processing system methods, reagents and solvents

The second consideration regarding the effect of sampling on the antibody assay system is the possible transfer of organic solvents from the sample processing system into the assay chamber. It is known that traditional monoclonal and polyclonal antibodies are not suited to function in non-polar solvents. While modified recombinant antibodies may have an increased survival and performance, these are also not thought to survive and function in many non-polar solvents (Sims *et al.*, 2005). In addition there is the consideration that protein conjugates and fluorescently labelled control proteins that may be used for control spots or as a part of a competitive assay system must also be functional in the final solvent in which the assay takes place.

As discussed in section 2.2.8, due to the desire to detect both polar and a-polar biomarkers, there are likely to be two independent sample extraction lines. The first will be based on aqueous solvents and used to extract proteins and water-soluble polar biomarkers, while the second will use non-polar organic solvents to extract a-polar biomarkers. Many of the most efficient methods to extract proteins from soil samples are based on guanidine-hydrochloride (see for example Simoneit *et al.*, 1998). Since this reagent at the high concentrations it is normally used at will denature any proteins it encounters, including antibodies, it may denature both some target molecules of interest and any antibodies it encounters (Schweitzer *et al.*, 2005). This is clearly not compatible with the Life Marker Chip, so the antibody assay must be tested with guanidine-HCl to determine the significance of any adverse effects. Other extractions

based on phosphate buffers can be used instead of a guanidine-HCl extraction, but these are less efficient (Schweitzer *et al.*, 2005).

A typical organic solvent extraction of lipids and polyaromatic hydrocarbons from a soil sample is carried out in two stages; firstly the organic molecules of interest are removed by dissolving the sample in a mixture of solvents of different polarity, e.g. dichloromethane, methanol and phosphate buffer, and passing this solvent through a solid phase extraction cartridge to trap the target molecules in the solid phase. In the second stage specific targets are eluted with a series of different solvents of increasing polarity, such as hexane, chloroform, acetone, ethyl acetate and methanol (Aga & Thurman, 1993, Fang and Findlay, 1996). However, modifying this traditional approach to fit the mass and volume constraints of an instrument for space flight is not straightforward, partly due to the availability and selection of SPE columns of appropriate sizes and materials, and partly because the mass limits the number of different solvents that can be used.

The proposal therefore is to use a single extraction medium in the a-polar extraction line, to capture as many targets of interest as possible simultaneously. This may be achieved by combining a number of solvents as described in the first stage of lipid extraction by Fang and Findlay (1996) or by using a single organic solvent that provides the best compromise between extracting target molecules of interest and compatibility with the antibody assay system e.g. propanol (Buch *et al.*, 2003). Water-methanol mixtures are also being considered as previous work has shown that ELISA assays are tolerant to limited presence of methanol, dependant on the specific antibody-antigen pair (Aga & Thurman, 1993).

2.4.1.4 Additional considerations

In addition to the effect of dissolved mineral salts there is also the possibility that oxidants are present in the Maritan regolith, inferred by the failure of the Viking experiments to detect any organics (Klein, 1979, Parnell *et al.*, 2006). This is most commonly thought to be hydrogen peroxide (H₂O₂), but other oxidising species e.g. superoxide, hydroxide and perhydroxyl radicals have also been proposed. Regardless of

the specific oxidising agent present, if oxidising species come in to contact with antibodies or other assay reagents they may damage them and disable the assay (Parnell *et al.*, 2006). To counter this possibility, an antioxidant such as ascorbic acid may be added to the assay buffer to prevent oxidising reactions (see section 5.3.3.2).

2.4.1.5 Summary of possible environmental and sample processing reagents that may have an effect on antibody assays

The likely target areas of interest for Life detection include areas of the Martian surface that contain rocks altered by the presence of water, including large deposits of evaporite minerals such as iron, calcium and magnesium sulphates. At present the sample processing system for the Life Marker Chip is in the early design stage, but is likely to be based on standard solid phase extraction in which the sample is passed over a column that selectively binds to organic species of interest, then these species are removed from the column in a single stage with a single solvent (or combination of solvents). Due to the extreme range of polarities of the target molecules of interest, two lines of extraction may be required, one for polar and one for a-polar targets (see section 2.2.8). Examples of possible reagents and organics solvents that could be used in the sample processing system include guanidine-HCl, methanol and n-hexane, and these are the solvents used to test the effect of organic solvents on immunoassays in section 3.3.4.

It is prudent prior to further development of the sample processing system to determine any limitations imposed on the sample extraction methods required by any effects of Martian regolith components or carry-over of solvents used in the sample extractions system on the assay. Antioxidants may be required to counter and chemical reactions caused by the presents of oxidising agents in the sample. Very little previous work has been done in this area, so the generation of experimental data to support the development of the LMC sample processing system is timely and will be explored in this thesis.

2.5 Literature Review Summary

Four key areas of scientific interest and knowledge have been discussed in this literature review. Firstly, we have considered whether it appears feasible to use an antibody-based assay in space due to the effects of radiation on the biological components of the assay, particularly proteins including antibodies. The balance of evidence on studies using gamma radiation suggests that while antibodies in a liquid state are likely to be inactivated by radiation particularly at the levels required for pre-flight sterilisation, antibodies in a dried state are much more stable since they cannot be attacked by the secondary radiolytic products of water. Very little work has been done to study the effects of particle radiation on antibodies. This is an area that is critical to the development of the Life Marker Chip and it was important at the time this study began that some initial experiments were carried out to validate the use of antibodies in space environments.

The second area of importance, which includes sections 2.2 and 2.3 of this literature review, is the analytical problem to be addressed by the Life Marker Chip. The Biomarker workshop held by members of the SMILE LMC consortium identified a large number of target biomarker molecules that would be of interest to the Life Marker Chip, many of which are beyond the detection capabilities of other instruments in the Pasteur Payload. In order to detect as many of these targets as possible simultaneously with the likely amount of material available, it was proposed to utilise immunoassays in a microarray format within a microfluidic channel, that would enable the detection of up to 25 different 'targets' (as discussed in section 1.1.1), with each target being one epitope (some of which may be parts of a molecule allowing detection of an entire class of biomarkers) in any particular channel. It was also recommended that each sample was divided into two, and different sample extractions performed on the two parts in order to achieve detection of both polar targets, mainly indicative of extant life, and a-polar targets, which are more closely linked to extinct life. The most suitable technology available to base this instrument on appeared to be a fluorescent assay on a mono-mode planar waveguide, since this type of instrumentation has extremely high sensitivity. Previous work has also been carried out with fluorescent assays on planar waveguides within microfluidic channels, although not with the number of assay spots required for the Life Marker Chip assay. Although the technology in this area is already

at an advanced stage, further development and optimisation of an instrument platform is required for the Life Marker Chip and was carried out during this thesis as part of the European Space Agency Technology Readiness Level Upgrade Study.

The final area of importance is consideration of the effects of the Martian environment on the assay system, particularly with regard to the development of the sample processing system. It is likely that target areas of interest for the ExoMars rover will include deposits of sulphates and evaporite minerals, including specifically magnesium sulphate, calcium sulphate and iron (II) and iron (III) sulphates, that are not normally present in biological assays. The sample processing system may use guanidine-HCl and / or organic solvents in order to remove organic target molecules of interest from rock samples. It is possible that these reagents may pass through the sample processing system into the assay chamber and therefore affect the assay in some way. Work is therefore required to determine what effects these salts and organic solvents may have on the assay so that the design of the sample processing system can be modified to prevent any harmful reagents reaching the assay chamber e.g. by addition of a demineralisation step or evaporation of organic solvents.

In this chapter the current state of knowledge in the areas of literature relevant to this thesis has been reviewed. In the following three chapters, the work carried out in the three key areas of work; radiation and pre-flight sterilisation, development of the instrumentation platform, and studies on the effect of Mars related media and sample processing of the assay system, will be reported.

Chapter 3: Exposure of Fluorescent Dyes and Antibodies to simulated Radiation and Sterilisation protocols¹

3.1 Introduction

As discussed in section 2.1, a key unknown in terms of the use of antibody-based Life detection technologies in space is the effect of radiation and other environments associated with space missions. The range of radiation environments encountered during a flight to Mars, includes gamma rays, protons, neutrons and heavy ions at energies ranging from a few MeV to thousands of GeV and beyond, peaking at around 1 GeV (Benton, 2001). Low energy radiation has a higher level of interaction with substances, while higher energy radiation can do significantly greater damage on the occasions when it does interact.

In order to consider designing instrument for use on Mars, such as the Life Marker Chip to be included on the ExoMars rover, i.e. for use in these radiation conditions, it is necessary to understand the effects of this radiation exposure on both the individual components and the assembled device. In the case of an optical biosensing system, many of the hardware components such as microfluidic systems and electronics can be designed based upon materials and systems that have been established as suitable for space flight in previous missions. However, the critical biological components of the Life Marker Chip (LMC) have never been used in space before. The effect of each radiation type and combinations of radiation effects therefore needed to be investigated and understood before significant instrument development was carried out, particularly ensuring that any effects of radiation on the peak emission wavelengths of fluorescent dyes, since this would affect the decision on appropriate dyes, light sources and optical systems. The effect of radiation on antibodies is also critical since damage to antibodies could prevent or inhibit antibody-antigen interaction, and / or reduce the specificity of the antibody to its target.

As described in section 2.1.1.4, planetary protection procedures are in place to prevent contamination of planetary surfaces with terrestrial Life and reduce the likelihood of false positive detection of extraterrestrial life due to spacecraft contamination. This is implemented in the form of an acceptable “bioburden” which is measured by bacterial spore count per m² of surface. The acceptable bioburden varies depending on the potential of the spacecraft to come into contact with the planetary surface i.e. surface

1: Much of the experimental work in this section was carried out jointly with Daniel Thompson and Dr. Mark Sims from the University of Leicester, and Dr. David Cullen from Cranfield University. The authors main responsibilities in these experiments were the optimisation of sample preparation techniques, preparation and analysis of antibody and fluorophore samples for radiation and heat sterilisation exposures, and sample handling during test procedures. Other group members contributed to the calculation of appropriate radiation doses, developing the experimental design for radiation and heat exposures, and proving access to the radiation testing facilities.

rovers have a more stringent sterilisation requirement than orbiters. For surface rovers on Mars, such as the ExoMars rover that will carry the Life Marker Chip, the bioburden of the material surfaces must be by six orders of magnitude during the pre-flight assembly of the rover. (Mahaffey *et al.*, 2004, Divincenzi *et al.*, 1996,1984). This is typically achieved by a dry heat sterilisation protocol, normally a minimum of 50 hours at 120°C, as was carried out for the Viking missions (Mahaffey *et al.*, 2004).

The effect of this treatment on fluorescent dyes and antibodies at the time of this study was unknown, although it was considered highly unlikely that an antibody would survive such treatment. The reason for this expectation is that antibodies are proteins with a highly complex structure, and much of this structure is held together by relatively low strength molecular interactions e.g. hydrogen bonding. These weak molecular interactions are low energy bonds, and heating to high temperatures would be expected to destabilise these and so change the protein structure, thus inactivating any structure-dependent binding. Given the likely detrimental effects of heat sterilisation on biological materials, gamma irradiation is being considered as a potential sterilisation technology that may be more suitable for biological components than the dry heat method.

In this section, the results of a series of experiments in which antibodies and fluorescent dyes commonly used as labels in biological assays were exposed to different types of radiation and a heat sterilisation procedure will be described and discussed. As discussed in the literature review, prior to these studies very few studies had been carried out using gamma irradiation on antibodies, and we are not aware of any previous work in which fluorescent dyes have been exposed to gamma radiation. Similarly, we are not aware of any reported particle irradiation exposures of either antibodies or fluorescent dyes. Therefore, in this section both the methods and the results are novel. The results of a heat sterilisation tests are also included. As far as the author is aware, no previous work has been carried out to determine whether antibodies and fluorescent dyes survive dry heat sterilisation procedures, although in the case of antibodies this is largely because it is considered unlikely that any specific binding activity would be retained.

Since it is impractical to expose samples to all of the types of radiation encountered in a mission scenario simultaneously (there are no facilities capable of simulating the

complete spectrum of radiation types and energies simultaneously), the effect of each type of radiation was investigated, and will be reported, separately.

3.2 Proton and helium ion exposures – introduction

Proton and helium ion exposures were both carried out at Birmingham University using a cyclotron to generate a beam of either a protons or helium ions. This facility was selected because it is capable of generating an essentially mono-energetic particle beam (protons or helium ions) at any single energy between 9 and 35 MeV, and is capable of providing equivalent mission fluences of protons in a convenient timescale (however, the calculated mission fluences used are near the lower limit of the cyclotron facility's range). The term fluence is used to describe the amount of protons that the sample is exposed to rather than dose, since dose implies that a known amount of radiation has been absorbed by the sample (while in the case of antibodies and fluorescent dyes the absorption characteristics are unknown). The available range of energies using the cyclotron facility (9 to 35MeV) covers a significant proportion of the lower energies of particle radiation likely to be present during flight. The most desirable energy range to study would be at 3 MeV or higher, since protons at lower energies are likely to be absorbed by the spacecraft shielding, and the lower energy radiation is expected to be more damaging. However at the time of this study the cyclotron provided the best compromise between most appropriate energy range, availability and convenience of generating appropriate fluences of particles.

It is worth noting that whilst Galactic Cosmic Rays (GCR) are generally much higher energy than the radiation used in these experiments, the actual Life Marker Chip device will be positioned inside the spacecraft where lower energy secondary radiation and fragments generated by GCR will play a large role. The spacecraft shielding is likely to prevent much damage from the lowest energy radiation particles incident upon it from space, but an understanding of the effect of radiation on unshielded fluorescent dyes and antibodies is useful to know from a basic science viewpoint, and a “worst case” scenario in terms of the mission. The effects of radiation shielding were therefore not considered when calculating estimated mission fluences of particle radiation for the tests reported in this thesis.

Since the cyclotron facility generates mono-energetic proton beams, we¹ were unable to produce an energy spectrum such as that one would expect the samples to see in

space. Instead we divided the energy spectrum into two parts; 9-35 MeV, and 35 MeV upwards. The SPace ENVironment Information System (SPENVIS) model (see section 2.1.2.4) was used to calculate the total fluence of protons with energies lying within these two energy ranges for an Earth-Mars transit, basing the transit parameters on those suggested in the Mars Transportation Environment Definition Document (Alexander *et al.*, 2001), which gives a 179-day Earth–Mars transfer period during the ‘on’ season for solar particle events within the JPL model (Thompson *et al.*, 2006).

An “over test” philosophy was adopted where the exposure times were based on an integrated fluence over a large energy range, but the range of energies was replaced with exposure at a single energy (the lowest in the range). Noting that the cross-section for proton damage for example in water peaks at low energies ~0.1MeV we assumed using the lowest energy in the range would be potentially more damaging to the sample than if it were exposed to the same fluence using the range of (higher) energies. Given the cross-section of water to protons the beam was expected to penetrate significantly into the samples and distribute energy throughout the samples (Thompson *et al.*, 2006).

Cyclotron beam currents of 50pA and 500nA were used to achieve the required fluences. Using these beam currents, which were the lowest currents at which a stable particle beam could be generated, it was not possible to expose the sample to 1X the mission fluence of protons. This is because the exposure would take only 0.7 seconds, and the proton beam exposures could not be accurately controlled to achieve an accurate exposure of that timescale. The test samples were therefore exposed to various multiples of this basic fluence, namely 10X, 100X and 10,000X, including some very high exposures to enhance the “over test” principle adopted within this work. In order to validate the exposures and assess the uniformity of the proton beam across the exposed area, radiochromic film was exposed to the same fluence of protons immediately after each sample exposure.

3.2.1 Preliminary particle radiation testing

The goal of this section is to expose representative biological materials for the Life Marker Chip, in the form of an antibody, and representative fluorescent dyes that may be used as labels in the Life Marker Chip immunoassays, to a series of proton and helium ion fluences. The fluorescent dyes selected for the initial tests were fluorescein,

a commonly used dye in biological assays, and Alexa Fluor[®] 633, a modified rhodamine dye that is being considered for use in the Life Marker Chip due to its resistance to photobleaching and compatibility with low mass light sources. The antibody selected for proton radiation exposure was an anti-atrazine single chain recombinant antibody (scAb). This antibody was selected as it is raised against a broadly similar target to many biomarkers i.e. a small organic compound, atrazine is extremely unlikely to be present on the surface of Mars so the assay could be used as a control assay in the flight instrument, and the anti-atrazine scAb was conveniently available as it was kindly provided to Cranfield University by Haptogen (Aberdeen, UK).

Since these experiments were carried out and developed at the same time and using the same basic sample preparation techniques as the gamma irradiation studies reported in section 3.3, the changes in experimental protocol for these sections were made concurrently and the result sections refer to one another.

3.2.1.1 Preliminary particle radiation testing – materials and methods

As described in the introduction to this chapter, all proton and helium ion exposures were carried out at the cyclotron facility at the University of Birmingham. At this facility, the selected energy level and current of protons generated leave the cyclotron through a 1cm² beam port (see Figure 3.1). The particle beam could be ‘turned on and off’ by moving a Faraday cup, which prevents protons entering the beam port when in the ‘closed’ position. The fluence could therefore be controlled by calculating the required number of particles for a particular exposure using the HZETRN model described in section 2.1.2.2, and using the beam current to calculate the time taken for the required number of particles to pass through the sample. The Faraday cup was then removed from the beam path for that calculated time period and replaced when the exposure was complete.

In order to expose multiple samples to the same radiation treatment, an 864 well microtitre plate (Helix BioMedical Accessories, Ramona, USA) was customised to fit onto the end mounting of the Cyclotron beam port such that a 3 x 3 well area could be held directly in the 1cm x 1cm particle beam. This was done by drilling holes corresponding to the size and position of the spigots above and below the beam port (shown in Figure 3.1) in 4 locations across the microtitre plate (one location is shown in

Figure 3.2). An additional 9 wells elsewhere on the plate, which were not in the beam line, were used as control wells (shown in Figure 3.2). These wells were used to expose triplicate samples of antibodies or fluorescent dyes to proton radiation in this initial experiment.

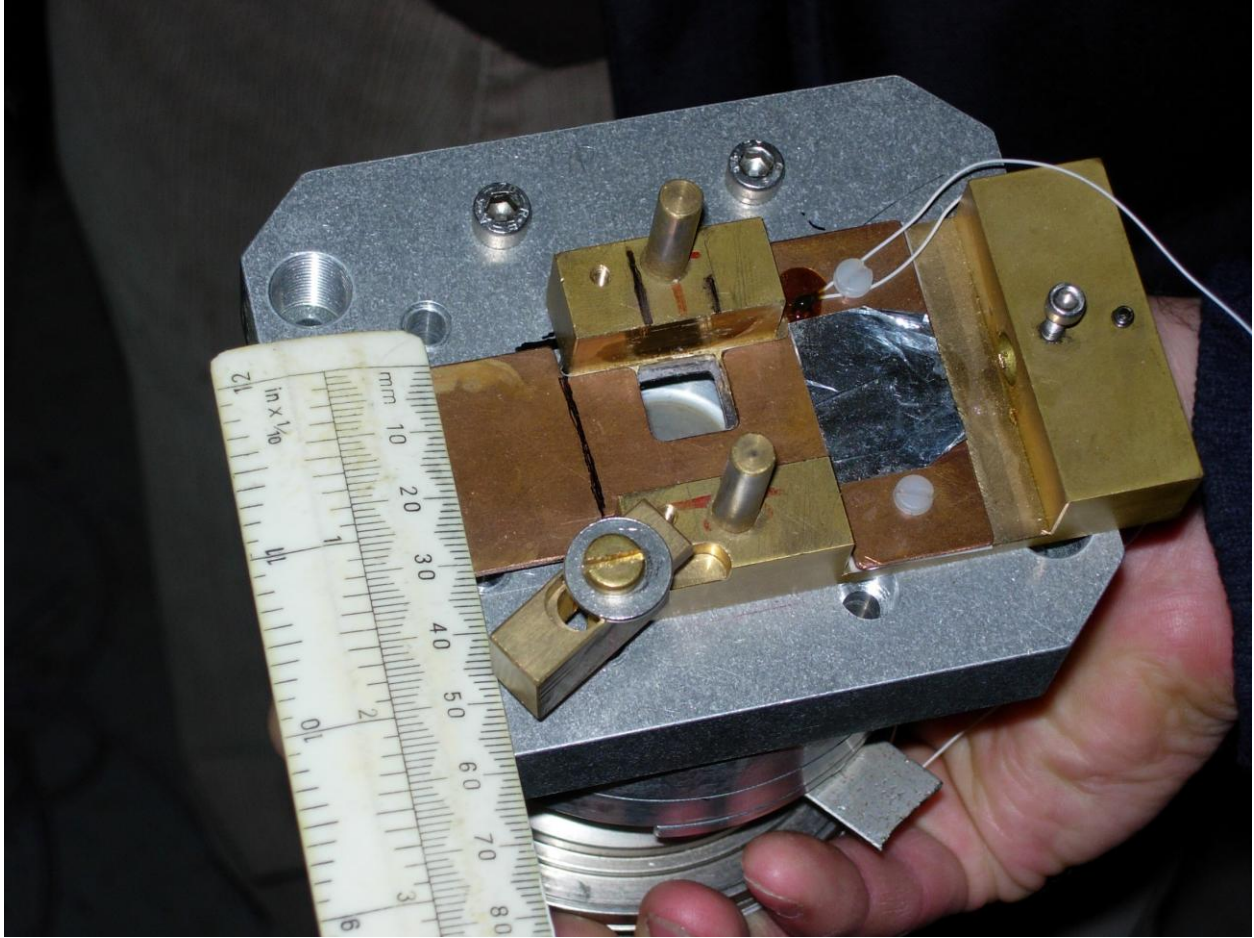


Figure 3.1: Cyclotron beam port attachment used to mount samples in front of the 1cm x 1cm particle radiation beam



Figure 3.2: Customised 864 well microtitre plate with 9-well sample and control areas marked

In this initial experiment only fluorescein was used as an example of a fluorescent dye, since the Alexa Fluor[®] 633 dye is more expensive and it was desirable to have a greater understanding of the experimental procedure before using the more expensive dye in an experiment. 10µl of 0.5mg.ml⁻¹ fluorescein (Sigma-Aldrich Poole, UK, Product Code 32615) or 10µl of ~0.075mg.ml⁻¹ anti-atrazine scAb (Haptogen, Aberdeen, UK) antibody

were pipetted into the two sample areas in a random known pattern. The microtitre plate was then placed into a -80°C freezer for 4 hours, then transferred as rapidly as possible (to prevent melting of the frozen samples) into a freeze-drier (Edwards Modulyo) and dried overnight. After freeze-drying the microtitre plate was wrapped in aluminium foil, in an attempt to prevent material entering the wells while minimising the chance of electrostatic interactions removing material from an insulating cover, and transported to the University of Birmingham. In order to minimise physical disturbance of the samples, the aluminium foil was left in place over the sample areas during the exposure, only pierced sufficiently to allow the microtitre plate to be mounted on the mounting rods (see Figure 3.3). The assumption was made that this very thin layer of shielding would have little effect on the radiation exposure.

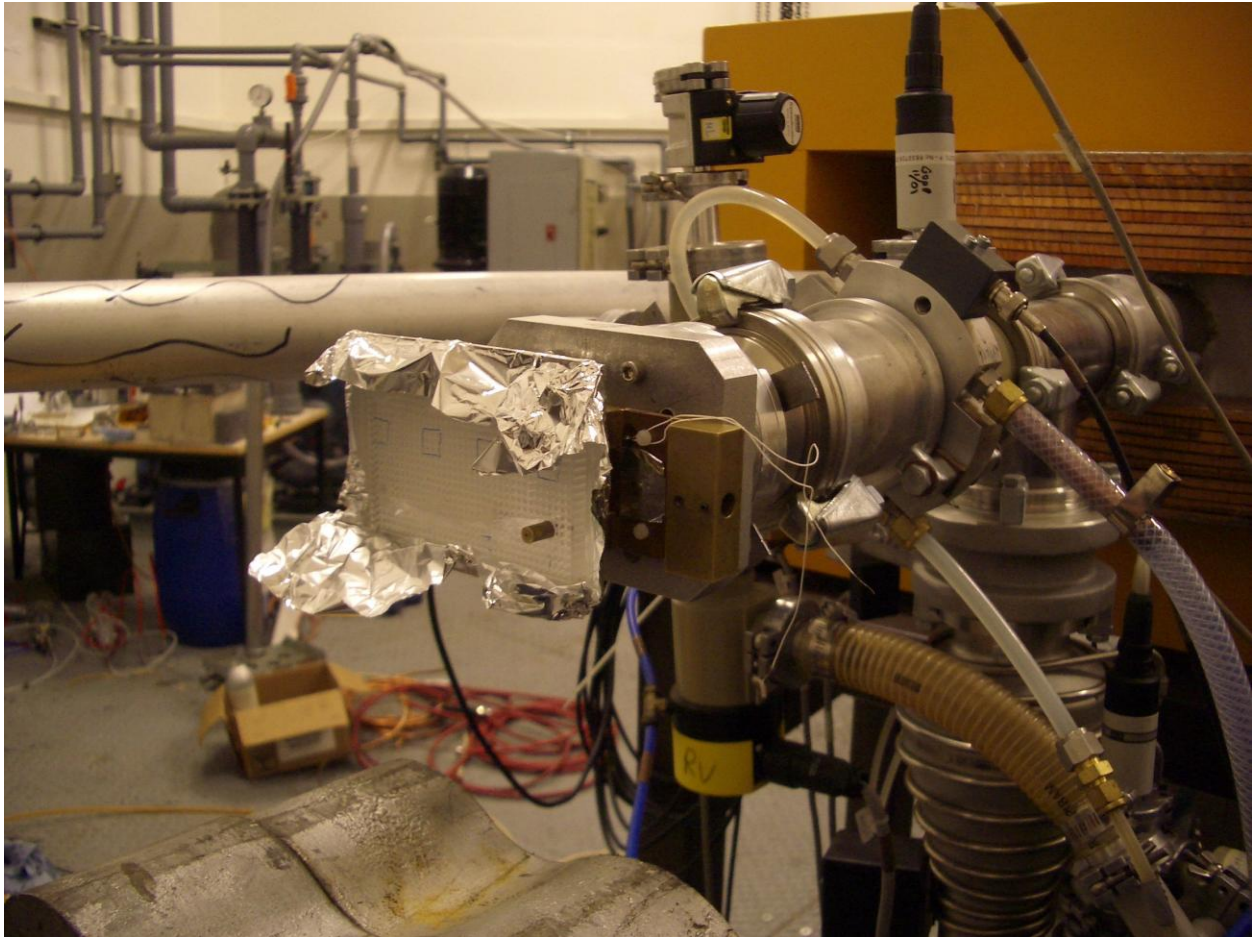


Figure 3.3: Modified 864 well microtitre plate mounted on the cyclotron beam port. The aluminium foil was left in place since it was considered difficult to remove it without disturbing the dried material in the samples and it would have a negligible shielding effect.

The proton exposures were carried out using a cyclotron beam current of 5pA. This equates to 2.12×10^7 protons per second. The samples were exposed to two proton fluences, 1.38×10^{10} and 1.48×10^8 protons, taking 653 and 6-7 seconds exposure respectively. These proton fluences are low compared to the expected mission fluence

discussed in section 2.1.2.4. This is due primarily to a miscalculation of the proton fluences in this initial experiment. However the experiment was continued as this error was realised at a very late stage, and it was useful to continue the experiment to validate and develop the protocol.

After exposure, the microtitre plate was transported back to Cranfield University for analysis. Each fluorescein sample was reconstituted in 15 μ l deionised water and transferred to an Eppendorf vial containing 850 μ l of RO water. Each sample well was then washed 9 times with 15 μ l of deionised water, adding this water to its corresponding Eppendorf vial, to produce a final concentration of 0.05mg.ml⁻¹ fluorescein.

3.2.2 Fluorimeter analysis of Fluorescein and Alexa Fluor[®] 633 samples

The fluorimeter used throughout this work was a Cary Eclipse Varian spectrophotometer. The fluorimeter was controlled with Cary Eclipse Scan Software (version 1.0(78)). In this first experiment only fluorescein was used, but the settings for Alexa Fluor[®] 633 are also included here as this protocol will be referred to in later sections.

In all of these experiments, the software was used with the default settings with the following specific details and exceptions. The excitation and emission slit widths were set to 5nm. The photomultiplier tube gain for fluorescein was set to 600, and for Alexa Fluor[®] 633 it was set to 800. For some samples, different photomultiplier tube gains were required to obtain a signal within the working range. Where this was the case, the output signal was normalised. This normalisation was based the experimental observation that the measured signal for a given sample doubled with a photomultiplier gain increase of 8%.

The emission and excitation spectra of the dyes were both measured, and the peak wavelengths and intensities determined automatically by the software. For fluorescein the excitation wavelength was scanned between 400nm and 510nm, (with emission measured at 520nm), and the emission wavelength was scanned between 500nm and 600nm (with the excitation wavelength set to 488nm). In the case of Alexa Fluor[®] 633, the excitation spectra was scanned between 550 and 650nm, (with the emission wavelength set to 650nm), and the emission wavelength was scanned between 635 and 720nm (with the excitation wavelength set at 633nm).

The peak emission and excitation wavelengths and intensities were recorded and analysed in Microsoft Excel 2000.

3.2.3 ELISA method

All antibody assays were based on an ELISA, testing the antibody over a range of antibody concentrations, in order to observe changes in the shape and signal in the antibody binding curve. This method was used throughout sections 3.1 and 3.3

The ELISA method used was as follows:

- Microtitre plates (Immulon 4 ELISA, Fisher Scientific, UK) were coated with BSA-atrazine conjugate by adding 100 μl of 10 $\mu\text{g}\cdot\text{ml}^{-1}$ BSA-atrazine conjugate (kindly provided by Haptogen Ltd., Aberdeen, UK) in 10mm HEPES buffer (pH 7.4) to each well. The plate was covered with aluminium foil and incubated overnight at 20°C. (approximately 14 hrs).
- The antigen solution was removed by flicking to empty and slapping the plate onto a bench surface covered with absorbent paper (Kimwipe) to remove residual liquid. 200 μl of blocking buffer (0.25g. ml^{-1} skimmed milk powder (Marvel brand) in HEPES buffer) was added to each well to block non-specific protein binding. The plate was then incubated at 20°C for 4 hrs.
- The blocking buffer was removed by flicking and slapping the plate. The plate wells were washed twice with 200 μl HEPES buffer, flicking and slapping the plate to remove the washing buffer.
- 100 μl of the appropriate dilution of primary antibody sample (humanised anti-atrazine scAb) was added to each wells. The plate was then incubated at 20°C for 2 hrs. See below for details of preparation of test antibodies.
- The plate wells were washed three times with 200 μl of wash buffer (10mm HEPES buffer pH7.4 containing 0.05% Tween 20) followed by one wash with 200 μl of HEPES buffer.

- 100µl of secondary antibody (anti-human C-kappa light chain (bound & free) labelled with horseradish peroxidase enzyme) (Sigma-Aldrich, Poole, UK) diluted 1/1000 (from supplied stock) in HEPES buffer was added to each well, and the plate incubate for 1 hr at 20°C
- The plate wells were washed three times with 200µl of wash buffer followed by one wash with 200 µl of HEPES.
- One 3,3',5,5'-tetramethylbenzidine (TMB) tablet was dissolved in 10ml of 0.05M citric phosphate perbonate buffer. 100µl of this solution was added to each well and allowed to develop a desired colour intensity (measured after 10 minutes at 20°C). The reaction was stopped by adding 50µl of 1M H₂SO₄ to each well. The plate was read at a wavelength of 450 nm using a Lab Systems iEMS Reader MF microtitre plate reader.

3.2.3.1 Test antibody preparation methods

During this thesis, antibody samples for ELISA were prepared in a number of different ways and then included in the protocol described in section 3.2.3. This section describes how antibodies were prepared for the liquid control assays, antibodies exposed to radiation or heat treatments, and (as described in Chapter 5) ELISAs in buffers containing Martian regolith salts or organic solvents.

Liquid control assays:

Antibody serial dilutions were prepared in the desired concentration ranges, of which the first/highest anti-atrazin(e) antibody concentration was a 0.3mg.ml⁻¹ solution of the anti-atrazine scAb in HEPES buffer. The subsequent antibody solutions were prepared by double-diluting the antibody across the plate (10 times) (with HEPES buffer).

Dried antibody samples (for radiation, and heat sterilisation):

Dried antibodies were produced by adding a volume (typically 30 μl) of $0.3\text{mg}\cdot\text{ml}^{-1}$ anti-atrazine scAb to a plastic vial, and placing the vial(s) into a sealed vessel containing excess silica hydride desiccant in an oven at 30°C for 24 hours.

Dried antibodies were reconstituted in the same volume of deionised water from which they were dried (since equivalent buffer salts would be present in the dried sample). They were then diluted to $0.03\text{mg}\cdot\text{ml}^{-1}$ in HEPES buffer. The subsequent antibody solutions were prepared by double-diluting the antibody across the plate (10 times) (with HEPES buffer or other test solution as specified below). The remaining 2 wells were used for control assays.

Assays with buffers containing sulphate minerals:

Anti-atrazine scAb was dried (as above) and reconstituted to a concentration of $0.3\text{mg}\cdot\text{ml}^{-1}$ in 10mm HEPES buffer (pH 7.4) containing commercially available calcium, magnesium or iron(II) sulphate (Sigma-Aldrich, Poole, UK), dissolved at specified concentrations. The subsequent antibody solutions were prepared by double-diluting the antibody across the plate (10 times) (with the HEPES buffer containing the appropriate concentration of sulphate). The remaining 2 wells were used for control assays.

Assays with buffers containing organic solvents:

Anti-atrazine scAb was dried (as above) and reconstituted to concentration of $0.3\text{mg}\cdot\text{ml}^{-1}$ in a specified (combination of) organic solvent(s). The subsequent antibody solutions were prepared by double-diluting the antibody across the plate (10 times) (with appropriate organic solvent). The remaining 2 wells were used for control assays. During the antibody incubation step the microtitre plates were sealed with AlumaSeal (Sigma-Aldrich, Poole, UK), a foil coated with adhesive, to prevent evaporation of the solvent.

Assays with buffers containing guanidine-HCl:

Anti-atrazine scAb was dried (as above) and reconstituted to concentration of $0.3\text{mg}\cdot\text{ml}^{-1}$ in a specified concentration of Guanidine-HCl or Guanidine-HCl – HEPES buffer mix.

Only 0.3mg.ml⁻¹ antibody concentrations have been tested. A control assay was carried out by reconstituting dried anti-atrazine scAb in HEPES buffer.

3.2.3.2 Preliminary particle radiation testing – fluorescent dyes results and discussion

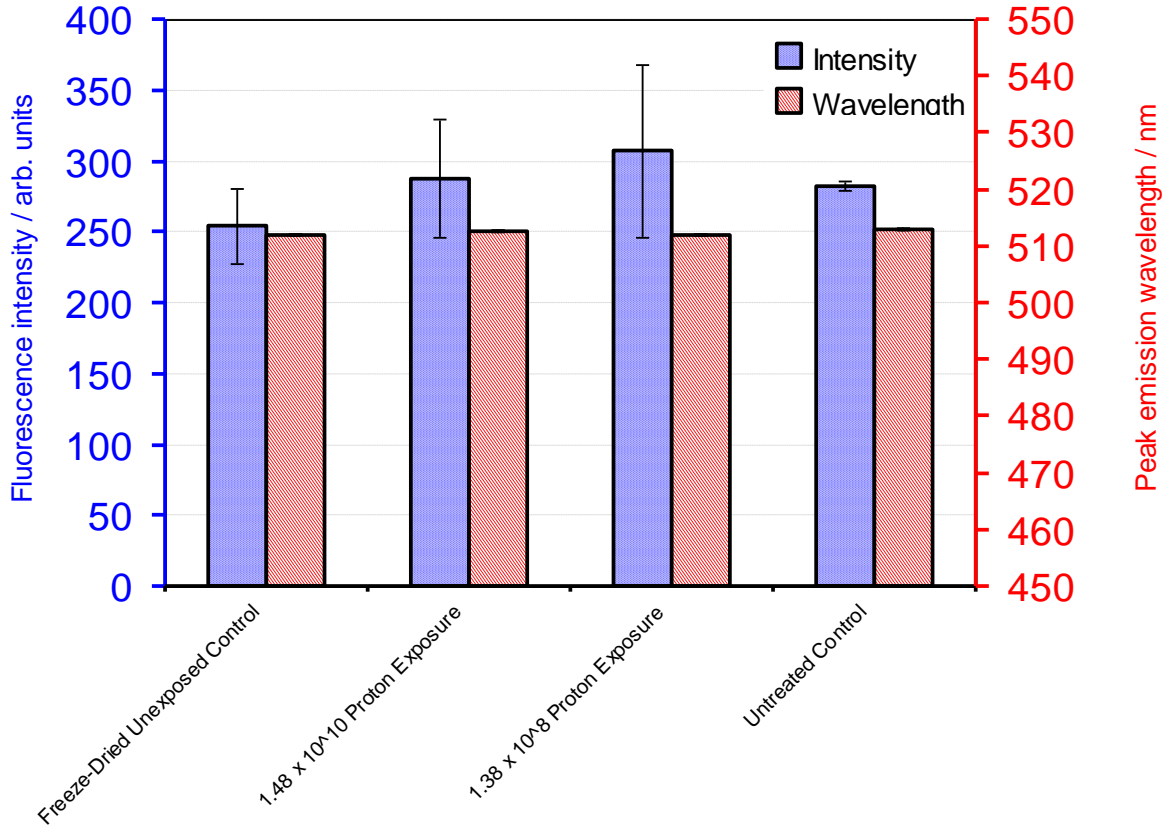


Figure 3.4: Effect of proton irradiation on fluorescent properties of fluorescein. The error bars indicate standard errors of the mean from three scans of the each sample.

Figure 3.4 shows the results of the 1.38 x 10¹⁰ and 1.48 x 10⁸ proton fluence exposures on the fluorescent properties of fluorescein. Since these proton fluences were later found to be very low, the results of this experiment were considered to be largely a test of the reproducibility of the sample preparation i.e. freeze-drying and reconstituting the samples. It appears from Figure 3.4 that the fluorescent properties of untreated fluorescein, the freeze-dried control and the freeze-dried samples exposed to proton radiation all have similar fluorescent properties, although the large error bars indicate that the process is not very reproducible.

With hindsight, it was considered that the reproducibility issues in this data, particularly in the fluorescent intensity, could be attributed to a small loss of material from the sample wells during the freeze-drying process. Given that this poor reproducibility could be explained by a loss of material from the sample wells, and that there was no change

in the peak emission or absorption wavelengths, the implication of the results in Figure 3.4 is that these levels of proton irradiation does not have a significant effect on the fluorescent properties of fluorescein. In addition, the fluorescein free acid preparation used in this experiment was near its solubility limit in water at the concentrations used to prepare the samples. While this is unlikely to have had a significant effect on the results of this experiment because all of the samples were prepared from the same stock solution of fluorescein, in all subsequent proton radiation tests a more water-soluble fluorescein sodium salt was used.

3.2.3.3 Preliminary particle radiation testing – anti-atrazine scAb results and discussion

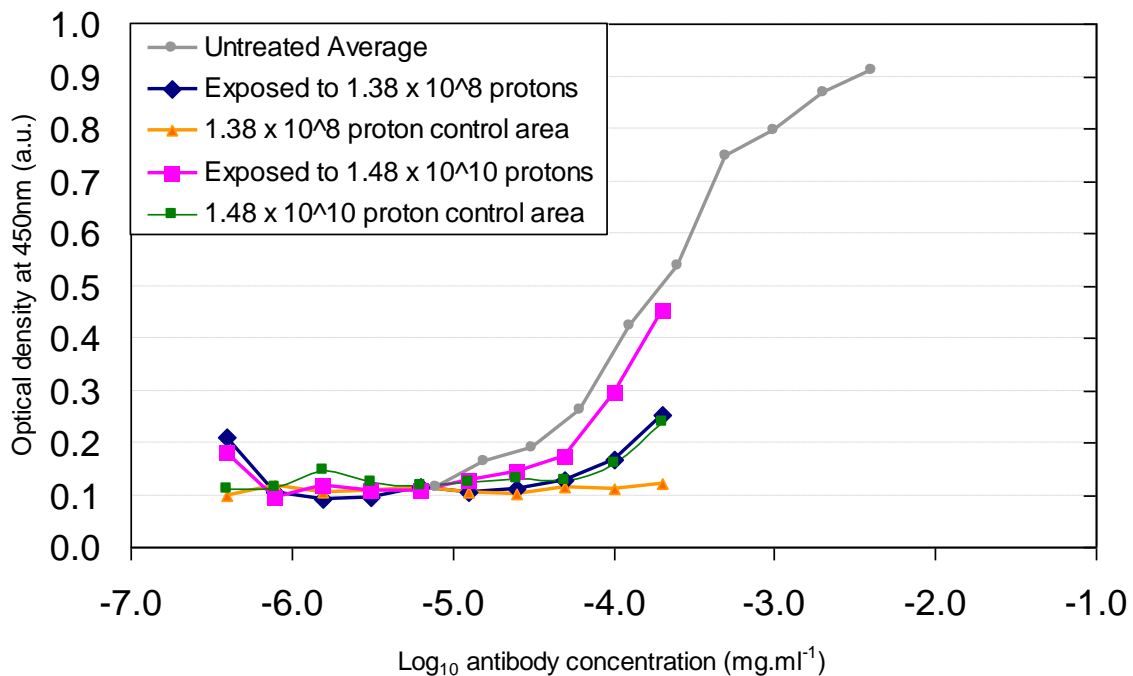


Figure 3.5: Effect of initial proton exposures on anti-atrazine scAb antibody, compared to samples outside the beam line and a stock antibody sample that was not included in the cyclotron tests.

Figure 3.5 shows the results of an ELISA carried out with the anti-atrazine scAb after the proton radiation exposures. What is immediately clear from this graph is that the test samples only have data points at relatively low concentrations. This is because the relatively low concentration of the stock solution of antibody meant that it was not possible to achieve a high concentration of reconstituted antibody. The maximum concentration achievable was limited because of the volume of the 864 microtitre plate wells, and difficulty of inserting and removing liquids from these wells, limited the sample volume to a maximum of 10 μ l. This sample then had to be diluted to a minimum

of 200µl in order to carry out the ELISA, resulting in a 20-fold dilution of the stock antibody concentration. It was therefore decided to adapt the protocol in future experiments to start with a higher stock concentration of antibody such that a higher concentration of reconstituted antibody could be used in the ELISA after particle radiation exposures.

In Figure 3.5, the binding curves of the antibodies exposed to proton radiation appear to show a higher binding affinity than the corresponding control samples. However, this result is highly questionable, and may be explained by two key factors. Firstly, it is possible that a greater amount of dried antibody was lost from the control wells during the sample handling process, therefore reducing the amount of antibody available in the assay. Secondly, as is discussed in the following paragraph, the control antibody samples would also have been exposed to a significant amount of proton radiation, so may not be appropriate as control samples. Therefore it is not possible to draw any conclusions about the effect of the proton radiation exposures on the antibody from this experiment. As mentioned in the discussion of the results of the fluorescein exposed to protons in this experiment (see section 3.2.3.2), this variability was thought, with the benefit of hindsight, to be due primarily to the loss of material during the freeze-drying process (this will be discussed further in section 3.2.4.2).

Also, in the light of practical experience of carrying out experiments within the cyclotron facility, it was realised that the experimental controls in this experiment were not the most reliable. This is because while the control sample wells were not in the beam path, when the particle radiation beam is active, a high background level of radiation (arising from scattered and secondary radiation from the beam and shielding of the cyclotron chamber) is generated around the cyclotron equipment. The cyclotron is housed in a 2m thick concrete shielding known as a cyclotron vault to contain this radiation. Therefore anything in the cyclotron vault during the exposure is subjected to a relatively high level of particle radiation, including the control samples in this experiment.

As a final point of consideration it was realised after this initial experiment had been carried out that there had been a calculation error in the proton fluence, such that the highest amount of protons used in this experiment was significantly lower than the calculated mission fluence of protons. However, since the principal goal of this initial

experiment was to develop the experimental method, this was not critical and the calculations were corrected for the subsequent experiments.

3.2.4 Evaluation and refinement of sample preparation procedure for ion beam exposures

To overcome the issue of the control samples being exposed to a significant radiation dose, the format of the sample exposures was changed. 1 cm² squares containing 3 x 3 wells were cut out of a 864 well microtitre plate, and a custom aluminium holder was fabricated at the University of Leicester to hold the sample blocks in front of the beam for the exposures. This sample holding block (shown in Figure 3.26) was made from aluminium, simply because it was a conveniently available material, and contained a cut out section in which the blocks of 864 well microtitre plate could be inserted, and holes for the mounting spigots on the cyclotron beam port such that the sample block could be mounted in front of the beam port. With these sample blocks each radiation exposure could be carried out by taking an individual sample block into the cyclotron chamber for the exposure on that block, storing the remaining sample blocks including the control samples outside the cyclotron vault for all other exposures.

At this stage in the project, the initial experimental results for both particle and gamma irradiation tests (reported in section 3.3.1) showed poor reproducibility. The common factor in both of these sample preparation procedures was the freeze-drying stage, and a likely explanation for the results was thought to be that freeze-dried dye or antibody material, which is very light and susceptible to both physical disturbance and electrostatic interactions with nearby materials, could be escaping the vials or sample wells during the freeze-drying process. This would explain some of the variation between samples within each batch of results behaving differently, since a lower mass of dye or antibody present in the sample well or vial would mean a lower concentration in the reconstituted sample, and therefore a lower fluorescent intensity or antibody binding signal.

Since at this stage in the work the loss of material from gamma radiation samples during freeze-drying had become apparent, a series of experiments were carried out with the new sample blocks to optimise the drying process prior to further particle radiation tests.

3.2.4.1 Initial freeze-drying experiment with sample blocks – materials and methods

The sample blocks for each experiment were prepared in the same way. 10 μ l of either 1mg.ml⁻¹ fluorescein in RO water or 1mg.ml⁻¹ chicken egg albumin in 10mM PBS pH7.4 were added to a number of sample wells in each block. Chicken egg albumin was used as the anti-atrazine scAb was available in only limited quantity, whereas chicken egg albumin is a similar size protein readily available and was expected to have very similar physical properties to the antibody fragment. The sample blocks were then placed into a freezer at -80°C for at least 3 hours. Immediately prior to freeze-drying, the sample blocks were placed into a petri dish, in an attempt to prevent the initial rapid depressurisation and re-pressurisation of the freeze-drier sample chamber by application and removal of the vacuum which could produce air flows. Air flows could disturb the frozen or dried material and remove bulk amounts of samples from the wells. The petri dish was then placed in the freeze-drier and the vacuum applied as quickly as reasonably achievable to minimise the chance of the fluorescein and antibody samples melting. After the freeze-drying process was complete the samples were examined for any signs of material disturbance. They were not used in radiation exposures or analysed except by visual inspection, since the purpose of this series of experiments was simply to determine whether material loss from the sample wells was a cause of poor reproducibility in the previous work.

3.2.4.2 Initial freeze-drying experiment with sample blocks – results and discussion

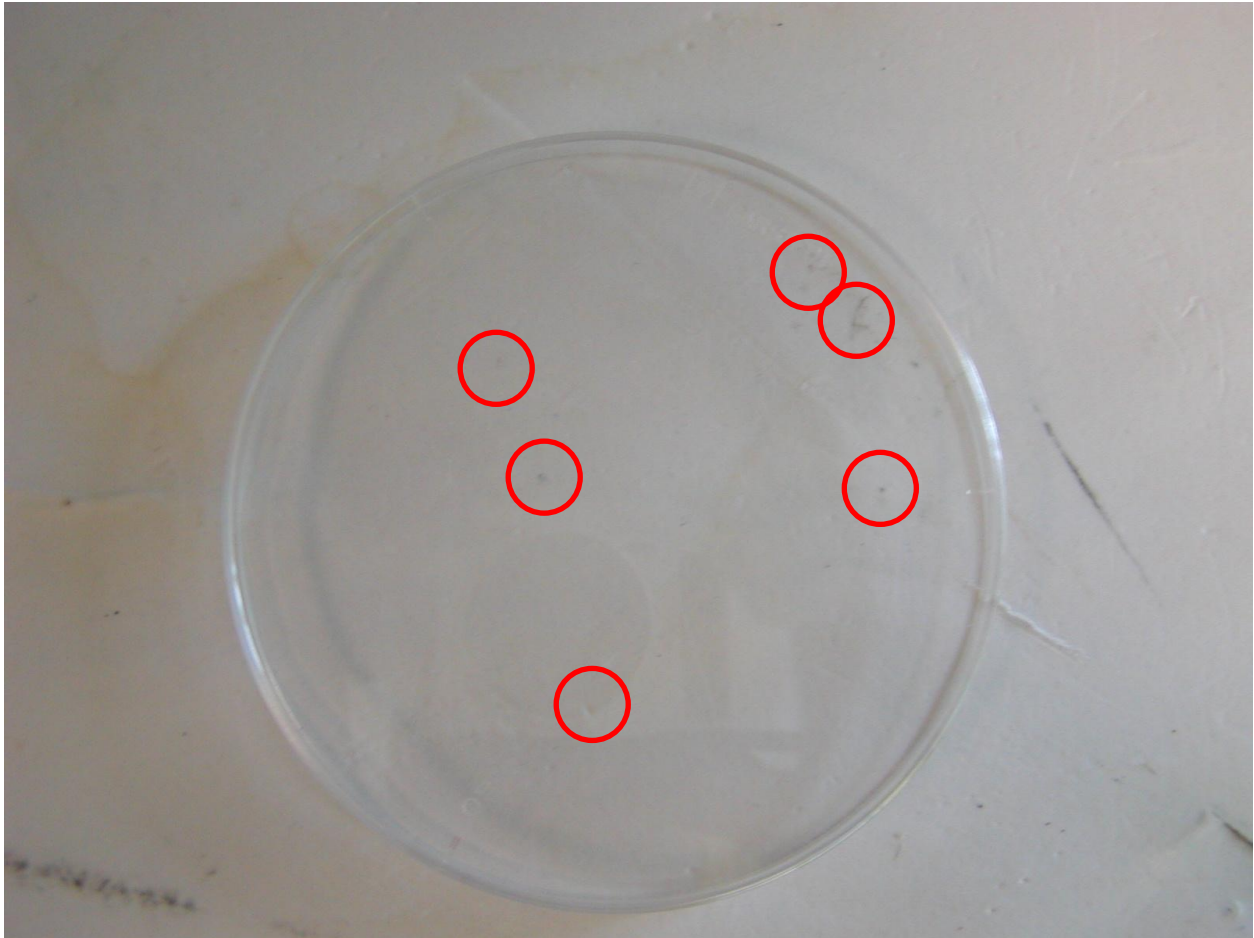


Figure 3.6: A petri dish used as a baffle to protect sample clocks during the freeze-drying process.

Figure 3.6 shows a photograph of a petri dish used to protect the sample blocks from the pressure change on application or deactivation of the vacuum pump, after completion of the freeze-drying cycle and removal of the sample blocks. There are blue deposits visible on the inner surface of the petri dish lid (areas circled in red in Figure 3.6). These match up precisely with the locations of the sample blocks within this petri dish during the freeze-drying protocol. This indicated that sample was being transported from the sample block well to the inner surface of the petri dish by some mechanism. Importantly this observation confirmed that the freeze-drying protocol was a source of experimental error that could be the cause of the discrepancy between control samples and those exposed to protons in the initial experiments (see sections 3.2.3.2 and 3.2.3.3).

There are a number of potential causes of this transportation of sample material, of which the most likely were considered to be electrostatic charge build-up between the polypropylene sample blocks and the polystyrene petri-dish, or the presence of an air

bubble in the liquid samples after pipetting into the sample block which would be a source of outward pressure under vacuum and could cause frozen material to be ejected from the sample block. Melting of the frozen sample material particularly at the interfaces could also contribute to enabling either of these processes to remove sample material from the wells.

3.2.4.3 Experiment to eliminate causes of material loss from sample wells – materials and methods

A number of alternative sample preparation protocols were tested to try to find a way to prevent this sample loss, using chicken egg albumin as a model protein solution and fluorescein as a fluorescent dye solution, since it is cheaper than Alexa Fluor[®] 633 and has similar physical properties.

The first of these was to try to minimise or eliminate electrostatic charge build-up as a potential cause of material loss, by wrapping both the petri dish and individual sample blocks in aluminium foil (see Figure 3.7). The sample blocks were pierced above each the wells in order to allow sublimed water to easily escape from the wells during freeze-drying.



Figure 3.7: Petri-dish and sample blocks wrapped in aluminium foil

These sample blocks and petri dishes wrapped in aluminium foil were used in two experiments, firstly as in the previous experiment using them directly after the 3 hour incubation at -80°C , and secondly with the addition of an immersion of the sample blocks in liquid nitrogen (see Figure 3.8) immediately prior to the freeze-drying, as this would ensure that the samples were at a lower temperature at the start of the freeze-drying process and would therefore be less likely to melt during transfer into the freeze-drier. Samples were held partly immersed in liquid nitrogen until they had been cooled sufficiently to ensure that they had cooled to the temperature of the liquid nitrogen (as judged by the cessation of boiling liquid nitrogen around the sample block), then fully immersed for approximately 2 minutes. The sample blocks were then immediately transferring into the freeze-drier and the freeze-drying cycle started.

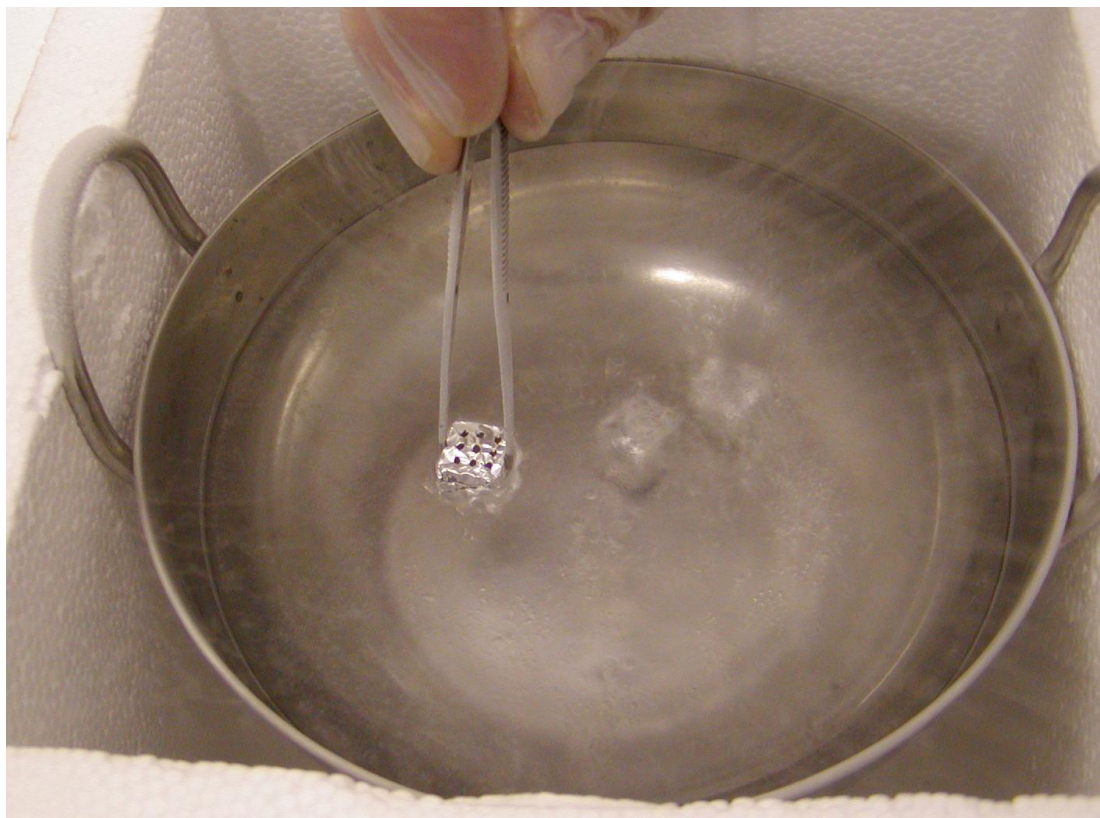


Figure 3.8: Immersion of Sample Blocks in Liquid Nitrogen

3.2.4.4 Experiment to eliminate causes of material loss from sample wells – results and discussion

The foil-covered petri dish top used in this experiment is shown in Figure 3.8. Spots of a white material, the chicken egg albumin, have been deposited on the foil covering and are clearly visible above each location where a sample block had been placed during the freeze-drying. Orange-red spots are also present near the white spots, indicating that some fluorescein has also been deposited on the petri-dish lid, therefore both proteins and dyes escape the sample wells during the freeze-drying process.

There are two possible explanations for this. The first is that air bubbles are present in the liquid samples when they are placed in the wells prior to freeze-drying. Throughout this series of sample preparation development experiments, various pipetting techniques were used in order to try to minimise or prevent the inclusion of air bubbles within the solutions when placing them into the sample blocks. While bubble formation could be prevented in most cases by a skilled operator, it was not possible to prevent completely.

An alternative explanation is that material is removed from the well either as it is freeze-dried (and therefore changes to a free powder rather than being frozen in ice) due to electrostatic interactions, or when the sample chamber is re-pressurised at the end of the freeze-drying sample, as the in-rush of air disturbs the dried materials in the sample wells. This was tested by visually observing a petri-dish containing sample blocks prepared as described in section 3.2.4.3 (without foil wrapping) during a freeze-drying cycle. Observation during this test revealed that some material was removed from the sample block wells almost immediately after the vacuum was applied, and built up on the petri-dish lid throughout the freeze-dry cycle. This eliminated the presence of bubbles in the samples when they were frozen as a cause of material loss (since such an effect would result in the rapid removal of a large amount of sample from the wells almost immediately after applying the vacuum). However, the cause of material loss was still unknown, since coating the surfaces with aluminium foil should have prevented electrostatic effects.



Figure 3.9: The foil coated lid of a petri-dish after a freeze-drying cycle, clearly showing material escaping the sample block wells and building up on the surface of the aluminium foil.

3.2.4.5 Solution to sample preparation issues associated with freeze-drying

Since neither of the protocols described in sections 3.2.4.1 and 3.2.4.3 were successful in preventing the loss of material from the wells in the sample block, and the difficulties with freeze-drying the samples to prepare them for radiation treatments could not be overcome easily, a different approach was adopted. In all subsequent experiments the antibody and fluorescent dye samples were dried down instead of freeze-dried. This was carried out by placing filled sample blocks in a sealed container containing excess self-indicating silica gel desiccant, and placing the container in a 37°C oven overnight. This simple drying procedure overcame the difficulties with sample preparation by freeze-drying, although the samples were likely to contain trace amounts of water absorbed from the ambient environment during the radiation exposures. It is also likely that the presence of water would enhance any damage caused by particle irradiation, so these conditions are consistent with the over-test philosophy adopted throughout this series of experiments.

3.2.5 Particle radiation testing with modified sample preparation and exposure procedures

At this stage an experimental method had been developed that allowed samples exposed to the cyclotron beam in sample blocks (which contained nine wells and were used to carry out triplicate exposures of up to three sample types), rather than doing multiple exposures in different locations on the same microtitre plate. This development of the method significantly reduced the level of background radiation during the particle radiation exposures because each sample block was only placed into the cyclotron vault during one exposure. In addition the sample preparation procedure had been modified to prevent the loss of material from the sample block wells by drying down the samples rather than freeze-drying. As mentioned in section 3.2.3.3, the calculation of the mission fluence of protons for the cruise phase of a nominal Mars mission during the 'on' season for solar flares was modified to correct for the error in the previous experiment. With these new methods, a second round of testing was carried out at the cyclotron facility at the University of Birmingham.

The final value for the mission fluence of protons would have been difficult to use for sample exposures. This is because, even with the lowest stable beam current from the cyclotron, the exposure time would be in the order of seconds, which would be difficult to carry out accurately and reproducibly given that the proton beam was turned on and off by manually controlling a Faraday cup (as described in section 3.2.1.1). Therefore the lowest level of exposure used in this experiment was ten times the mission fluence.

3.2.5.1 Proton radiation testing with modified sample preparation and exposure procedures – materials and methods

10 μ l of either 1 mg.ml⁻¹ fluorescein in RO water, 1mg.ml⁻¹ Alexa Fluor 633 in RO water or 0.3mg.ml⁻¹ anti-atrazine scAb in 10mM PBS pH 7.4 was carefully pipetted into the sample block wells in a random known pattern. The sample blocks were then placed into a sealed container with excess self-indicating silica hydride desiccant, and the container stored in a 37°C oven overnight to remove the water from the solutions.

In an attempt to test the samples to destruction, exposures of 10 times, 100 times and 10,000 times the mission fluence of protons were carried out. The proton exposures in this experiment were carried out at 9MeV, the lowest energy proton beam the cyclotron

can generate. The current used for the 10 and 100 times mission fluence was 50pA, and a 500pA current was used for the 10,000 times mission fluence.

After the exposures the samples were transported to Cranfield University. The fluorescein and Alexa Fluor[®] 633 samples were reconstituted as described in section 3.2.1.1, such that the final concentration of both fluorescein and Alexa Fluor[®] 633 was 0.05mg.ml⁻¹, and their peak emission and excitation wavelengths and intensities measures in a Cary Eclipse Varian Spectrophotometer. The anti-atrazine scAb samples were reconstituted and an ELISA assay carried out as described in section 3.2.1.1.

3.2.5.2 Proton radiation testing with modified sample preparation and exposure procedures – fluorescent dye results and discussion

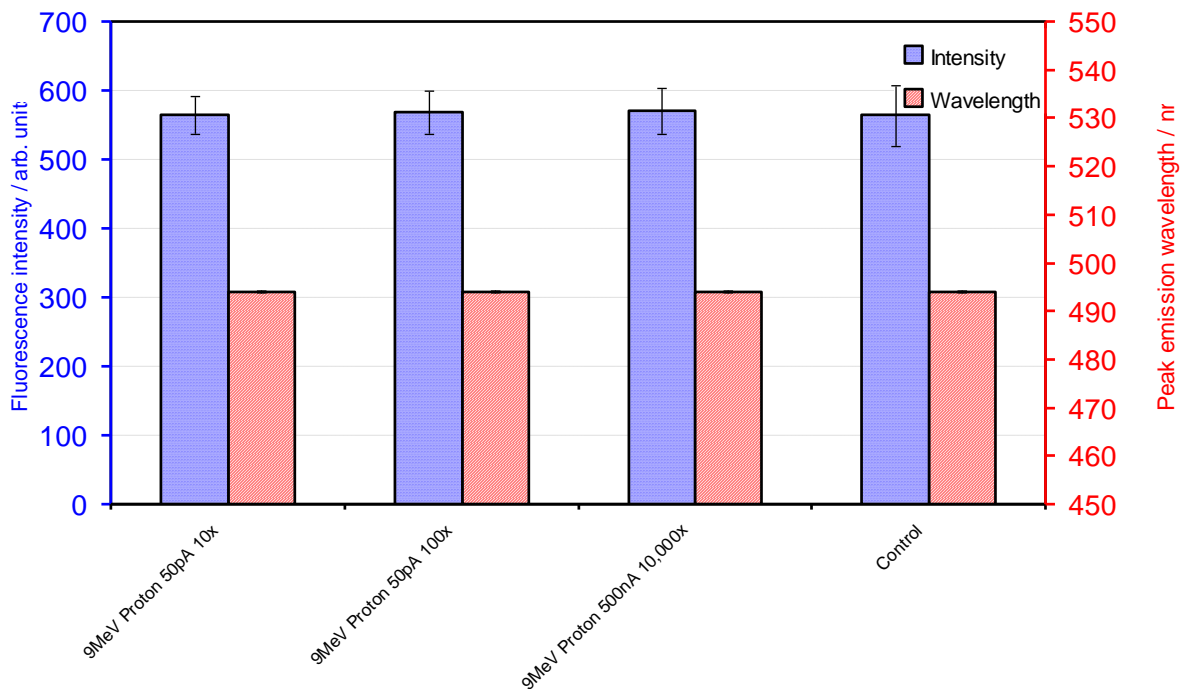


Figure 3.10: Effect of proton radiation (10, 100 and 10,000 times the mission fluence) on the fluorescent properties of fluorescein. The error bars represent the standard errors of the mean values of triplicate samples.

Figure 3.10 shows the effects of the proton radiation exposures on the fluorescent emission properties of fluorescein. Only the emission data is shown, but the absorption properties were also tested and found to correlate with the emission results i.e. no changed in peak excitation wavelength were observed, and slight variations in emission intensity were matched the excitation intensity results. It is apparent that none of the 9MeV proton exposures, even up to 10,000 times the expected mission fluence, had a

significant effect on either the peak emission wavelength or emission intensity of fluorescein, and this was confirmed by Student's T test ($P = 42.87\%$, 51.59% and 65.54% for 10x, 100x and 10,000x the mission fluence of protons, respectively) compared to the control sample which was not exposed to any particle radiation.

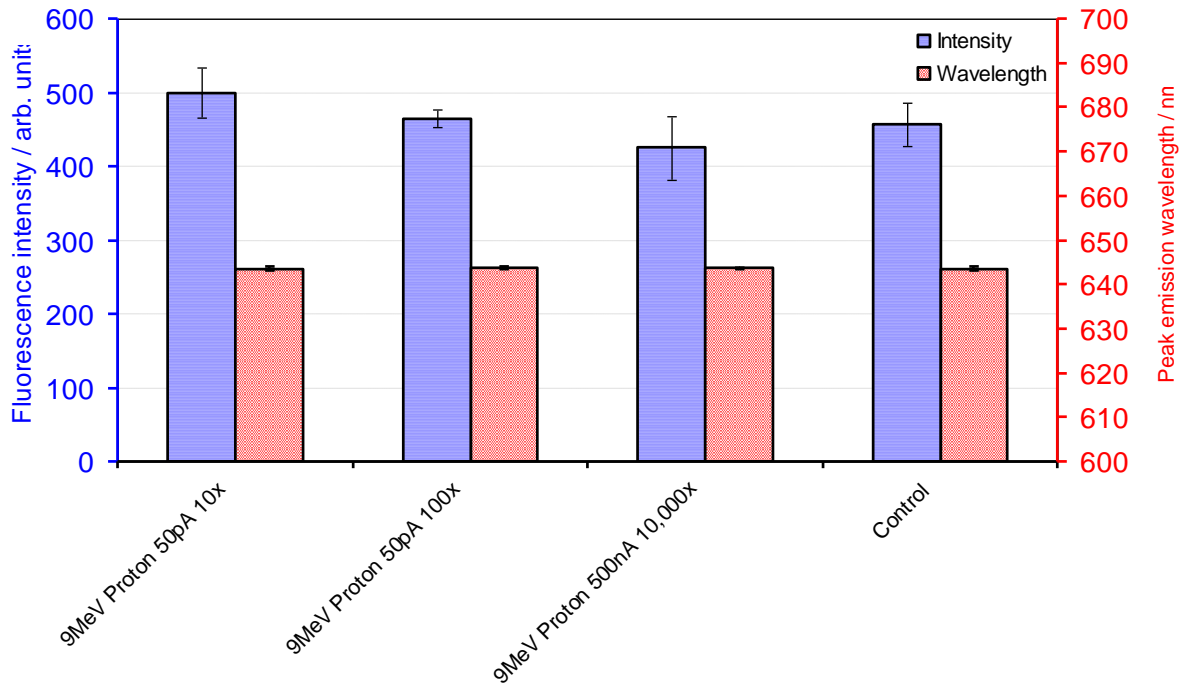


Figure 3.11: Effect of proton radiation (10, 100 and 10,000 times the expected mission fluence) on the fluorescent emission properties of Alexa Fluor[®] 633. The error bars represent the standard errors of the mean values of triplicate samples.

Figure 3.11 shows the effects of the proton radiation exposures on the fluorescent emission properties of Alexa Fluor[®] 633. As for the fluorescein, only the emission data is shown in this thesis, but the absorption properties were also tested and found to correlate with the emission results. It was also found that none of these 9MeV proton exposures significantly affected either the peak emission wavelength or emission intensity of Alexa Fluor[®] 633, as Student's T tests on the fluorescent intensity gave probabilities of 70.53%, 48.95% and 44.98% of the samples exposed to 10x, 100x and 10,000 times the mission fluence of protons (respectively) being different from the control sample which was not exposed to any particle radiation.

3.2.5.3 Proton radiation testing with modified sample preparation and exposure procedures – antibody results and discussion

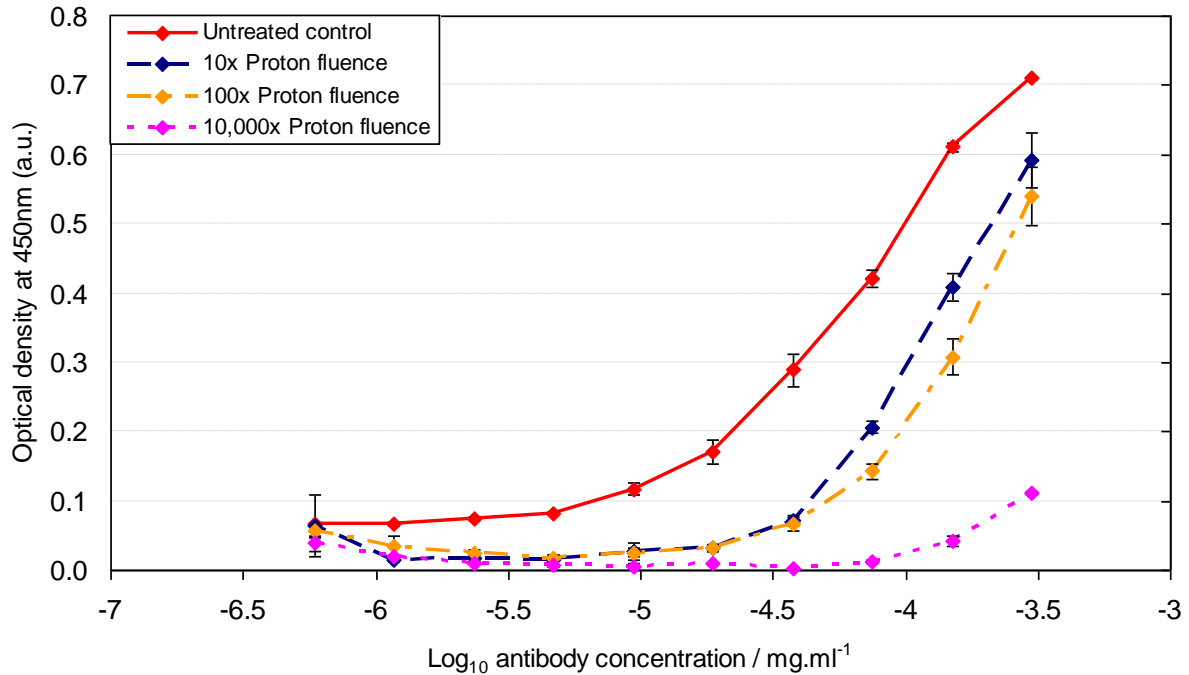


Figure 3.12: Effect of proton radiation (10, 100 and 10,000 times the mission fluence) on the binding properties of a representative recombinant antibody (anti-atrazine scAb). The error bars represent the standard errors of the mean values of triplicate samples.

Figure 3.12 shows the effect of 10, 100 and 10,000 times the calculated mission fluence of protons on the antigen binding properties of the anti-atrazine antibody fragment. The red solid line curve shows the binding curve of the untreated control. This shows a sigmoid binding curve as expected, although the top of the curve is not visible at the range of antibody concentrations used in this experiment. The binding curves for anti-atrazine scAb exposed to 10 and 100 times the mission fluence appear to show that the binding affinity of the antibody decreases with exposures to greater proton fluences. Overall the antibody binding signal (indicated by optical density) has been reduced to 50-75% of the untreated antibody. There are two possible causes of this effect. One is that all antibody molecules were equally affected by proton damage, although it is difficult to conceive of a mechanism by which many antibody molecules would lose a similar level of activity when damaged by ionising radiation at an energy level easily sufficient to break a covalent bond. The second explanation is that antibody molecules damaged by ionising radiation would in most cases be rendered inactive and possibly be fragmented, but that a significant proportion of antibody molecules would not be affected by such interactions. Further tests, such as analysis of irradiated antibody

samples by electrophoresis, MALDI-TOF-MS and thin layer chromatography need to be carried out to determine which of these hypotheses is correct.

Although the precise mechanism of damage remains unconfirmed, it is apparent that the antibody is damaged in some way by proton irradiation. However, a significant proportion of the antibody signal (<50%) is retained even at 100 times the expected mission fluence of protons for the ExoMars mission. This is a key result, particularly considering the “worst case” scenarios used for this proton damage test i.e. that the radiation model used to calculate the proton fluences did not take into account any spacecraft radiation shielding, and no attempt was made to reduce the effect of ionising radiation on the antibody e.g. by the addition of ascorbate or other free-radical scavengers. This result indicates that the expected mission fluence of protons for ExoMars does not cause a critical level of damage to antibodies, therefore supporting the use of antibodies in the Life Marker Chip.

The exposure to 10,000 times the mission fluence of protons appears to have shown that the antibody has lost almost all of its activity. However, observation of the sample blocks after the exposures indicated that a different factor may have contributed to this. Figure 3.13 shows the sample blocks after the particle radiation exposures and removal of the fluorescent dye and antibody fragment samples. Note that sample block 3 in the lower right of the image appears to have a more curved and reflective upper surface than the other sample blocks. This change in appearance was thought to be due to the higher beam current of protons used in this exposure (500pA) compared to the other proton exposures (50pA). A higher beam current would mean a faster rate of proton impacts i.e. energy generation and less time for heat loss from the sample block, and this build up of energy could have caused the surface of the sample block to begin melting.

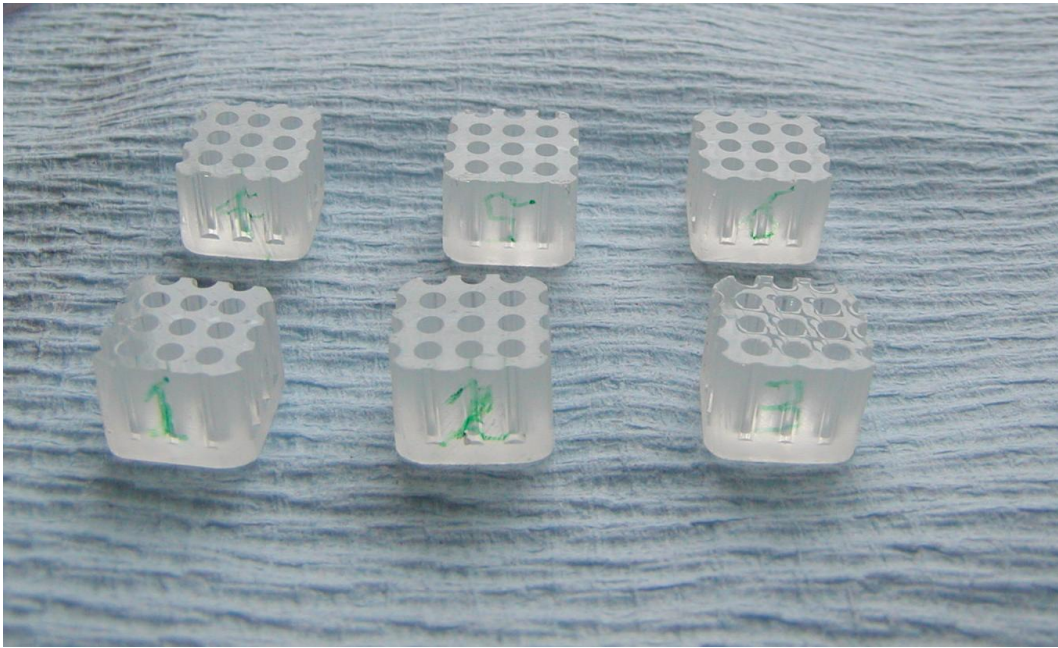


Figure 3.13: Sample blocks after proton and helium ion exposures. Note the surface appearance of block no. 3 (bottom right) is different from the other sample blocks

This melting would in turn transfer heat into the samples, which in the case of antibodies would disrupt hydrogen bonding and therefore cause significant structural damage, resulting in the loss of the specific binding properties of the antibody to its antigen. This would considerably reduce the binding signal for this sample block regardless of the effect of the proton radiation alone.

3.2.5.4 Helium ion radiation testing with modified sample preparation and exposure procedures – materials and methods

Helium ion exposures were also carried out in this experiment. Since less data was available regarding the expected mission fluence of helium ions than for protons, the assumption was made that the same number of helium ion particles as protons would be encountered. This is a greatly exaggerated value, since the number of helium ions would in fact be approximately one third of the number of protons (see Figure 3.13), but the same value was used to ensure an 'over-test' was carried out in the absence of accurate data. The helium ion fluences used in this experiment were ten and 100 times this overestimated mission fluence. The helium ion exposures in this experiment were carried out at 30MeV using a beam current of 50pA.

After exposure to the particle radiation beam the sample blocks were wrapped in aluminium foil and stored in a sealed petri dish containing silica hydride desiccant, to prevent moisture affecting the samples. The fluorescent dyes were then reconstituted as described in 3.2.1.1, and analysed in the Cary Eclipse Varian Spectrophotometer.

The scAb antibody fragments were reconstituted to a concentration of $0.3\mu\text{g.ml}^{-1}$ and analysed by ELISA, following the same protocol described in section 3.2.1.1

3.2.5.5 Helium ion radiation testing with modified sample preparation and exposure procedures – fluorescent dye results and discussion

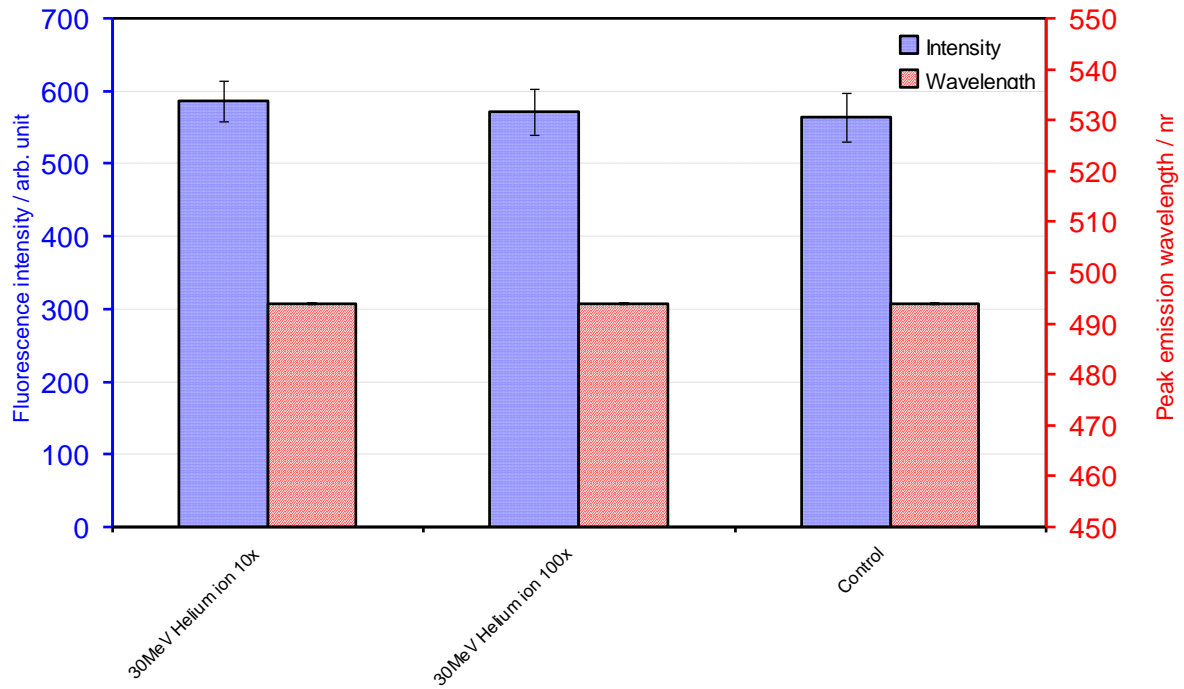


Figure 3.14: Effect of helium ion radiation (10 and 100 times the mission fluence) on the fluorescent properties of fluorescein. The error bars represent the standard errors of the mean values of triplicate samples.

Figure 3.14 shows the effects of the helium ion radiation exposures on the fluorescent emission properties of fluorescein. As in the previous experiments, only the emission data is shown but the absorption properties were also tested and found to correlate with the emission results. It is immediately clear that neither of the 30MeV helium ion radiation exposures had a significant effect on either the peak emission wavelength or emission intensity of fluorescein, since all of the exposed samples have very similar emission properties to the control sample, which was not exposed to any particle radiation. This was confirmed by Student's T test on the fluorescent intensity of the samples (P = 68.41% and 61.25% for 10x and 100x the expected mission fluence of helium ions, respectively).

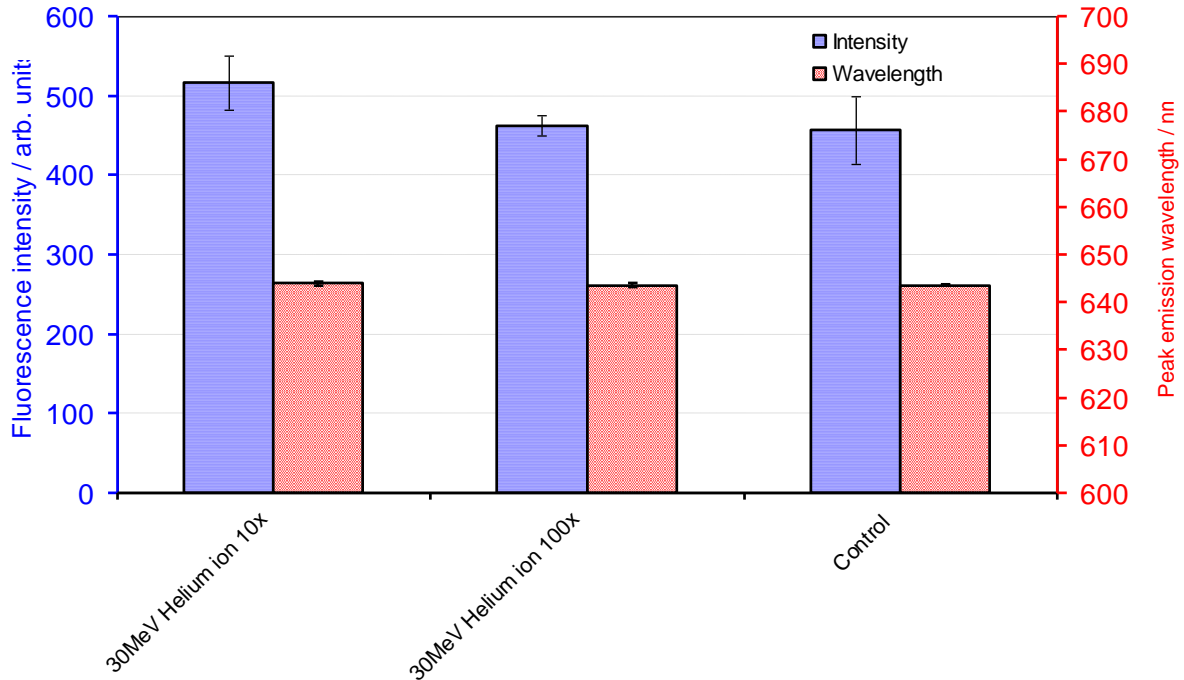


Figure 3.15: Effect of helium ion (10 and 100 times the mission fluence) radiation on the fluorescent properties of Alexa Fluor® 633. The error bars represent the standard errors of the mean values of triplicate samples.

Figure 3.15 shows the effects of these radiation exposures on the fluorescent emission properties of Alexa Fluor® 633. As for the results of the analysis of the fluorescein samples, 30MeV helium ion radiation exposures have not had a significant effect on either the peak emission wavelength or peak emission intensity of Alexa Fluor® 633 (P values for the fluorescent intensities being different from the control samples were 79.74% and 46.05% for 10x and 100x the mission fluence of helium ions respectively, calculated by Student’s T test). These results indicate that particle radiation does not induce changes in the peak absorption or emission wavelengths of fluorescent dyes. This is an important finding for the LMC instrument development, as it means that the choice of wavelength for the excitation light source in the flight instrument and the wavelength for which the fluorescent readout system will be optimised, will not be complicated by radiation-induced changes to the fluorescent dyes.

3.2.5.6 Helium ion radiation testing with modified sample preparation and exposure procedures – antibody results and discussion

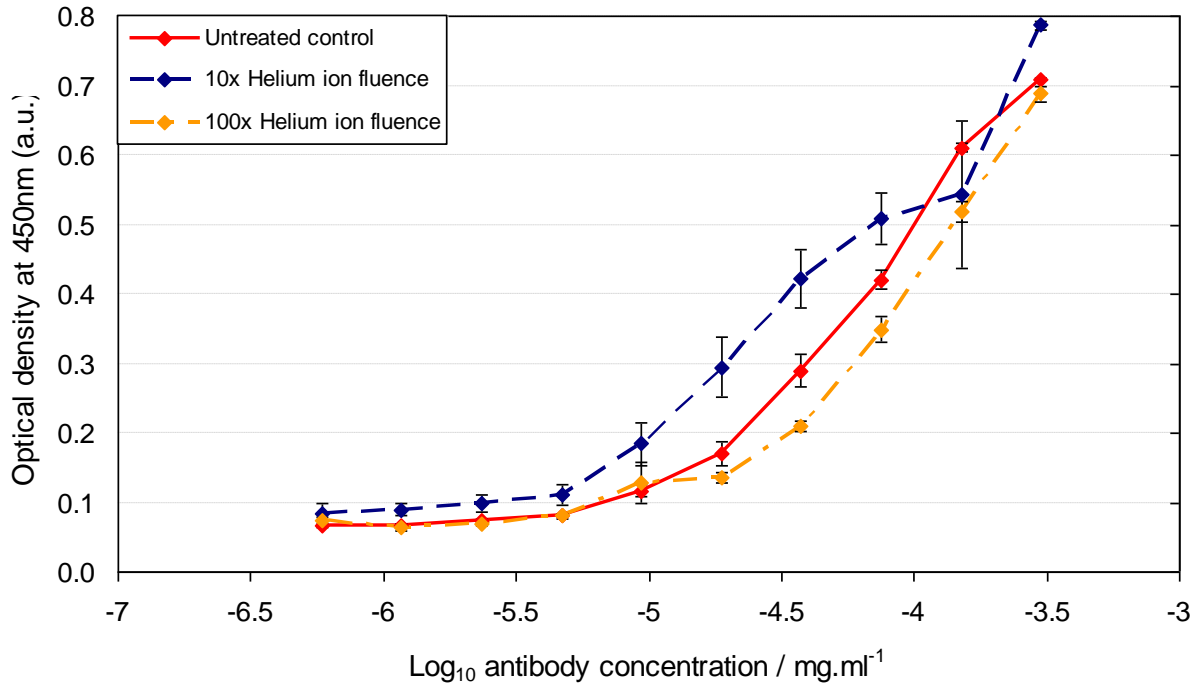


Figure 3.16: Effect of helium ion radiation (10 and 100 times mission fluence) on the binding properties of a representative recombinant antibody (anti-atrazine scAb). The error bars represent the standard errors of the mean values of triplicate samples.

Figure 3.16 shows the effect of 30MeV helium ions at 10 and 100 times the calculated mission fluence on the binding affinity of anti-atrazine antibody fragment. While the antibody exposed to ten times the mission fluence of helium ions at 30MeV shows a slightly misshapen binding curve, this could be due to experimental error rather than an affect on the antibody caused by radiation damage. Neither the 10 nor 100 times the mission fluence of helium ions have resulted in complete inactivation of the antibody, in fact neither treatment appears to have had a significant effect. As was the case for all previous radiation treatments, this result shows that radiation effects do not fundamentally rule out the use of antibodies in the ExoMars mission scenario.

3.2.5.7 Particle radiation testing with modified sample preparation and exposure procedures – reproducibility

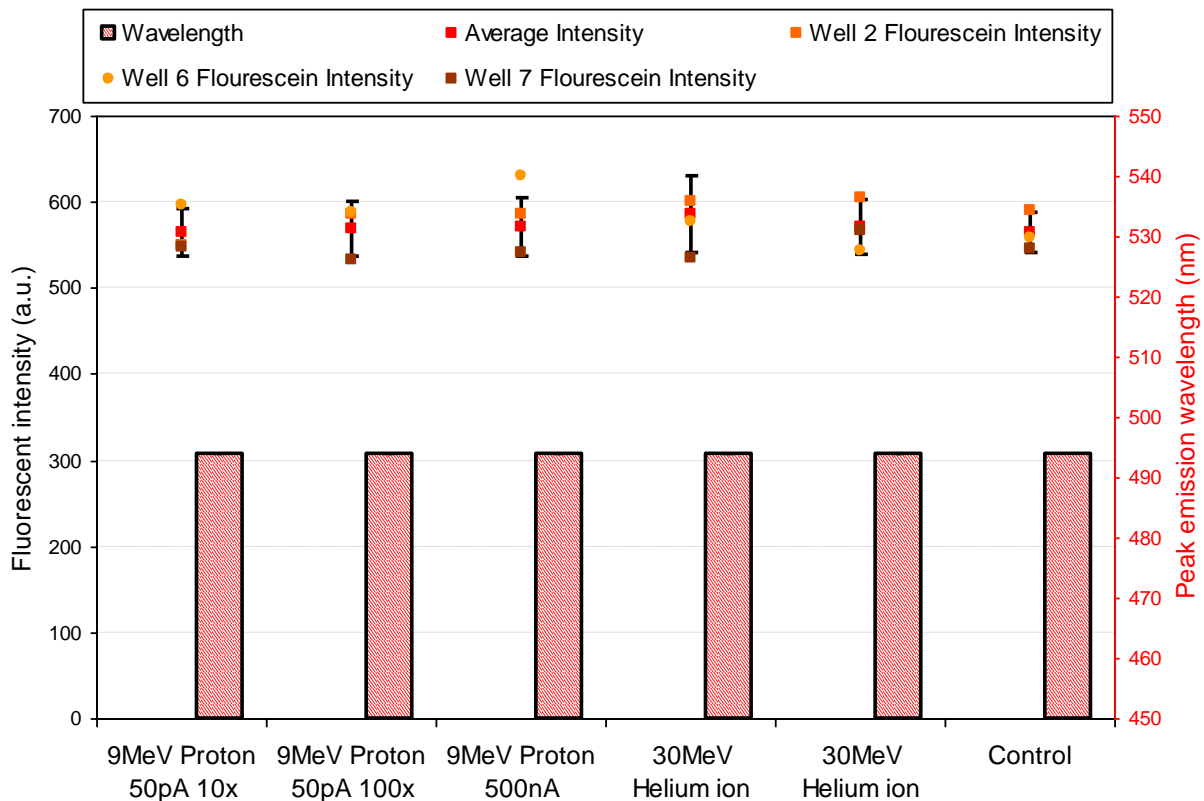


Figure 3.17: Effect of proton and helium ion radiation on the fluorescent properties of fluorescein samples in Figure 3.10 and Figure 3.14 showing the intensities of each sample. The well numbers refer to the sample block wells containing fluorescein samples (wells 1, 5 and 9 contained Alexa Fluor® 633, and wells 3, 4 and 8 contained anti-atrazine scAb) The error bars represent the standard errors of the mean values of triplicate samples.

Figure 3.17 shows the reproducibility of the data in Figure 3.10 and Figure 3.14, by including all the individual data points for fluorescent intensity. This is included as a demonstration that the drying-down protocol overcame the reproducibility issues that were encountered with the freeze-drying method.

3.2.6 Summary and discussion of particle radiation testing results

In this section, methods for exposing fluorescent dyes and antibodies to particle radiation at a cyclotron facility have been developed and the protocols refined to improve the reproducibility of the results. The method was then used to carry out a series of proton and helium ion radiation exposures on representative immunoassay components of the Life Marker Chip, including two fluorescent dyes and a recombinant antibody. The results overall support the use of antibodies and fluorescent dyes in

astrobiology missions to Mars, since the peak emission and excitation wavelengths of the dyes were not affected by any of the particle radiation treatments, and the fluorescent intensity of both dyes was not greatly reduced even at radiation levels far in excess of the expected mission dose for ExoMars. A significant loss of antibody binding signal (~50%) was observed at 10 and 100 times the expected unshielded proton radiation dose for the ExoMars mission. However, since a large amount of activity remained this could be taken into account in the configuration of the final instrument, for example by including excess antibody and adjusting the level of dye labelling and optical readout setting to allow for some loss of antibody activity. In addition, these tests were carried out with a “worst case scenario” philosophy in particular assuming that there was no spacecraft shielding in the dose calculations.

A number of other particle radiation tests are still to be carried out, including lower energy levels of protons and helium ions, neutrons and if possible heavy ions. Work is in progress towards carrying out these tests and will be discussed further in section 6.2. In addition to particle radiation, gamma radiation is an important radiation source not only because it is a common secondary radiation type generated from spacecraft shielding, but also because it has been used to sterilise biological materials including antibodies (Grieb *et al.*, 2002) and therefore may provide a method to sterilise the Life Marker Chip for ExoMars. A number of gamma radiation tests were carried out during this work, and will be reported in the following section.

3.3 Gamma irradiation exposure of fluorescent dyes and antibodies

While the spacecraft shielding will significantly reduce the amount of gamma radiation from space reaching the instrument, gamma radiation is likely to be generated as a secondary radiation product when particle radiation interacts with the shielding. As discussed in section 2.1.2.12, the expected gamma radiation levels encountered for the ExoMars mission scenario were calculated based on the NASA Mars Science Laboratory Proposal Information Package, which states that an instrument in the payload module can expect to encounter a total ionising dose of 3.0krads during a 300-day transfer to Mars and one Martian year (687 earth days) of surface operations (MSL PIP, 2004). This was broadly in agreement with the European Space Agency calculation for the ExoMars mission (ESA, 2005).

Based on this, samples were exposed to a range of gamma radiation doses. The initial experiment was a very low dose 150mrad, because at that time only a low energy gamma radiation source was available. This experiment was used to develop the experimental method. A series of gamma radiation exposures from 3krad to 2.5Mrad was then performed using a GammaCell Cobalt-60 source with an output of $\sim 50\text{krad hr}^{-1}$. This GammaCell unit was conveniently available at the University of Leicester and had an output that was compatible with completing exposure to these levels of gamma irradiation in a convenient time period (a few minutes for mission doses, and a few days for sterilisation doses). In addition, GammaCell units are widely used in previous gamma irradiation work in the literature so their use for this type of work has some precedent (Caballero *et al.*, 2004, Grieb *et al.*, 2002).

All of the samples were tested in a dried state, achieved either by freeze-drying or dried at 37°C with desiccant. This was done because the indications from the literature were that biological materials are less likely to be damaged by radiation in a dried state. Liquid controls were also used to determine any effect of the drying procedure on the fluorescent dyes and antibodies.

3.3.1 Preliminary Gamma Irradiation Experiment

Since the exposure of dried biological materials to gamma irradiation is not carried out routinely, the work reported here focuses initially on establishing and developing an experimental protocol, and moves on to using this protocol in a controlled experiment to represent various mission environments. Since this work was carried out concurrently with the proton and helium ion work (reported in section 3.1), there are similarities between the sample preparation methods used and development of the experimental protocols.

3.3.1.1 Preliminary Gamma Irradiation Experiment - Materials and Methods

In the initial experiment, 100 μl of 0.5 $\text{mg}\cdot\text{ml}^{-1}$ fluorescein (Sigma-Aldrich, Poole, UK, Product Code 32615) in RO water was placed into four polypropylene vials. Two of these samples were then dried in a freeze-drier (Edwards Modulyo) overnight, while the samples that were not freeze-dried were stored at room temperature. The samples were then transported to the University of Leicester, where one liquid and one dried

sample were exposed to 150mrad of Gamma radiation in a GammaCell unit. This Gamma cell unit was used because it was conveniently available and similar units have been used in the literature (Caballero *et al.*, 2004, Grieb *et al.*, 2002). The samples that were not exposed to the gamma radiation were subjected to the same transportation and environmental conditions as the dried sample to provide a liquid and a freeze-dried control, which would indicate any effect of the sample handling procedure on the samples. The samples were then returned to Cranfield University, reconstituted in RO water to a concentration of 0.05 mg.ml^{-1} , and the fluorescent properties tested in fluorimeter as described in section 3.2.2.

3.3.1.2 Preliminary gamma irradiation experiment – results and discussion

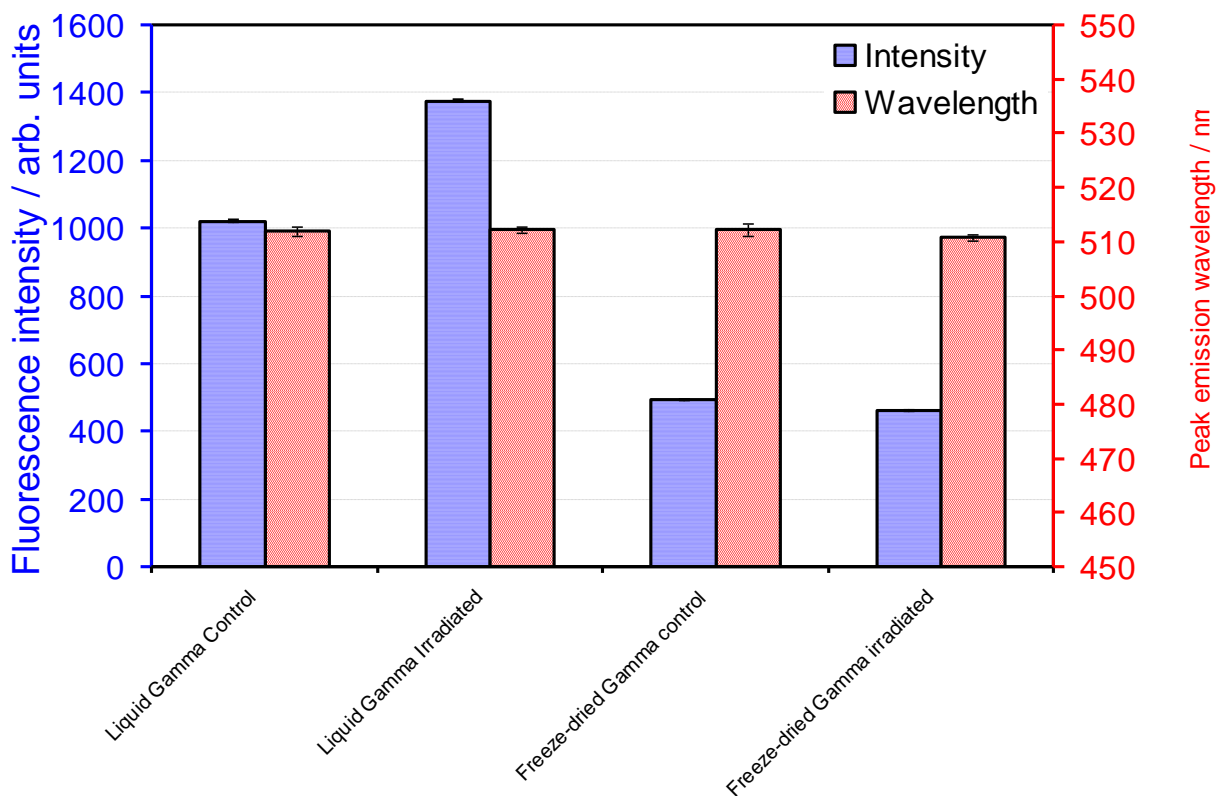


Figure 3.18: Effect of preliminary 150mrad gamma radiation exposure on peak emission wavelength and intensity of fluorescein. The blue bars indicate fluorescent intensity, while the red bars indicate the peak emission wavelength. Since these tests were carried out on single samples, the error bars indicate the reproducibility of the fluorimeter measurements.

Figure 3.18 shows the results of this experiment. The peak emission and excitation wavelengths of each sample were measured, but since the results are directly related i.e. a reduction in fluorescent excitation corresponds to a reduction in fluorescence intensity, and no change in peak emission or absorption wavelengths was observed, only the emission data is shown here. The liquid control sample gives a baseline on where the intensities would be expected if the sample processing and irradiation had no

effect on the fluorescent properties of the dyes. The fluorescein samples that were freeze-dried both appear to have the same peak emission wavelength as the liquid control, but a lower emission intensity. This indicates that while the freeze-drying process may have affected the dye in some way, gamma irradiation of dried fluorescein has little or no effect on the fluorescent properties. The samples exposed to gamma radiation in the liquid state appear to have a higher emission intensity than the control. However in this experiment there was one 1 of each sample type, so it is possible that this variation is caused by the sample handling method. Therefore none of these results can be considered significant other than to state that low dose gamma irradiation does not have a great effect on fluorescein in either the liquid or dried state.

In this initial experiment the free acid form of fluorescein was used, but since this was found to have poor solubility in water (possibly contributing to the variability in experimental results above) it was decided to use a more water-soluble fluorescein sodium salt (Sigma-Aldrich, Poole, UK, Product code 46960) in all future experiments.

3.3.2 Gamma irradiation method development and reproducibility study

Taking the observations from the initial experiment in section 3.2.3.2, including that the use of the fluorescein free acid resulted in problems of making solutions of known concentration due to solubility issues, the methodology for exposing fluorescent dyes to gamma radiation was adapted and a more detailed experiment carried out. In this second experiment, a more representative dye for the Life Marker Chip was also exposed to gamma radiation, namely Alexa Fluor[®] 633. This dye was not used in the initial experiment since it is more expensive than fluorescein and it was desirable to have an established method before using it. Since the Alexa Fluor[®] dye has a higher quantum yield than fluorescein, and is more expensive, the mass of Alexa Fluor[®] 633 dye exposed to gamma radiation in this experiment was lower than the mass of fluorescein, and similarly the concentration of Alexa Fluor[®] 633 tested in the fluorimeter is lower than the concentration of fluorescein used.

3.3.2.1 Gamma irradiation method development and reproducibility study – materials and methods

Triplicate samples containing 100µl of 1.0mg.ml⁻¹ fluorescein sodium salt in RO water, and 10µl 0.1 mg ml⁻¹ Alexa Fluor[®] 633 were prepared in polypropylene vials and dried in

a freeze-drier (Edwards Modulyo) overnight. Corresponding control samples were also prepared and stored in darkness at room temperature during the freeze-drying step. A larger number of control vials (9) containing fluorescein were prepared in this experiment to determine the reproducibility of the sample preparation with fluorescein sodium salt with no gamma radiation exposure. Three samples were exposed to gamma radiation doses of 30 and 300kRad using the GammaCell facility at the University of Leicester. Higher doses were not carried out at this stage since they involved overnight exposures, and it was considered prudent to ensure the exposure method was reproducible before performing longer experiments. The samples were then transported back to Cranfield University, where the fluorescein samples were reconstituted in RO water to a final concentration of $0.01\text{mg}\cdot\text{ml}^{-1}$, and Alexa Flour[®] 633 samples were reconstituted in RO water to a concentration of $0.0001\text{mg}\cdot\text{ml}^{-1}$.

3.3.2.2 Gamma irradiation method development and reproducibility study – fluorescein results

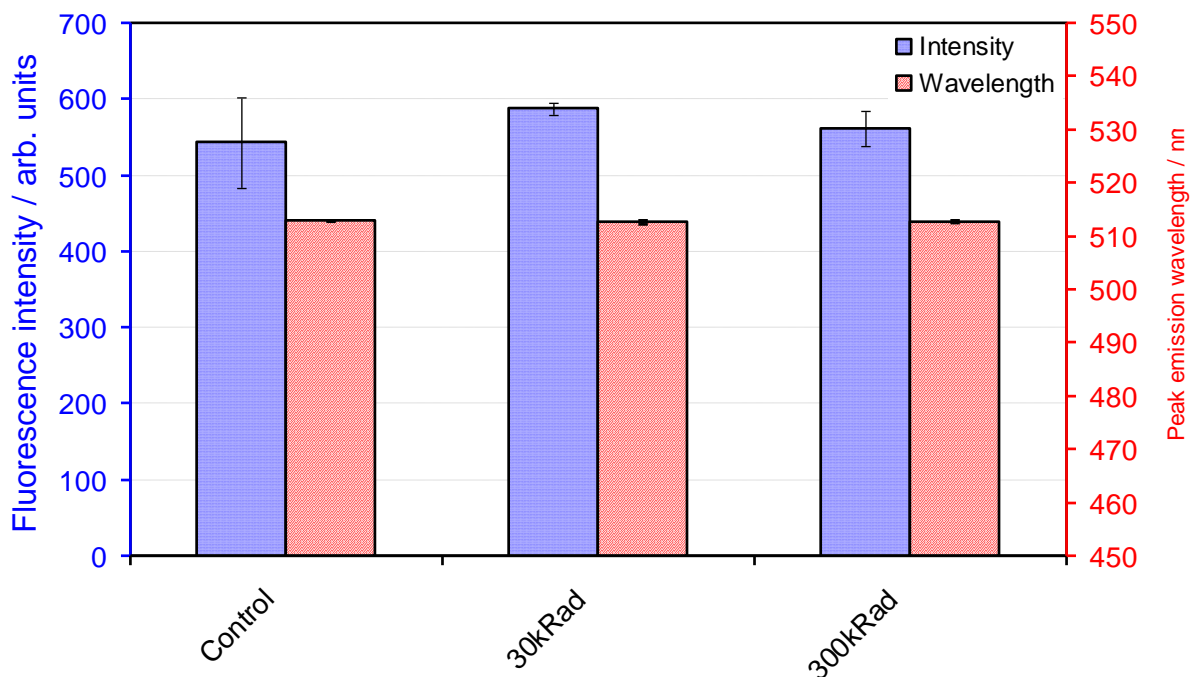


Figure 3.19: Effect of 30krad and 300krad of gamma irradiation on the fluorescent emission properties of fluorescein. The error bars indicate standard errors of the mean intensity. The control result is based on 8 samples, and the 30krad and 300krad gamma exposure results were from triplicate samples.

Figure 3.19 clearly shows that the intensity variation between samples of fluorescein in this experiment was relatively small for the 30krad and 300krad samples, having CV of 4.0% and 10.9% respectively from triplicate samples. The control samples had a CV of

59.2%, but this large value was largely influenced by one particular sample which gave a very low intensity signal, possibly due to an operator error in sample handling. When this sample was removed from the analysis the CV was reduced to 10.4%. The standard error used to calculate the error bar in Figure 3.19 does not include this much lower sample. These results indicate that the drying protocol with fluorescein sodium salt is a reproducible method of preparing fluorescein samples for gamma radiation exposures. Figure 3.19 shows that neither 30krad nor 300krad of gamma radiation had a large effect on either the fluorescent peak emission wavelength or intensity of fluorescein.

3.3.2.3 Gamma irradiation method development and reproducibility study – Alexa Fluor® 633 results

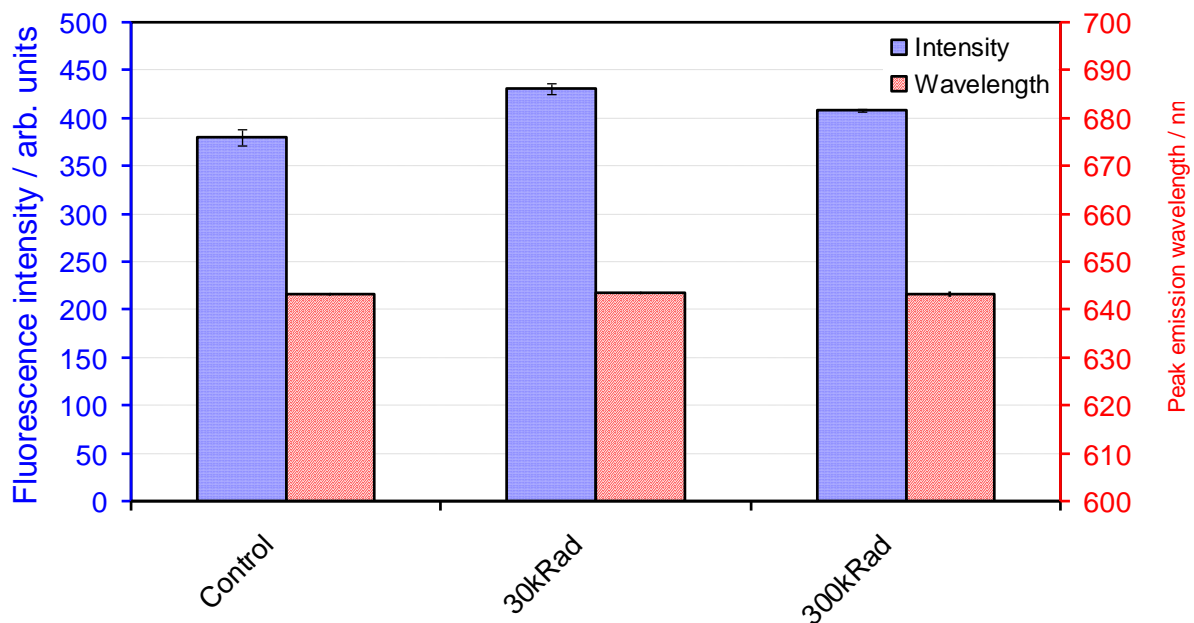


Figure 3.20: Effect of 30krad and 300krad of gamma irradiation on the fluorescent emission properties of Alexa Fluor® 633.

Figure 3.20 shows that neither 30krad nor 300krad of gamma radiation had a significant effect on the fluorescent peak emission wavelength or intensity of Alexa Fluor® 633. Solubility was not considered to be a problem for the Alexa Fluor® 633 dye since this dye is modified to have a high solubility in water. This was supported by observations during the experiment.

3.3.2.4 Gamma irradiation method development and reproducibility study – discussion

Since the nominal mission dose of gamma irradiation for the ExoMars mission is expected to be 3krad and both of these fluorescent dyes appear not to be affected by a ten-fold excess of this mission dose, Gamma radiation damage alone does not rule out use of these dyes for use in the mission. However resistance to other radiation types not tested in this work e.g. neutrons and lower energy levels of protons and helium ions, and combinations of gamma irradiation with other types of radiation must also be considered in future experiments (see Section 6.2). A further experiment was then designed to evaluate the possibility of using a gamma radiation as a sterilisation method, which would require a significantly higher radiation dose than the mission itself.

3.3.3 Investigating the potential for sterilisation of the Life Marker Chip by gamma irradiation

The experiment described in section (3.3.1) had demonstrated that two fluorescent dyes (fluorescein and Alexa Fluor[®] 633) could be exposed to gamma radiation doses significantly higher than the expected mission dose. In this experiment, the same dyes were exposed to the actually mission dose of gamma radiation, and a higher dose corresponding to a gamma sterilisation procedure, in order to build up evidence as to whether gamma sterilisation could be used as a sterilisation technique for the Life Marker Chip.

3.3.3.1 Use of gamma irradiation as a sterilisation technique for fluorescent dyes – Materials and Methods

In a slight modification of the protocol used in the previous experiment (see section 3.3.1), 100µl of 1.0ml.ml⁻¹ fluorescein sodium salt or 10µl of 0.1 mg ml⁻¹ Alexa Fluor[®] 633, both in RO water, was added to polypropylene vials and dried down at 37°C overnight in a sealed vessel containing excess silica gel desiccant. This change was made based on methods developed for the proton and helium ion exposures described in section 3.2.4, which had been found to be more reproducible than freeze-drying. Unlike freeze-drying, trace amounts of water may remain in the sample with this method, as the samples are stored and exposed to gamma radiation in the ambient atmosphere and could absorb water. However, this is not a critical factor for this

experiment since the samples in the flight instrument will be prepared differently, by freeze-drying biological samples into glass-fibre pads (see section 6.2), and the atmosphere and pressure in the flight instrument will be controlled and will remain at low pressure and temperature for most of the mission radiation exposure (Sims *et al.*, 2004). Any enhanced radiation damage due to the presence of water was considered a contribution to the over-test philosophy adopted throughout these radiation tests.

The samples were then exposed to doses of 3kRad and 2.5MRad of gamma radiation in the Gammacell unit at the University of Leicester. The 3kRad dose was representative of the expected mission dose of gamma radiation (MSL PIP, 2004, ESA, 2005), and 2.5MRad was selected as it is in the mid-range of the values selected for sterilisation of antibodies by Grieb *et al.* (2002) and could be carried out in a convenient exposure time at the University of Leicester GammaCell facility.

3.3.3.2 Use of gamma irradiation as a sterilisation technique for fluorescent dyes – results and discussion

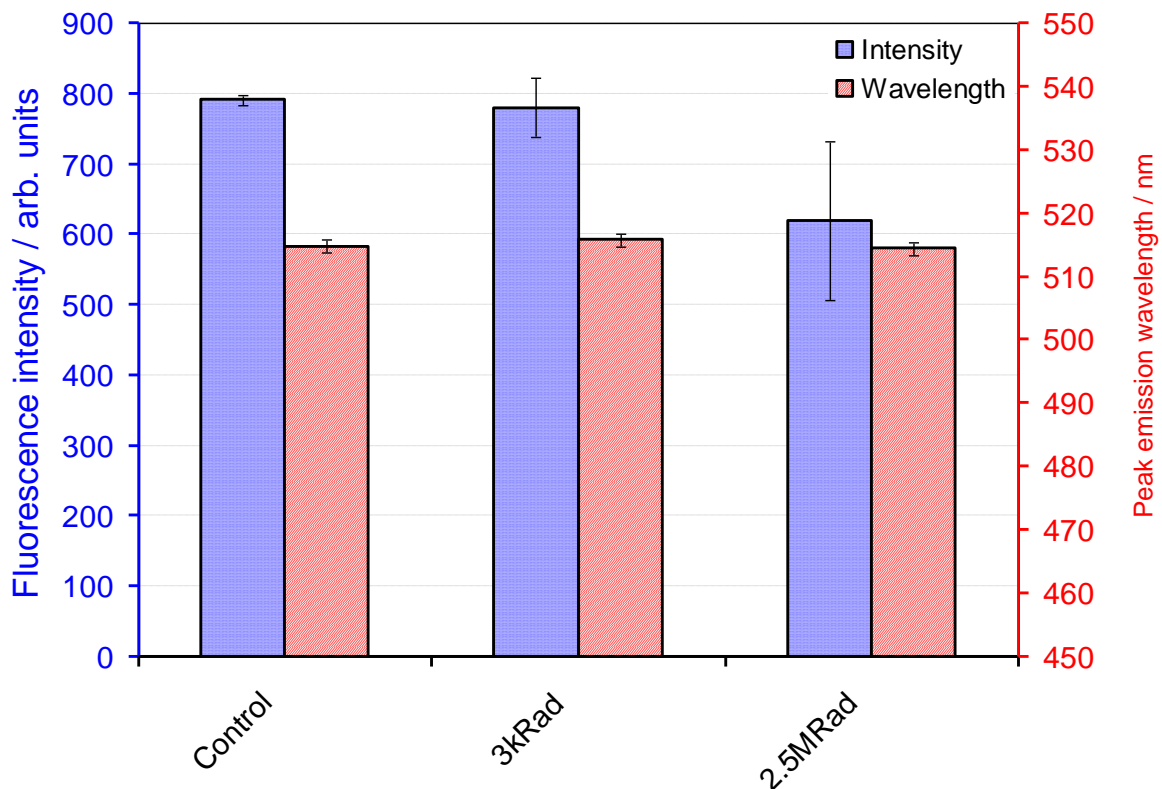


Figure 3.21: Effect of mission and sterilisation doses of gamma irradiation on the fluorescent emission properties of fluorescein

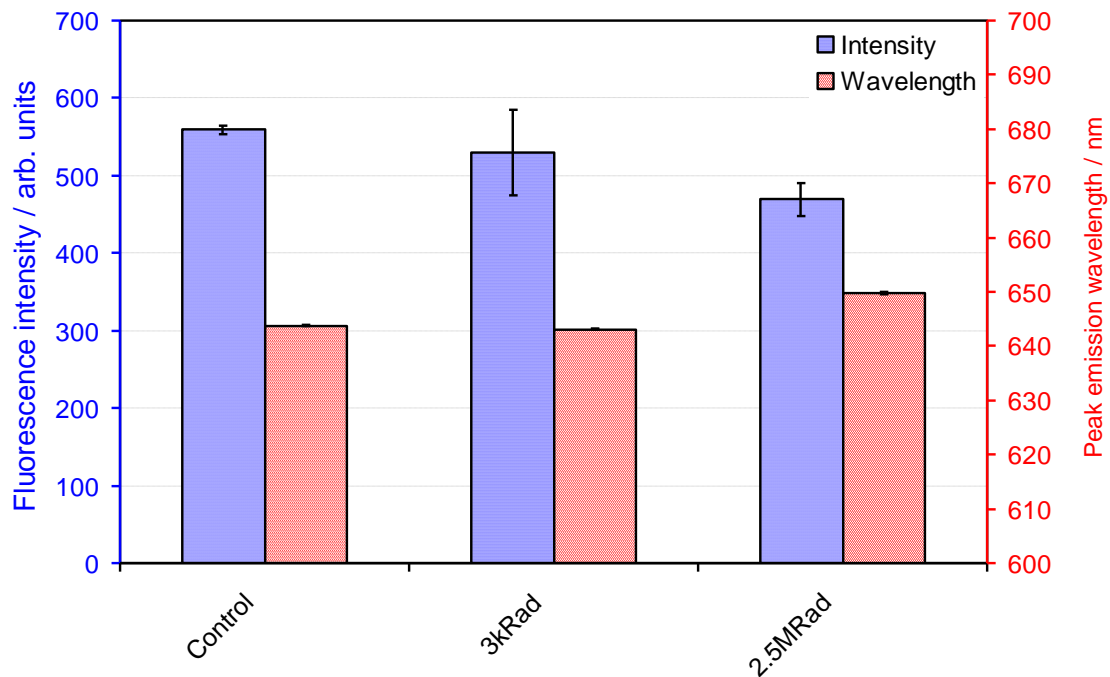


Figure 3.22: Effect of mission and sterilisation doses of gamma irradiation on the fluorescent emission properties of Alexa Fluor[®] 633. The error bars represent standard errors of the mean intensities from triplicate samples.

Figure 3.21 and Figure 3.22 show the effect of these 3kRad and 2.5MRad gamma radiation exposures on the fluorescent emission properties of fluorescein and Alexa Fluor[®] 633 respectively. As expected from the result of the earlier experiments at higher radiation doses (reported in sections 3.3.2.2 and 3.3.2.3), the 3kRad exposure had no significant effect on the peak emission intensity or peak emission intensity of either fluorescein ($P=48.54\%$ by Student's t-test) or Alexa Fluor[®] 633 ($P=67.73\%$ by Student's t-test). The 2.5MRad exposure did appear to reduce the fluorescent intensity of both fluorescein and Alexa Fluor[®] 633. In the case of fluorescein this effect was not statistically significant ($P=84.54\%$ by Student's t-test). For Alexa Fluor[®] 633, the intensity reduction was significantly different from the control ($P=98.04\%$ by Student's t-test), but was not significantly lower than the 3krad exposure ($P=97.39\%$ by Student's t-test). A small reduction in the emission intensity of the dyes would not be expected to be a problem in the flight instrument, since intensity controls, e.g. assay spots containing only fluorescently labelled protein, could be included and used to calibrate the Life Marker Chip for any loss in signal caused by radiation damage to the fluorescent dyes.

Having observed a loss of fluorescent intensity, it is important to understand the mechanism that causes it. Since there has been little or no previous work to characterise the effects of radiation on fluorescent dyes, the potential causes of

intensity loss here are the opinions of the author. There are two possible structural causes of a change in fluorescent intensity in a fluorescent dye. The first is a rearrangement of chemical bonds within the dye to create a new molecular structure that is either not fluorescent or has significantly different fluorescent properties, and the second is fragmentation of the molecule leading to loss of active fluorescent dye. Given that there was no observed change in peak emission or excitation wavelength, fragmentation of the dye seems the more likely explanation since a structural rearrangement would be likely to produce structures that show fluorescence. In addition, gamma radiation is likely to break covalent bonds, also favouring dye fragmentation as the likely mechanism. This could be verified by a chromatography method such as thin layer chromatography, or spectroscopic methods such as nuclear magnetic resonance (NMR) or infra-red spectroscopy. This was not carried out during the work reported here because the primary goal of this work was to determine the functionality of the dyes under radiation conditions rather than to identify any mechanisms of damage. This loss of fluorescent intensity shows that further work is required to characterise any radiation damage to fluorescent dyes at sterilisation doses, and determine possible solutions to any issues this may cause for the Life Marker Chip. These further tests to characterise radiation damage will be discussed further in section 6.2.

3.3.4 Determination of the maximum tolerated gamma radiation dose for fluorescein

The final experiment carried out in this series of gamma radiation tests on fluorescent dyes aimed to establish the point at which gamma radiation would cause complete deactivation of the fluorescent properties of a fluorescent dye. In addition, this was used as an opportunity to carry out a gamma radiation exposure at a number of different doses using samples that were all prepared and analysed at the same time, since the results of the two previous experiments (in sections 3.3.1 and 3.3.2) cannot be directly compared with each other as the sample preparation methods were different. In this experiment, gamma radiation doses of 3krad and 30krad were used for consistency with the expected mission dose and previous experiments, 3Mrad was used as a sterilisation dose rather than the 2.5Mrad used in section 3.3.2.1 since this dose was a more convenient exposure time for this experiment, and 9Mrad was added as a very high dose in the expectation that it would cause a greater level of damage to the dyes than 3Mrad.

3.3.4.1 Determination of the maximum tolerated gamma radiation dose for fluorescein - materials and methods

In order to demonstrate the benefit of removing water from the dyes prior to radiation exposure, and the fluorescein was exposed to a series of gamma radiation doses in both the liquid (aqueous solution) and dried (heated at 37°C overnight) state. 100µl of 1.0ml.ml⁻¹ fluorescein sodium salt in RO water was added to polypropylene vials, then the vials were placed either open (to dry down the dye) or closed (to prepare samples to be exposed to radiation in the liquid state) into a sealed vessel containing excess silica gel desiccant, and the vessel was heated to 37°C overnight. Triplicate samples were then exposed to a series of different doses of gamma radiation (3krad, 30krad, 3Mrad, and 9Mrad) in the Gammacell unit at the University of Leicester. Control samples were also prepared and transported to the University of Leicester under the same conditions as the exposed samples, but were stored at room temperature and not exposed to gamma radiation during the experiment. After the exposures the samples were transported to Cranfield University and the fluorescent properties analysed in the Cary Eclipse Varian Spectrophotometer.

3.3.4.2 Determination of the maximum tolerated gamma radiation dose for fluorescein – results and discussion

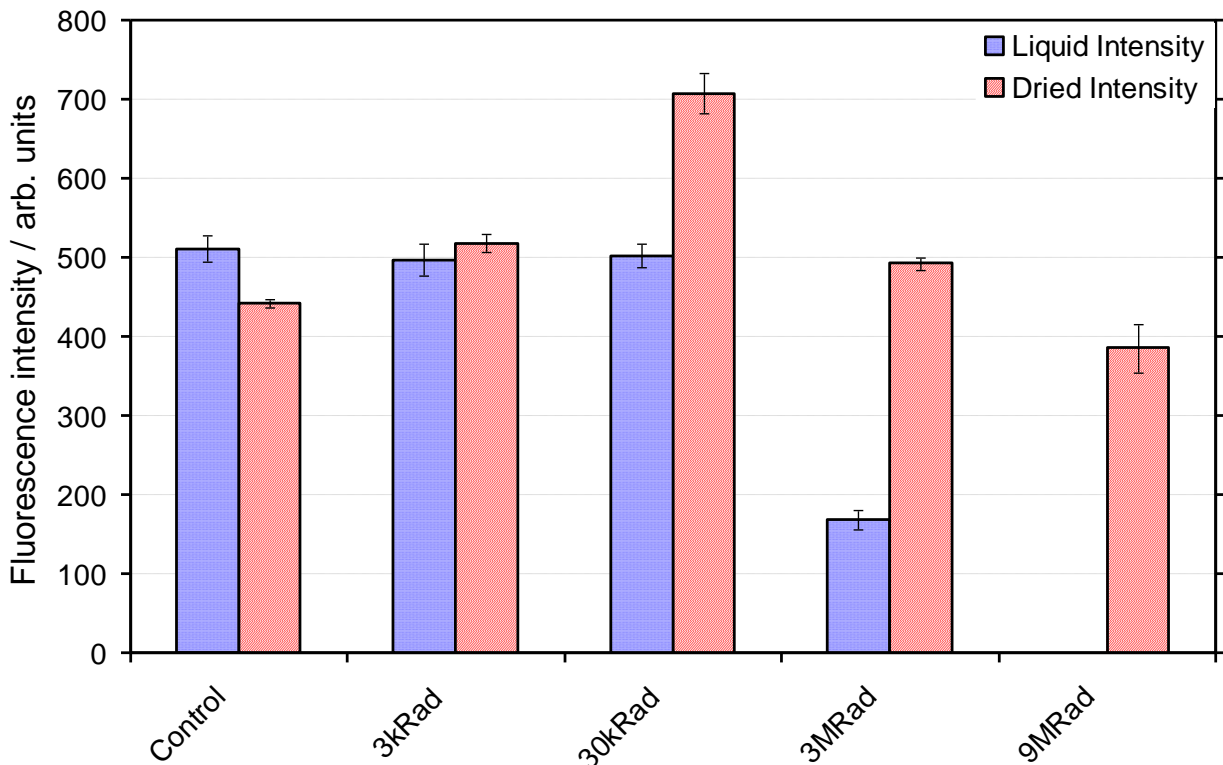


Figure 3.23: Effect of Gamma irradiation on fluorescent emission intensity of dried down and liquid fluorescein. The error bars represent standard errors of the mean intensities from triplicate samples.

Figure 3.23 shows the effect of this series of gamma irradiation doses on the peak emission intensity of fluorescein. It is clear that, in contrast to the initial experiment (section 3.3.1.2), the peak emission intensity of dried fluorescein samples appears to be very similar or slightly greater than the corresponding samples in the liquid state. This shows that the modifications to sample preparation methods throughout this work have resulted in a significantly more reliable protocol. As with the particle radiation sample preparation described in section 3.2.1, this is due to the freeze-drying procedure causing significant loss of material from the sample vials, in particular when the vacuum is applied. The drying down method based on heating at 37°C in a sealed vessel containing desiccant removed the problem of poor reproducibility in sample preparation since a vacuum was not required. Additionally, there appears to be a trend in the dried samples in which lower radiation doses, 3krad and 30krad, show a significantly higher peak emission intensity than the control sample (P=98.59% and 98.72% by Student's t-test, respectively). However at higher gamma exposures, 3Mrad and 9Mrad, the fluorescent intensity is not significantly different from the controls (P=91.18% and 74.23% by Student's t-test, respectively). If this effect were proven to be reproducible with larger sample numbers, gamma radiation treatment could have applications in increasing the emission intensity of fluorescein and possibly other fluorescent dyes.

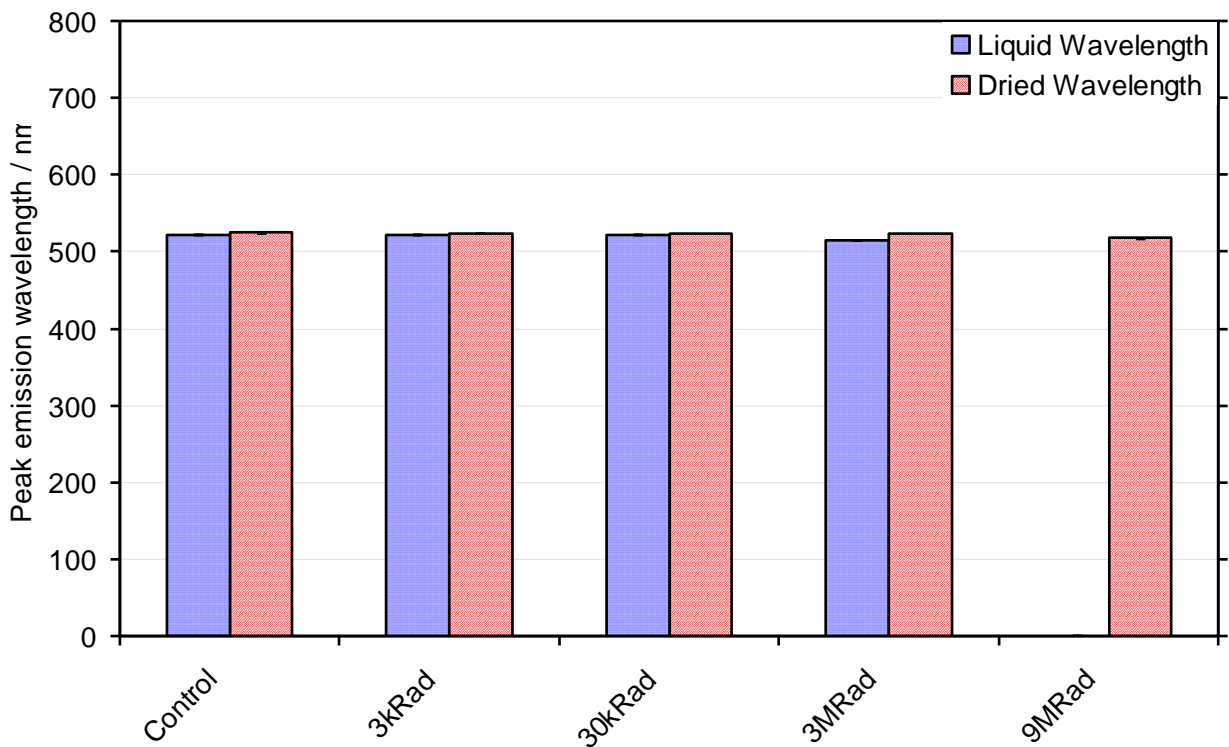


Figure 3.24: Effect of Gamma irradiation on fluorescent peak emission wavelength of dried down and liquid fluorescein. The error bars represent standard errors of the mean intensities from triplicate samples.

Figure 3.24 shows the effect of these gamma radiation exposures on the peak emission wavelength of fluorescein. All of the results appear very similar, so it is clear that any changes in peak emission wavelength have been very small, except in the case of the 9Mrad liquid sample. In this sample the fluorescent emission intensity when the sample was excited at 488nm (the excitation wavelength of fluorescein used throughout these experiments) was below the detection limit of the spectrophotometer, so no peak emission wavelength could be recorded. This result is consistent with the previous experiment (see section 3.3.3.2), and continues to support the conclusion that changes in the peak fluorescent wavelengths are unlikely to occur during the ExoMars mission and therefore the selection of components such as light sources and filters will not be complicated by changes in the wavelengths of the dye due to radiation exposure.

3.3.4.3 Determination of the maximum tolerated gamma radiation dose for fluorescein – conclusions

As observed in previous experiments (see sections 3.3.1 and 3.3.2), gamma radiation up to 3Mrad does not appear to have a great effect on fluorescein exposed in the dried state. However, after exposure to 9Mrad of gamma radiation the emission intensity of dried fluorescein has been reduced by ~10% compared to the control. However, in the liquid state, while the dye appears to be unaffected by gamma radiation up to exposures of 30krad, after a 3Mrad exposure the emission intensity has been reduced to below 25% of the untreated sample, and no fluorescence is observed at all after a 9Mrad exposure.

This experiment supports the initial hypotheses that samples in the liquid state would be less resistant to radiation damage due to the possible interaction of the radiolytic products of water (free radicals and ions) with the dye structure. It has also provided some evidence that gamma irradiation could be used as a sterilisation method for astrobiology instruments, such as the Life Marker Chip, that contain labelled biological molecules, since the fluorescent properties of the dyes were not significantly affected at representative sterilisation doses (3Mrad) (as given by Grieb *et al.*, 2002). It may be of scientific interest in the future to investigate the cause of the small loss of fluorescent intensity observed after the 9Mrad exposure (for example by carrying out thin layer chromatography and/or Nuclear magnetic resonance on exposed dye samples to identify degradation products). This is discussed further in section 6.2.

3.3.5 Summary of Gamma Irradiation Experiments

In this series of gamma irradiation experiments, the potential for the use of the fluorescent dyes fluorescein and Alexa Fluor[®] 633 has been investigated. Methods have been developed to expose these or similar dyes to gamma irradiation in the dried state in a reproducible way, such that dried and reconstituted control samples have similar fluorescent emission intensity and identical peak wavelength to liquid control samples (see Figure 3.23 and Figure 3.24). This method development is, in itself, an important step towards the validation of biological assays utilising fluorescent dyes in astrobiology instruments such as the Life Marker Chip.

The experiments have shown that in addition to retaining their fluorescent properties after exposure to equivalent mission doses of gamma irradiation in both the liquid and dried state, a sterilisation dose of gamma irradiation does not significantly degrade the dyes used in these experiments in a dried down form. The finding that up to a hundred times the expected mission dose (in the case of Alexa Fluor[®] 633) and up to 3Mrad (in the case of fluorescein), does not significantly affect the fluorescent properties of these dyes in terms of their peak emission wavelength and fluorescent intensity, is a key result supporting the use of biological assays based on fluorescent dye labels in astrobiology missions to Mars. In addition, these results support gamma irradiation as a potential method for sterilising the instrument prior to launch, another important consideration for astrobiology instruments since it is paramount that viable organisms from terrestrial sources are eliminated, for the purpose of meeting planetary protection requirements (see section 2.1.1.4). However further work needs to be done to establish the reasons for some loss of fluorescence, particularly if this arises from fragmentation of dye molecules.

The expectation would be that structurally similar dyes, for example Alexa Fluor[®] 750, would behave in a similar way to the specific dyes used in these experiments, so the instrument design could potentially be modified to use different dyes if required. This is important for the flexibility of the design of the Life Marker Chip, since at the time of writing the breadboard model of the SMILE Life Marker Chip is designed to be based on Alexa Fluor[®] 633, but due to the availability of lower mass and more intense optical sources other dyes including Alexa Fluor[®] 750 are still being considered for the flight instrument. Therefore if a different dye was selected further gamma radiation testing would be required to confirm this hypothesis that the effects would be similar.

No gamma irradiation studies on antibodies were performed during this work. This was in part due to time constraints, and the finding that in previous publications antibodies have been exposed to sterilisation doses of gamma radiation and found to show little structural damage and retain their binding affinity for their specific antigen in immunoassays (Cabalero *et al.*, 2004, Grieb *et al.*, 2002). These findings indicate that antibodies will be suitable for use in the Life Marker Chip, but tests are planned in the future to confirm the findings in the literature (see section 6.2).

3.3.6 Particle and gamma radiation testing summary

In sections 3.1 and 3.3 a number of radiation tests have been carried out on fluorescent dyes and antibodies to determine firstly whether these reagents could survive the likely levels of radiation encountered during a mission to Mars, and secondly whether gamma irradiation could be considered as a possible radiation treatment.

None of the radiation conditions tested to date have resulted in complete inactivation of either the dye or antibody under exposures at levels comparable with the (un-shielded) mission scenario, or even a 10-100 times greater exposure than the levels expected for the ExoMars mission. This was critical in establishing that a labelled antibody-antigen based detection system was a feasible technology for the detection of organic biomarkers on Mars in the Life Marker Chip.

Further work still needs to be carried out particularly testing the effect of gamma irradiation on antibodies and lower energy protons and helium ions on both antibodies and fluorescent dyes, and whether irradiation of assembled devices has a different effect than irradiation of dried antibody in isolation (see section 6.2). The effect of neutrons and combinations of radiation types also need to be investigated, and tests are planned to investigate this. The SMILE Life Marker Chip consortium are preparing a set of samples of LMC components for exposure to the space environment including launch and re-entry on the BIOPAN-6 mission in September 2007. This opportunity will allow antibody and fluorescent dye samples and microarrays mounted on silicon wafers to be exposed to the complete spectrum of space radiation (although at dose levels significantly lower than those expected for ExoMars) and will take into account different levels of shielding.

Since these radiation tests have proved that gamma radiation at the expected mission levels for ExoMars did not cause significant degradation of fluorescent dyes, sterilisation doses were also tested. The results of gamma irradiation of fluorescein at sterilisation doses showed that while a sterilisation dose of gamma irradiation would significantly degrade fluorescein in aqueous solution, dried fluorescein was much less susceptible to damage. Antibodies have been used in immunoassays after exposure to sterilisation doses of gamma radiation (Grieb *et al.*, 2002), indicating that they would survive the ExoMars mission environment.

In order to confirm the need for an alternative sterilisation method for the Life Marker Chip, a number of heat sterilisation tests were carried out, and the results of these are included in the following section.

3.4 Heat sterilisation tests on antibodies and fluorescent dyes

As stated in section 2.1.1.4, heat sterilisation is a standard method to reduce the spacecraft bioburden, i.e. the spore count per m². While this may inactivate viable organisms, it may not remove all potential contamination from the Life Marker Chip, since organic materials e.g. cellular components and their degradation products may remain and could be a source of false positive measurements. A higher level of cleanliness may be required to remove all organic contamination from the LMC, but the purpose of the experiments carried out in this work was to establish whether antibody-based assays could be incorporated into the ExoMars rover prior to the heat sterilisation procedure. The critical components i.e. antibodies and fluorescent dyes were therefore subjected to a heat sterilisation procedure to determine how much, if any, activity they retained. There are several standard protocols for heat sterilisation, but during these experiments we adopted a method from the NASA Procedures and Guidelines document NPG: 8020.12B, which consisted of holding the samples under vacuum at 125°C for 50 hours. The heat sterilisation is performed under vacuum, which removes water and oxygen. This therefore prevents degradation of the antibodies and fluorescent dyes by reaction with water and oxygen, and may increase their stability.

The exposures were carried out in a vacuum oven chamber at the University of Leicester. This equipment was capable of generating a high vacuum and maintaining the required temperature for 50 hours.

3.4.1 Preliminary heat sterilisation test – materials and methods

A custom aluminium sample holder was designed and fabricated for the exposure of fluorescent dyes and antibodies to heat sterilisation protocols. This consisted of sample wells 1.5mm in diameter and 8mm deep, machined in an aluminium block (see Figure 3.26). The dimensions of the wells were based on the approximate dimensions of the 864 well microtitre plate wells used in the second run of particle radiation experiments, since controlled sample handling in the microtitre plate wells was possible. Aluminium was selected as the sample holder material because it was conveniently available, easy to machine and has a high thermal conductivity, thus would transfer the maximum amount of heat to the samples (continuing the “worst-case” scenario testing philosophy used throughout this work).

As was the case for the early work in both gamma and particle radiation studies, this work was carried out in parallel so the same reagents were as used in early experiments. 25µl of fluorescein (Sigma-Aldrich, Poole, UK, product code 32615) in RO water at a concentration of 0.5mg.ml⁻¹ was added to each sample well. The sample block was then placed into a freezer at -80°C for 3 hours to ensure complete freezing of the sample. The sample block was then transported in a cool box and dried in a freeze-drier (Edwards Modulyo) for 3 hours, starting the freeze-drying process as quickly as possible, to ensure minimum thawing of the samples.

The sample block was then wrapped in aluminium foil and placed in a petri dish containing excess self-indicating silica gel desiccant while the samples were transported to the University of Leicester, to minimise the amount of water present in the sample prior to the heat sterilisation and prevent particulate contaminants entering the sample wells.

A Mars environment simulation chamber (University of Leicester) consisting of a pressure-sealed chamber with access to a vacuum pump and oven was used for all heat sterilisation tests. The sample block was placed inside and a high vacuum applied, then the chamber was heated to 125°C for 3 hours. After this treatment the sample block was returned to Cranfield University under the same transportation conditions as described. The fluorescein was reconstituted into 1ml of deionised water to a final concentration of 0.0025 mg.ml⁻¹. This was carried out by adding 10µl of RO water to each of the wells in the aluminium block and incubating for 1 minute to allow the fluorescein to dissolve, then transferring that 10µl from the wells to a vial containing 900µl deionised water. This was repeated 9 times to give a total of 10 washes with RO water. The peak emission and absorption wavelengths and intensities of the dye samples were then tested in the Cary Eclipse Varian Spectrophotometer.

3.4.2 Preliminary heat sterilisation testing - results and discussion

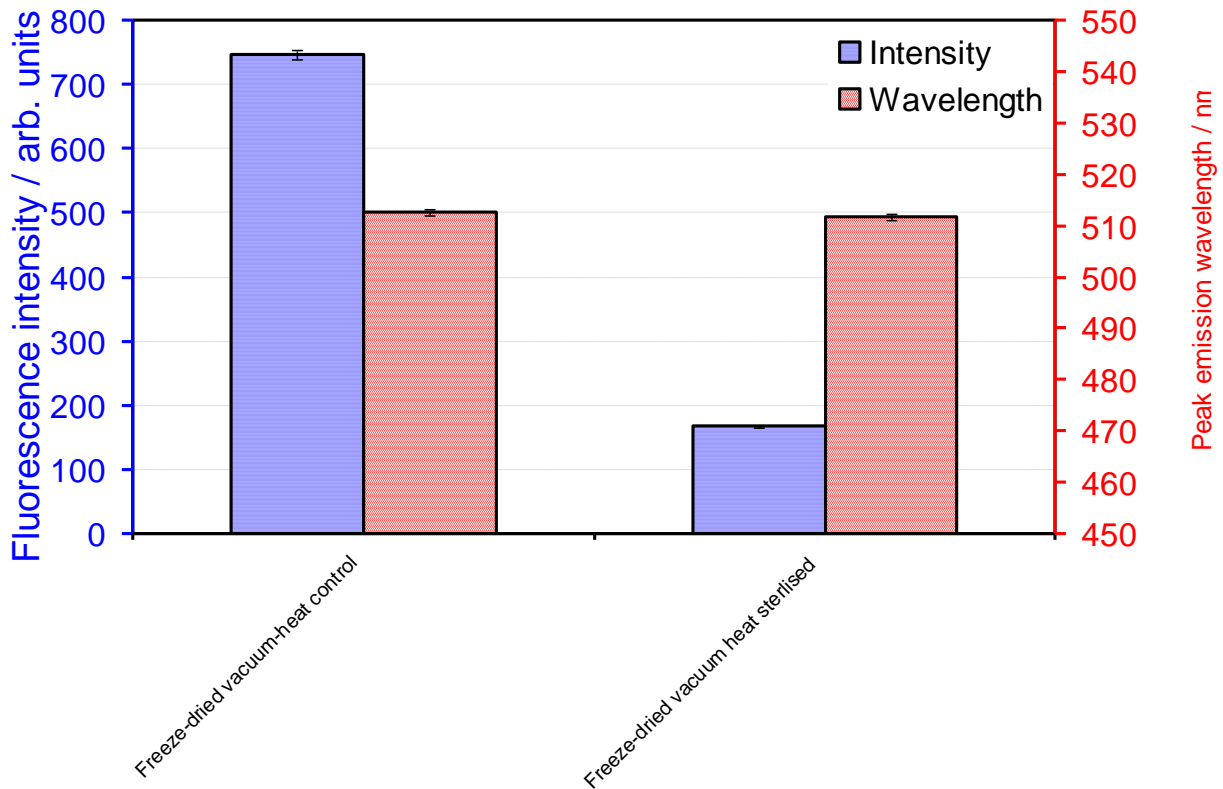


Figure 3.25: Effect of a heat sterilisation run consisting of 125°C for 3 hours on the fluorescent properties of fluorescein. The error bars represent standard errors of the mean intensities from triplicate samples.

In this initial test only one sample was exposed to the heat sterilisation procedure. Given that the results of the proton and gamma radiation tests carried out using similar sample preparation procedures were not very reproducible (see sections 3.2.3.2 and 3.3.1.2), few definite conclusions can be drawn from the result in Figure 3.25. The results only confirm that the fluorescent properties of fluorescein were not completely inactivated by this heat treatment, and that the peak emission wavelength was not affected. A similar set of changes in procedure to those implemented for the gamma and proton work after the initial test run were also considered and incorporated into the next heat sterilisation run.

An additional factor that would contribute to poor reproducibility heat sterilisation test was that manually inserting and particularly removing samples from the 1.5mm diameter aluminium block wells was extremely difficult to do in a reproducible way. In contrast to the polystyrene 864 well microtitre plates and sample blocks used for the particle radiation exposures, the aluminium block is not transparent and has a much more hydrophilic surface. These two factors in combination meant that even using a thinner

than standard pipette tip it was extremely difficult to avoid creating air bubbles inside the wells when filling them with solution, and consequently over-filling the wells and contaminating adjacent wells.

3.4.3 Modified protocol for heat sterilisation testing

The simplest solution to the difficulty in manually placing and removing liquid samples from the aluminium block wells was to machine larger plate wells into the block, therefore wells of 3mm diameter and 8mm depth were drilled into the aluminium block and used for all subsequent heat sterilisation experiments (see Figure 3.26). In addition, as for the gamma and particle radiation tests (see sections 3.2.3.2 and 3.3.1.2), in the second run fluorescein sodium salt (Sigma-Aldrich, Poole, UK, Product Code 46960) was used in the second run to increase the reproducibility of the results.

3.4.3.1 Modified protocol for heat sterilisation testing – materials and methods

10 μ l of either 1mg.ml⁻¹ fluorescein sodium salt or 1mg.ml⁻¹ Alexa Fluor[®] 633 in RO water was placed in each well. The freeze-drying protocol was modified to include immersing the sample block in liquid nitrogen for 1 minute immediately prior to freeze-drying. This was done to prevent the sample melting at the interface and therefore allowing trapped air to cause samples to be ejected from the block under vacuum.

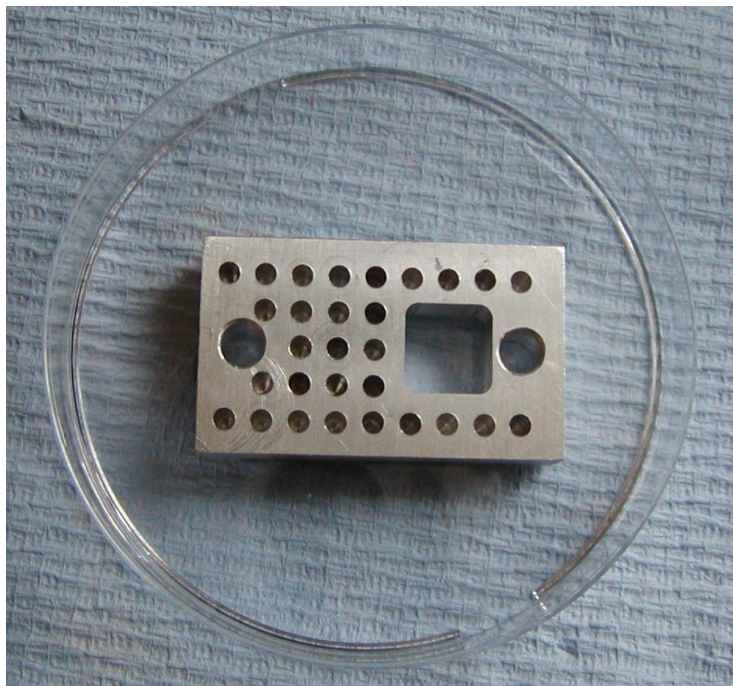


Figure 3.26: Second design of the heat sterilisation sample block.

After immersion in liquid nitrogen the sample block was immediately placed into the freeze-drier and the freeze-drying process started. As in the previous experiment, the samples were freeze-dried for 3 hours, and after removal from the freeze-drier the sample was stored with excess silica gel desiccant for transportation to the Mars environment simulation chamber.

After placing the sample block in the heating chamber, a high vacuum was applied, and then the chamber was heated to 125°C and held at that temperature for 50 hours. The sample block was then returned to Cranfield University under the same transportation conditions as described. The fluorescein and Alexa Fluor[®] 633 samples were reconstituted into 1ml of deionised water to a final concentration of 0.0025 mg.ml⁻¹, using the protocol described in section 3.4.1. The peak emission and excitation wavelength and intensity of the dye samples were then tested in the Cary Eclipse Varian Spectrophotometer.

3.4.3.2 Modified protocol for heat sterilisation testing – results and discussion

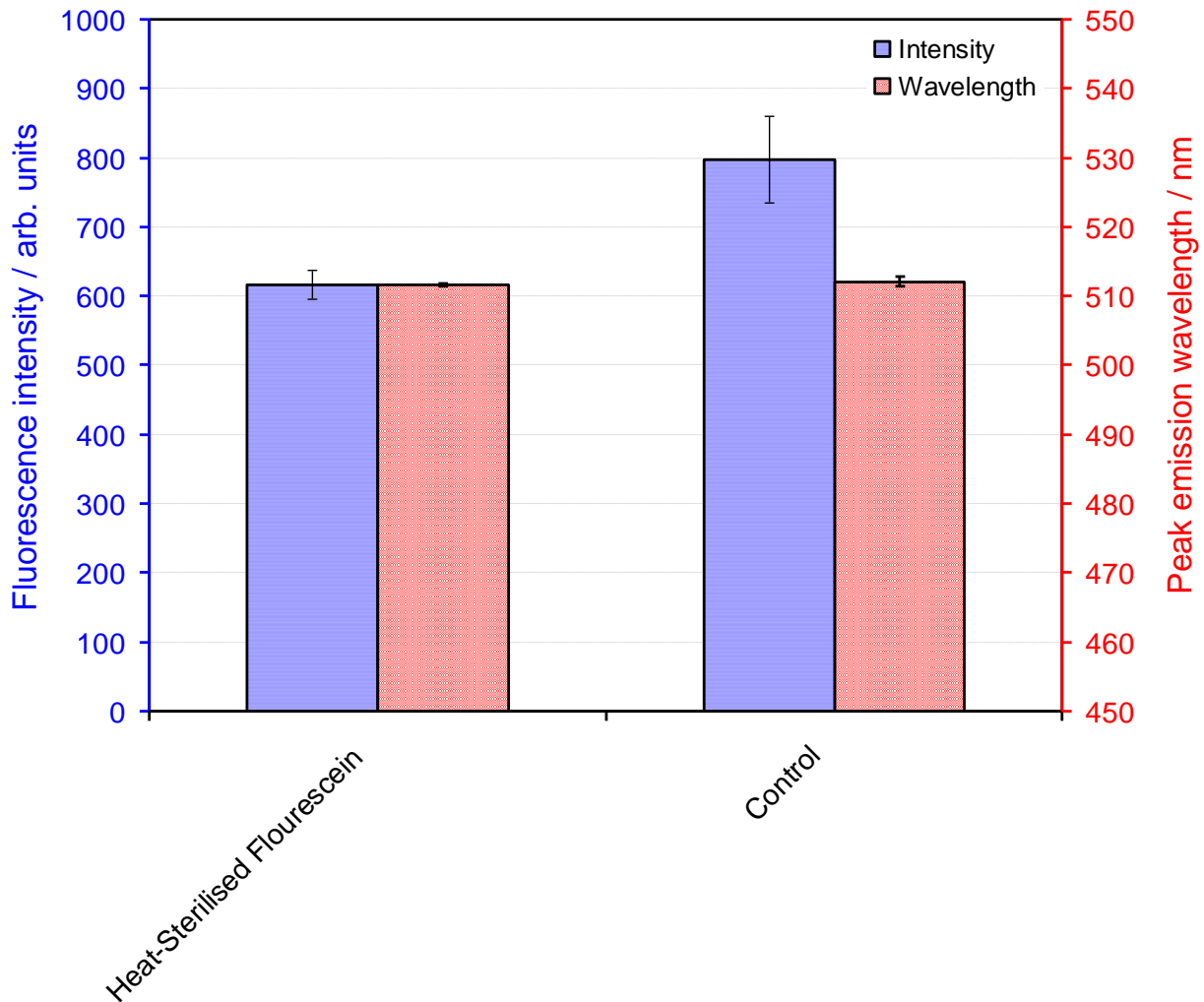


Figure 3.27: Effect of modified heat sterilisation on the fluorescent emission properties of fluorescein. Error bars represent the standard error of the mean fluorescent intensity from 5 samples exposed to radiation and 4 control samples.

Figure 3.27 shows the results of this heat sterilisation protocol on the fluorescent emission properties of fluorescein. While there are still some problems with reproducibility of the intensity, which was thought to be due to further issues with the freeze-drying sample preparation method (as seen from the relatively large error bars), it is clear that the 50 hour heat sterilisation treatment has not had a significant adverse effect on the fluorescent properties of fluorescein. The peak emission wavelength was not affected, and while the average emission intensity is lower after the heat sterilisation treatment this is within the experimental error, so no conclusions can be drawn from this in terms of significant differences.

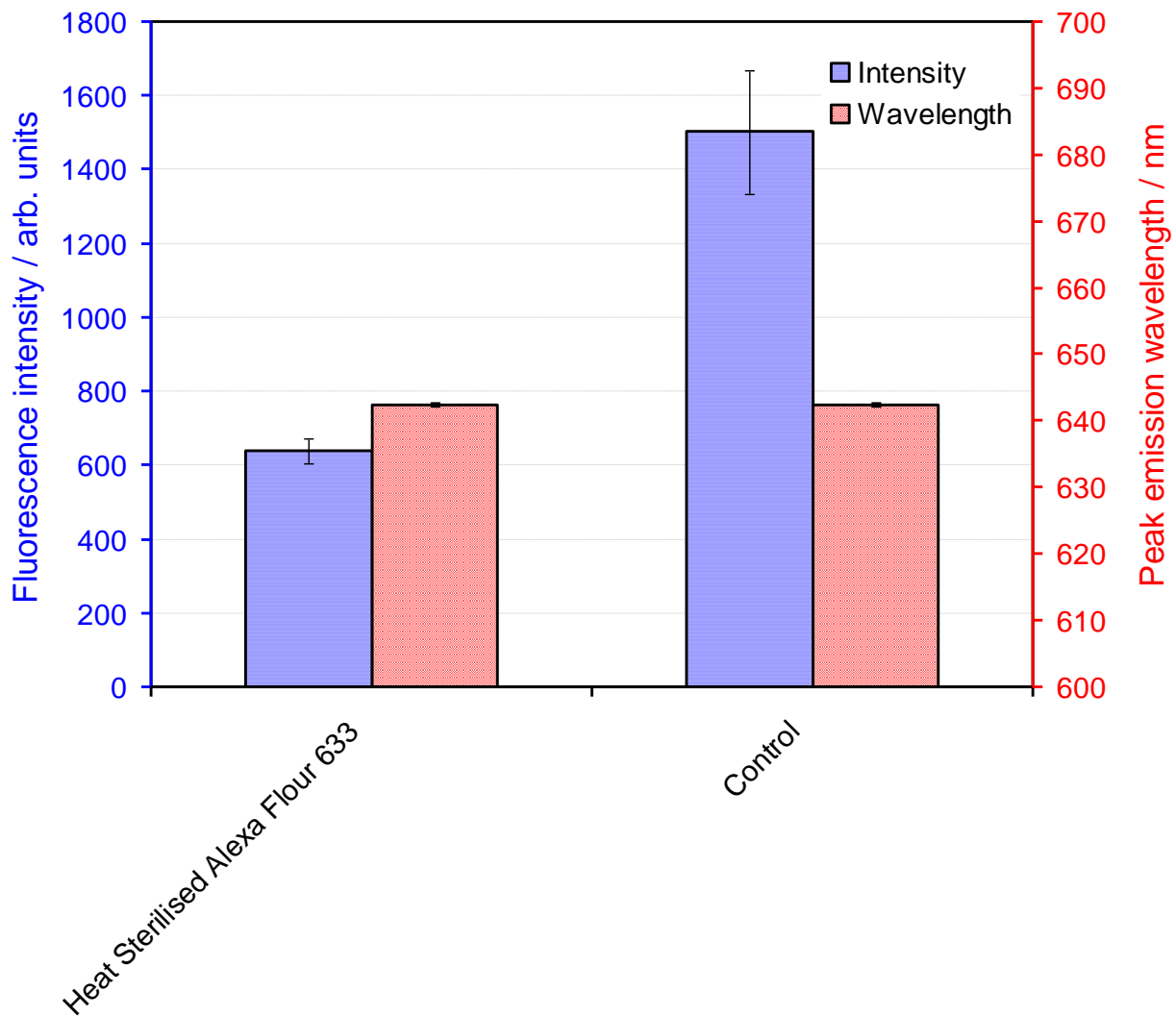


Figure 3.28: Effect of modified heat sterilisation on the fluorescent emission properties of Alexa Fluor[®] 633. Error bars represent the standard error of the mean fluorescent intensity from 3 samples exposed to radiation and 3 control samples.

Figure 3.28 shows the results of this heat sterilisation protocol on the fluorescent emission properties of Alexa Fluor[®] 633. In this case, the emission intensity of the heat-sterilised dye is significantly lower than the control. However, since the control dye was not exposed to either freeze-drying or heat sterilisation, it is not possible to determine whether this was due to material loss caused by the freeze-drying process or any effect of the heat treatment. Regardless of the cause of this loss of intensity, the effect of this reduced fluorescence on the detection limit of the instrument must be determined if heat sterilisation is used in the flight instrument. Importantly, the peak excitation and emission wavelength was not affected so changes in fluorescent wavelengths do not have to be considered in the selection of the excitation light source or excitation and emission filters on the flight instrument,

Since at this stage in the project drying down fluorescent dye and antibody samples into sample wells and vials had been proven to increase the reproducibility of the fluorescent

dye signal in particle and gamma radiation exposures, this approach was also adopted for the following heat sterilisation experiment.

3.4.4 Improved reproducibility heat sterilisation test

In order to improve the reproducibility of the results for heat sterilisation tests, a third round of testing was carried out in which the fluorescent dye and antibody samples were dried down into the aluminium block wells using the same procedure as for the particle and gamma radiation tests (see section 3.2.4.5), i.e. placing the sample block in a sealed vessel containing silica gel desiccant and heating it to 37°C overnight.

3.4.4.1 Improved reproducibility heat sterilisation test – materials and methods

In this heat sterilisation test run, 30µl of 1mg.ml⁻¹ fluorescein sodium salt (five samples), 30µl of 0.1 mg.ml⁻¹ Alexa or 30µl (three samples), or 0.3mg.ml⁻¹ anti-atrazine scAb (three samples) were placed into 3mm diameter wells in the aluminium block. The sample block was then placed into a sealed vessel containing excess silica gel desiccant, and the vessel placed into an oven at 37°C overnight to remove the water from the samples. The method used for the previous heat sterilisation test was then repeated for this test run (see section 3.4.3.1).

3.4.4.2 Improved reproducibility heat sterilisation test – fluorescein results and discussion

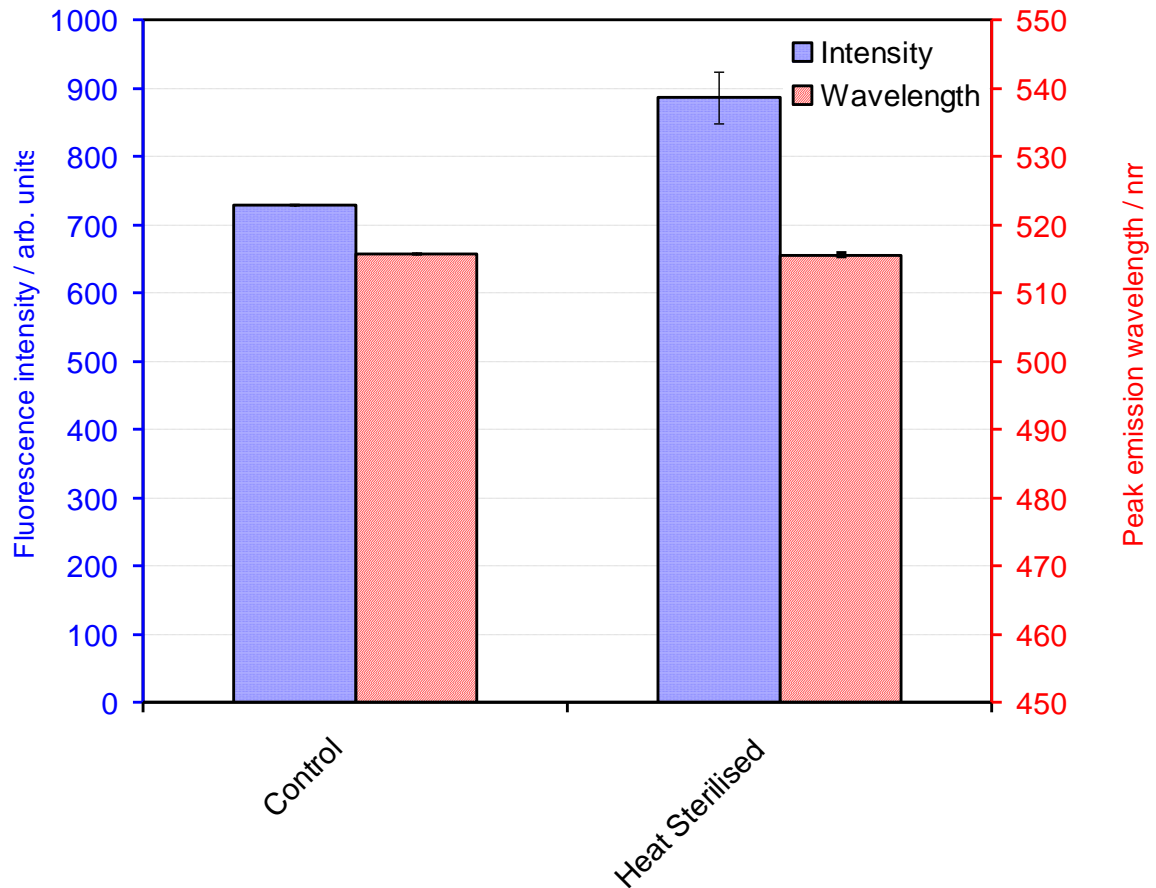


Figure 3.29: Effect of optimised heat sterilisation on the fluorescent emission properties of fluorescein. Error bars represent the standard error of the mean fluorescent intensity from 5 samples exposed to radiation and 3 control samples.

Figure 3.29 shows the effect of this 125°C heat sterilisation for 50 hours on fluorescein. It is clear that the reproducibility has improved compared to the previous experiments, as more samples were tested (only single samples were tested in the preliminary experiment) and the error bars have become smaller. However, this procedure could be developed to further improve the quality of the results. Nonetheless, Figure 3.29 shows that the heat sterilisation procedure does not have a significant effect on dried down fluorescein, either on the peak emission wavelength or intensity. Similar results were found for the excitation properties (data not shown).

In the previous heat sterilisation experiment, the poor reproducibility of the sample handling process was a big contributor to the result. In contrast the improved reproducibility of these results allows more reliable interpretation of the effect of heat sterilisation on the biological material than the previous heat sterilisation experiment, so the conclusions for this section are based primarily on these results.

3.4.4.3 Improved reproducibility heat sterilisation test – Alexa Fluor® 633 results and discussion

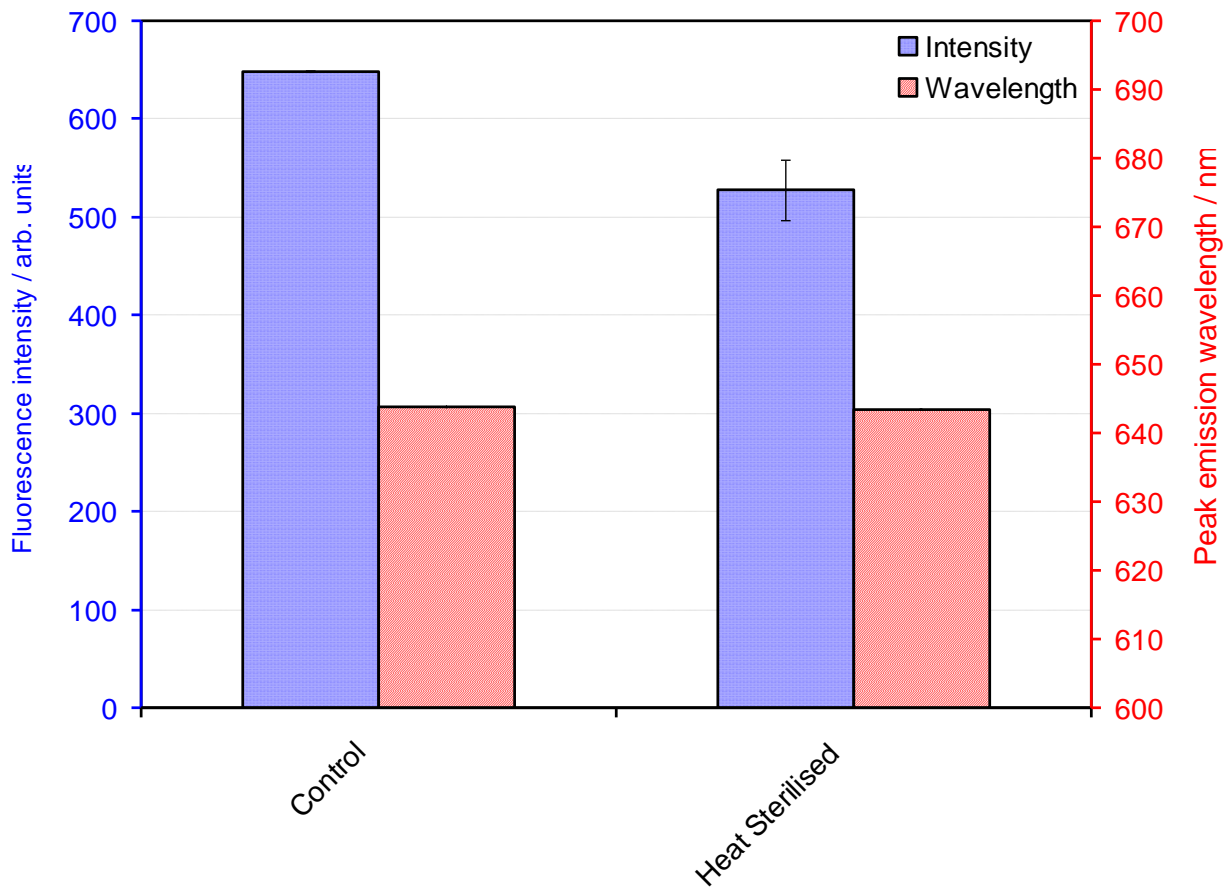


Figure 3.30: Effect of optimised heat sterilisation on the fluorescent emission properties of Alexa Fluor® 633. Error bars represent the standard error of the mean fluorescent intensity from 5 samples exposed to radiation and 3 control samples.

Figure 3.30 shows the effect of the 50 hour 125°C heat sterilisation on Alexa Fluor® 633. As for the fluorescein, it is clear that the reproducibility has improved compared to the previous experiments, but further improvements to the quality of the results could be made. However, this result demonstrates that the peak emission wavelength is not affected by heat sterilisation at all, and any reduction in emission intensity is small. Similar results were found for the excitation properties (data not shown). As for the fluorescein results for this experiment, these results were far more reproducible than the previous experiment which gave the opposite conclusions (see section 3.4.3.2), therefore these results are considered to be more reliable.

3.4.4.4 Improved reproducibility heat sterilisation test – anti-atrazine scAb results and discussion

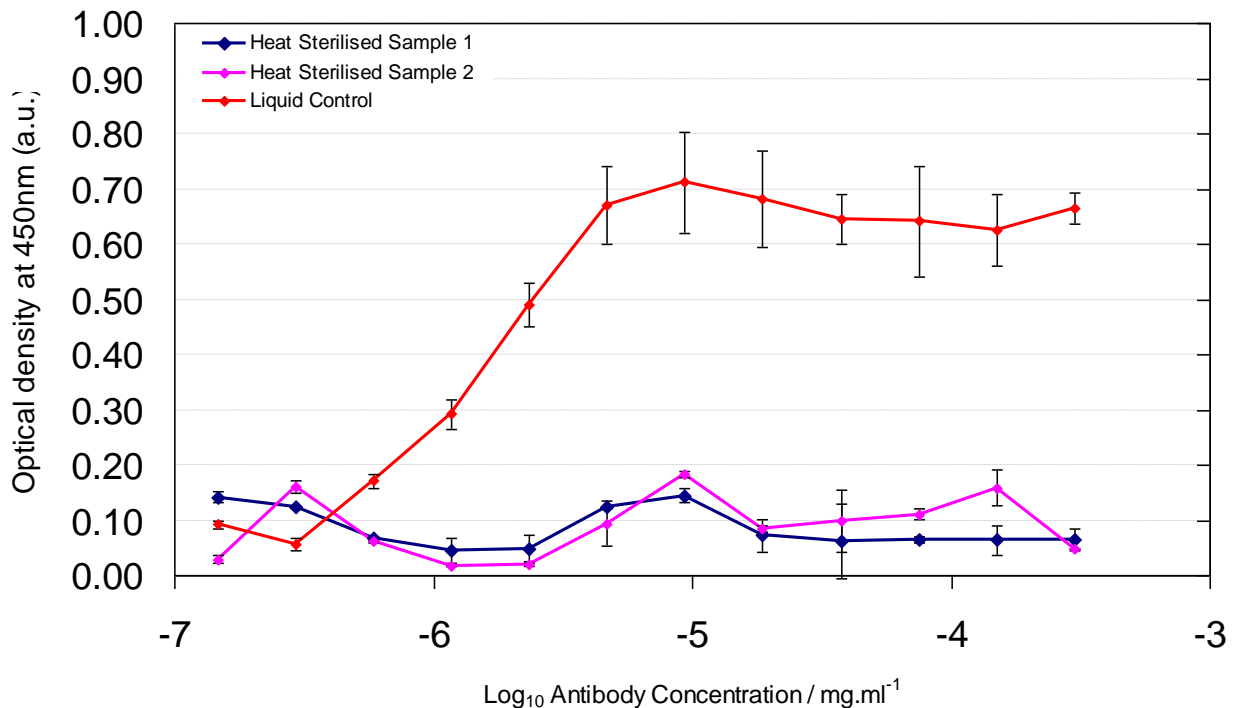


Figure 3.31: Effect of heat sterilisation on the antigen binding properties of anti-atrazine scAb assessed by binding ELISA. The error bars represent the standard error of the mean binding signal from triplicate samples.

Figure 3.31 shows conclusively that antibody fragments do not withstand heat sterilisation at 125°C for 50 hours. This is not an unexpected result, and could be due to a number of factors. These include denaturation of the antibody, which would destroy the binding site for the target molecule and render the antibody inactive in the assay. Also in this experiment since a secondary antibody (anti-human kappa light chain) was used in the assay, damage to the region targeted by this secondary antibody may also affect the antibody binding signal measured. It is likely that all antibodies and proteins that may be used in the Life Marker Chip would behave in a similar way under these heat sterilisation conditions, so dry heat sterilisation appears to be an unsuitable approach for preventing terrestrial contamination of the Life Marker Chip.

3.5 Summary and conclusions from radiation and sterilisation experiments

In sections 3.1, 3.3 and 3.4 of this chapter, three sets of experiments were carried out in parallel to determine the effect of different aspects of the mission environment; gamma radiation, particle radiation and heat sterilisation, on both fluorescent dyes and antibodies. Through a series of experiments, a protocol was developed to expose the antibody and fluorescent dyes to each of these environments in a controlled and reproducible way. In the final experimental formats, none of the heat sterilisation tests

has shown a large enough detrimental effect on the fluorescent dyes to invalidate their use in the conditions that they would encounter in Life Marker Chip instrument. Heat sterilisation has been shown to be inappropriate for antibodies. However, this work has demonstrated that fluorescent dyes survive gamma radiation sterilisation doses, albeit with some degradation of their excitation and emission intensities, and gamma radiation for the sterilisation of antibodies have been reported in the literature (Grieb *et al.*, 2002). Therefore, it may be possible to sterilise the Life Marker Chip by gamma radiation, and therefore dry heat sterilisation would not be required.

Both fluorescein and Alexa Fluor[®] 633 in a dried down state appeared to retain their fluorescent properties with little or no change in fluorescent intensity or peak emission or excitation wavelengths under a number conditions. These included gamma radiation up to and beyond the 3Mrad levels used for sterilisation, 9MeV protons up to and beyond 10,000 times the expected mission fluence, 30MeV helium ions at least 100 times greater than the expected mission fluence, and heat sterilisation at 125°C for 50 hours. In addition, in the liquid state the fluorescent dyes were not significantly affected by the expected mission dose of gamma radiation.

The anti-atrazine scAb, representative of one of the types of antibody proposed for the flight instrument, was also not rendered inactive by the environments used in these experiments. The antibody was found to lose approximately half of its binding affinity after exposure to 10 or 100 times the expected mission fluence of 9MeV protons, and was not affected by up to 100 times the expected fluence of 30MeV helium ions. The antibody did not however retain any function after the heat sterilisation treatment, confirming that an alternative sterilisation method must be identified for the flight instrument. Unfortunately there was no opportunity to expose the anti-atrazine scAb to gamma irradiation in the timescale of this work, however this will be carried out in future work as part of the development of the Life marker Chip.

Since this work none of the mission environments tested to date proved to be fundamentally incompatible with the use of antibodies and fluorescent dyes in astrobiology mission to Mars, the development of the Life Marker Chip was continued in the area of developing a suitable instrument platform in which the fluorescently labelled antibody assay could be incorporated into the mission design specifications including mass and size. This involved miniaturising standard biological assays from the ELISA plate format to a protein microarray design. This work is described in the following chapter.

Chapter 4: Development of the Life Marker Chip Microarray Readout Breadboard System

4.1 Introduction

As discussed in the literature review, all of the proposed instrument designs for the Life Marker Chip (LMC) are based on a protein microarray assay system operating within microfluidic channels. While the technologies required to achieve the proposed specification of each component do exist, no complete system incorporating all aspects had been developed prior to this work. In this chapter, the development of an example assay and breadboard instrument using representative assay systems (utilising anti-atrazine scAb and anti-GroEL antibody receptors) will be described.

The main objectives of this instrument development work were to demonstrate the following:

- Printing of homogeneous microarray spots within a microfluidic channel
- Imaging of fluorescent microarray spots within a microfluidic channel
- Demonstration of an immunoassay in a microarray spot format within a channel
- Developing a suitable blocking protocol to minimise non-specific binding
- Functionalisation of glass and silicon surfaces to enable covalent attachment of proteins and antibodies
- Demonstration of covalent immobilisation of spotted reagents onto surfaces

Since demonstration of pin-printing of microarray spots was a critical step for many of these objectives, and had not previously been carried out at Cranfield University, a series of experiments were conducted in order to confirm that the microarray equipment was functioning as expected. Initially the printed spots were imaged with a fluorescent microscope or a Digital Blue QX3 microscope, and dyes and fluorophores compatible with these imaging systems were used. The fluorescent microscope readout was used in an initial demonstration that fluorescence-based immunoassays of the type proposed for the SMILE Life Marker Chip instrument could be carried out and imaged fluorescently with available equipment. The results of these experiments were not analysed in detail, since they were not directly relevant to the development of the Life Marker Chip, but are included in Appendix A.

After the initial work had been completed, additional funding became available and allowed the assembly of a breadboard imaging system that was more representative of the flight design of the Life Marker Chip. The breadboard system was used to establish readout protocols for immunoassays for relevant biomarker molecules in the proposed microarray format, test additional fluorescent dyes, develop an additional assay, and to investigate means to reduce non-specific binding. The flight design of the Life Marker Chip is based on silicon wafers, which, unlike the glass microscope slides used in this study, are not available pre-treated with a surface chemistry to allow the covalent attachment of proteins and antibodies. Therefore a standard method to functionalise glass and silicon surfaces was adopted and demonstrated on silicon and glass components, in order to show that these materials could be functionalised for inclusion in the breadboard system and the flight instrument. The first key development in this area was the assembly of the breadboard system, which is described in the following section.

4.2 Development of a breadboard imaging system and adaptation of assay protocols to use representative Life Marker Chip biomarker targets and Alexa Flour[®] 633 dye

4.2.1 LMC readout design considerations and development of the breadboard imaging system – introduction

The preliminary experiments and method developments made in Appendix A confirmed that it is possible to fabricate an antibody or protein microarray chip with the desired array and spot sizes (100 - 200 μ m) for the flight Life Marker Chip instrument (as described in section 2.3.1). However, the readout and immobilisation methods in these experiments were not representative of the proposed instrument, and the assay used was not directly representative of a true biomarker target. In this section, the development of an imaging system more closely representative of the flight model designed for the Life Marker Chip is described, followed by the development of an additional assay using a biomarker target relevant to Life detection, and the optimisation of this assay protocol. In addition, protocols for the surface modification of glass and silicon services to introduce functional groups for the covalent attachment of proteins to the surface were developed.

Throughout the Life Marker Chip development, fluorescent dyes of higher wavelengths (red and near infra-red) were always thought to be more suitable for space flight and use in a radiation environment than lower wavelength dyes (green and blue). There are a number of reasons for this, including that longer wavelength dyes are less prone to interference from auto-fluorescence that could reduce the sensitivity. Use of longer wavelength dyes would

therefore mean that the instrument could achieve a higher sensitivity, which is important since the concentration of biomarker targets in the samples is likely to be very low, in the parts per billion range (Sims *et al.*, 2005). Another factor is that optical glasses (for example in lenses in the imaging system) can lose some of their transmission properties when exposed to radiation, particularly at blue end of spectrum (Firestone & Harada, 1979), therefore potentially reducing their transmission of light at lower wavelengths. Other considerations for dye selection include some resistance to photobleaching in ambient light, since some experiments such as the radiation tests in Chapter 3 require handling the dye in ambient light for small amounts of time, and availability in a convenient format for protein labelling, as developing a protocol for *in-situ* labelling of proteins is a key objective of this section.

Taking these factors into consideration, the dye selected for further investigation for use in the Life Marker Chip was Alexa Fluor[®] 633, which operates at a long wavelength (in the near infra red region), and has a high resistance to photobleaching. It is available in a succinimidyl ester form, which allows it to be covalently attached to both proteins and functionalised surfaces if required. Another potential benefit of Alexa Fluor[®] 633 is that structurally similar dyes operating at other wavelengths are available, so that if the development of the Life Marker Chip indicated that a change of wavelength would aid in design of the flight instrument, the work done with the fluorescent dye would still have some relevance if a similar dye was used.

4.2.2 Breadboard imaging system development - specifications and assembly

In order to be able to detect these longer wavelength dyes with reasonable sensitivity and exposure times, and in a format similar to a possible LMC flight instrument design, a breadboard system was assembled for optical imaging of microarrays at 633nm. The layout of this breadboard is shown in Figure 3.2.1. A microscope slide holder was attached to an X-Y-Z translation stage, which was in turn mounted on a manual rotation stage. This entire assembly was placed onto an optical rail (all components were from Edmund Optics York, UK). A 10mW Helium-Neon 633 laser (Polytec, Waldbrom, Germany) was mounted in front of the microscope slide holder, and positioned such that the central position of the stage movement axes was directly in front of the laser. The rotation stage was adjusted such that the microscope slide holder was at an angle of $\sim 30^\circ$ from the laser beam. A second optical rail was placed facing directly towards the microscope slide holder. A low light level Peliter-cooled CCD camera (SXV-H9, Starlight Express, Holyport, Berkshire, UK) was mounted on

an X-Y stage, and this assembly mounted on the second optical rail facing the microscope slide. The X-Y stage allowed movement of the camera for focussing images. The SXV-H9 camera was selected because it is black and white camera, and was a reasonable compromise between cost and pixel density on the CCD chip (it has 1392 x 1040 pixels in a 8.9 x 6.7mm area). A number of optical spacers (Edmund Optics, York, UK) were mounted onto the CCD camera to reduce the focal distance to approximately 2.5cm, as to achieve maximum sensitivity, the objective should be as close to the surface as possible. 2.5cm was the smallest focal length that could be practically achieved with the available equipment, and offered the best compromise between having a wide field of view and imaging detail within the spots. A x4 microscope objective was also added to provide some magnification of the image of the surface. The images taken with the CCD camera in this configuration show an area of approximately 2mm x 2mm. A notch filter with an optical density of 6 at 633nm was mounted within a specialised optical spacer in front of the CCD camera. This filter is designed to block out much of the reflected and scattered 633nm light from the surface, to allow images to be taken without fluorescent light being saturated out by reflected or scattered incident light (as would be the case without the notch filter present).

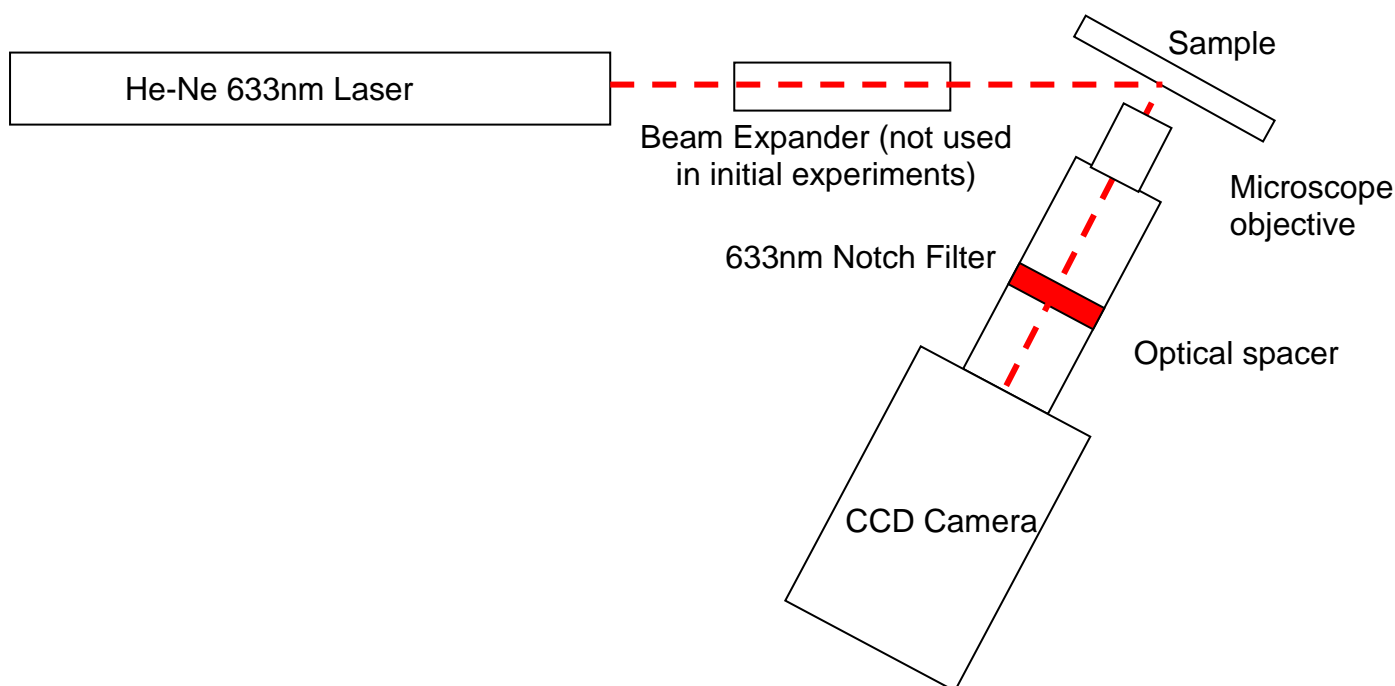


Figure 4.1 Schematic layout of the breadboard imaging system.

4.3 Determining the detection limits of the new breadboard imaging system – introduction

In order for this imaging system to be used for the readout of immunoassays it was necessary to be able to produce images of monolayers of fluorescently labelled proteins or

antibodies in microarray spots. Therefore, to show that this was possible before attempting an immunoassay, the detection limit of the newly assembled imaging system was determined by printing microarray spots from different concentrations Alexa Fluor® 633 in RO water onto a glass microscope slide, drying the slide to remove the liquid, and then imaging the slide. A series of appropriate concentrations of Alexa Fluor® 633 dye to model a monolayer was calculated as follows.

Given that the nominal spot diameter of the SMP3B spotting pin spots is 110µm (<http://arrayit.com/Products/Printing/Stealth/stealth.html>, accessed 03 April 2007) (see Appendix A), and that the molecular footprint area of a protein is typically $\sim 100\text{\AA}^2$, one can calculate that a monolayer of protein molecules covering the whole spot area would contain $\sim 95,000,000$ protein molecules.

Since the nominal volume of liquid deposited by the SMP3B spotting pin is 900 pl (<http://arrayit.com/Products/Printing/Stealth/stealth.html>, accessed 03 April 2007) (see Appendix A), and the molecular weight of the Alexa Fluor® 633 dye is 1200Da, one can calculate approximate values for the number of dye molecules per protein footprint area for Alexa Fluor® 633 dye solutions of different concentrations, assuming that the dye is dried down evenly across the whole of the spot area as the spot solution evaporates. Since during a covalent immobilisation, not all of the immobilised protein may be available for antibody-antigen interaction, in this simple model it is assumed that 50% of the protein footprint sites may contain immobilised antibody / antigen. A series of calculations of relevant Alexa Fluor® 633 concentrations are shown in Table 4.1

Table 4.1 Calculation of the resulting number of dye molecules per protein for a series of Alexa Fluor® 633 dye concentrations after the spotting solution was evaporated away from the surface. This calculation assumes a monolayer of protein covering the whole spot area, a molecular footprint size of 100\AA^2 for the protein or antibody on the surface and an even distribution of dye across the spot area when the spotting solution is evaporated off.

Concentration of Alexa Fluor® 633 in spotting solution ($\text{mg}\cdot\text{ml}^{-1}$)	Mass of dye per spot (g)	Molecular Weight of Alexa Fluor® 633 (Da)	Moles of dye per spot (Moles)	Number of dye molecules per spot	50% of no. of dye molecules per protein footprint
10^{-2}	9E-12	1200	7.5E-15	4515000000	23.754862
10^{-3}	9E-13	1200	7.5E-16	451500000	2.3754862
10^{-4}	9E-14	1200	7.5E-17	45150000	0.2375486
10^{-5}	9E-15	1200	7.5E-18	4515000	0.02337548

In immunoassays targets are typically labelled with between 5 and 20 dye molecules per protein (Document No. MP10168 (Alexa Fluor® Succinidyl Esters), Molecular Probes).

Table 4.1 shows that, if the simple modelling scenario used was valid, printing and imaging spots from a range of Alexa Fluor[®] 633 concentrations between 10^{-2} and 10^{-5} mg.ml⁻¹ would be appropriate to confirm that the imaging system could image protein microarray spots both at typical labelling levels, and with fluorescent labelling levels down to ~0.02 dye molecules per available protein binding site. If such spots could be imaged, the levels of fluorescence would correspond to the level of fluorescence from a monolayer of labelled material bound to a protein or antibody on the surface that would be present in an immunoassay.

4.3.1 Determining the detection limits of the new breadboard imaging system – materials and methods

Alexa Fluor[®] 633 dye in RO water was spotted on untreated glass microscope slides (Fisher Scientific, Loughborough, UK) at a number of different concentrations (1×10^{-2} mg.ml⁻¹ and a series of 10-fold dilutions down to 1×10^{-5} mg.ml⁻¹) to cover the range of surface dye concentrations representing those calculated for a monolayer in Table 4.1.

The microarray equipment and robotic control software used for microarray printing throughout this work are described in detail in Appendix A. Briefly, the equipment comprises Stealth[™] SMP3B spotting pins (Telechem International, Sunnydale, CA, USA) with a nominal spot size of 110µm diameter placed in a Stealth[™] print head. The print head is mounted on an optically controlled robot which can be programmed to move to a series of locations with sub-micron positional accuracy.

The spotting program for this experiment printed the microarray with a 600µm centre-to-centre spacing between adjacent spots, in both horizontal and vertical directions. The spotting robot program printed each dye solution in increasing order of dye concentration i.e. the lowest concentration of dye was printed first to form the top row of the array, the next highest concentration was printed in the second row, etc.. This protocol required some washing of the spotting pin to remove one concentration of dye solution before printing the following solution. A study on Stealth[™] SMP3 spotting pins (<http://www.fda.gov/nctr/science/journals/text/vol6iss1/rrp0306.htm> Accessed: 23-Oct-06) showed that 5 cycles of washing in deionised water with sonication removed all carry over between two oligonucleotide solutions. Since the Alexa Fluor[®] dyes are highly soluble in water and less likely to adhere to the pin surface, the pin was washed by moving it in and out of a reservoir of deionised water five times in between different dye concentrations. The slides with printed arrays of dye were then left to dry in darkness under ambient conditions

for at least 2 hours, and then placed into the breadboard imaging system and imaged in darkness with a 60 second exposure.

4.3.2 Determining the detection limits of the new breadboard imaging system – results and discussion

Figure 4.2 is an image of the array described in section 4.3 taken with the imaging system described in section 4.2.2 with a 60 second exposure time. Two rows of spots are clearly visible in the centre of image, and appear by visual inspection to be of different intensities, i.e. of different fluorescent intensities. Since this image covers the entire area in which microarray spots of Alexa Fluor® 633 dye was printed, one can surmise that these two rows of spots were the dye rows printed at 1×10^{-2} and 1×10^{-3} mg.ml⁻¹ respectively.

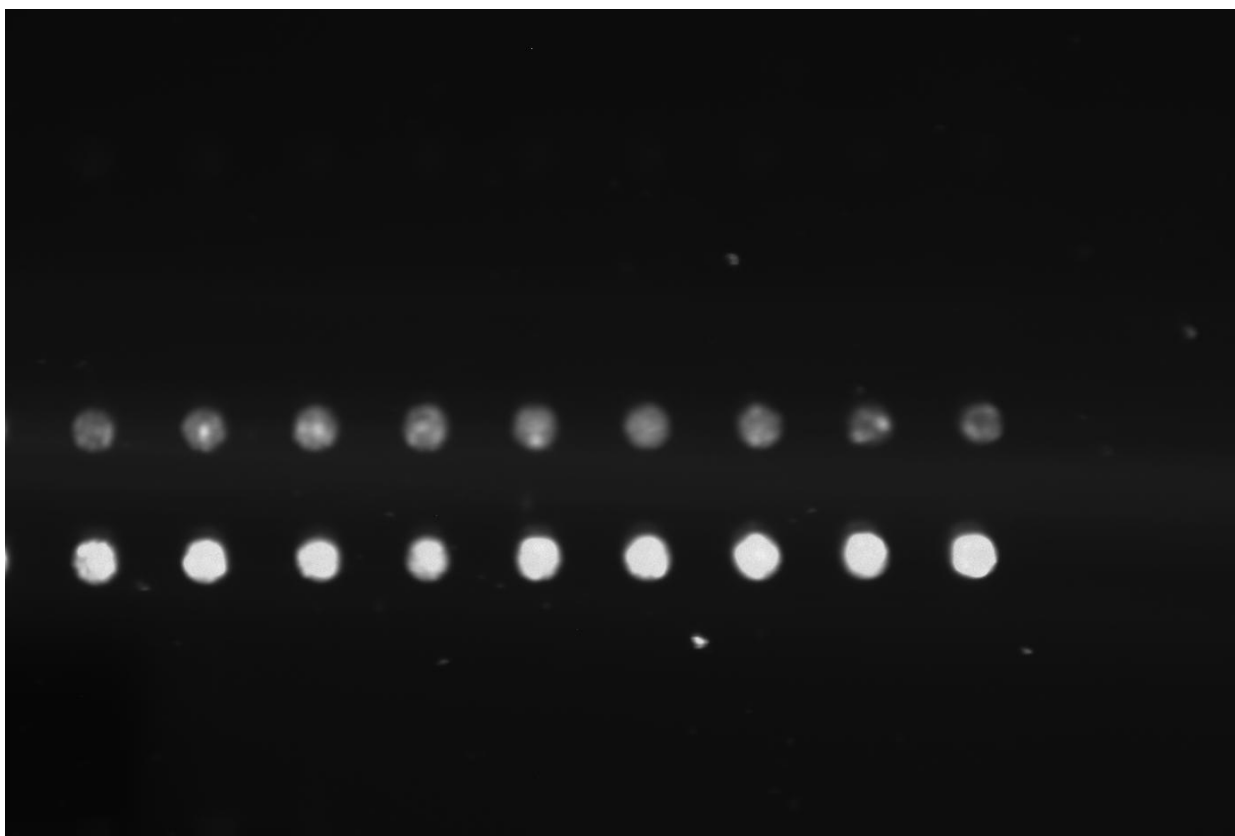


Figure 4.2: A 60 second exposure image of an array of difference concentrations of Alexa Fluor® 633 dye taken with the Starlight Express CCD camera with a 60 second exposure time.

Figure 4.2 was processed using the Starlight Express SXV-H9 camera software (version 3.5), such that the palette was readjusted to highlight weaker features. This analysis produce the following image (Figure 4.3), which also shows a lower concentration of Alexa Fluor® 633 spots

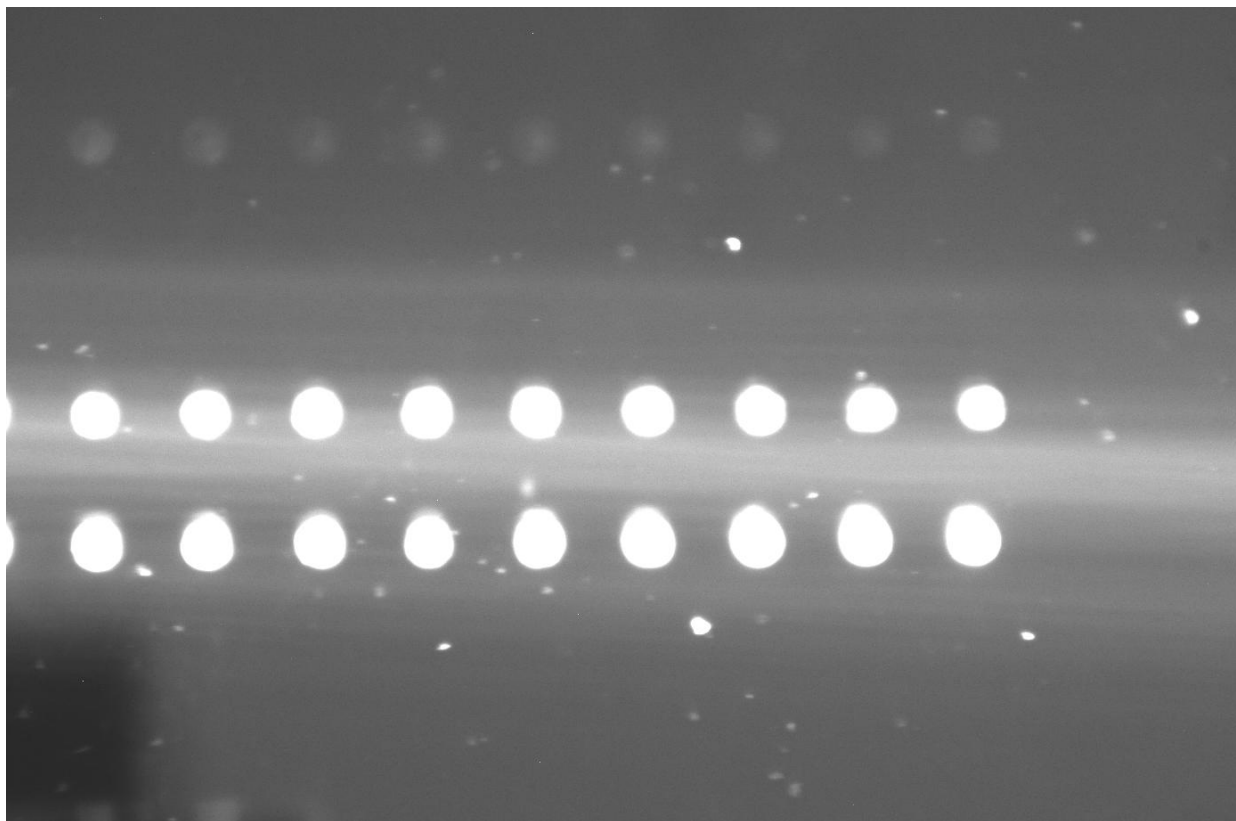


Figure 4.3: A 60 second exposure image of an array of difference concentrations of Alexa Fluor® 633 dye taken with the Starlight Express CCD camera and enhanced with the software filters

The enhanced image in Figure 4.3 shows that a third row of dye spots at a lower concentration is visible, at the top of the image, in the location corresponding to the Alexa Fluor® dye printed from a solution of $1 \times 10^{-5} \text{ mg.ml}^{-1}$ concentration. The appearance of this row of spots after image processing indicated that they could be imaged directly with a longer exposure time. This was not investigated at this time, but was noted for future experiments. The location where it would be expected to see a row of spots corresponding to Alexa Fluor® 633 dye printed at $1 \times 10^{-4} \text{ mg.ml}^{-1}$ does not contain any spots, and it was later found that this was due to an error in the printing program. The intensity of the top two visible rows of spots in this image (Figure 4.3) corresponding to Alexa Fluor® 633 dye printed at 1×10^{-5} and $1 \times 10^{-3} \text{ mg.ml}^{-1}$ were analysed using the find objects function of ImageTool (version 3.0), and exporting the intensity values into Microsoft Excel. The results of this analysis are shown in Figure 4.4 below.

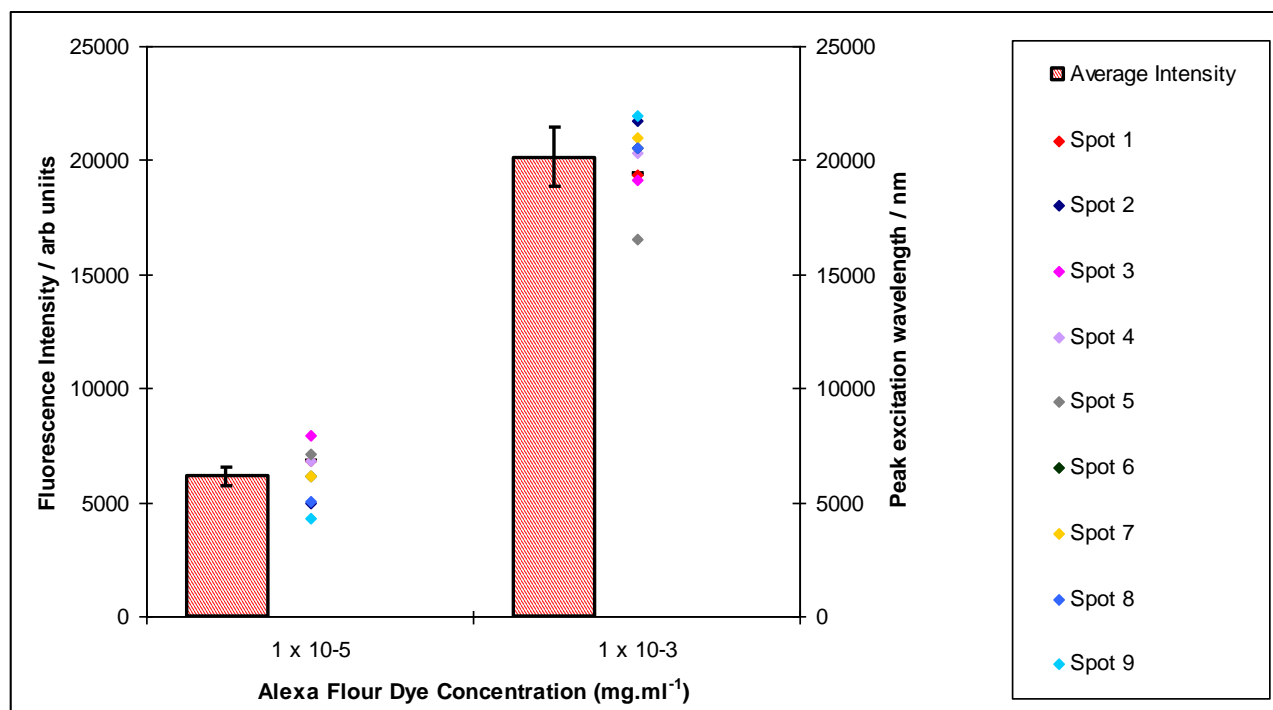


Figure 4.4: Analysis of the 60-second exposure image of Alexa Flour 633 spots at different concentrations (Figure 4.2).

This analysis shows that there is a significant difference in the pixel intensity of these two rows of spots. The dye spotted at a concentration of 1×10^{-5} mg.ml⁻¹ gave a mean signal of 6150 arb. units with a 20% CV, and the spots printed from 1×10^{-3} mg.ml⁻¹ dye solution have a mean signal of ~20130 arb. units with a CV of 19.1%. Although the difference in measured intensity is not a factor of 100, this could be because the pixels for the 1×10^{-3} row of spots are saturated in the processed image.

Figure 4.4 shows that a numerical analysis confirms what appears to be the case in the Figure 4.3 there is a clear difference in the average intensity of spots printed at the 1×10^{-5} and 1×10^{-3} mg.ml⁻¹, and the intensities of spots at the same concentration is broadly similar. There is some variation due to the presence of particulates and drying effects over some spots.

Having now confirmed that the imaging system was able to detect Alexa Flour[®] 633 dye at relevant concentrations and clearly resolve the concentrations, an initial assay experiment was carried out.

4.4 Immunoassay protocols used during the assay development

During the development of the immunoassays in a microarray format, a number of variations of immunoassay protocols were used in an attempt to overcome some non-specific binding issues. In this section, all of these protocol variations will be summarised. The specific protocol for each experiment and reasons for the selection of that method will be described in the appropriate materials and methods section for that experiment.

4.4.1 Anti-atrazine scAb immunoassay

When amine coated slides were used, the assay areas of the slides were activated by a 15 minute incubation in a freshly prepared solution of 2.5×10^{-5} M BS3 (Pierce, Rockford, IL, USA) in pH 9.0 sodium carbonate-bicarbonate. The BS3 solution was then washed off in deionised water and the slide dried under a nitrogen gas stream. Epoxy slides were used directly as supplied with no preparation step.

The assay protocol was then carried out as follows, using one of the methods:

- 20 μ l of 0.03mg.ml⁻¹ anti-atrazine antibody (kindly provided by Haptogen, Aberdeen, UK) (a humanised recombinant antibody fragment), in printing buffer (PBS-30% glycerol (AnaIR grad, Merck)) was pooled over each assay area and the slide incubated in a humidity chamber for 2 hours.
 - The slide was then placed into a blocking solution of 0.1mg.ml⁻¹ skimmed milk powder (Marvel), agitated to wash remaining anti-atrazine in printing buffer from the slide surface, and incubated in a humidity chamber for 2 hours.
 - Each assay area was washed five times with 1ml of 10mM PBS pH 7.4 with 0.1% TWEEN-20 and then five times with 1ml of deionised water, by pipetting the water onto the assay area at an acute angle downwards. The slide was then dried under a nitrogen line.
- 20 μ l of 0.02mg.ml⁻¹ goat anti-human IgG (H+L) labelled with Alexa Fluor[®] 633 (Molecular Probes, Paisley, UK) in 10mM PBS pH 7.4 was then pooled over the test assay area. 20 μ l of 10mM PBS pH 7.4 was pooled over the control assay area, and the slide incubated in a humidity chamber for 2 hours.
- The chip was then placed into the imaging system and an image taken with a 60 second exposure.

4.4.2 GroEL immunoassay

When amine coated slides were used, the assay areas of the slides were activated by a 15 minute incubation in a freshly prepared solution of 2.5×10^{-5} M BS3 (Pierce, Rockford, IL, USA) in pH 9.0 sodium carbonate-bicarbonate. The BS3 solution was then washed off in

deionised water and the slide dried under a nitrogen gas stream. Epoxy slides were used directly as supplied with no preparation step.

4.5 Initial assays using Alexa Fluor[®] 633 labelled reagents in the optical breadboard

The aim of this section was to show that an immunoassay could be carried out in a microarray format in a microfluidic channel structure. The first experiment was designed to demonstrate an immunoassay based on immobilising material on the surface of a microfluidic channel, using an Alexa Fluor[®] 633 labelled secondary antibody, to show that an assay could be carried out with appropriate reagents for image readout with the breadboard system. This was followed by an experiment in which the assay was carried out in a microarray spot format, in order to establish a protocol for an immunoassay in a microarray format, and to show that the imaging system was suitable for producing images to readout this type of immunoassay.

4.5.1 Initial assay using Alexa Fluor[®] 633 labelled reagents in the optical breadboard – materials and methods

In a previous experiment (see Appendix A), a polystyrene surface was used to physically immobilise proteins to a material surface to carry out an immunoassay. In this experiment, rather than using a physical adsorption method, a covalent protein immobilisation method was selected. A covalent immobilisation was chosen because, at this stage in the project, silicon waveguide wafers or chips were being considered as potential materials for the optical waveguides and microfluidic structures in the flight instrument. These materials were not expected to be suitable for the physical adsorption of proteins since their surfaces are relatively hydrophilic. Since the chemical properties of silicone oxide and silicon nitride are similar to glass, it was expected that standard surface chemistry reactions could be used to functionalise the surface with amine or epoxy surface chemistries. The surface reactions were investigated in a later experiment (see section 4.10). In this initial experiment commercially available amine-coated slides (Genetix, Loughborough, UK) were used, as they have a similar surface chemistry to an amine functionalised silicon wafer.

The slides were first activated with BS3 linker (Pierce, Rockford, IL, USA). 20µl of a freshly prepared solution of 2.5×10^{-5} M BS3 in pH 9.0 sodium carbonate-bicarbonate buffer was

pooled over each assay area as defined by laser cut microfluidic structures (cut from ARCare AR8939 adhesive tape - see Appendix A and Figure A.4), and incubated in a humidity chamber for 30 minutes. Each assay area was then washed five times with 1ml of deionised water, by pipetting the water onto the assay area at an acute angle downwards. The slide was then dried under a nitrogen gas line.

In this experiment, the entire assay area of the microfluidic structure was coated with antibody, rather than using the microarray spot format. This change was made because there were a number of modifications in the protocol compared to the previous immunoassay in a microarray format, including a different immobilisation chemistry and the use of a slightly less specific anti-human antibody. It was considered that since all of these methodological changes would have to be successful in order for the immunoassay to work, carrying out the assay in a microarray spot format may further complicate the interpretation of the results of this experiment. The aim of the experiment therefore was to determine whether the surface chemistry and antibody changes were compatible with reading out an immunoassay on the breadboard system. The method was as follows:

- 20 μ l of 0.03mg.ml⁻¹ anti-atrazine antibody (kindly provided by Haptogen, Aberdeen, UK) in PBS-30% glycerol (AnalR grad, Merck) (a humanised recombinant antibody fragment) was pooled over each assay area and incubated in a humidity chamber for 2 hours.
- The slide was then placed into a blocking solution of 0.1mg.ml⁻¹ skimmed milk powder (Marvel), agitated to wash remaining anti-atrazine, in PBS from the slide surface and incubated in a humidity chamber for 2 hours.
- Each assay area was washed five times with 1ml of 10mM PBS pH 7.4 with 0.1% TWEEN-20 and then five times with 1ml of deionised water, by pipetting the water onto the assay area at an acute angle downwards. The slide was then dried under a nitrogen line.
- 20 μ l of 0.02mg.ml⁻¹ goat anti-human IgG (H+L) labelled with Alexa Fluor[®] 633 (Molecular Probes, Paisley, UK) in 10mM PBS pH 7.4 was then pooled over the test assay area. 20 μ l of 10mM PBS pH 7.4 was pooled over the control assay area, and the slide incubated in a humidity chamber for 2 hours.
- The chip was then placed into the imaging system and an image taken with a 60 second exposure.

4.5.2 Initial assay using Alexa Fluor[®] 633 labelled reagents in the optical breadboard – results and discussion

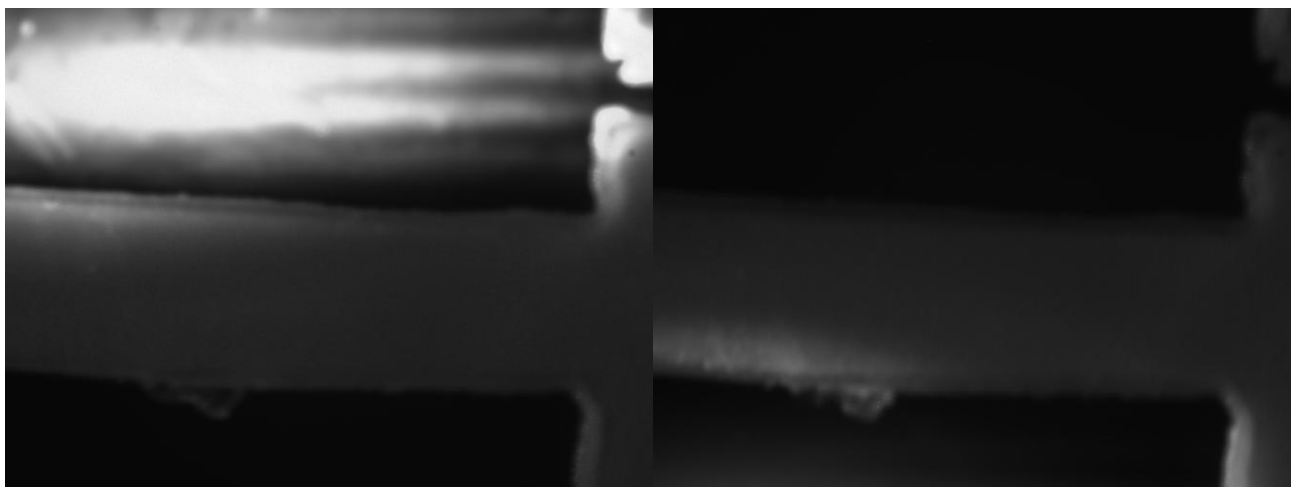


Figure 4.5: 60 second exposures of the assay area (~ 1 x 2mm) of a microfluidic channel on which a binding immunoassay was carried out. In both images, the top area is a complete immunoassay, the bottom area is a control area in which the secondary antibody was not included in the assay protocol. Left: laser illumination directed onto the complete assay area. Right: laser illumination directed onto the control area.

Figure 4.5 shows that while the experiment in which the complete assay was performed (top) gives a strong fluorescent signal when the laser is directed at that area, the control assay with no Alexa Fluor[®] 633 labelled secondary antibody present does not give any fluorescence. Neither assay area produces any fluorescence when the laser is not directed at it, because the laser illuminates only a small area of the surface. This suggested that all stages of the assay, including the covalent immobilisation of anti-atrazine antibody on the slide surface, were functioning as expected, and that it was possible to obtain images of bound Alexa Fluor[®] 633 labelled secondary antibody. The anti-human (H+L) secondary antibody labelled with Alexa Fluor[®] 633 may have a lower binding affinity than the anti-human kappa light chain antibody (which was used as a secondary antibody to bind to the anti-atrazine scAb in section 3.1.2.3), because it is raised against a less specific target (personal communication, Haptogen, Aberdeen). While this may be the case, this experiment confirmed that the anti-human (H+L) antibody would bind to the anti-atrazine scAb strongly enough for it to be detected with the breadboard imaging system, and therefore that the binding immunoassay appeared to be working under the conditions of this experiment. However, it should be noted that if the anti-human (H+L) antibody does have a lower binding affinity for the recombinant anti-atrazine scAb than anti-human kappa light chain antibodies, it may not be possible to achieve very low limits of detection with this assay. Since the immunoassay had been shown to work under the conditions used, an experiment to carry out an immunoassay with the same reagents and conditions in a microarray spot format was attempted.

4.5.3 Preliminary immunoassay in microarray format – materials and methods

The assay area was activated with BS3 linker as described in section 4.4. The protocol for the assay was as follows:

- An array of 5 rows in a controlled pattern of spots was then printed with the Spotting Robot using of $0.03\text{mg}\cdot\text{ml}^{-1}$ anti-atrazine antibody (kindly provided by Haptogen, Aberdeen, UK) in PBS-30% glycerol.
- The slide was then placed into a solution of $0.1\text{mg}\cdot\text{ml}^{-1}$ skimmed milk powder (Marvel), agitated to wash remaining anti-atrazine in PBS-30% glycerol from the slide surface. The slide was then incubated in a humidity chamber for 2 hours.
- Each assay area was washed five times with 1ml of 10mM PBS pH 7.4 with 0.1% TWEEN-20 and then five times with 1ml of deionised water, by pipetting the solutions onto the assay area at an acute angle downwards. The slide was then dried under a nitrogen line.
- $20\mu\text{l}$ of $0.02\text{mg}\cdot\text{ml}^{-1}$ labelled anti-human IgG (H+L) labelled with Alexa Fluor[®] 633 in 10mM PBS pH 7.4 was then pooled over the test assay area. The slide was then incubated in a humidity chamber for 2 hours.
- The assay area was then washed five times with 1ml of 10mM PBS pH 7.4 containing 0.1% TWEEN-20 and then five times with 1ml of deionised water, by pipetting the solutions onto the assay area at an acute angle downwards.
- The chip was then placed into the imaging system and an image taken with a 60 second exposure (see Figure 4.6).

4.5.4 Preliminary immunoassay in microarray format – results and discussion

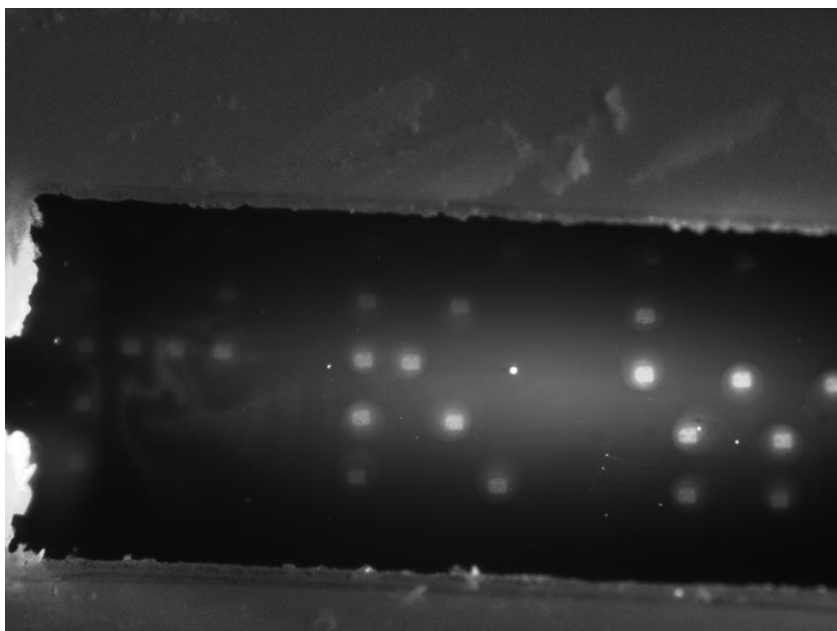


Figure 4.6: An immunoassay in which $110\mu\text{m}$ diameter spots of anti-atrazine scAb were deposited onto an activated amine surface and exposed to Alexa Fluor[®] 633 labelled secondary antibody. This 60 second image was taken on the optical breadboard.

Figure 4.6 shows a 60 second exposure image of the chip after the assay was carried out, and shows fluorescence in the positions where the anti-atrazine scAb was spotted onto the surface, but not from other parts of the blocked assay area. The low level of fluorescence

between the spots indicates that the blocking and washing protocols were reasonably effective in preventing non-specific binding. This result was a clear demonstration that all stages of the assay system were fundamentally working. Another important development was that even though the configuration did not allow maximum light collection efficiency from the array, Figure 4.6 showed that the breadboard imaging system could be used to readout immunoassays of this type with a convenient exposure time.

However, it is apparent that the assay area has a non-uniform illumination, such that the spots in the centre of the image appear to be brighter than those at the outside. This was interpreted as a result of the laser spot having an uneven intensity, and being smaller than the assay area, thus giving an uneven intensity distribution across the assay area. In order to resolve this problem, a 10x beam expander (Intelite Inc., Genoa, USA) was incorporated into the imaging system. This spread the point source of the laser over the area of a 1cm diameter circle, providing much more uniform illumination of the assay area (note, however, that this does not affect the energy distribution profile). Spreading the laser illumination over a larger area reduces the intensity of the illumination at any given point, potentially making a longer exposure time necessary.

The same chip imaged in Figure 4.6 was re-imaged with the beam expander in the system. Figure 4.7 below shows the result of this experiment. It is clear by visual inspection of the image that the addition of the beam expander has resulted in a much more even illumination of the surface and correspondingly more even intensity of the array spots. Also, the central spots also appear less bright than in Figure 4.6, as expected due to the reduced illumination intensity.

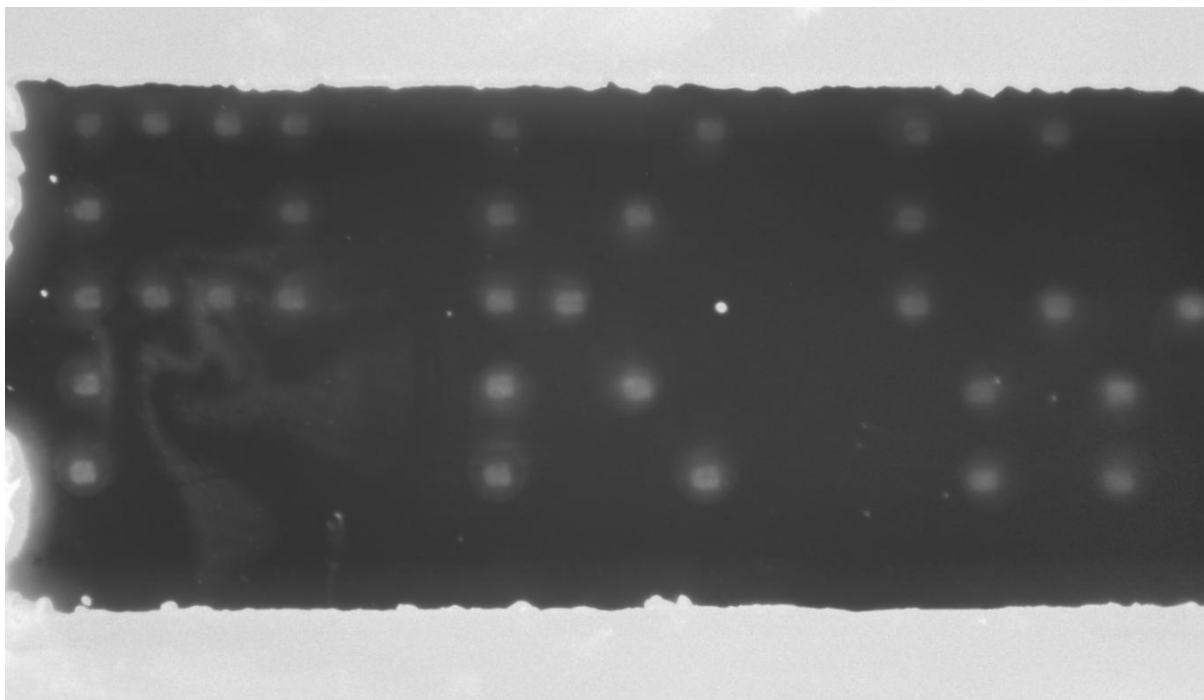


Figure 4.7: An immunoassay in which 110 μ m diameter spots of anti-atrazine scAb were deposited onto an activated amine surface and exposed to Alexa Flour[®] 633 labelled secondary antibody. This 60-second exposure image was taken on the breadboard imaging system in darkness with the beam expander present.

All of the spots present in Figure 4.7 and Figure 4.6 appear to consist of a brighter square area with a 'halo' of less bright fluorescence around them. This 'halo' effect is much clearer in Figure 4.7 than in Figure 4.6, due to the uneven illumination in Figure 4.6. In order to try to prevent this halo effect from appearing, a series of experiments were carried out with variations on the blocking and washing protocols used in the immunoassay. These are reported in the following section.

4.6 Optimisation of blocking and washing protocols

In the previous experiment (see section 4.5.4), the immunoassay in a microarray format was proved successful, but the spots appear to have a 'halo' around them. In order to try to remove this halo effect, a number of approaches to the blocking and washing stages were devised. Three assay areas per chip were prepared using each of these approaches, to compare the effects and reproducibility of each method.

4.6.1 Optimisation of blocking and washing protocols – materials and methods

The approaches used in this experiment to find a suitable blocking and washing protocol included the use of alternative washing methods, different blocking solutions and sonication. The halo effect observed was thought to be occur between completion of pin printing and incubation in the blocking solution, so this is the stage at which the blocking and washing protocol was altered. A 0.2M TRIS buffer pH 9.0 was used in some blocking protocols since

TRIS buffers contain free amine groups, and would inactivate any remaining epoxy groups on the slide surface prior to the protein blocking stage. Ultrasonication was used in some protocols to try to remove the spotting buffer containing glycerol from the slide surface more effectively than by manual agitation.

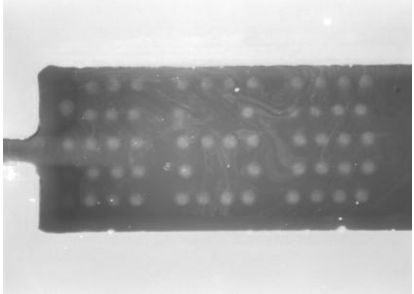
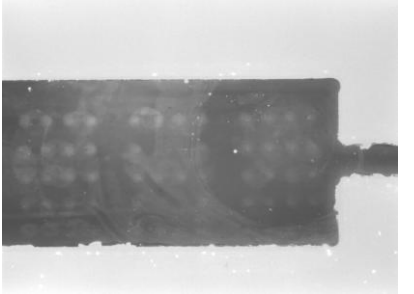
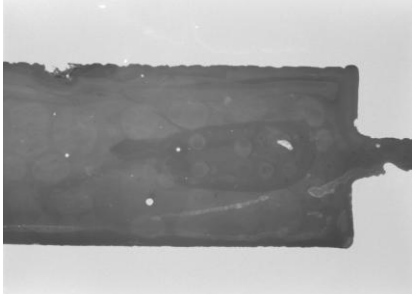
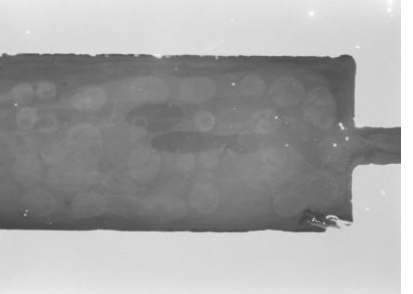
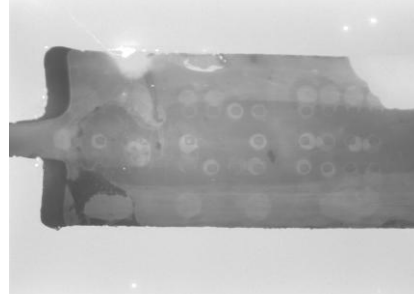
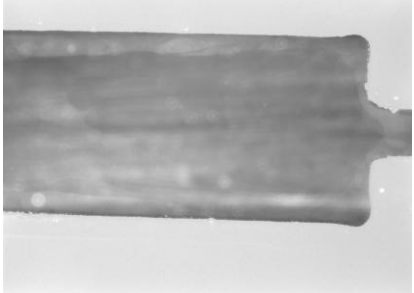
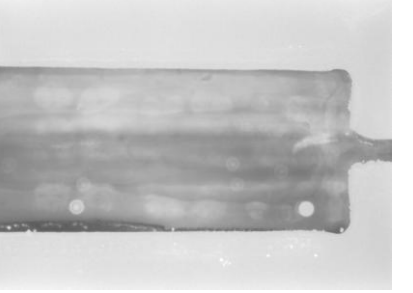
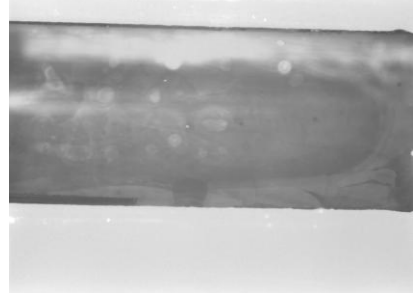
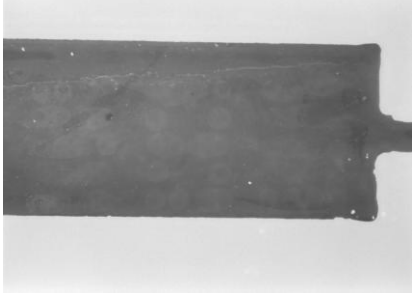
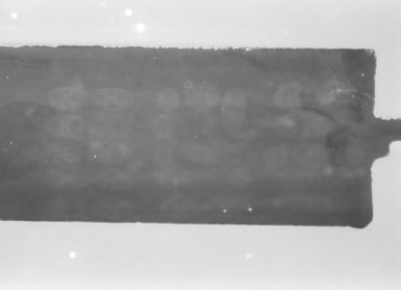
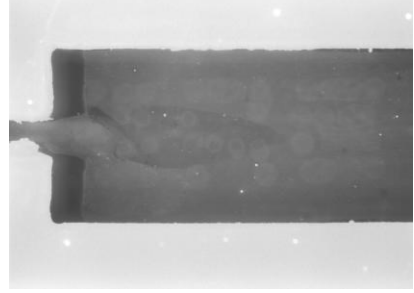
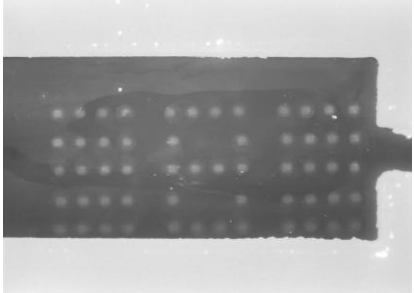
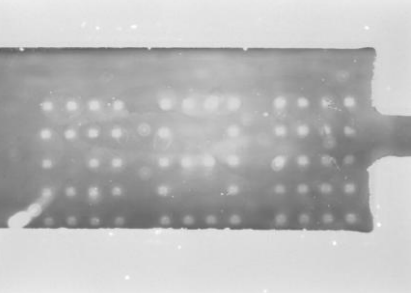
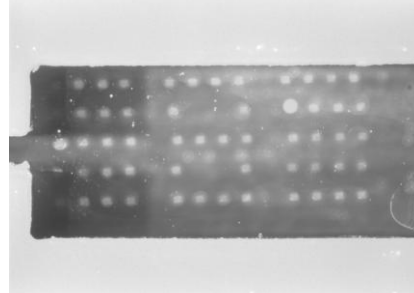
In each of these experiments the following protocol was followed:

- An array of 5 rows in a controlled pattern of spots was printed onto BS3-activated amine coated slides (Genetic, Loughborough, UK) with the Spotting Robot using 20 μ l of 0.03mg.ml⁻¹ anti-atrazine scAb in PBS-30% glycerol.
- Blocking step (one of the following was used for each experiment):
 - Assay areas were washed five times with 1ml blocking solution of 0.1mg.ml⁻¹ skimmed milk powder, then 20 μ l blocking solution was pooled over the assay area and incubated in a humidity chamber for 2 hours. (Table 4.1 top row left).
 - Assay areas were washed five times with 1ml 0.2M TRIS buffer pH9.0, then 20 μ l blocking solution of 0.1mg.ml⁻¹ skimmed milk powder was pooled over the assay area and incubated in a humidity chamber for 2 hours (Table 4.1 top row centre).
 - Assay areas were washed five times with 1ml of 0.2M TRIS buffer pH9.0, then the slide was sonicated at 15000Hz for 1 minute in 0.2M TRIS buffer with additional manual agitation. The slide was then placed in a beaker of blocking buffer for 2 hours (Table 4.1 row 2).
 - The slide was washed for 1 minute in a beaker of blocking solution of 0.1mg.ml⁻¹ skimmed milk powder with manual agitation, then the slide was placed in a beaker of blocking buffer for 2 hours. (Table 4.1 row 3).
 - The slide was sonicated at 15000Hz for 1 minute in blocking buffer with additional manual agitation for 1 minute, then the slide was then placed in a beaker of blocking buffer for 2 hours. (Table 4.1 row 4).
 - The slide was washed in a beaker of PBS-0.1% TWEEN 20 high-speed magnetic stirring for 1 minute, then each assay area washed three times with 1ml of deionised water, then the slide was then placed in a beaker of blocking solution of 0.1mg.ml⁻¹ skimmed milk powder for 2 hours (Table 4.1 row 5).
- Each assay area was then washed five times with 1ml of 10mM PBS pH 7.4 with 0.1% TWEEN-20 and then five times with 1ml of deionised water, by pipetting the water onto the assay area at an acute angle downwards. The slide was then dried under a nitrogen line.
- 20 μ l of 0.02mg.ml⁻¹ labelled goat anti-human IgG (H+L) (Molecular Probes / Invitrogen, Paisley, UK) labelled with Alexa Fluor[®] 633 in 10mM PBS pH 7.4 was then pooled over the test assay area, and the slide incubated in a humidity chamber for 2 hours.
- The chip was then placed into the breadboard imaging system, and an image taken with a 60 second exposure (see Figure 4.6).

4.6.2 Optimisation of blocking and washing protocols – results and discussion

The results of this study are shown in Table 4.1.

Table 4.1: Results of a number of different blocking and washing experiments on amine coated slides.

			
<p>5 x 1ml Blocking Buffer, 5x 1ml dH₂O incubate 10µl</p>		<p>5 x 1ml 0.2M TRIS pH 9.0, 5x 1ml dH₂O incubate 10µl</p>	
			
<p>60 second sonication with manual agitation in blocking buffer, incubate 10µl blocking 1</p>	<p>60 second sonication with manual agitation in blocking buffer, incubate 10µl blocking 2</p>	<p>60 second sonication with manual agitation in blocking buffer, incubate 10µl blocking 3</p>	
			
<p>60 second sonication with manual agitation in 0.2M TRIS pH 9.0, incubate 10µl blocking 1</p>	<p>60 second sonication with manual agitation in 0.2M TRIS pH 9.0, incubate 10µl blocking 2</p>	<p>60 second sonication with manual agitation in 0.2M TRIS pH 9.0, incubate 10µl blocking 3</p>	
			
<p>60 second sonication in blocking buffer, beaker blocking incubation 1</p>	<p>60 second sonication in blocking buffer, beaker blocking incubation 2</p>	<p>60 second sonication in blocking buffer, beaker blocking incubation 3</p>	
			
<p>60 second washing in PBS-0.1% TWEEN 20 under magnetic stirring, incubation in beaker of blocking 1</p>	<p>60 second washing in PBS-0.1% TWEEN 20 under magnetic stirring, incubation in beaker of blocking 2</p>	<p>60 second washing in PBS-0.1% TWEEN 20 under magnetic stirring, incubation in beaker of blocking 3</p>	

The first row of Table 4.1 shows the results of two experiments in which the slide was washed by pipetting 1ml of either blocking buffer or in 0.2M TRIS pH 9.0 over the assay area at an acute angle five times and then blocked by placing 10 μ l of blocking buffer over the assay area and incubating for two hours in a humidity chamber. In the image on the left the blocking buffer used for washing and blocking was 0.1% w/v skimmed milk powder in 10mM HEPES pH 7.4. The image on the right shows a slide that was washed in 0.2M TRIS pH 9.0 before blocking with 0.1% w/v skimmed milk powder in 10mM HEPES pH 7.4. While microarray spots are visible in both of these images, the spots are clearer when 0.1% w/v skimmed milk powder in 10mM HEPES pH 7.4 was used as a washing buffer rather than 0.2M TRIS pH 9.0.

The second row of Table 4.1 shows triplicate results of an experiment in which the slides were washed by sonication for 60 seconds in a beaker of blocking buffer (0.1% w/v skimmed milk powder in 10mM HEPES pH 7.4) while being manually agitated in the beaker, and then blocked by incubation in 10 μ l of blocking buffer. In this case, no microarray spots are visible in any of the images. A similar result was obtained in the third and fourth rows of Table 4.1, in which slides were washed by sonication for 60 seconds in a beaker of in 0.2M TRIS pH 9.0 and then blocked by incubation in either 10 μ l of blocking buffer, or a beaker of blocking buffer, respectively. The images in rows two to four indicate that sonication may disturb the microarray spots on the surface of the slide, causing the anti-atrazine antibody in the printing solution to spread and immobilise over the entire surface. The labelled anti-human (H_L) antibody would then bind to the whole of the assay area resulting in the observed high background signal. It was therefore decided not to include a sonication step in any future experiments.

The fifth row of Table 4.1 shows triplicate results of an experiment in which the slides were washed in a beaker of 10mM PBS buffer pH 7.4 containing 0.1% TWEEN 20 surfactant before blocking by incubation in a beaker of blocking buffer. Microarray spots are visible in these images, but they have a similar level of background fluorescence as the image in Figure 4.7, and also have the same 'halo' effect around the spots observed in Figure 4.7 (although this is difficult to observe in the images in Table 4.1, it is clear when the images are larger as in Figure 4.7). This method therefore does not offer any clear advantages over the previous protocol.

In summary, a number of conclusions were drawn from this series of experiments:

- The inclusion of a sonication step resulted in an extremely high level of non-specific binding signal around the spots. This could be because while removing the printing buffer containing antibody from around the spot area, the sonication was spreading the printing buffer over the surface and causing the anti-atrazine scAb to be immobilised across the entire assay area.
- The use of TRIS buffer in the blocking protocol to neutralise any remaining active epoxy groups on the slide surface appeared to either have no effect or increase the background level. Protocols including this step were eliminated as potential methods to overcome the problem of non-specific binding.
- Manual agitation alone improved the blocking results in some cases but not reproducibly.

Given that none of the above experiments appeared to have resolved either the background fluorescence or presence of 'halo' effects around the spots, the slide surface chemistry was changed in the next series of experiments in order to circumvent some of these issues.

4.7 Development of immunoassay on epoxy coated slides

Since a number of the issues causing high background fluorescence in the assay images appeared to be difficult to resolve by modification of the blocking step using amine-coated slides, the pragmatic approach of attempting the assay on epoxy-coated slides was adopted. Both amine (Cras *et al.*, 1999) and epoxy (Guilleaume *et al.*, 2005) functionalised surfaces have been used for protein immobilisations in literature, and this change would have little effect on the existing experimental protocol other than to remove the BS3 activation step. The literature also indicated that epoxy coated slides are more commonly used for protein microarray work than amine-coated slides (Guilleaume *et al.*, 2005). Slide functionalisation methods are discussed in more detail in section 4.10.

The epoxy coated slides (Genetix, product code K2652, New Milton, UK) were used directly as supplied, as no surface activation step was necessary. For the initial experiments with epoxy coated slides the blocking and washing method selected was washing with five times with 1ml of RO water and incubating in a beaker of blocking solution.

4.7.1 Validation of epoxy coated slides – materials and methods

Initially, an experiment was carried out to confirm that the assay performed similarly on epoxy-coated slides as for the amine slides, by repeating the same immunoassay protocol described in section 4.5.4 with minor modifications to adapt the protocol for epoxy coated slides. This included increasing the imaging time from 60 seconds to 300 seconds, as this was found to improve the image quality for immunoassay on epoxy-coated slides.

- An array of spots of $0.03\text{mg}\cdot\text{ml}^{-1}$ anti-atrazine in 10mM PBS pH 7.4 containing 30% glycerol was printed directly onto the epoxy-coated slide, then the slide was incubated for 2 hours in a humidity chamber.
- The slide was then blocked by immersion in a beaker of blocking solution of $0.1\text{mg}\cdot\text{ml}^{-1}$ skimmed milk powder for 2 hours.
- Each assay area was washed five times with 1ml RO water, by pipetting the liquid over the surface at an acute angle.
- $20\mu\text{l}$ of anti-human Alexa Fluor® 633 labelled secondary antibody was pooled over the assay areas and the slide incubated in a humidity chamber for 2 hours.
- The assay areas were then washed three times with 1ml of 10mM PBS pH 7.4 containing 0.1% TWEEN 20, then twice with 1ml RO water and dried for 1 minute under a nitrogen line.
- The slide was placed into the breadboard imaging system and an image taken using a 300 second exposure time.

4.7.2 Validation of epoxy coated slides – results and discussion

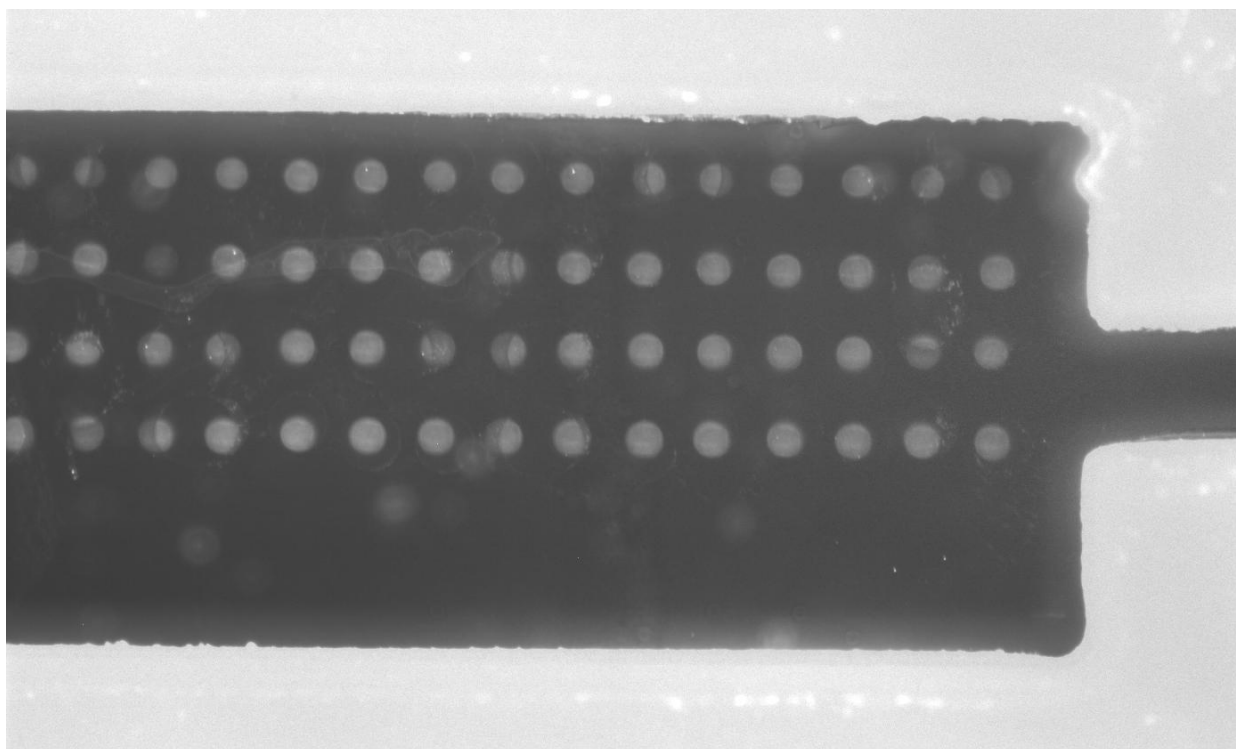


Figure 4.8: An immunoassay in which a 4×20 array of $110\mu\text{m}$ diameter spots of anti-atrazine scAb were deposited onto an epoxy coated slide (Genetix) and exposed to Alexa Fluor® 633 labelled secondary antibody. This 300-second exposure image was taken on the optical rig in darkness with the beam expander present.

Figure 4.8 shows an example of a microarray produced in this experiment (one sample of three). It is clear that all of the spots appear to be present and emitting similar levels of fluorescence. It is also immediately clear that the 'halo' effect observed in Figure 4.7 is not present here. This result was a clear demonstration that the assay system was fundamentally working, confirming that the assay protocol could be transferred to epoxy coated slides with improved results in terms of non-specific binding. However, there are some undesirable features present such as 'half-spots' and drying effects. In order to achieve the goals of optimising the immunoassay protocol and developing a relevant assay for a biomarker target, a number of protocol variations were carried out during the development of a new immunoassay system.

4.8 Selection of an assay system directly relevant to Martian samples

In order to make the immunoassay development work more relevant to the final instrument, the decision was taken to change the both the target molecule and the assay format. The new assay system selected was based on the detection of GroEL (chaperonin-60), a molecular chaperone involved in protein synthesis and ubiquitous to many forms of terrestrial life (see section 2.2.6.1). A commercially available GroEL protein (Cat. No. C7688, Sigma-Aldrich, Poole, UK.) and anti-GroEL antibody (Cat. No. G6532, Sigma Aldrich, Poole, UK) were selected for this assay because they were available in a convenient form (freeze-dried protein and IgG antiserum fraction, respectively), and had also been used in earlier work by collaborators (Steel, A., personal communication).

In the proposed SMILE Life Marker Chip, one of the key elements of the assay system was the *in-situ* labelling of biomarker targets with fluorescent dyes to allow direct detection of biomarkers in the sample (Sims *et al.*, 2005). As far as the author is aware, such labelling reactions have not been attempted in this format before. Since neither the anti-GroEL antibody nor the GroEL protein were available pre-labelled with Alexa Fluor[®] 633, a small scale *in-situ* labelling method was developed. The addition of this *in-situ* labelling step made the assay protocol being used more relevant to the proposed final format for the flight instrument, and provided a way to readout GroEL immunoassays in a microarray format with the optical breadboard system in the absence of commercially available reagents.

4.9 Initial *in-situ* labelling protocol for GroEL protein

As mentioned in section 4.2.1, the Alexa Fluor[®] 633 dye used was selected in part because it is available with a succinidyl ester functional group. The succinidyl group will react with amine groups causing the dye to covalently attach to the amine, and this can be utilised in

protein labelling since proteins contain many free amine groups at their surface (Document No. MP00143 (Amine-reactive probes), Molecular Probes). This section describes how Alexa Fluor[®] 633 succinidyl ester was used to label GroEL protein.

4.9.1 Initial *in-situ* labelling protocol for GroEL protein – materials and method

The GroEL protein was aliquotted into a number of vials each containing 20 μ l of 1 mg.ml⁻¹ GroEL as supplied by the manufacturer, in TRIS buffer. Since, as described above TRIS buffer contains free amine groups which react with succinidyl ester groups, and this would have a quenching effect on any labelling reaction. To avoid this problem without the need for a large excess of reactive dye, prior to use the GroEL aliquots were made up to 500 μ l by addition of HEPES buffer (pH 7.4, 10mM), then the 500 μ l volume was passed through a Microcon 10,000 molecular weight cut-off filter (Fisher Scientific, Loughborough, UK) by centrifuging at 13,000 RPM for 30 minutes. The 60,000Da GroEL held back by the membrane was reconstituted into HEPES buffer (pH 7.4, 10mM), by adding 100 μ l of the buffer to the filter, inverting the filter and centrifuging the product out into a clean vial for 1 minute at 6,500 RPM. The final concentration of GroEL in HEPES buffer was 0.2 mg.ml⁻¹, assuming that no GroEL was lost during the filtration step.

In preparing this labelling reaction, Alexa Fluor[®] 633 succinidyl ester was dissolved in anhydrous methanol (Sigma-Aldrich, Poole, UK) to a concentration of 1 mg.ml⁻¹. The succinidyl ester groups will hydrolyse in water (Document No. MP10168 (Alexa Fluor[®] Succinidyl Esters), Molecular Probes) and have a half-life of 30 minutes. Anhydrous methanol was selected as a suitable solvent as it was sufficiently polar to dissolve the dye, but does not contain water and so would not significantly affect the reactivity of the succinidyl groups. The dye was then diluted to a concentration of 0.2mg.ml⁻¹ in anhydrous methanol, and 100 μ l of this dye solution was added to a number of 1.5ml Eppendorf vials. The open aliquots and remaining stock solution of 1mg.ml⁻¹ Alexa Fluor[®] 633 in anhydrous methanol were then placed into a sealed vessel containing excess self-indicating silica gel desiccant (to prevent the dye absorbing water from the ambient atmosphere), and the vessel placed into an oven at 37°C overnight to drive off the methanol and leave only reactive dye in the aliquots. This left a mass of 0.02mg of reactive Alexa Fluor[®] 633 dried in the vials.

The ratio of dye to protein was calculated such that there was a fifty times molar excess of dye compared to protein molecules in the reaction mixture. This was thought to be sufficient as a typical labelling reaction of this type attaches 20-40 dye molecules per protein molecule for a typical protein such as BSA. 100 μ l of 0.2 mg.ml⁻¹ protein was added to the Eppendorf

vials of Alexa Flour[®] 633, and the dye dissolved and mixed thoroughly by pipetting and agitation. This reaction mixture was left in a sealed vial at ambient temperature for 30 minutes. Effective dye labelling was verified by passing the dye reaction mixture through a 10,000 MWCO filter after completion of the labelling reaction (see Figure 4.9 below). Since the protein would be held back by the filter while any unreacted dye would pass through it, a blue colour in the separated high molecular weight fraction would indicate that dye was attached to the protein i.e. the reaction was successful.

4.9.2 Initial *in-situ* labelling protocol for GroEL Protein – results and discussion

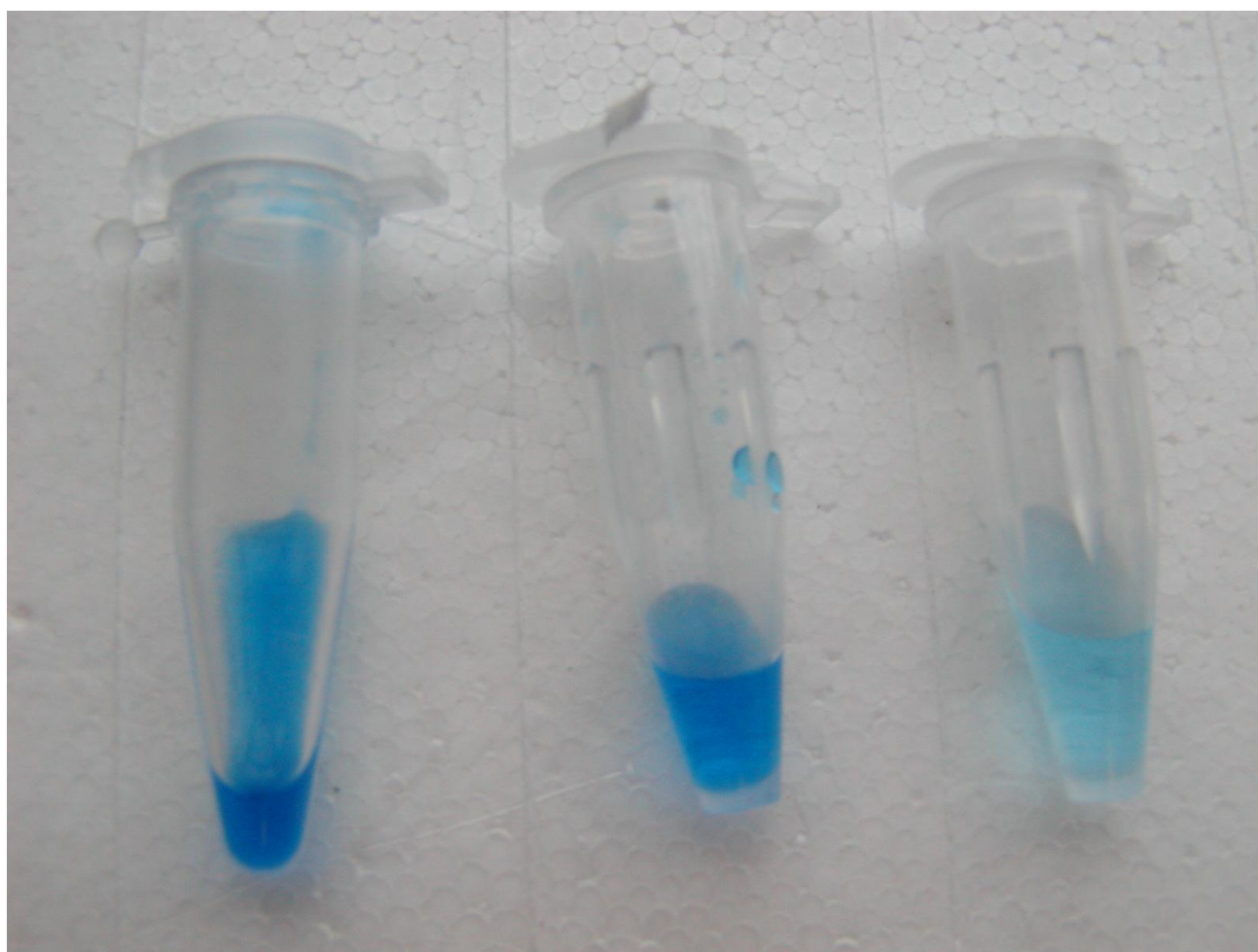


Figure 4.9: Photograph of labelled GroEL protein under different conditions: Left: Complete reaction mixture. Centre: Fraction of reaction mixture retained after filtration through a 10,000 MWCO filter and reconstituted in 10mM HEPES pH 7.4. Right: Filtrate of complete reaction mixture.

Figure 4.9 showed that the majority of the dye was held back by the filter after the reaction had taken place, indicating a high degree of successful labelling. However, some dye passed through the filter confirming that the amount of dye initially in the reaction mixture was an excess, as intended. This experiment established that the labelling process appeared to be successful, and that the anti-GroEL antibody could bind to the labelled GroEL

protein, and the labelling reaction was scaled down to the level of a single batch in subsequent experiments.

The next goal of this section of work was to confirm that the GroEL immunoassay system could be applied to epoxy-functionalised slides in a microarray format. The previous experiments had demonstrated that a number of requirements for a working GroEL immunoassay in this format were established. Figure 4.9 had confirmed that the GroEL labelling reaction was working, since Alexa Fluor[®] 633 would only be retained by the molecular weight cut-off filter if it was attached to the GroEL protein. The experiment in section 4.7 had shown that an immunoassay protocol was working on epoxy-coated slides, and could be read out with the breadboard imaging system. Therefore, the main unknown factors involved in performing a GroEL immunoassay were whether the anti-GroEL antibody would bind to GroEL labelled with a large amount of Alexa Fluor[®] 633, and what binding affinity the antibody would have if it did bind. To minimise the potential effect of a low antibody binding affinity, a high concentration of labelled GroEL was used in the first GroEL immunoassay in a microarray format, to ensure that binding would be detected if it occurred.

In the LMC flight instrument design the base material of the optical waveguides is proposed to be a silicon wafer, with a surface of either silicon oxide or silicon nitride. Silicon oxide and silicon nitride waveguides are not commercially available with an epoxy surface chemistry, and would need to be functionalised in-house. This meant that one of the key goals of the LMC development was to demonstrate immunoassays on in-house epoxy functionalised silicon surfaces. In order to progress towards such a demonstration, the decision was taken to develop the GroEL immunoassay on both commercial and in-house epoxy-coated surfaces in parallel. The next key requirement was to establish a procedure for the in-house epoxy functionalisation of surfaces, and the following section describes the epoxy functionalisation protocol that was adopted.

4.10 (3-glycidoxypropyl)trimethoxysilane (GOPS) functionalisation protocol

A standard method to covalently immobilise proteins on a glass or silica surface is to modify the surface with a functionalised silane containing an epoxy group. The silane group reacts with free hydroxyl groups on the surface and under ideal conditions produces a monolayer surface coating with a high density of reactive epoxy groups available for immobilisation of proteins (Kambhampati, 2004, Cras *et al.*, 1999, Van Der Voort & Vansant, 1996). Protein

molecules are immobilised by the formation of a covalent bond between the epoxy group on the surface and free amine groups on the protein (Kambhampati, 2004)

A number of epoxy functionalisation protocols were reviewed (Cras *et al.*, 2006, Guilleaume *et al.*, 2005, Han *et al.*, 1999, Lamure *et al.*, 1994), and for convenience the simplest approach identified in the literature was adopted (Cras *et al.*, 2006). Briefly the protocol involves an overnight incubation in an anhydrous organic solvent containing an appropriate epoxy-functionalised silane at room temperature and under an inert gas, either argon or helium. The inert gas prevents water from entering the system via the ambient atmosphere. Other adaptations of this basic protocol were present in the literature, including higher temperature incubations, refluxing, agitation and sonication, but for this work it was considered that if a simple approach was successful, a more complex protocol was not necessary.

4.10.1 (3-glycidoxypropyl)trimethoxysilane (GOPS) functionalisation protocol – materials and methods

(3-glycidoxypropyl)trimethoxysilane (GOPS) (Cat. No. 440167, Sigma Aldrich, Poole, UK) was selected as an appropriate silane reagent because it has been used extensively in the literature and is commercially available. It is used diluted to an appropriate concentration in anhydrous toluene.

The critical factors in the success of any silane functionalisation are the cleaning of the surface to be functionalised and all equipment used in the experiment (to remove organic contamination which could inhibit the functionalisation reaction), and removal of water from the reaction chamber (Cras *et al.*, 1999). Water must be removed to prevent polymerisation of the silane, which would result in a thicker and non-uniform deposition, which, in the context of the Life Marker Chip, could extend beyond the evanescent field (Cras *et al.*, 1999). To achieve the required level of cleanliness, all glassware used in the procedure (a 500ml reaction vessel with three Quickfit access ports, three Quickfit glass stoppers to seal the reaction vessel, two 20ml Hamilton syringes, and one 2ml Hamilton syringe) and a metal spatula were thoroughly washed with detergent and rinsed with RO water. All of this equipment was placed in an oven (OMT oven, Sanyo, Loughborough, UK) at 200°C for four hours to remove adsorbed water.

The glass chips were cleaned during the oven drying of other equipment. In the first run glass microscope slides were used, and these were cut into the same dimensions as the silicon chips to be supplied by collaborators. This was because the functionalisation chemistry would be expected to be the same and the availability of silicon chips was limited. A 500ml plastic beaker was thoroughly cleaned with detergent and rinsed with RO water. Working in a laminar flow cabinet to reduce particulate contamination from the atmosphere, four 20 x 20mm glass microscope slide chips were placed inside the beaker with plastic wafer tweezers, and moved to space them evenly around the base. The first washing step was ultrasonication in a detergent, to remove any organic contamination from the surface of the glass chips. Approximately 200ml of a 1% w/v Dri-Decon solution in RO water was added to the beaker slowly, to cover the chips with minimal disturbance. The beaker was then covered in aluminium foil and placed in an ultrasonic water bath (275W, 15000Hz) for 10 minutes.

After ultrasonication, the next stage of cleaning was a water washing step to remove all organic material cleaned from the chip surface, and the bulk of the surfactant cleaner, from the beaker. A water vacuum pump was used to remove the Dri-Decon solution from the plastic beaker. The beaker was then re-filled with approximately 200ml of RO water, gently agitated for approximately 30 seconds, and then the RO water removed through the water pump. This was repeated two more times to a total of three washes with RO water. The next stage was to remove both water and residual surfactant from the chip and beaker simultaneously.

Approximately 100ml of anhydrous methanol (Sigma-Aldrich, Poole, UK) was added to the plastic beaker, agitated for approximately 30 seconds and removed through the water pump. A second volume of approximately 100ml of anhydrous methanol was added, and then the beaker was covered in aluminium foil and placed in an ultrasonic water bath for 10 minutes in 1-2cm of water. The methanol was then removed through the water pump, and the beaker re-filled with approximately 100ml of anhydrous methanol, gently agitated for approximately 30 seconds and the methanol removed through the water pump. This was repeated two more times to a total of three washes with anhydrous methanol. The final methanol wash solution was not removed until the reaction chamber was assembled – i.e. the glassware was ready for the slides / chips to be placed into the reaction vessel.

The glassware was removed from the drying oven and allowed to cool in air sufficiently that it could be handled, and placed in the laminar flow cabinet for assembly. An argon gas line

was placed into the reaction vessel through one of the access plugs, and gas released such that a small flow of argon was filling the vessel and gently overflowing from it. This was validated by carefully feeling the flow from the remaining reaction chamber exits. An argon atmosphere prevents water from the ambient atmosphere entering the reaction vessel.

The chips were then removed from the final anhydrous methanol wash and dried under a nitrogen gas flow. The dried chips were then gently placed onto the side of the reaction vessel using clean plastic wafer tweezers, and the reaction vessel gently moved or shaken to slide them in to the bottom of the vessel.

The anhydrous toluene solvent (Cat. No. Sigma-Aldrich, Poole, UK) was then added to the reaction vessel. A 20ml Hamilton syringe was assembled from the dried clean glassware. In order to remove any humidity from the ambient atmosphere from the Hamilton syringe, it was filled with argon gas from the reaction vessel and the argon ejected into the ambient atmosphere. This was repeated nine times to a total of ten cycles of argon through the syringe.

The toluene was supplied under an inert gas, so removal of toluene from the supplied vessel required adding a volume of gas to the stock bottle to replace the volume to be removed. To achieve this, the Hamilton syringe was filled with 20ml argon gas, inserted into the anhydrous toluene vessel, and the gas injected. The Hamilton syringe was then filled with 20ml toluene, removed from the toluene vessel and the 20ml toluene injected into the reaction vessel.

The GOPS was then added to the toluene in the reaction vessel. The 2ml Hamilton syringe was assembled and purged with argon from the reaction vessel ten times as for the 20ml Hamilton syringe. The syringe was then filled with 2ml argon and inserted into the GOPS (Sigma-Aldrich, Poole, UK) bottle. The 2ml argon was injected into the GOPS, and the syringe filled with 2ml of GOPS. The syringe was then removed from the GOPS bottle and the 2ml GOPS injected into the toluene in the reaction vessel. The final concentration of GOPS in toluene was therefore 0.40M.

The argon gas line was removed from the reaction vessel, and the remaining reaction vessel ports sealed with their Quickfit stoppers. The reaction vessel was then agitated gently to mix the GOPS and toluene with minimal disturbance of the glass chips. The reaction vessel was incubated for 24 hours at room temperature, with gently agitation every few hours to mix the solutions. Care was taken to ensure that the chips did not lie on top of each other at any point during incubation, as this could result in uneven GOPS coating.

After the 24 hour incubation, the reaction vessel was opened and an argon line placed into the reaction vessel as before. A clean 20ml Hamilton syringe was assembled and purged with 20ml argon from the reaction vessel ten times to remove air and moisture from the atmosphere. The toluene / GOPS solution was removed from the reaction vessel and disposed of.

The chips were then washed in toluene to remove any excess un-reacted GOPS on the chip surface. A second clean 10ml Hamilton syringe was filled and purged with 20ml argon 10 times, then filled with 20ml argon. 20ml anhydrous toluene was removed vessel as described previously and injected into the reaction vessel. The reaction vessel was agitated to wash the chips in toluene. The Hamilton syringe used to remove the reacted GOPS / toluene mixture was then used to remove the toluene from the reaction vessel. This was repeated two further times to a total of 3 washes in anhydrous toluene.

The glass chips were carefully removed from the reaction vessel, and placed into a clean 500ml plastic beaker. Excess toluene on the chip surface was then removed by covering the chips with approximately 50ml anhydrous methanol, agitating the beaker for 30 seconds, and removing the methanol with a water vacuum pump. This was repeated two further times to a total of three washes in anhydrous methanol. Finally, the methanol was removed by a series of washes in RO water. As for the anhydrous methanol washes, the chips were immersed in approximately 50ml of RO water, agitated for 30 seconds and the water removed with a water vacuum pump, and this process repeated two further times to a total of three washes in RO water. The chips were then removed from the plastic beaker, dried under nitrogen, and stored in a sealed container with excess self indicating silica gel desiccant at room temperature until used.

One glass chip was removed at each stage of the protocol to verify the effect of that step on the surface by contact angle measurements. It was expected that the cleaning steps would remove organic contamination from the chip surface and thus reduce the contact angle, while the GOPS incubation, if successful, would increase the contact angle to $\sim 60^\circ$ (Cras *et al.*, 2006). Three contact angle measurements were made on each of the chips on a KVS CAM 100 contact angle system (KSV Instruments, Helsinki, Finland).

4.10.2 Silane (GOPS) functionalisation of glass – results and discussion

Table 4.2: Results of contact angle measurements at different stages of GOPS functionalisation. One chip was removed from the process at each stage, and three measurements made on each chip at different locations.

Stage of protocol	Contact angle
Untreated glass slides	$<5^\circ$
After detergent wash	$<5^\circ$
After anhydrous methanol wash	$12 \pm 2^\circ$
After GOPS incubation and washing	$61.5 \pm 2^\circ$
Untreated commercial GOPS slide	$49.7 \pm 1^\circ$

Table 4.2 shows the results of the contact angle measurements. These indicate that prior to the GOPS immobilisation the microscope slide was very hydrophilic, having a contact angle of $<5^\circ$. This increased slightly to 12° after the methanol wash, and after incubation in the 0.4M GOPS solution in toluene the contact angle increased to 61.5° , which is in agreement with the range of contact angle measurements for similar methods in the literature (Cras *et al.*, 1999). The commercial GOPS coated slides were found to have a contact angle of 49.7° , possibly due to differences in the GOPS protocol used.

4.11 Silane (GOPS) functionalisation of silicon

For the Life Marker Chip demonstrator and flight instrument, the optical waveguides are proposed to be made from silicon, and coated with a cladding layer of either silicon oxide or silicon nitride. The immunoassay reagents in the microarray must therefore be immobilised onto one of these surfaces. Since the GOPS functionalisation protocol had been shown to be successful on glass, which was expected to have a similar surface chemistry to both silicon oxide and silicon nitride, the next experiment was to test GOPS coating protocol described in section 4.10 on silicon nitride and silicon oxide chips (kindly provided by Lionix, Leiden, Netherlands) (see section 2.3.6). In both silicon based and glass surfaces, silane groups are believed to react with exposed silanol groups on the surface (Van Der Voort and Vansant, 1996), so no fundamental changes were required in the functionalisation protocol.

4.11.1 Silane (GOPS) functionalisation of silicon - materials and methods

The silicon chips were found to have an unexpectedly high contact angle before cleaning which was assumed to be due to organic material contaminating the surface. To remove this, prior to the Dri-Decon and methanol washes the chips were incubated in 1M NaOH for 30 minutes. Otherwise, the protocol was unchanged from that in section 4.10.

4.11.2 Silane (GOPS) functionalisation of silicon – results and discussion

The chip surfaces have been assessed by several methods to determine the quality of the GOPS coating. These methods include visual inspection, contact angle measurement and atomic force microscopy. Visual inspection under good lighting allows the surface to be assessed for roughness or large particulates on the surface and drying stains. No particulates or uneven surface features were observed by visual inspection.

Changes in contact angle indicate a chemical alteration of the surface. Glass has a very low contact angle of $<5^\circ$, and the silicon surfaces used also have a low contact angle. Silicon nitride and silicon oxide have contact angles of approximately 35° (A. Prack, Lionix, The Netherlands, personal communication) while GOPS modified surfaces have a contact angle of $60^\circ - 70^\circ$ (Cras *et al.*, 1999). The contact angles found after cleaning the surfaces and after GOPS functionalisation are shown in **Error! Reference source not found.**

It is clear from **Error! Reference source not found.** that both the silicon nitride and silicon oxide surfaces have a similar contact angle to that expected after cleaning, and that both materials have a contact angle very close to 60° after the functionalisation. This was a good indication that the protocol successfully coated the surface with an epoxy surface chemistry, as intended. Having demonstrated this, the next stage was to develop the assay on epoxy functionalised surfaces, and this was carried out in the following section.

Table 4.3: Contact angle measurement of silicon nitride and silicon oxide surfaces before and after GOPS functionalisation. Typical images and the average values \pm one standard deviation from three measurements are shown.

	Cleaned chip surface	GOPS coated surface
Silicon Nitride	<p>Contact angle $37.6 \pm 2.9^\circ$</p>	<p>Contact angle $58.2 \pm 2.7^\circ$</p>
Silicon Oxide	<p>Contact angle $31.4 \pm 2.0^\circ$</p>	<p>Contact angle $59.6 \pm 2.0^\circ$</p>

4.12 Use of *in-situ* labelled GroEL in microarray assays on in-house GOPS functionalised surfaces

As described in section 4.9.2, establishing a procedure for the in-house epoxy functionalisation of surfaces was a requirement for the parallel development of the GroEL immunoassay on commercial and in-house surfaces. In this section, a series of experiments were carried out in which the *in-situ* GroEL labelling protocol was used to develop a GroEL immunoassay on both commercial epoxy coated microscope slides and glass slides treated with the in-house GOPS functionalisation protocol. A successful immunoassay on the surface functionalised in-house would demonstrate that GOPS functionalisation was a suitable method to prepare silicon or glass surfaces for immunoassays in a microarray format. In addition, this immunoassay utilises custom reagents and a target directly relevant to the Life Marker Chip, and would therefore show that the techniques could be applied for the detection of other suitable biomarkers. Optimisation of the same immunoassay on commercially available GOPS treated slides would show that the more conveniently available commercial slides were suitable for use during the development of the assays. The initial assay showed that GroEL protein was not being removed from the slide surfaces during the assay, possibly due to non-specific binding. This effect was much greater on the commercial

GOPS coated slides. To overcome this, the protocol for *in-situ* labelling of GroEL was modified and a number of changes were made to the immunoassay protocol to try to reduce this effect.

4.12.1 Initial assay using *in-situ* labelled GroEL in microarray assays – materials and methods

At this point in the project, *in-situ* labelling of GroEL had been carried out and verified by filtration and an assay on a commercial GOPS coated slide, and in-house surface functionalisation of glass and silicon surfaces had been optimised and confirmed by contact angle measurement. The next stage of development was to combine these protocols by using the GroEL assay system on the in-house GOPS coated slide, since this is how the assays would be prepared and carried out in the flight instrument. In addition, an assay using the previous anti-atrazine assay was carried out on both in-house and commercial GOPS microscope slides as a control for the immunoassay protocol (since this protocol was known to be successful on amine-coated slides).

The protocol used for these experiments were as follows:

- A 5 x 5 array of either 1/10 v/v anti-GroEL IgG fraction (Sigma-Aldrich, Poole, UK) or 0.3mg.ml⁻¹ anti-atrazine scAb in PBS containing 30% v/v glycerol was spotted onto either commercial or in-house GOPS coated glass slides, and incubated in a humidity chamber for 2 hours.
- The slide was washed and incubated for 4 hours in 0.1mg.ml⁻¹ skimmed milk powder in HEPES 10mM, pH 7.4 buffer, to remove excess spotting buffer and block the remaining slide surface.
- Each assay area was washed five times by pipetting 1ml RO water over it at an acute angle.
- The appropriate Alexa Fluor[®] 633 labelled analyte was pooled over the assay area and incubated for 1 hour (one of the following).
 - 0.2mg.ml⁻¹ Alexa Fluor[®] 633 labelled anti-human IgG (H+L) antibody in HEPES 10mM, pH 7.4 was pooled over anti-atrazine scAb arrays.
 - 0.1mg.ml⁻¹ Alexa Fluor 633[®] labelled GroEL protein total reaction mixture, in 10mM PBS pH 7.4 was pooled over anti-GroEL arrays.
- Each assay area was washed five times with 1ml of HEPES 10mM, pH 7.4 with 0.1% v/v Tween 20, and then five times with 1ml RO water, by pipetting the solution over the assay area at an acute angle.
- The slide was dried under a nitrogen gas line for 1 minute.
- The chip was placed into the breadboard imaging system, and each assay area was imaged with a 300 second exposure.

4.12.2 Initial assay using *in-situ* labelled GroEL in microarray assays – results and discussion

Table 4.4: Images showing the results of the experiments described in section 4.12.1. Top Left: Commercial GOPS slide scAb assay. Top Right: Commercial GroEL Assay. Bottom Left: In-House GOPS slide scAb assay. Bottom Right: In-House GOPS slide GroEL assay.

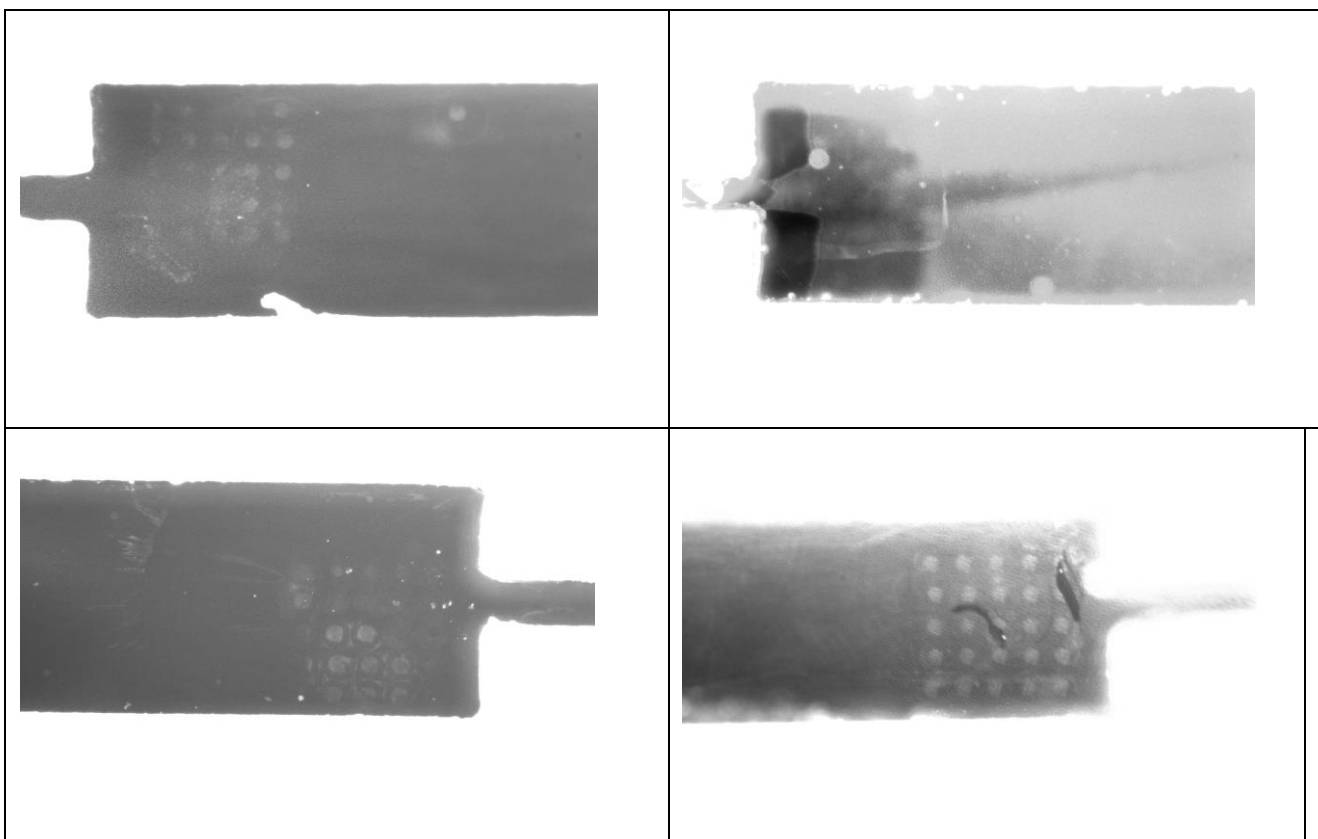


Table 4.5: Results and observations from initial assays on commercial and in-house GOPS coated slides.

	ScAb Spotting	Anti-scAb IgG labelled with Alexa Fluor 633	Anti-GroEL Spotting	GroEL “in situ” labelled with Alexa Fluor
GOPS – commercial coated glass microscope slides	Antibody “successfully” spotted	“High” binding Low background	Spotting not verified	Binding not verified Very high background
GOPS – in-house coated glass microscope slides	Antibody partially “successfully” spotted	“High” binding Partial arrays only Low background	Antibody “successfully” spotted	“High” binding High background compared to scAb assay

Table 4.4 contains the images obtained from each of these experiments using a 300 second exposure on the optical breadboard. Table 4.5 summarises the conclusions that can be drawn from these images, both in terms of the microarray spotting process on each surface and the assay itself, including factors such as non-specific binding.

The important points are that the anti-atrazine scAb assay used in the previous experiments was at least partially successful on both the commercial and in-house epoxy functionalised surfaces. This indicated that the in-house GOPS coating procedure had produced active epoxy groups on the glass surface enabling covalent immobilisation of the anti-atrazine scAb onto the surface, and the assay protocol did not create large amount of non-specific binding on either GOPS surface. However, only partial arrays of spots were visible, so further optimisation was still required.

The GroEL assay appeared to be successful on the GOPS surface prepared in-house, but produced a high background when carried out on the commercial GOPS slide. This indicated that there were some differences in the properties of the commercial and in-house surface chemistries, possibly due to differences in the immobilisation protocol. The high level of background could be caused by un-reacted Alexa Fluor[®] 633 dye in the GroEL reaction mixture binding non-specifically to one surface more than the other. There was also a higher level on non-specific binding observed for GroEL assay on in-house GOPS surfaces than the anti-atrazine scAb assay on the same surface.

Although this initial GroEL assay was not very successful on commercial GOPS slides, there was a practical advantage in using commercially available surfaces to pursue the GroEL assay on, since the GOPS functionalisation procedure was quite time consuming so a higher throughput of assay experiments could be achieved by purchasing commercial slides. As this experiment established that the basic surface chemistry of the in-house GOPS functionalisation was similar to the commercially prepared GOPS surfaces, GroEL assays on commercial GOPS slides were used to try to eliminate the high level of non-specific binding, by varying the blocking and washing protocols.

4.12.3 Modification of *in-situ* labelling protocol to include ethanolamine as a quenching reagent for un-reacted dye – materials and methods

Initially, the assay protocol was modified by the addition of a ten times molar excess of ethanolamine (relative to the initial dye concentration) to the reaction mixture prior to applying the reaction mixture to the assay area. Ethanolamine (Sigma-Aldrich, Poole, UK) was diluted to 1 / 500 to a concentration of 30mM in 10mM PBS pH7.4 and 5µl of this solution was added to the reaction mixture to inactivate any remaining succinidyl groups on un-reacted dye molecules. The complete experimental protocol was as follows:

- A 5 x5 array of 1/10 anti-GroEL IgG fraction (30 to 100 µg/ml) in 30% v/v glycerol in PBS was spotted onto a commercial GOPS coated slide, and the slide placed into a humidity chamber and incubated for 2 hours.
- The slides were washed and incubated in 0.1g.ml⁻¹ skimmed milk powder in HEPES 10mM, pH 7.4 buffer, to block the remaining slide surface.
- Each assay area was then washed five times with 1ml RO water, by pipetting the water over the slide surface at an acute angle.
- 20µl of 0.1mg.ml⁻¹ Alexa Fluor 633[®] labelled GroEL total reaction mixture (in 10mM PBS pH 7.4) containing 30mM ethanolamine was pooled over each assay area and incubated for 1 hour in a humidity chamber.
- Each assay area was washed five times with 1ml of HEPES 10mM, pH 7.4 with 0.1% w/v Tween 20, followed by five washes with 1ml RO water, pipetted across the assay area at an acute angle.
- The slide was dried under nitrogen for 1 minute
- The chip was placed into the optical rig and each assay area was imaged with a 300 second exposure in darkness.

4.12.4 Modification of *in-situ* labelling protocol to include ethanolamine as a quenching reagent for un-reacted dye – results and discussion

Two replicate results of this experiment are shown in Figure 4.10 and Figure 4.11 below.

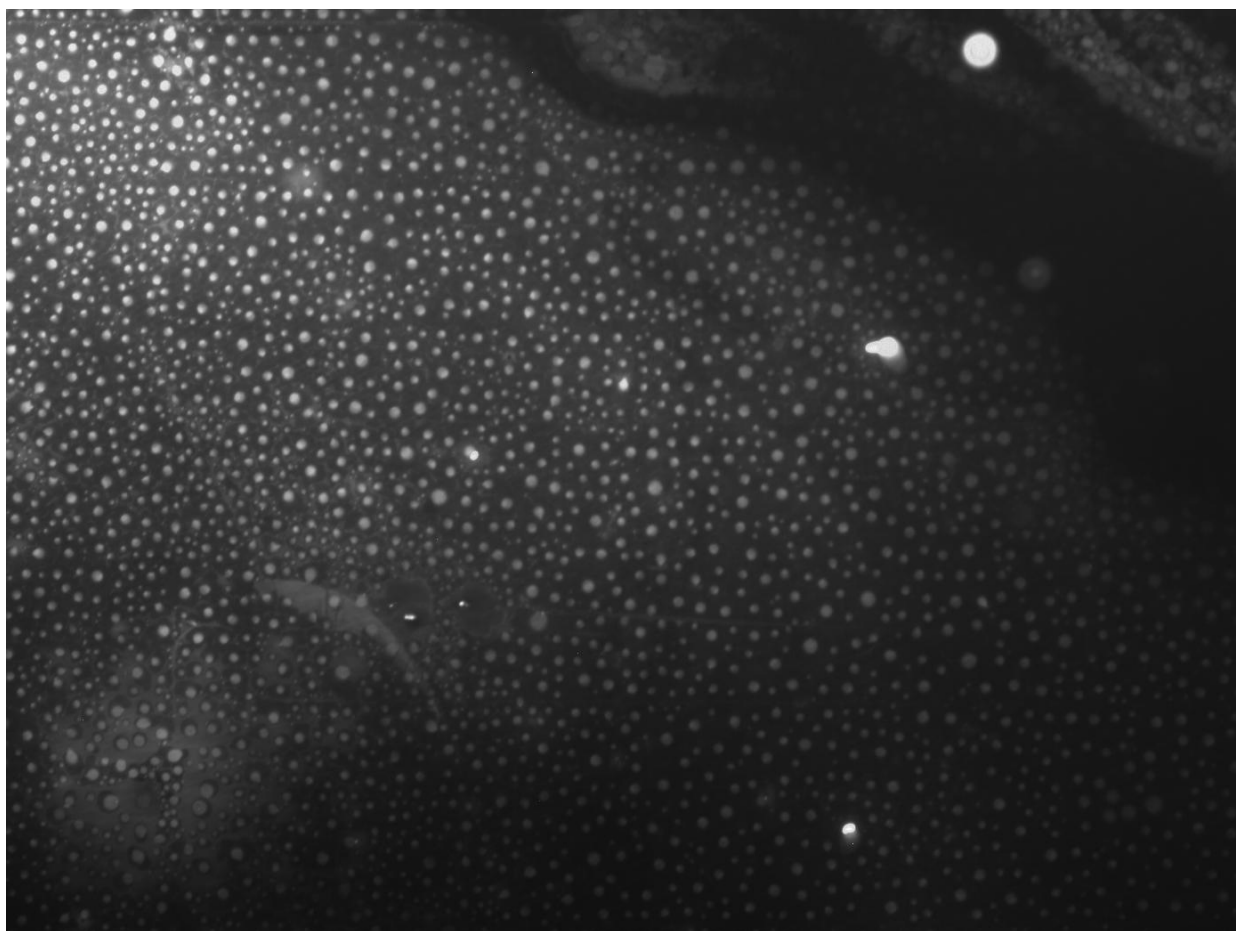


Figure 4.10: 300 second exposure image of an assay area in which a 5 x 5 array of anti-GroEL was printed and exposed to Alexa Fluor[®] 633 labelled GroEL protein after addition of ethanolamine.

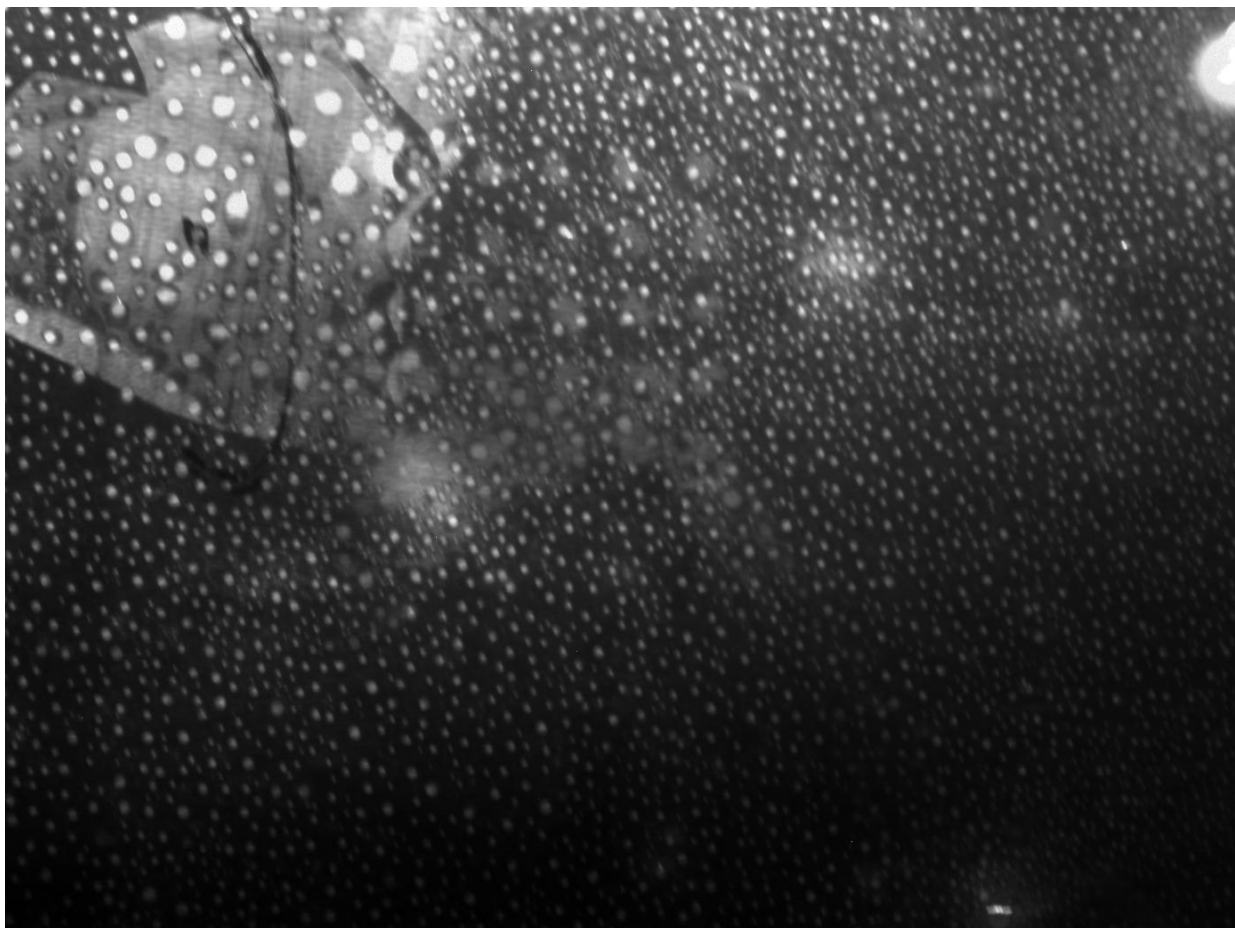


Figure 4.11: 300 second exposure image of an assay area in which a 5 x 5 array of anti-GroEL was printed and exposed to Alexa Flour[®] 633 labelled GroEL protein after addition of ethanalamine.

This experiment produced an interesting result. There is a strong non-specific signal present, in the form of spots that are approximately equal in size and evenly spaced. Also, in between the spots faint fracture lines can be seen. There were two likely explanations for these observations. The most probable is that when the slide is dried after washing away the labelled protein reaction mixture, the remaining reaction mixture is de-wetting from the surface as it dries, leaving circular deposits of material containing dye. This is supported by the observations that the circular features are all similar in size and equally distributed, and that small fracture lines are present in between the features, which are effects characteristic of the de-wetting of liquid films from homogeneous surfaces (Sharma & Khanna, 1998). The presence of inactivated dye in the reaction mixture could be contributing to this effect, since it was not observed in previous experiments where commercially prepared products that do not contain unreacted dye were used (see section 4.12.2). Other possible explanations were that un-reacted dye was binding to areas of the surface that were not fully blocked, or that the circular objects being observed were particles. However both of these alternative explanations are made less likely by the even size and distribution of the features and the presence of fracture lines between them.

4.12.5 Assay including test with inactivated dye filtrate – materials and methods

In order to test the theory that the deposition of the circular features in Figure 4.11 might be caused by the presence of inactivated dye in the reaction mixture, an experiment was carried out in which two different conditions were used. After the GroEL labelling reaction had been completed, ethanolamine (Sigma-Aldrich, Poole, UK) diluted to 1 / 500 in 10mM PBS pH7.4 to a concentration of 30mM, was added to the reaction mixture to inactivate any remaining succinimidyl groups on un-reacted dye molecules. In one slide, this complete reaction mixture was applied directly onto the slide. In a second slide, the reaction mixture was filtered again through a 10,000 MWCO filter (Fisher Scientific UK, Loughborough, UK) to remove the labelled GroEL protein, and the filtrate (containing only un-reacted dye and buffer) was applied to the microarray spots.

4.12.6 Assay including a test with inactivated dye filtrate – results and discussion



Figure 4.12: A 60 second exposure image of an assay area in which a 5 x 5 array of anti-GroEL was printed and exposed to Alexa Fluor[®] 633 labelled GroEL protein after addition of ethanolamine.

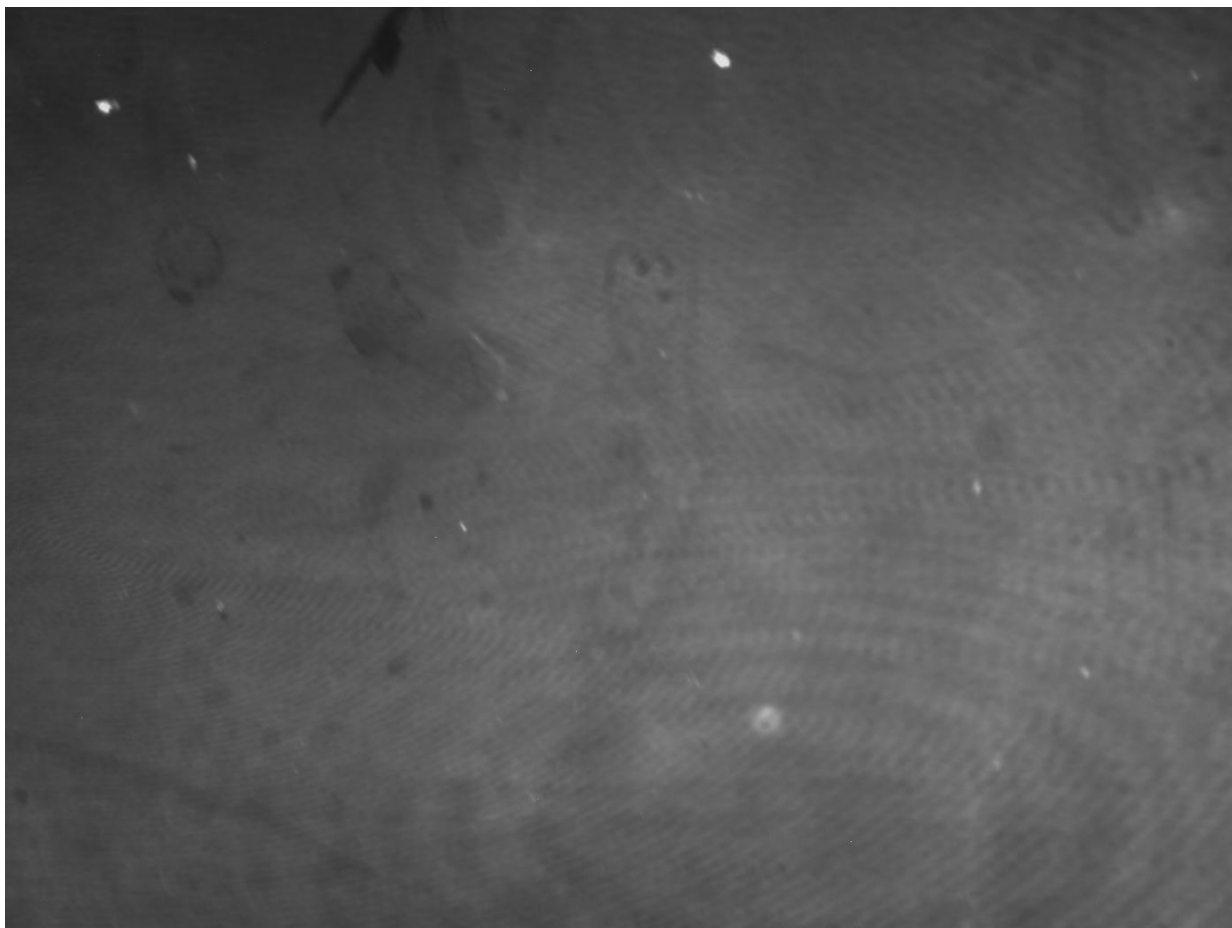


Figure 4.13: A 60 second exposure image of an assay area in which a 5 x 5 array of anti-GroEL was printed and exposed to filtrate produced from the GroEL reaction mixture after the addition of ethanolamine.

The fact that the filtrate containing no protein did not produce the non-specific binding signal that was observed when labelled protein was present indicated that the labelled protein, and not un-reacted Alexa Flour[®] 633 dye, must be non-specifically binding to something on the slide surface. The most likely cause of this was thought to be a problem with the blocking step, so in the next experiment the blocking method was revised by replacing the five washes with 1ml of deionised water after blocking with a more thorough one minute wash in a beaker of deionised water with manual agitation. This experiment will be described and discussed in section 4.13.

In this section a number of experiments were carried out attempting to develop a GroEL immunoassay on microscope slides functionalised with GOPS either commercially or in-house. The initial experiment showed that the scAb assay was successful on both surfaces to a limited extent, and that the GroEL assay was partly successful only on the in-house GOPS treated slide. In order to optimise the protocol, a series of experiments using the GroEL assay or components of it on GOPS coated slides was carried out. This led to the development of a protocol which could be used to further characterise the performance of antibody assays in a microarray format. This final protocol is described in the following

section, in which assays using a range of concentrations of labelled GroEL protein were carried out and used to produce a calibration curve for the immunoassay in a microarray format.

4.13 Calibration curve for an immunoassay in a microarray format

The problem of labelled GroEL non-specifically binding to the epoxy slide surface appeared to be resolved by replacing the five 1ml washes in deionised water after the blocking step with a one minute manual agitation in a beaker of deionised water. This method considerably reduced the level of non-specific binding, and was used to produce a calibration curve by carrying out immunoassays with different concentrations of GroEL labelled *in-situ* with Alexa Fluor® 633.

4.13.1 Calibration curve for an immunoassay in a microarray format - materials and methods

Since the non-specific binding issue had been considerably improved by modifying the washing procedure as described in section 4.12.6, the next stage of development was to produce a calibration curve to demonstrate reproducibility of the immunoassay, and determine the binding affinity of the antibody and detection limit of the assay. The complete final protocol was as follows:

- A 5 x 5 array of spots of 1/10 anti-GroEL IgG in PBS-30% glycerol was printed onto commercially available epoxy functionalised slides, and the slide incubated in a humidity chamber for 2 hours.
- The slide was then placed into a beaker of blocking buffer (0.1g.ml⁻¹ Skimmed milk powder in 10mM HEPES pH7.4), agitated for 30 seconds and then immersed in the blocking buffer for 4 hours.
- The slide was then removed from the blocking buffer and vigorously agitated in a beaker of RO water to remove excess blocking buffer, and dried under nitrogen.
- 20µl of Alexa Fluor® 633 labelled GroEL protein at different concentrations was 'pooled' over each assay area, and the slide incubated for 1 hour in the humidity chamber.
- Each assay area was washed five times with 1ml of 10mM HEPES pH7.4 containing 0.1% TWEEN 20, then five times with 1ml of RO water and dried under nitrogen.
- The slide was then placed into the optical breadboard, and an image of each assay area was taken with a 300 second exposure time.

4.13.2 Calibration curve for an immunoassay in a microarray format – results and discussion

Table 4.6: Images used to form a calibration curve for the GroEL Assay system.

	Assay Area 1	Assay Area 2	Assay Area 3
0.002 mg.ml ⁻¹			
0.02 mg.ml ⁻¹			
0.1 mg.ml ⁻¹			
0.2 mg.ml ⁻¹			
1 mg.ml ⁻¹			

The images in Table 4.6 show the results of carrying out the GroEL assay at a number of different concentrations of GroEL. It is immediately clear that these images show a considerable reduction in the level of background fluorescence than the image in the top-right box of Table 4.4, which was taken using the previous protocol. However, there are still areas where background fluorescence is present, mainly in the form of circular features which are likely to be caused by the presence of particulates in the assay solutions, and various pattern features across the area of the image which appear to be a drying effect. The images in Table 4.6 were of a sufficient quality to analyse and produce data to include in the calibration curve in all cases except the central image of the 1mg.ml⁻¹ assay, in which almost all of the spots were obscured by an area of non-specific binding. In all other images, spots partially

or wholly obscured by a feature considered to be caused by non-specific binding were not included in the analysis. This illustrates that while an analysis could be carried out on these images, further work needs to be done to prevent the appearance of these features.

In order to carry out a quantitative assessment of the spots rather than a qualitative assessment of the images, image analysis software was required. There are many image analysis programs available for microarray images. In this project, ScanAlyze (v2.35, Stanford University) was selected as a convenient program to use after a brief trial of a number of alternatives, as it is freely available to download for academic use, and offers a more user-friendly interface than other similar software. In order to analyse the FITS images generated by the CCD camera in ScanAlyze, they had to be exported into TIF format. This was done using the Starlight Express software (version 3.5) associated with the CCD camera in the breadboard imaging system. The TIF images were then analysed using ScanAlyze. This software is designed for analysing microarrays using two different dyes but was used here to analyse images with a single dye as follows:

- The TIF image of each array were loaded into both image analysis areas in the ScanAlyze software.
- A 6 x 5 grid was then created and adapted so that the spot sizes and spacing approximately matched those on the images, and one column of spots was on a blank area of the slide and used to provide a background measurement. This grid was used as a starting point to analyse all images. At this point spots obscured by non-specific binding features were removed from the analysis.
- The grid was then placed over the array, and the 'align' feature used several times to achieve the optimum spot alignment.
- The data was then saved and imported into Microsoft Excel, where the value for 'channel 1 pixel intensity' was subtracted from the average value of the 'channel 1 pixel intensity' from the background spots. This value was used as the binding signal in the calibration curve in Figure 4.14.

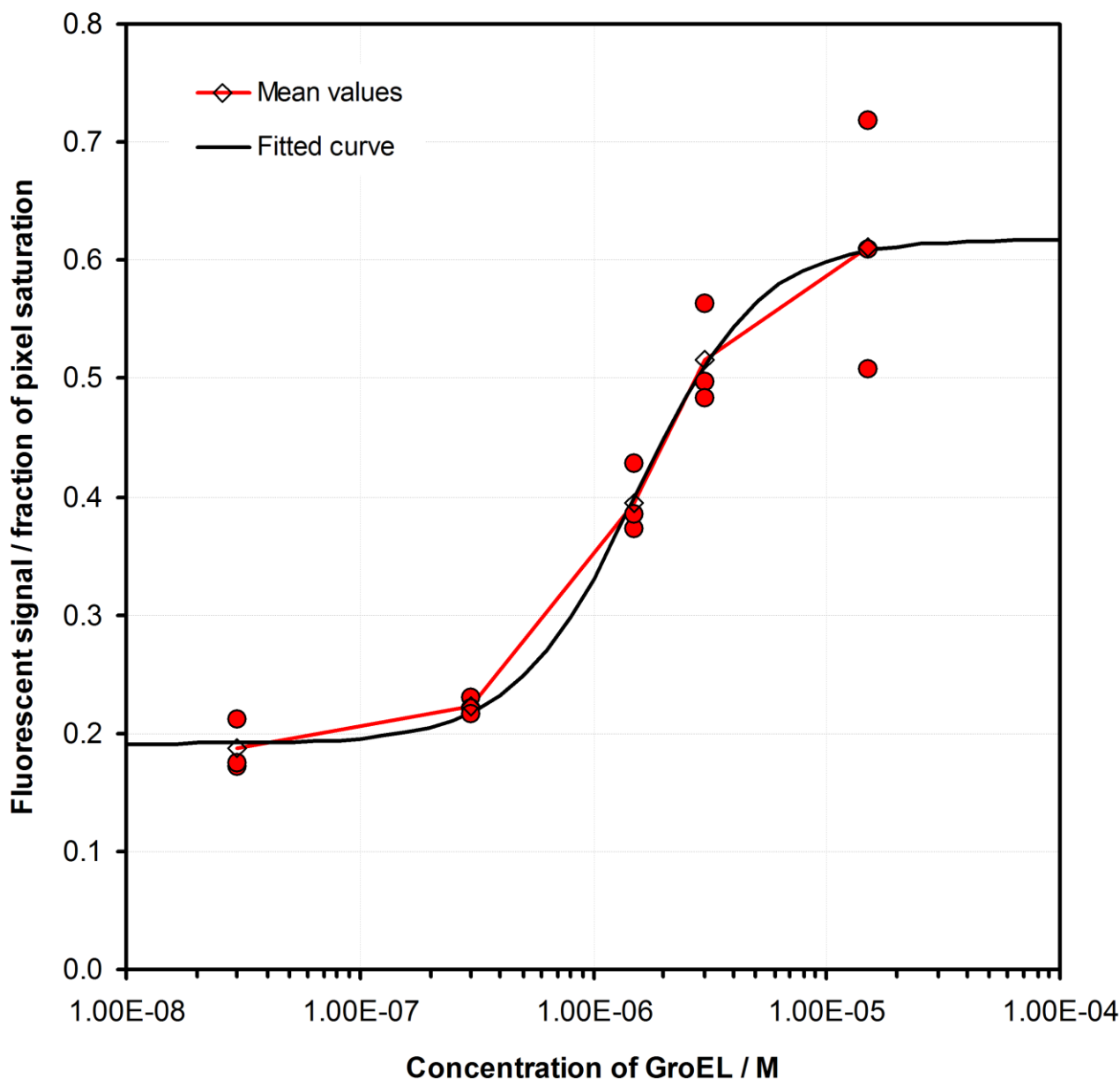


Figure 4.14: GroEL calibration results including a fitted curve.

The Microsoft Excel Solver Add-In feature was used to determine the best-fitting sigmoid curve for this data. A sigmoid function was selected because this is the typical shape of a binding antibody assay curve. This allowed the antibody dissociation constant (K_D) (which is inversely proportional to the antibody binding affinity) to be measured and indicated the range of concentrations at which labelled GroEL protein can be detected with this system.

The K_D value for the antibody was found to be $1.9 \times 10^{-5} \text{M}$, approximately two orders of magnitude higher than the typical range of K_D values for antibody-antigen binding (which is 10^{-7} to 10^{-11}) (Garcia *et al.*, 1999), indicating that the antibody binding affinity was lower than expected. This was assumed to be due to the high level of labelling of the GroEL protein with Alexa Flour[®] 633, as the presence of the dye may have altered the protein enough to reduce the antibody's affinity for it. Since the anti-GroEL antibody used was an IgG fraction,

it may contain a number of different epitopes of antibody which bind to different regions of the GroEL protein, so a low K_D value could indicate that dye molecules could have been attached on or near the binding site of one or more epitopes, but others are still able to bind to the protein. It is possible that the labelling reaction could be adjusted to reduce the level of labelling to counter this, or that antibodies could be raised against labelled proteins such that they have a greater affinity for the labelled protein, and this will be investigated in future work. Nonetheless, this finding highlighted that it may be necessary to use antibodies raised against labelled targets for some assays in the flight instrument, where an *in-situ* labelling / direct detection assay is proposed.

4.14 Summary and conclusions from instrument platform development experiments

The first stage of development of the instrumentation platform was to carry out preliminary experiments to validate the equipment and early readout methods (see Appendix A). Once this was completed, a breadboard system representative of the design of the Life Marker Chip instrument was assembled. Tests were carried out with dried down dye material to confirm that this breadboard system was suitable for the readout of immunoassays carried out in a microarray format.

Having confirmed the suitability of the breadboard imaging system, an immunoassay based on conveniently available reagents (anti-atrazine scAb and commercially available Alexa Fluor[®] 633 labelled anti-human IgG) similar to those used in Chapter 3 were used to establish a basic protocol for carrying out an immunoassay in a microarray format on commercially available amine-coated slides. The immunoassay protocol did produce microarray spots that could be imaged on the breadboard system, but a number of features indicative of non-specific binding of material to the surface and “halo” effects around the microarray spots were present. A number of different blocking and washing protocols were explored to try to resolve this, however a satisfactory solution was not found. In an attempt to circumvent these problems, commercially available epoxy-functionalised slides were used in place of the amine-coated slides. When the immunoassay was carried out on epoxy-coated slides, the ‘halos’ around the microarray spots were no longer present and the non-specific binding problems were reduced for the anti-atrazine scAb immunoassay.

At this point, two changes were made to make the immunoassay more relevant to the final Life Marker Chip instrument. First, a procedure for in-house silane modification of glass and

silica to produce epoxy-functionalised surfaces was adopted from the literature. This procedure was found to give reproducible contact angle measurements when carried out on glass, silicon oxide and silicon nitride samples. These procedures are well established, however confirming a successful protocol within the Life Marker Chip consortium is an important step in de-risking the instrument development. Secondly, a new immunoassay for the detection of a biomarker target molecule of astrobiological interest (GroEL / chaperonin-60), which may be included in the flight instrument Life Marker Chip, was developed. This involved establishing a protocol for *in-situ* Alexa Fluor[®] labelling of GroEL protein which could be adapted for the flight instrument and labelling of any amine-containing biomarker target, another key step in the development of the Life Marker Chip.

The GroEL immunoassay was carried out in a microarray format on both commercially available and in-house epoxy-coated microscope slides. Although the initial experiment indicated that the in-house epoxy surface showed less non-specific binding than the commercial epoxy coating, the more conveniently available commercial slides were used for further development of the assay. The development work involved a series of experiments to optimise blocking and washing protocols, which yielded a protocol that, although not fully optimised in terms of preventing non-specific binding, was consistent enough that most of the immunoassay images taken could be used to analyse microarray spot intensity. This protocol was used to produce a calibration curve for an immunoassay in a microarray format carried out in an open microfluidic channel structure. Although this calibration is not directly representative of the final format, since a closed microfluidic channel will restrict the volume of solution available and therefore the amount of material available to bind to the microarray spots, it is still an important development. An important point highlighted by the results of this experiment is that the binding affinity of the antibody as calculated from the calibration curve appeared to be higher than typical values, which may be due to the Alexa Fluor[®] 633 labelling of the GroEL affecting the binding affinity of the anti-GroEL antibody. This raises the point that antibodies raised against labelled biomarkers may be more suitable for the Life Marker Chip than antibodies against the unmodified target molecules.

Although the development of the Life Marker Chip instrumentation is ongoing and future work will be discussed in section 6.2, Chapter 4 has described the developments made during the timescale of this PhD work. The following chapter describes a number of experiments that were carried out in order to determine if, and how, the Martian environment and sample processing techniques may affect immunoassays and thereby how the design of the Life Marker Chip and sample processing system could reduce or prevent any effects.

Chapter 5: Effect of Martian regolith salts and sample extraction solvents on antibody-based assays

5.1 Introduction

As described in section 2.3, Martian regolith samples, especially those of interest for astrobiology, may contain different salts of which the most interesting ones for the Life Marker Chip (LMC) are particularly iron (II) and iron (III) sulphates, magnesium sulphate and calcium sulphate (Parnell *et al.*, 2004, Harland, 2005, Amaral, Martinez-Frias & Vázquez, 2005, Clarke *et al.*, 2005, Squyres *et al.*, 2005, Marion *et al.*, 2006, Peterson & Wang, 2006). Iron (III) sulphate is a lower priority target, since while it is formed in water the primary sites of interest for Life detection are areas that have been exposed to aqueous environments for extended periods of time, and are more likely to contain iron (II) sulphate produced by paragenesis (Squyres *et al.*, 2005, Marion *et al.*, 2006) (see section 2.4.1.2). Iron (III) sulphate (jarosite) has therefore not been tested for compatibility with biological buffers at the time of writing, but is intended for future work.

The SMILE LMC sample processing system will extract polar and a-polar biomarkers from the sample using solvents, which for biomolecules from extant Life may involve the use of agents such as guanidine-HCl to extract proteins. For a-polar biomarkers the sample processing and extraction may include highly a-polar organic solvents such as dichloromethane and n-hexane with or without other more polar organic solvents *e.g.* methanol, propanol.

At present it is unknown whether, or how much of, these salts and organic solvents will pass through the sample processing system and into the LMC assays. Thus a series of preliminary experiments have been carried out to determine what effect these might have on antibody assays, using an existing anti-atrazine binding ELISA based on a recombinant scAb antibody as a model system. As described in section 3.2, this anti-atrazine scAb antibody was used because it is an antibody against a small organic molecule similar to some of the proposed targets, and could be used in the flight as a positive control marker since it is unlikely that atrazine will be present on Mars. The antibody was also conveniently available in the laboratory. This antibody is a recombinant antibody, so it is representative of some antibodies that may be used in the flight instrument (Sims *et al.*, 2005). The detailed protocol for this assay is described in Section 3.2.

The experiments carried out in this section include assays with the anti-atrazine scAb in buffers containing the representative Martian salts iron (II) sulphate, magnesium sulphate and calcium sulphate at different percentages of their solubility limit. During the preliminary experiment, precipitation and oxidation of iron (II) to iron (III) was observed, so a second experiment was performed to define the conditions under which this occurred. In a further experiment, an attempt was made to prevent this precipitation by the addition of an anti-oxidant (ascorbate). An assay to determine the effect of different concentrations of guanidine-HCl varying from 8M (the most commonly used concentration for extraction) to 1M diluted in buffer was also carried out. Initial experiments to determine the need to remove organic solvents from the sample after processing were also done by performing assays with the anti-atrazine scAb in a number of organic solvents (hexane, hexane-methanol mixture and methanol-buffer mixtures).

5.2 Effect of representative Martian regolith salts on antibody assays

In order to determine the effect of representative Martian regolith salts on antibody assays, commercially available pure salts were dissolved in standard biological buffers to identify any effect of each salt individually. The assay was carried out exactly as described in section 3.1.1.4, but instead of using standard buffers for the antibody incubation step, buffers containing dissolved salts at different concentrations (depending on the solubility limit of the salt) were used. In this way, the salt was only present during the critical stage of antibody binding to its target antigen, and would not affect other aspects of the experiment. This is representative of the proposed assay system for the LMC, in which samples will flow in to a pre-fabricated microfluidic channel containing dried-down reagents and pass directly over the immobilised antibodies (Sims *et al.*, 2005). In this proposed assay system no other stages in the assay would be carried out in buffers containing Martian salts.

In the LMC itself, the buffer used for the immunoassays may be mixed with an organic solvent. However, this was not considered in these initial tests with Martian regolith salts, in order to determine the effects of each salt, and each organic solvent, individually before moving on to study more complex buffer combinations.

5.2.1 Effect of calcium sulphate (CaSO_4) on anti-atrazine binding ELISA – materials and methods

A literature survey indicated that the solubility limit of CaSO_4 (pure) in water at 25°C is $0.205\text{g}\cdot 100\text{ml}^{-1}$ ($2.05\text{mg}\cdot\text{ml}^{-1}$) (CRC Manual, 2007). 0.4g of CaSO_4 (Sigma-Aldrich, Poole, UK) was dissolved in 100ml of 10mM HEPES buffer pH 7.4 and vigorously shaking for 10 minutes. 0.4g of CaSO_4 in 100ml of HEPES exceeded the solubility limit of CaSO_4 at 20°C , as determined by the presence of visible precipitate in the solution after 24 hours incubation. Precipitates were left to settle, and removed by decanting the solution into a fresh container. HEPES buffer was used for this experiment in preference to PBS, which had been used in the radiation testing work (see section 3.1.1.4), to avoid precipitation of calcium phosphate. In the future a similar experiment with a real sample of gypsum ($\text{CaSO}_4\cdot 2\text{H}_2\text{O}$), a calcium sulphate mineral, from the Houghton impact crater, is planned. This is discussed in section 4.2.

5.2.2 Effect of calcium sulphate (CaSO_4) on anti-atrazine binding ELISA – results and discussion

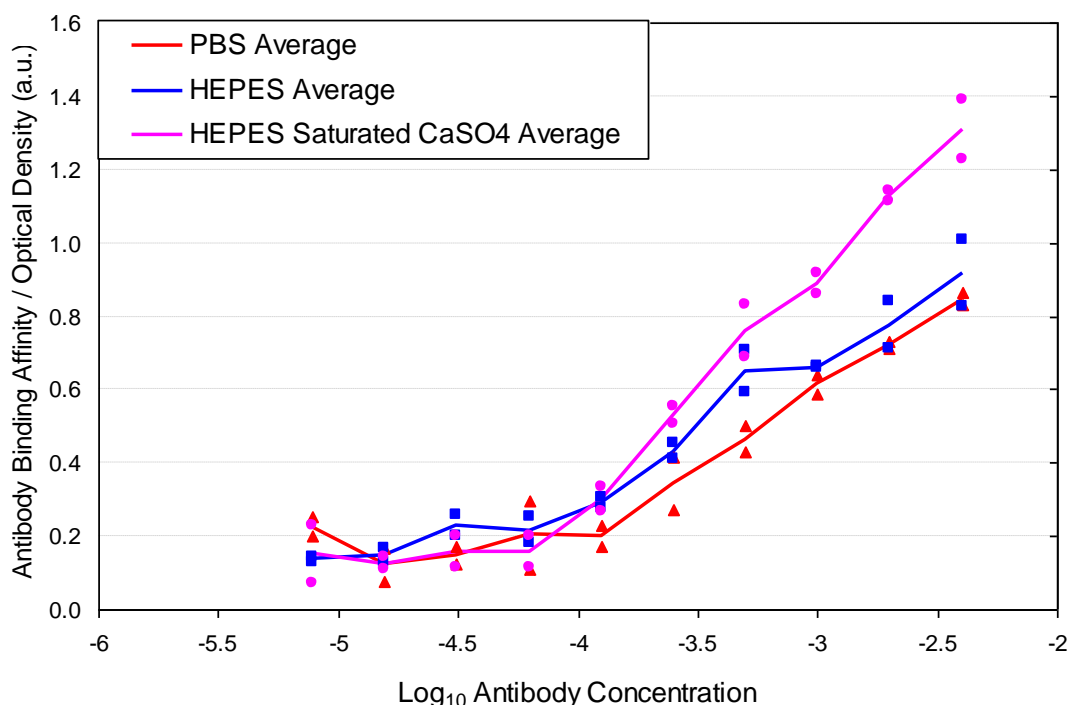


Figure 5.1: Comparison of anti-atrazine scAb binding ELISA run in PBS, HEPES and HEPES saturated with CaSO_4 . The average lines show the average for duplicate wells for the assay in each buffer, with symbols in the corresponding colour showing the data points for each well.

Figure 5.1: confirms that changing the assay buffer from 10mM PBS pH7.4 to 10mM HEPES pH7.4 had no significant effect on the assay. Figure 5.1: also shows that the

presence of calcium sulphate at its solubility limit has no negative effect on the antibody assay. Indeed, the antibody binding signal observed was slightly higher with calcium sulphate present. This demonstrates that calcium sulphate passing through into the assay chamber of the Life Marker Chip would not appear to present a problem for this particular assay. As this anti-atrazine antibody is representative of the type of antibody-antigen system for other LMC targets, it is reasonable to assume that the presence of calcium sulphate will not affect other immunoassays. However this will need to be tested and has been identified as future work in section 6.2.

5.2.3 Effect of magnesium sulphate (MgSO_4) on anti-atrazine ELISA – materials and methods

Magnesium sulphate (MgSO_4) (Epsom salt) was found in a literature survey to have a solubility limit in water of $35.7\text{g}\cdot 100\text{ml}^{-1}$ at 25°C (CRC handbook, 2007). Since this solubility is very high, it was decided to test the effect of MgSO_4 at 10, 50 and 100% of this solubility limit (i.e. 3.56, 17.3 and $35.6\text{g}\cdot 100\text{ml}^{-1}$) on the antibody assay. These solutions were prepared by adding 3.56, 17.3 or 35.6g of MgSO_4 (Sigma-Aldrich, Poole, UK) to 100ml of 10mM HEPES buffer pH 7.4 and shaking for 10 minutes. WARNING - This solution preparation was observed to be highly exothermic, sufficiently so that the $35.6\text{g}\cdot 100\text{ml}^{-1}$ solution damaged the glassware it was prepared. In the future representative real MgSO_4 samples e.g. epsomite could be tested with this system.

5.2.4 Effect of magnesium sulphate (MgSO_4) on anti-atrazine binding ELISA – results and discussion

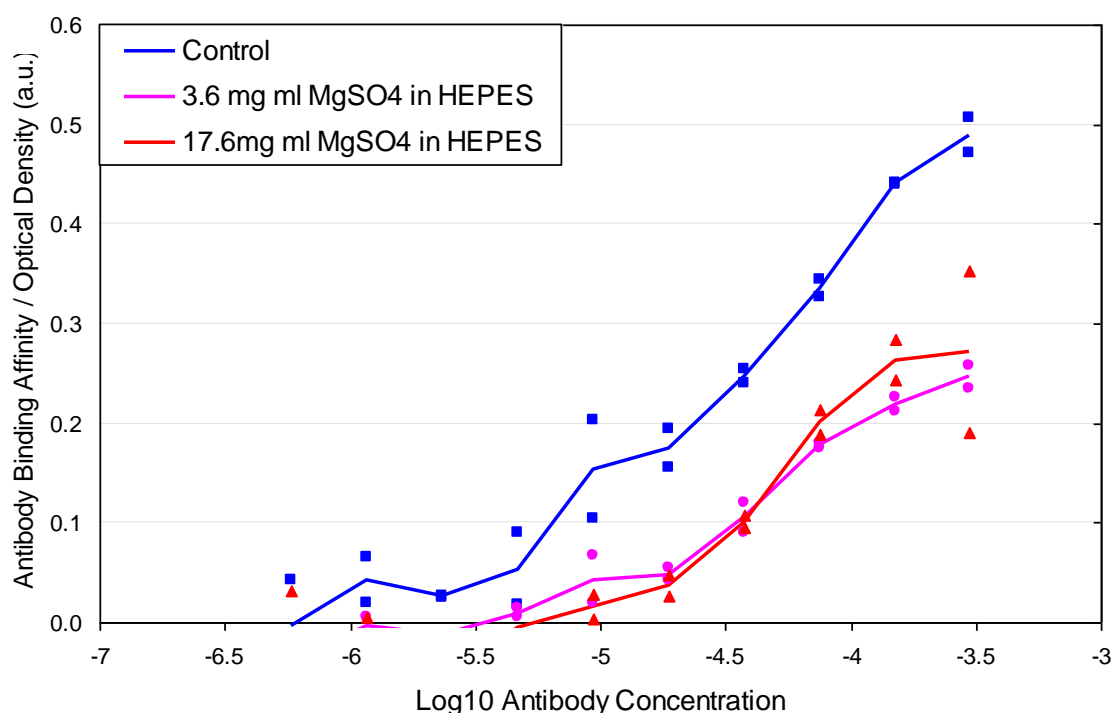


Figure 5.2: Comparison of Anti-Atrazine scAb binding ELISA run in HEPES containing MgSO_4 at 3.6 and 17.3mg.ml⁻¹. Data points for each well are shown in the corresponding colour for each assay. Some of the lower data points drop below 0 binding signal due to an anomalously high background signal during this experiment. The experiment will be repeated to resolve this problem.

Figure 5.2 shows that while the presence of magnesium sulphate at 3.6 and 17.6mg.ml⁻¹ causes a reduction in antibody binding of approximately 50%, significant activity remains. This shows that the high solubility of magnesium sulphate and therefore high salt content

of the buffers does have an adverse effect on antibody-antigen interaction, but significant binding activity remains even at 50% of the solubility limit. Assuming that other antibody-antigen systems are similarly affected, this reduction in binding is something that must be considered in the development of the LMC sample processing system. If this reduced binding is found to have a significant effect on the lower limit of detection of the LMC, a demineralisation step to remove mineral ions from the sample will have to be considered.

5.2.5 Effect of iron II sulphate (FeSO_4) on anti-atrazine binding ELISA – materials and methods

As discussed in section 3.3.1, while iron (III) sulphate (jarosite) is present on the Martian surface in much greater quantities than iron (II) sulphate, iron (II) sulphate is present in areas where paragenesis has occurred, i.e. where the presence of water for extended periods of time caused iron (III) sulphate to be reduced to iron (II) sulphate. Sites where this has occurred are of greater relevance to the Life Marker Chip since they indicate an environment in which Life may have evolved, and so the effect of iron (II) sulphate on the immunoassay, and the consequences of this for the sample processing system, was investigated in this work while iron (III) sulphate remains an important regolith component to be tested in future experiments (see section 4.2).

Iron (II) sulphate (FeSO_4) (also known as ferrous sulphate) was found to have a solubility limit in water of $29.56\text{g}\cdot 100\text{ml}^{-1}$ at 25°C (CRC Manual, 2007). Since this solubility is very high, it was decided to test the effect of FeSO_4 at 10, 50 and 100% of this solubility limit i.e. 2.66 , 13.3 and $26.6\text{g}\cdot 100\text{ml}^{-1}$ on the antibody assay. These solutions were prepared by adding 2.66 , 13.3 and 26.6g of FeSO_4 (Sigma-Aldrich, Poole, UK) to 100ml of 10mM HEPES buffer, $\text{pH } 7.4$ and shaking for 10 minutes.

5.2.6 Effect of iron II sulphate (FeSO_4) on anti-atrazine binding ELISA – results and discussion

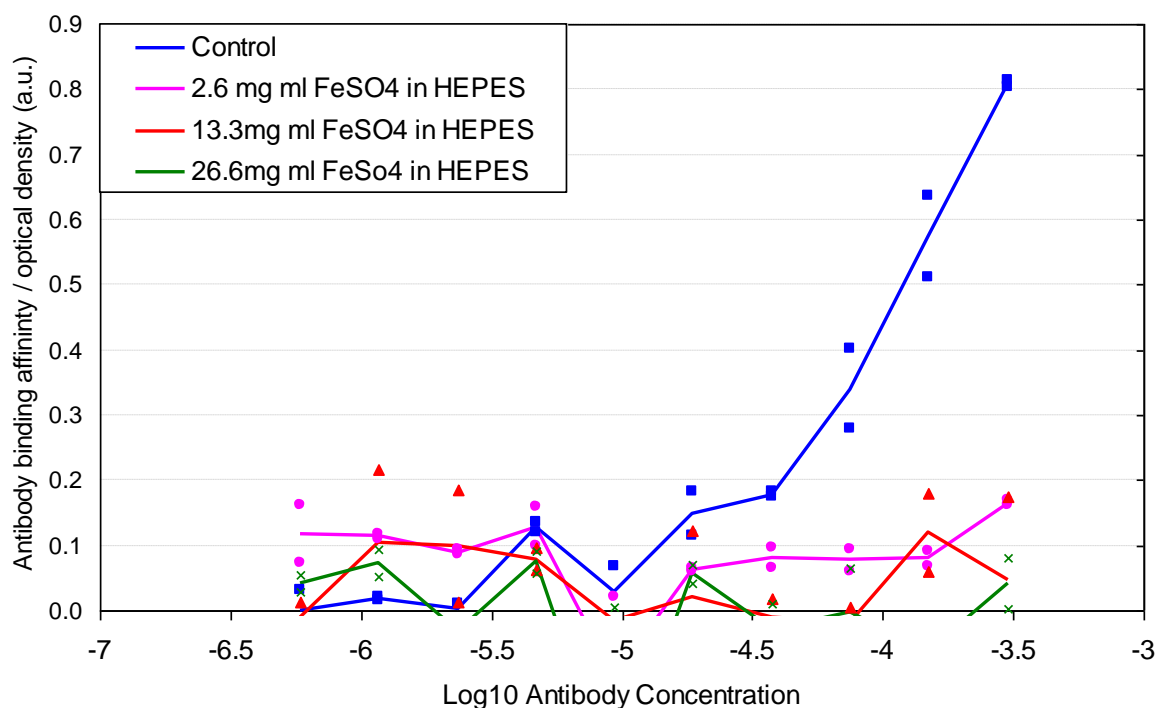


Figure 5.3: Comparison of Anti-Atrazine scAb binding ELISA run in HEPES containing FeSO_4 at 2.6, 13.3 and 26.6mg.ml⁻¹

Figure 5.3 shows the results of the assay with FeSO_4 present at different concentrations, and indicates that no significant antibody binding has been observed. However this does not illustrate other issues with this experiment. The results in Figure 5.3 were derived by subtracting the signal of microtitre plate wells containing antibody from wells containing only FeSO_4 in HEPES buffer. In this experiment, all of the microtitre plate wells to which FeSO_4 was added, including those with no antibody, gave a very high signal. In addition, the HEPES buffers containing FeSO_4 were observed to contain red precipitates after completion of the assay, indicative of the presence of iron (III) compounds. It is possible that the products of this reaction affected the protein blocking of these wells, resulting in non-specific binding of the anti-atrazine scAb and a high signal in all wells. Due to this very high background signal it was not possible to determine whether the antibody-antigen was affected by the presence of iron(II) sulphate.

We conclude from this that iron (II) sulphate was oxidised to iron (III) in the HEPES buffer, and that this oxidation generated insoluble iron (III) precipitates. Since this is incompatible

with the microfluidics in the sample processing system and the LMC, an alternative buffer in which these precipitates are not formed must be identified. Further experiments (see section 5.3) were carried out to investigate the timescale of this precipitation and ways to prevent it.

5.3 Investigation of buffer compatibility with Martian regolith salts

5.3.1 Preliminary experiment to determine compatibility of biological buffers with iron (II) sulphate – materials and methods

A preliminary experiment to identify an alternative buffer was carried out in order to validate the precipitation observation in section 5.2.6, and find out if this occurred with a number of buffer types. Approximately similar amounts of iron (II) sulphate (a low fraction of the solubility limit) were added to ~400ml of RO water, and uncontrolled concentrations and pH (of similar weight/volume ratio solutions) of different buffers used in biological assays (HEPES, TRIS, and MOPS). After the buffers were prepared they were photographed with a digital camera (Figure 5.4 and Figure 5.5).

5.3.2 Preliminary experiment to determine compatibility of biological buffers with iron (II) sulphate – results and discussion

Immediately after the iron (II) sulphate was added water the solution was clear. After 10 minutes incubation in water, HEPES and MOPS buffer solutions became a yellow-orange colour and contained precipitates. This indicates that oxidation of iron (II) to iron (III) has occurred, since iron (II) compounds are green in colour while iron (III) compounds are orange / red. When iron (II) sulphate was added to TRIS buffer, large amounts of a dark green precipitate were formed immediately and the solution became 'milky' in texture. These solutions were left for one hour more, and greater redness was observed in the TRIS solution and the RO water, suggesting that further oxidation of iron (II) had occurred. The HEPES and MOPS buffer solutions appeared to be similar in colour after one hour suggesting that they had reached equilibrium.

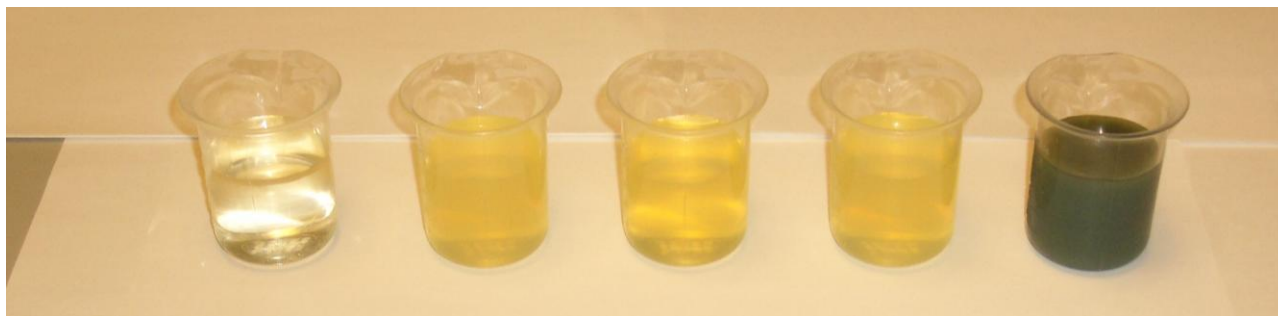


Figure 5.4: Photograph of iron (II) sulphate in different solutions. From left to right, a fresh solution in water, 10 minutes incubation in water, HEPES, MOPS and TRIS buffers. The buffer solutions were uncontrolled in terms of their concentration and pH, but were similar weight / volume ratios.

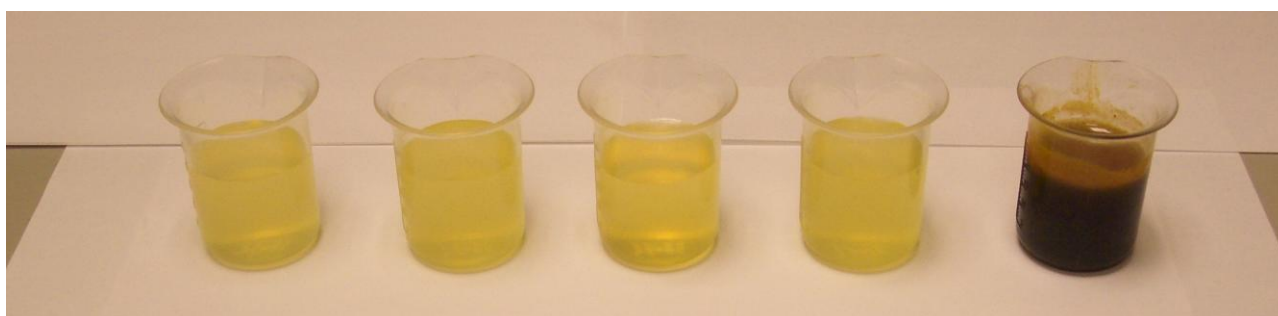


Figure 5.5: Photograph of iron (II) sulphate in different solutions. From left to right, 1 hour incubation of a solution in water, 1 hour 10 minutes incubation in water, HEPES, MOPS and TRIS buffers (the same solutions shown in Figure 5.4 after incubation at room temperature for 1 hour). The buffer solutions were uncontrolled in terms of their concentration and pH, but were similar weight / volume ratios.

This result clearly eliminates TRIS as a candidate for a biological buffer, since the precipitation reaction was immediate. The other buffers all behaved in a similar way and the reaction appeared to occur more slowly, indicating that it may be possible to inhibit it with an antioxidant e.g. ascorbic acid. Since ascorbic acid was already being considered for incorporation into the buffer salts to prevent or reduce radiation damage (see section 2.1.3.6), it was the first choice of antioxidant for preventing precipitation of buffer salts by oxidation reactions.

5.3.3 Controlled experiment to characterise precipitation in different buffers – materials and methods

A further experiment was carried out to monitor the effects observed in section 5.3.2 in a more controlled experiment and to determine whether the presence of an antioxidant (ascorbic acid) would prevent or reduce oxidation of iron (II) and the formation of precipitates in different buffers. The buffers HEPES, MOPS and TRIS were prepared at a concentration of 10mM (the concentration used in the previous assays). RO water was used as a control, to verify that effects observed were due to the presence of the buffer salts. Iron (II) sulphate was dissolved in 50ml of each buffer at a concentration of 26.6

$\text{mg}\cdot\text{ml}^{-1}$, 10% of its solubility limit in water at 25°C . The buffers were then photographed immediately after addition of the iron (II) sulphate and after 1 hour.

5.3.4 Controlled experiment to characterise precipitation in different buffers – results and discussion



Figure 5.6: Photograph showing different buffers immediately after the addition of $26.6\text{mg}\cdot\text{ml}^{-1}$ iron (II) sulphate. From left to right the solutions are RO water, 10mM HEPES, 10mM TRIS, and 10mM MOPS all at pH 7.4.



Figure 5.7: Photograph showing different buffers 1 hour after the addition of $26.6\text{mg}\cdot\text{ml}^{-1}$ iron (II) sulphate. From left to right the solutions are RO water, 10mM HEPES, 10mM TRIS, and 10mM MOPS all pH 7.4.

The visible presence of iron (III) in the RO water in this experiment is likely to be because the concentration of iron (II) sulphate added to the solutions in this experiment was much greater than that used in Figure 5.4, so the red precipitate is visible in Figure 5.6. It is immediately clear from the colour change in the solutions in Figure 5.6 that the iron (II) is oxidised to iron (III) immediately in both RO water and 10mM TRIS buffer. The 10mM HEPES buffer also appears to have a slight red colour, indicating that some oxidation of iron (II) also occurred in HEPES buffer. Very little oxidation was observed in the MOPS buffer. The results were very similar after a 1-hour incubation (Figure 5.7), except that in the TRIS buffer the iron (III) precipitate appears to have accumulated in the centre of the

solution. This accumulation of precipitate did not occur in RO water, indicating that the precipitate was formed by reaction of the iron (II) with the TRIS buffer salt. The clear conclusion from this and the assay carried out with the HEPES buffer is that pure TRIS and pure HEPES are clearly not appropriate for use in the Life Marker Chip since the formation of precipitates is incompatible with a microfluidic channel system.

5.3.5 Controlled experiment with buffer salts and antioxidant (ascorbic acid) – materials and methods

The experiment described in section 5.3.3 was then repeated, but this time with the addition of ascorbic acid, which was dissolved in the buffer prior to addition of the iron (II) sulphate. Ascorbic acid was added to each solution at a concentration of $20.6\text{mg}\cdot\text{ml}^{-1}$, a 2.5 times molar excess of ascorbic acid for the concentration of iron (II) sulphate added. No other changes were made to the protocol.

5.3.6 Controlled experiment with buffer salts and antioxidant (ascorbic acid) – results and discussion



Figure 5.8: Buffer solutions after the addition of ascorbic acid at a concentration $20.6\text{mg}\cdot\text{ml}^{-1}$. From left to right the buffers are: RO water, 10mM HEPES, 10mM MOPS, 10mM TRIS all pH 7.4.

The buffer solutions were transferred into clean beakers to remove the un-dissolved ascorbic acid. Iron (II) sulphate was then added to these solutions at a concentration of $26.6\text{mg}\cdot\text{ml}^{-1}$.



Figure 5.9: Buffer solutions containing ascorbic acid immediately after the addition of iron (II) sulphate at a concentration of 26.6mg.ml⁻¹. From left to right the buffers are: RO water, 10mM HEPES, 10mM MOPS, 10mM TRIS.



Figure 5.10: Buffer solutions containing ascorbic acid 1 hour after the addition of iron (II) sulphate at a concentration of 26.6mg.ml⁻¹. From left to right the buffers are: RO water, 10mM HEPES, 10mM MOPS, 10mM TRIS all pH 7.4.

Figure 5.9 and Figure 5.10 show that, in contrast to the previous experiment, the buffers containing ascorbic acid are all a blue/ green colour characteristic of the presence of iron (II) ions. This blue/green colour this indicates that formation of red / orange iron (III) precipitates as in section 5.3.4 did not occur, either immediately or after one hour. This is a clear demonstration that the addition of an antioxidant to the buffer is an effective way to prevent the formation of iron (III) precipitates and ensure that iron (II) containing samples will not be problematic for the microfluidic system. Since ascorbic acid does not dissolve in the buffers used at a high enough concentration to give a large molar excess of antioxidant, even at an iron (II) sulphate concentration of 26.6mg.ml⁻¹ (only 10% of its solubility limit of in water), other antioxidants with a higher solubility may be considered in future experiments. Nonetheless, this experiment has demonstrated a method by which oxidation reactions which may prove damaging to the Life Marker Chip can be prevented.

No experiments to determine whether the buffers containing 20.6mg.ml⁻¹ ascorbic acid and 26.6 mg.ml⁻¹ iron (II) sulphate were compatible with immunoassays were carried out in this thesis. However, Grieb *et al.* (2002) demonstrated an antibody assay with antibody in

buffer containing 200mM ascorbic acid, showing that the presence of ascorbic acid does not prevent antibody-antigen interaction. The presence of iron (II) ions in the buffer may have an effect on the assay, but there are two possible solutions to this. One is the addition of an ion chelator e.g. EDTA to the buffer to prevent the Fe^{2+} ion interacting with the antibody, and the second would be the addition of a demineralisation step to the LMC sample processing system, which would prevent iron (II) salts reaching the antibody assay buffer in the flight instrument.

Although much further work is required to fully develop a buffer system that is fully tested and known to be compatible with the evaporite minerals most likely to be present on the Martian surface (see section 4.2), the experiments reported here summarise the work carried out to date. One of the key outcomes of this work was that it highlighted the possibility of dissolved evaporite minerals reaction with buffer salts to form insoluble precipitates that would be incompatible with a microfluidic channel based Life Marker Chip instrument, which had not previously been considered. Another key result was the finding that the inclusion of an antioxidant (ascorbate) that is compatible with immunoassays prevented the formation of these precipitates. Ascorbate is used routinely in some biological assay applications and antibody preparations (e.g. Grieb *et al.*, 2002), so would not be expected to have an adverse effect on the Life Marker Chip immunoassays. Thus although a buffer format that would be expected to be compatible with the Martian samples has not been fully tested in this work, it is believed that a solution had been found to the precipitation of buffer salt reaction products. The next stage in development was to determine the tolerance of immunoassays to the presence of organic solvents that may be considered in the development of the sample processing system, and this work is described in the following sections.

5.4 Sample extraction reagents and organic solvents

As described in section 2.4.4.5, the sample processing system for the SMILE LMC is currently based on the use of a solid phase extraction column, in which a single solvent is used to remove organics from the column and into the LMC assay area. Depending upon the detailed design of this system, dissolved Martian regolith salts and reagents for use in the sample processing and extraction system may pass through into the LMC assay reaction chamber. In polar biomarker extraction, guanidine-HCl is a common extraction reagent that may be used to extract biological target molecules from the regolith samples (see for example Schweitzer *et al.*, 2005). The a-polar biomarker extraction line, by the nature of the hydrophobic target molecules of interest, must use hydrophobic solvents e.g. n-hexane to extract the targets from the sample, and may transfer these into a solution more compatible with antibody-antigen interaction by use of an intermediate organic solvent such as methanol (Schweitzer *et al.*, 2005, Buch *et al.*, 2003).

Little previous work has been done to date to determine the effects of these reagents or organic solvents on the binding properties of antibodies. Aga & Thurman (1993) carried out ELISAs after solid phase extraction through a C₁₈ column with different solvents, and found an ELISA assay to be tolerant to up to 20% v/v methanol in water. However the tolerance of ELISAs to methanol was found to be highly variable (from 5-50%v/v) depending on the antibody-antigen pair (Aga & Thurman, 1993).

A series of experiments were devised and carried out to determine whether or how much of these solvents would be tolerated by an antibody-antigen interaction, using the anti-atrazine scAb binding ELISA described in section 3.1.1.4 as a representative system. This is broadly comparable with the proposed assay format in the flight instrument since one of the antibody-antigen pair is immobilised on a surface and the binding reaction occurs in solution over this functionalised surface. In all experiments in organic solvents, the antibody-antigen binding step was carried out in the solvent of interest, while the rest of the protocol remained unaltered as described in section 3.1.1.4.

5.4.1 Effect of guanidine-HCl on antibody-antigen interaction – materials and methods

Guanidine HCl can be used to extract proteins, amino acids and DNA from soil or regolith samples. It is normally used as a denaturant for proteins and therefore denaturation of the scAb antibody, i.e. loss of activity, is expected at higher concentrations, for example the 8M typically used in extraction protocols (Schweitzer *et al.*, 2005). In this experiment, anti-atrazine scAb was used only at a concentration of $0.3\mu\text{g}\cdot\text{ml}^{-1}$ rather than the serial dilution (2-fold dilutions from $0.3 - 5.9 \times 10^{-4}\mu\text{g}\cdot\text{ml}^{-1}$) used in previous experiments. This was because it is known that guanidine-HCl is a protein denaturant and would almost certainly reduce the antigen-binding ability of the antibody fragment significantly, especially at lower concentrations of antibody (since at lower concentrations any slight denaturation effect may be beyond the lower limit of detection of the assay). In order to achieve maximum similarity to the proposed final instrument, plastic Eppendorf vials were loaded with $1\mu\text{l}$ of $0.3\text{mg}\cdot\text{ml}^{-1}$ anti-atrazine scAb and placed into a sealed vessel containing excess silica hydride desiccant, and the vessel placed in an oven at 37°C overnight to remove all water present. The binding ELISA assay protocol was then carried out as described in section 3.1.1.4, except that the addition of the anti-atrazine scAb was carried out as follows. Immediately prior to the addition of anti-atrazine scAb to the plate wells, 1ml of guanidine HCl (Sigma-Aldrich, Poole, UK) was added to the vials containing dried anti-atrazine scAb at concentrations of 8M (as supplied) and 6M, 4M, 2M and 1M diluted in 10mM HEPES pH7.4. $100\mu\text{l}$ of this solution was then added to the appropriate wells on the ELISA plate and incubated for 2 hours at 20°C , and the remaining protocol was carried out according to section 3.1.1.4.

5.4.2 Effect of guanidine-HCl on antibody-antigen interaction – results and discussion

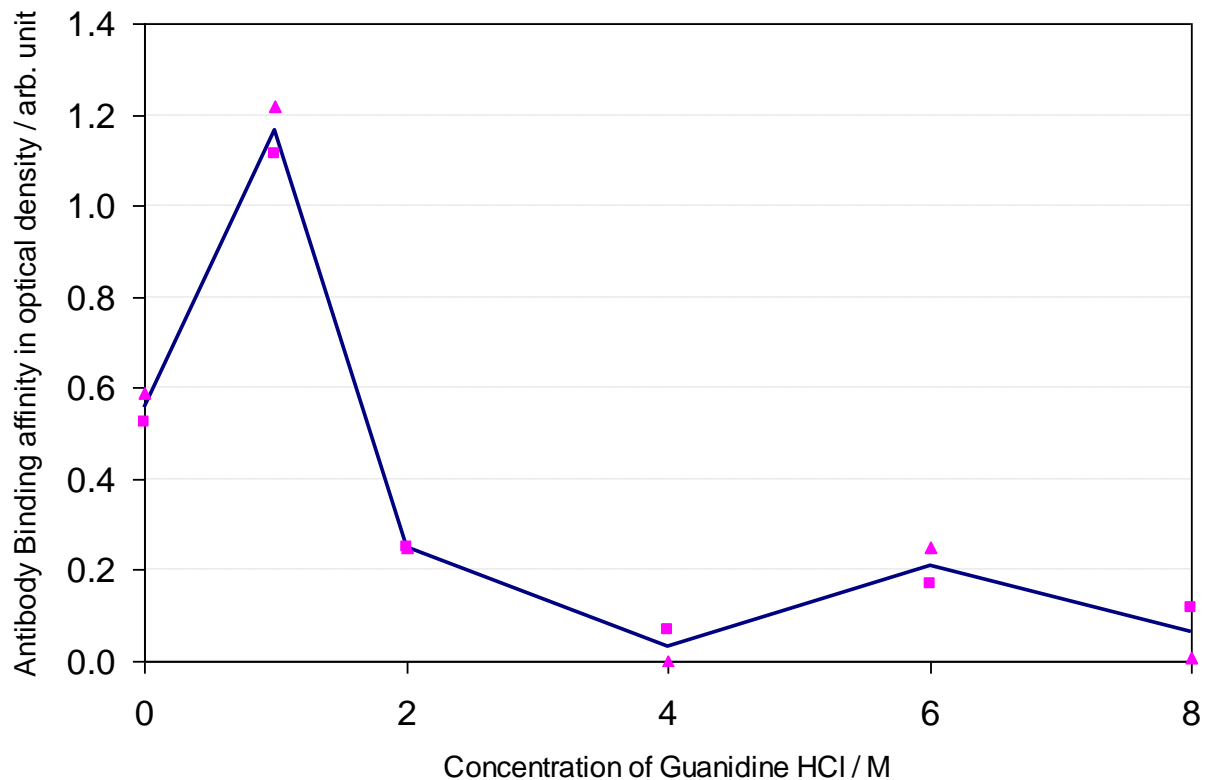


Figure 5.11: Effect of the presence of different dilutions of guanidine-HCl on anti-atrazine scAb in a binding ELISA format. Guanidine HCl was used at concentrations of 8M (directly from the stock solution) and diluted to 6M, 4M, 2M and 1M in 10mM HEPES buffer pH 7.4. The control antibody was reconstituted in 10mM HEPES pH 7.4. The line connects the average binding signal from the duplicate wells at each concentration, and filled triangles and squares represent replicates of the guanidine HCl serial dilutions.

Figure 5.11 shows that guanidine HCl at 1M appeared to increase the amount of bound antibody. This may be due to the diluted guanidine-HCl partially denaturing the scAb, and thereby increasing the binding affinity of the labelled secondary antibody, without adversely affecting the scAbs atrazine binding site (so the scAb still binds to its BSA-atrazine antigen). At concentrations 2M and above, no significant antibody binding is observed as expected (because guanidine-HCL denatures proteins).

This experiment has demonstrated that this ELISA, (and potentially immunoassays for other LMC targets) will not function in the presence of over 2M guanidine-HCl. This imposes a requirement on the LMC sample processing system to limit the amount of guanidine-HCL that passes through into the assay chamber to a maximum concentration of 2M, either by diluting the extracted solution (which given the low concentrations of target

analytes is unfavourable) or transferring the extracted biomarkers into a different solution before releasing it into the assay chamber.

5.4.3 Effect of sample extraction organic solvents on antibody assays – materials and methods

Sample extraction procedures use a variety of organic solvents to remove potential target molecules from their matrices. Antibodies are known to have variable tolerance to the presence of organic solvents (Aga & Thurman, 1993). Factors contributing to this can include poor solubility and changes in the secondary structure of the antibody due to the hydrophobic nature of the solvent (Aga & Thurman, 1993).

Dried antibody samples were prepared by pipetting 1 μ l of 0.3mg.ml⁻¹ anti-atrazine scAb into Eppendorf vials, and placing the vials in a sealed container with excess silica gel dessicant in an oven at 37°C overnight. These antibody samples were reconstituted in the desired solvent and used in the assay. A binding ELISA was then carried out according to the protocol in section 3.1.1.4. During incubation steps involving antibody in organic solvents, the plates were sealed with AlumaSeal™ adhesive aluminium foil sheets (Sigma-Aldrich, Poole, UK) to prevent evaporation of the solvent.

Two solvents have been tested to date. Methanol is used to elute some molecules of intermediate polarity from solid phase extraction columns as described in section 2.4.1.3, either in pure form or combined with other solvents, so was considered a useful solvent to test. Methanol was diluted in 10mM HEPES buffer pH 7.4 in volume fractions of 10, 25 and 50%, to represent different ratios of water-methanol that may be used to elute organics from the solid phase extraction column. Hexane is used to remove highly a-polar molecules from the solid phase extraction column and was tested as an example of a highly a-polar solvent. 100% hexane, hexane containing 12.5% volume fraction of Methanol (close to the solubility limit of methanol in hexane) and 100% methanol were tested in a separate experiment.

5.4.4 Effect of sample extraction organic solvents on antibody assays – results and discussion

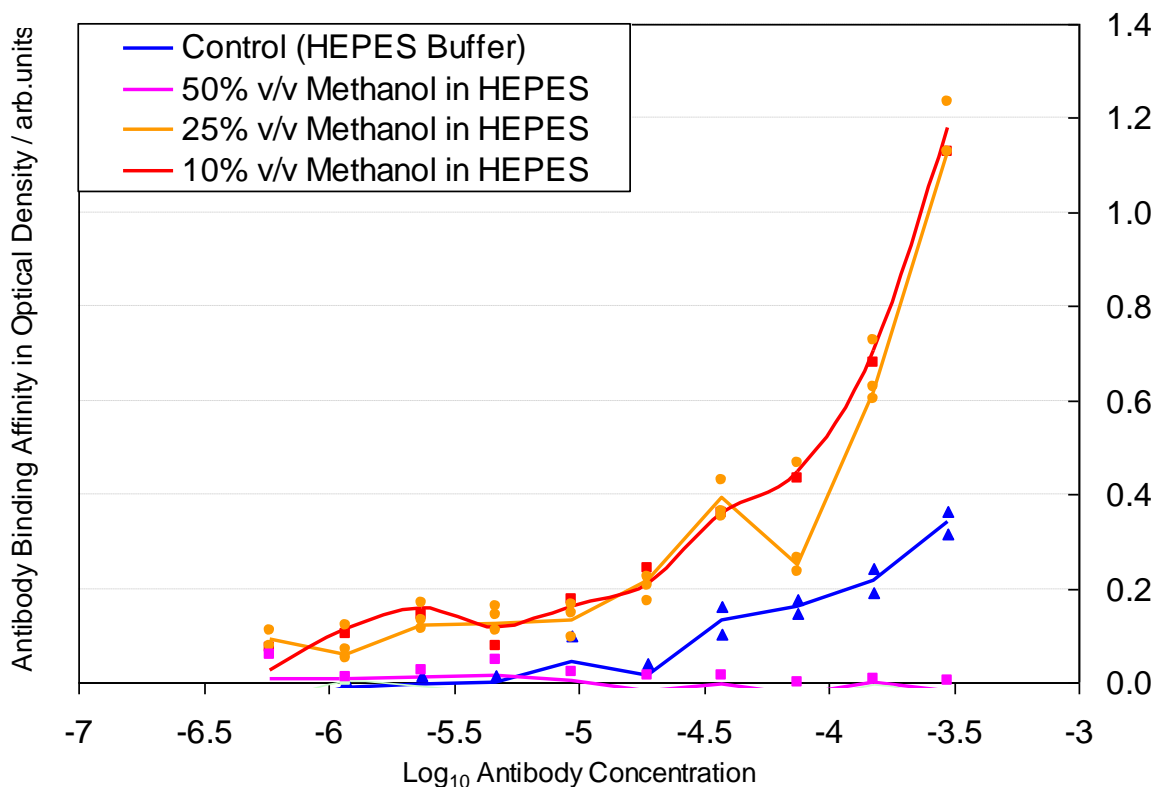


Figure 5.12: Effect of the presence of different concentrations of methanol in HEPES Buffer on the binding properties of anti-atrazine scAb recombinant antibody fragment.

Figure 5.12 shows that with up to 25% volume fraction of methanol in HEPES buffer antibody binding still occurs, and in fact a higher signal was observed. Similarly to guanidine-HCl, this increase in binding could be due to the different polarity of the methanol causing partial denaturation of the scAb, making it easier for the labelled secondary antibody to bind. Such an effect could increase the binding signal without affecting the binding site allowing the scAb to attach to the BSA-atrazine target. At 50% volume fraction of methanol in HEPES buffer, however, no signal is observed. This loss of signal could be caused by the organic solvent causing structural damage to the antibody, or a consequence of the antibody being insoluble in the methanol / HEPES buffer solution. This result is in broad agreement with the findings of Aga & Thurman (1993).

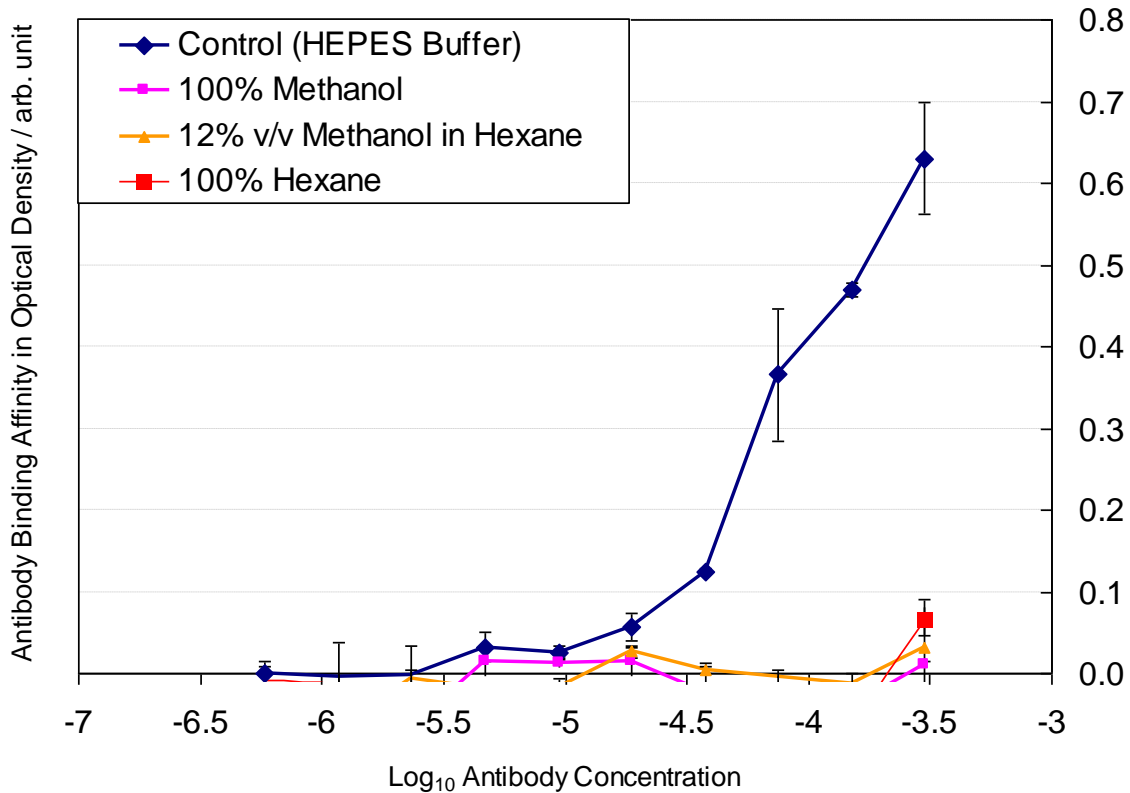


Figure 5.13: Effect of the presence of hexane, methanol and a hexane / methanol mixture on the binding properties of anti-atrazine scAb recombinant antibody fragment.

Figure 5.13 shows that no antibody binding was observed when the scAb incubation stage of the ELISA was carried out in 100% methanol, 100% hexane or hexane containing 12.5% volume fraction methanol. The most likely explanation for this is that the antibody is insoluble in the hexane, 100% methanol and hexane / methanol mixture. Further tests need to be done to establish what the contribution of each of these factors is to the loss of antibody binding signal. However, this result is a clear indication that pure hydrophobic solvents are unlikely to be compatible with the antibody assay in the flight instrument, so methods to dilute or remove the organic solvents from the extraction system while retaining the target molecules of interest in the sample will have to be considered.

5.5 Summary and discussion of the effects of Martian regolith salts and sample extraction solvents on antibody-based assays

The focus of this section has been to determine the effect of likely Martian samples on antibody assays, since the Life Marker Chip proposes to utilise antibody assays for the detection of biomarkers on Mars. The sample processing system for the LMC has not been fully defined at this stage, therefore some of these experiments were carried out to determine requirements for the sample processing system as well as determining the effect of different conditions on the assays.

The first area that was considered was the effect of Martian regolith salts. Since the target areas of most interest to the ExoMars mission are areas that may have supported Life on Mars, the mission will intend to place a rover on an area of the surface that may once have been covered by liquid water (Vago *et al.*, 2003). These areas are likely to contain large deposits of evaporite minerals including calcium sulphate, iron (II) and iron (III) sulphates and magnesium sulphate (see section 2.1.4.2). Assays were carried out using antibody in buffers containing these minerals at different fractions of their solubility limit. It was found that calcium sulphate had little effect on the assay, and magnesium sulphate reduced the binding signal by approximately 50%. The addition of iron (II) sulphate to buffers resulted in precipitation of an insoluble iron (III) compound and a very high background signal in the assay. A further set of experiments was carried out in which it was found that the formation of precipitates in the presence of iron (II) sulphate could be prevented by the addition of ascorbate (an antioxidant), but this new buffer was not tested in an assay format. However ascorbate is used in some biological assays and has no adverse effects (Grieb *et al.*, 2002), so this solution is expected to overcome the non-specific binding caused by the addition of iron (II) sulphate to buffers. This will be confirmed in future work (see section 4.2). Since an antioxidant was already being considered for addition into the LMC buffers to prevent oxidation by radiation damage, this does not significantly affect the design of the LMC.

The second area considered in this section was the possibility that reagents including organic solvents used in the sample extraction system may reach the assay area of the Life Marker Chip. Since the chemistry and solvents to be used in the LMC sample processing system have not yet been defined, experiments were carried out in which a

representative antibody (anti-atrazine scAb) was used in different concentrations of guanidine-HCl (a common sample extraction reagent for proteins) methanol / HEPES buffer mixtures, representing a polar organic solvent, n-hexane as an example a-polar solvent, and a methanol / n-hexane mixture to represent a mixture of organic solvents. Guanidine-HCl increased the antibody binding signal at a concentration of 1M, but at 2M and above the binding signal was very low. Since guanidine-HCl is a protein denaturant, this is likely to be due to denaturation of the antibody or the BSA-atrazine conjugate, or both. This result indicated that guanidine HCl can only be present in the antibody assay at concentrations of 1M and below, and the possibility of denaturing target proteins of interest in the sample limits it's usefulness in this application.

It was found the antibody assay had an enhanced signal when 25% v/v methanol was present in the buffer, but at 50% and higher concentrations of methanol no antibody binding signal was observed. No antibody binding was observed when the antibody was used in pure n-hexane or n-hexane containing 12.5% v/v methanol. These experiments indicate that methanol could be used in the sample processing system and diluted in buffer prior to reaching the antibody assay area of the LMC. However, if n-hexane or organic solvent mixtures are used, the biomarkers to be detected must be transferred into a different carrier solution before an antibody assay can be carried out.

This series of experiments has defined some of the limits of using an antibody assay based detection system for applications in the Martian environment, and provided a number of key design inputs for the sample processing system which is currently under development. Some of the results are positive, for example enhanced binding signal when low concentrations of methanol are present, and others have raised unexpected points for consideration such as the reaction of iron (II) sulphate with HEPES buffer. This area requires further investigation as the design of the sample processing system is developed. The organic solvents or mixtures present in the solution used for antibody-antigen binding is critical, and further work to confirm that the solution used in this assay step is compatible with all of the salts that may be present in the Martian regolith samples to be analysed is essential.

6 Discussion and Future Work

6.1 Discussion of developments in Life Marker Chip technology for *in-situ* Life detection on Mars made during this work

Since the three sections of practical work were carried out and reported as a series of experiments in which the results of each experiment and implications for subsequent work were discussed throughout Chapter 3, this final discussion presents a brief summary of the developments made and the status of each area of work at the conclusion of this PhD work.

The Life Marker Chip is an important instrument proposed for the Pasteur payload for the European Space Agency's flagship Life detection mission, ExoMars, since it has the ability to detect large number of molecular targets of interest that are beyond the detection capabilities of other instruments. However, at the time that work in this thesis began, a number of key areas of work critical to the development of the Life Marker Chip had not been carried out.

Firstly, the proposal to utilise the specific molecular recognition properties of antibodies and the sensitivity enabled by fluorescent dyes had to be confirmed as compatible with the radiation and sterilisation environments encountered during a space mission. The current state of knowledge initially was primarily the work of others using gamma radiation, which indicated that transporting or sterilising proteins in solution would not be successful due to degradation by the radiolytic products of water. However, protein in a dried state had been shown to be more resistant to damage. No work had been done exposing fluorescent dyes or antibodies to gamma, proton or helium ion radiation. In producing the literature review for this thesis a draft publication has been written and is awaiting submission to the journal *Astrobiology*, pending receipt of updated figures for the measured radiation environment during flight to Mars from the NASA MARIE team.

To address this, a protocol was developed which allowed dried samples of fluorescent dyes and antibodies to be exposed to fluences of protons and helium ions at level comparable to a mission to Mars and large excesses. Although some loss of activity

was observed in some experiments, none of the conditions used completely inactivated either the antibody used or representative fluorescent dyes. Fluorescent dyes were also shown to survive both heat sterilisation and gamma radiation exposure up to the levels used in sterilisation protocols in the dried state, although in water the dyes did not retain fluorescent properties when exposed to sterilisation doses. These results contributed towards the continuation of funding for the development of the Life Marker Chip by the European Space Agency, some results for the particle radiation tests have been published (Thompson *et al.*, 2006) and further publications are planned for other results including the exposure of fluorescent dyes to gamma radiation.

The second area of interest was the development of the instrumentation platform on which the Life Marker Chip would be based. Reviewing the literature indicates that the proposed design utilised a number of technologies that were already at an advanced stage of development in other fields, but have not been used in combination in previous work. In this thesis many of the components required for the assay system to be used in the final Life Marker Chip design have been demonstrated, including epoxy functionalisation of glass and silicon surfaces, printing protein and antibody microarray within microfluidic channel structures, covalent attachment of proteins and antibodies to these surfaces, optimising an assay protocol for carrying out an immunoassay in a microarray format in an open microfluidic channel, *in-situ* labelling and detection of a relevant target protein, and developing a breadboard system and imaging protocol that allows imaging of fluorescently labelled protein bound to antibody microarrays. This work has advanced the level of knowledge in this area by demonstrating deposition of protein and antibody microarrays in microfluidic structures for the first time, using spot assay areas much smaller than demonstrated in previous work, and successfully carrying out immunoassays using these microarrays. It has also provided strong support for the continuing development of the Life Marker Chip design by demonstrating capability within the consortium to carry out each of the assembly stages required to build the complete instrument.

The third and final aspect of the Life Marker Chip instrument considered in this work was the effect of real sample matrices and sample processing reagents and solvents on the proposed antibody assay detection system. While calcium sulphate and magnesium sulphate did reduce the antibody binding signal in the representative assay,

they did not present critical problems for the assay even at their solubility limits in water. However, iron (II) sulphate did present a problem for the antibody assay and a microfluidic design, specifically by forming precipitates of an iron (III) salt in both HEPES and TRIS buffers. The resulting HEPES buffer appeared to cause a very high binding signal in the antibody assay, indicating that they affected either the dissolved antibody or the protein conjugate in the plate wells, or both, in a way which caused a high degree of non-specific binding. However, on visual inspection the buffer MOPS did not appear to be affected in this way, and in HEPES, TRIS and MOPS buffers the addition of ascorbic acid as an antioxidant appeared to prevent the formation of precipitates. While ascorbic acid may not prove to be the best antioxidant for the flight instrument for the flight instrument because it does not have high enough solubility to provide a large excess over iron (II) sulphate (even at 10% of iron (II) sulphate's solubility limit), this work has demonstrated that the inclusion of an antioxidant in the final assay buffer is a suitable approach to preventing oxidation reactions and the formation of precipitates.

The use of Guanidine-HCl as an extraction reagent may increase the yield of protein from samples, but it is not compatible with an antibody assay system at concentrations of more than 1M. Since typical extraction protocols use guanidine-HCl at 8M or 6M, it would either have to be diluted or removed from the solution before it reached the antibody assay reaction chamber. Diluting the sample is likely to be impractical due to the likely low concentrations of target analytes, but reagents could be removed during a solid phase extraction step. Solid phase extraction was already being considered in the design for the sample processing system since it allows both concentration of the sample and exchange of buffer solutions between the extraction and assay stages.

The experiments with organic solvents demonstrated that completely organic solvents such as methanol, hexane or methanol-hexane mixtures are not compatible with antibody assays as expected. This suggests that if these solvents are to be used in the sample processing system the targets extracted from them must be transferred into an aqueous solvent prior to being passed over the antibody assay area, for example by a solid phase extraction. This is not a critical problem for the Life Marker Chip since, as mentioned above, a solid phase extraction step was already being considered for the sample processing system. Experiments with buffer-methanol mixtures suggested that solutions containing up to 25% methanol could be used in the antibody assay reaction.

This may allow buffer-methanol mixtures to be used to increase the solubility of organic target molecules in the solution used for the antibody assay without adversely affecting the assay. Buffer-methanol mixtures could therefore be used to remove targets from a solid phase extraction column after they had been extracted from the sample by other reagents or solvents that are incompatible with antibody assays. All of the work on Mars related media is believed to be novel especially for this application, and will be considered for publication when further experiments have been carried out to increase the range of conditions tested.

In summary, this thesis includes work that has advanced the current state of scientific knowledge in three key areas for the development of the Life Marker Chip; the effect of the radiation environment on biological assay components, development of the instrument platform and effect of Mars-related media and sample processing reagents on biological assays. This knowledge has contributed to both the continuation of developing the Life Marker Chip instrument by validating the use of biological reagents in space, and the design and development of the instrument platform and sample processing system. A number of publications have been produced or are being prepared that include data from work carried out in this project, in addition to contributions to the technical documentation required by the European Space Agency for the Technology Readiness Level Upgrade Study. This work is ongoing and will be expanded upon in future work, which will be discussed in the following section.

6.2 Future Work

While significant progress has been made during the work described in this thesis, further work is required in all three of the key areas in order to ensure the successful development of a breadboard and flight model of the Life Marker Chip by 2011, the target date set by the European Space Agency for delivery of the LMC instrument. Since the Life Marker Chip Technology Readiness Level Upgrade Study continues beyond the timescale of this PhD work, the information reported here may not represent the final state of development in any particular area.

In radiation testing, the key experiment that was not carried out during this work is the exposure of dried antibody samples to Gamma radiation, at a series of doses including

mission and sterilisation levels. Unfortunately due to time constraints and availability of equipment and personnel this could not be carried out in time for the submission of this thesis, but it remains a key test and is to be carried out at the earliest opportunity. Since the conclusion of the practical work reported in this thesis, a further series of proton radiation tests has begun. This involves the exposure of a number of types of sample to 2, 5 and 10 times the mission fluence of protons, using 60MeV protons. The samples exposed include antibody and fluorescent dye freeze-dried into glass-fibre pads, and silicon oxide and silicon nitride chips epoxy functionalised with GOPS and printed with a microarray containing 5 different reagents. At the time of writing these samples and other Life Marker Chip components including gasket materials have been exposed to these proton radiation fluences and are currently in quarantine until residual radioactivity drops to a safe background level. Other radiation tests that are planned are further exposures of both antibodies and fluorescent dyes to lower energy level protons and neutrons, both of which may be generated as secondary radiation from spacecraft shielding. This is to be carried out either using the Dynamitron at the University of Birmingham or facilities at the National Physics Laboratory.

For the instrument platform, the first priority is to develop an assay in a closed microfluidic channel. The assay may have a slightly different calibration curve than the open channel due to there being a restricted volume of sample solution. Early experiments attempting to achieve this were not successful due to problems with non-specific binding to one of the materials used to form the microfluidic channel, but this problem is not anticipated to be difficult to solve. In addition, assay using some of the protocols developed in different sections of this work together rather than independently are a key step, for example demonstrating a successful GroEl assay on a silicon oxide surface that had been modified with the GOPS functionalisation protocol is a logical development. Work is planned in which a consortium partner will supply silicon devices with microfluidic devices and optical waveguides integrated in to them, and these will be used to integrate some of the techniques demonstrated in this thesis.

The range of Mars media and sample processing reagents tested with antibody assays and buffer salts needs to be expanded as soon as possible, to establish a suitable buffer for the assay at an early stage. This will initially involve further testing of different buffers with the Martian regolith salts with and without the addition of ascorbic acid, to

identify a buffer that is suitable for all likely sampling environments, and then to test this buffer in antibody assays with different concentrations of each representative regolith salt. This may then be expanded in to mixing this final buffer with methanol to integrate it with the sample processing system. Work is already planned by other members of the SMILE consortium to develop the design of the sample processing system, and select an appropriate sample processing method based on the results generated in the initial work in this thesis. If this development identifies any other potentially suitable organic solvents or extraction reagents these will be tested for compatibility with the antibody assay.

The ultimate goal for this work is to develop a flight instrument Life Marker Chip and sample processing system for the Pasteur payload on board the ExoMars mission rover, and validate the use of this instrument and sample processing unit in the Mars environment. This is to be achieved by 2011, with a mission launch date in 2013. This thesis contains early development work towards this in three key areas, by providing evidence supporting the potential application of biological materials in Mars missions, validating the instrument design approach and confirming a number of immunoassay and imaging protocols, providing input into the design and development of the Life Marker Chip sample processing system, and indicates the areas of high importance for the next stage of development of the SMILE Life Marker Chip.

References

- Adams Jr., J.H. (1992) Cosmic radiation: constraints on space exploration. *Nuclear Tracks and Radiation Measurements*, 20, 397-40.
- Affara, N. A. (2003) Resource and Hardware Options for Microarray-Based Experimentation, *Briefings in Functional Genomics and Proteomics*, 2, 7-20.
- Aga, D. S. & Thurman, E. M. (1993) Coupling Solid-Phase Extraction and Enzyme-Linked Immunosorbent Assay for Ultratrace Determination of Herbicides in Pristine Water, *Analytical Chemistry*, 65, 2894-2898.
- Amaral, G., Martinez-Frias, J. Vázquez, L. Astrobiological Significance of Minerals on Mars Surface Environment: UV-Shielding Properties of Fe (jarosite) vs. Ca (Gypsum) Sulphates, *Reviews in Environmental Science and Biotechnology*, 5, 219-231
- Benton, E.R., and Benton, E.V. (2001) Space radiation in low-Earth orbit and beyond. *Nuclear Instrumentation and Methods B*, 184, 255-294.
- Benini, R., Cennamo, N., Minardo, A. & Zeni, L. (2006) Planar Waveguides for Fluorescence-Based Biosensing: Optimization and Analysis, *IEEE Sensors Journal*, 6, 1218-1226.
- Buch, A., Sternberg, R., Meunier, D., Rodierb, C., Laurenta, C., & Raulina, F. (2003) Solvent extraction of organic molecules of exobiological interest for in situ analysis of the Martian soil, *Journal of Chromatography A*, 999, 165-174.
- Bundo-Morita, K., Gobson, S. and Lenard, J. (1988) Radiation Inactivation of Analysis of Fusion and Hemolysis by Vesicular Stomatitis Virus. *Virology*, 163, 622-624.
- Butcher, G., Sims, M.R., Fraser, G., Klingelhofer, G., Bernhardt, B., and Davidson, A. (2006) Background Radiation Effects and Hazards in Planetary Instrumentation, *Nuclear Instrumentation and Methods in Physics Section A*, 2006, 564, 559-566.
- Bibring, J.-P., Langevin, Y., Gendrin, A., Gondet, B., Poulet, F., Berthé, M., Soufflot, A., Arvidson, R., Mangold, N., Mustard, J. & Drossart, P. (2005) Mars Surface Diversity as Revealed by the OMEGA/Mars Express Observations, *Science*, 307, 1576–1581.
- Caballero, I., Altanés, S., Castillo, A., Deridder, V., Gomez, T., Miralles, Y., Naydenov, V., Prieto, E. and Tilquin, B. (2004) Radiosensitivity Study of Freeze-dried Antibodies to Gamma Irradiation. *American Pharmaceutical Review*, 1-4.

Cho, Y. & Song, K.B. (2000) Effect of γ -Irradiation on the Molecular Properties of BSA and β -Lactoglobulin, *Journal of Biochemistry and Molecular Biology*, 33, 133-137.

Cho, Y., Yang, J.S. & Song, K.B. (1999) Effect of Ascorbic Acid and Protein Concentration on the Molecular Weight Profile of Bovine Serum Albumin and β -Lactoglobulin by γ -Irradiation, *Food Research International*, 32, 515-519.

Cheftel, J.C., Cuq, J.L. & Lorient, D (1985) Amino Acids, Peptides, and Proteins. In: Fennema, O.R. (Ed.), *Food Chemistry*, Marcel Dekker, New York, pp279-343.

Clark, B.C., Morris, R.V., McLennan, S.M., Gellert, R., Jolliff, B., Knoll, A.H., Squyres, S.W., Lowenstein, T.K., Ming, D.W., Tosca, N.J., Yen, A., Christensen, P.R., Gorevan, S., Brückner, J., Calvin, W., Dreibus, G., Farrand, W., Klingelhofer, G., Waenke, H., Zipfel, J., Bell III, J.F., Grotzinger, J., McSween & H.Y., Rieder, R. (2005) Chemistry and mineralogy of outcrops at Meridiani Planum, *Earth and Planetary Science Letters*, 240, 73-94.

Clark, B.C. & Van Hart, D. (1981) The Salts of Mars, *Icarus*, 45, 370-378.

Cras, J.J., Rowe-Taitt, C.A., Nivens, D.A. & Ligler, F.S (1999) Comparison of chemical cleaning methods of glass in preparation for silanization, *Biosensors & Bioelectronics*, 14, 683-688.

Darling, D. (2002) *Life Everywhere: The Maverick Science of Astrobiology*, Basic Books, New York, USA, ISBN 978-0465015641.

Dartnell, L.R., Desorgher, L.S., Ward, J.M. & Coates, A.J. (2007) Modelling the surface and subsurface radiation environment: implications for astrobiology, *Geophysical Research Letters*, 34, L02207

Davies, K.J.A. (1987) Protein Damage and Degradation by Oxygen Radicals I: General Review, *The Journal of Biological Chemistry*, 262, 9895-9901.

Davies, K.J.A., Delsignore, M.E. & Lin, S.W. (1987a) Protein Damage and Degradation by Oxygen Radicals II, Modification of Amino Acids, *The Journal of Biological Chemistry*, 262, 9902-9907.

Davies, K.J.A. & Delsignore, M.E. (1987) Protein Damage and Degradation by Oxygen Radicals III, Modification of Secondary Structure and Tertiary Structure, *The Journal of Biological Chemistry*, 262, 9908-9913.

- Davies, K.J.A., Lin, S.W. & Delsignore, M.E. (1987b) Protein Damage and Degradation by Oxygen Radicals IV: Degradation of Denatured Proteins, *The Journal of Biological Chemistry*, 262, 9914-99920.
- Deflora, S. & Badolati, G. (1973) Thermal Inactivation of Untreated and Gamma-Irradiated A2/Aichi/68 Influenza Virus, *Journal of General Virology*, 20, 261-265
- DiVincenzi, D.L. & Stabekis, P.D. (1984) Revised Planetary Protection Policy for Solar System Exploration, *Advanced Space Research*, 4, 291-295.
- DiVincenzi, D.L., Stabakis, P. & Barengoltz, J. (1996) Refinement of Planetary Protection Policy for Mars Missions, *Advanced Space Research*, 18, 311-316.
- Elliott, L.H., McKormick, J.B. & Johnson, K.M. (1992) Inactivation of Lassa, Marburg and Ebola Viruses by Gamma Irradiation, *Journal of Genetic Virology*, 20, 86-88.
- European Space Agency (2005) *Preliminary Requirements and specifications LIFE MARKER CHIP*, ESA document ref: TEC-MMG/2005/941. NOTE: Cited as "ESA, 2005".
- Filali-Mouhim, A., Audette, M., St-Louis, M., Thauvette, L., Denoroy, L., Penin, F., Chen, X., Rouleau, N., Le Caer, J.-P., Rossier, J., Potier, M., & Le Maire, M. (1997) Lysosome Fragmentation Induced by Radiolysis, *International Journal of Radiation Biology*, 72, 63-70.
- Firestone, R.F. & Harada, Y. (1979) Evaluation of the Effects of Solar Radiation on Glass, NASA CR-161247.
- Garrison, W.M. (1997) Reaction Mechanisms in the Radiolysis of Peptides, Polypeptides and Proteins, *Chemistry Review*, 87, 381-398.
- Gamble, W.C., Chappell, W.A. & George, E.H. (1980) Inactivation of Rabies Diagnostic Reagents by Gamma Radiation, *Journal of Clinical Microbiology*, 12, 676-678.
- Garcia, A.A., Bonen, M.R., Ramirez-Vick, J. Sadaka, M. & Vuppu, A. (1999) Chapter 6: Bioaffinity, *Bioseparation Process Science*, Malden, MA, Blackwell Science Incorporated, ISBN 0-86542-568-X.
- Grieb, T., Forng, R.-Y., Brown, R., Owolabi, T., Maddox, E., McBain, A., Drohan, W.N., Mann D.M. and Burgess, W.H. (2002) Effective use of Gamma Irradiation for Pathogen Inactivation of Monoclonal Antibody Preparations. *Biologicals*, 30, 207–216.

Golden, J.P. (1998) US Patent 5,827,748.

Gómez-Elvira, J.; Holm, N.; Briones, C.; Cokell, C.; Compostizo, C.; Dumont, M.; Gómez, F.; Parro, V.; Sebastián, E.; Steele, A.; Toporski, J. (2004) Molecular Biology for Life Detection (MoBiLD) on Mars, *In: Proceedings of the Third European Workshop on Exo-Astrobiology, 18 - 20 November 2003*, Madrid, Spain. Ed.: R. A. Harris & L. Ouwehand. ESA SP-545, Noordwijk, Netherlands: ESA Publications Division, 123 – 126, ISBN 92-9092-856-5.

Guillaume, B., Bune, A., Schmidt, C., Klimek, F., Moldenhauer, G., Huber, W., Dorit, D., Korf, U., Wiemann, S. & Poustka, A. (2005) Systematic comparison of surface coatings for protein microarrays, *Proteomics*, 5, 4705-4712.

Harland, D.M, (2005) *Water and the Search for Life on Mars*, Springer, Praxis Publishing Ltd, Chichester, UK, ISBN 0-387-26020-X.

Han, Y., Mayer, D., OffenHauser, A. & Ingebrandt, S. (2006) Surface activation of thin silicon oxides by wet cleaning and silanization, *Thin Solid Films*, 510, 175-180.

Holmes-Seidle and Adams (2002) *Handbook of Radiation Effects*, Oxford University Press, Oxford, UK, ISBN 978-0198563471.

Horneck, G., Rettberg, P., Reitz, G., Wehner, J., Eschweiler, U., Strauch, K., Panitz, C., Starke, V. & Baumstark-Khan, C. (2001) Protection Of Bacterial Spores In Space, A Contribution To The Discussion On Panspermia, *Origins of Life and Evolution of the Biosphere*, 31, 527–547.

Horneck, G., Bücker, H., Reitz, G., Requardt, H., Dose, K., Martens, K. D., Mennigmann, H. D. & Weber, P. (1984) Microorganisms in the Space Environment, *Science*, 225, 226–228.

Lamture, J.B., Beattie K.L., Burke B.E., Eggers M.D., Ehrlich D.J., Fowler R., Hollies M.A., Kosicki B.B., Reich R.K., Smith S.R., Varma, R.S., Hogan, M. E. (1994) Direct detection of nucleic acid hybridization on the surface of a charge coupled device, *Nucleic Acids Research*, 22, 2121–2125.

Lide, D. R. ed. (2007) *CRC Handbook of Chemistry and Physics, Internet Version 2007, (87th Edition)*, <<http://www.hbcnpnetbase.com>>, Taylor and Francis, Boca, Raton, FL. NOTE: Cited as “CRC Handbook”.

Kambhampati, D. (Ed.) (2004) Protein Microarray Technology, *Wiley-VCH*, Weinheim, Germany. ISBN: 978-3-527-30597-1.

Kato, A., Tsutsui, N., Matsudomi, N., Kobayashi, K. & Nakai, S. (1981) Effects of Partial Denaturation on Surface Properties of Ovalbumin and Lysozyme, *Agricultural Biology and Chemistry*, 45, 2755.

Kempner, E.S. (1993) Damage to Proteins Due to the Direct Action of Ionizing Radiation, *Quarterly Review of Biophysics*, 26, 27-48.

Klein, H. P. (1979) The Viking Mission and the Search for Life on Mars, *Reviews of Geophysics*, 17, 1655-1662.

Klingelhoefer, G., Knoll, A. H., McLennan, S. M., McSween Jr., H. Y., Morris, R. V., Rice Jr., J. W., Rieder, R. & Soderblom, L. A. (2005) In Situ Evidence for an Ancient Aqueous Environment at Meridiani Planum, Mars, *Science*, 306, 1709-1704.

Kume, T. & Matsuda, T. (1995) Changes in Structural and Antigenic Properties of Proteins by Radiation, *Radiation Physics and Chemistry*, 46, 225-231.

Krumhar, K.C. & Berry, J.W. (1990) Effect of Antioxidant and Conditions on Solubility of Irradiated Food Proteins in Aqueous Solutions, *Journal of Food Science*, 55, 1127-1132.

Le Maire, M., Thauvette, L., De Foresta, B., Viel, A., Beauregard, G. & Potier, M. (1990) Effects of Ionising Radiations on Proteins, *The Biochemical Journal*, 267, 431-439.

Lee, Y.W. & Song, K.B. (2002) Effect of γ -Irradiation on the Molecular Properties of Myoglobin, *Journal of Biochemistry and Molecular Biology*, 35, 590-594.

Lee, S., Lee, S. & Song, K.B. (2003) Effect of Gamma-Irradiation on the Physicochemical Properties of Porcine and Bovine Blood Plasma Proteins, *Food Chemistry*, 82, 521-526.

Lee, M., Lee, S. & Song, K.B. (2004) Effect of γ -Irradiation on the Physicochemical Properties of Soy Protein Isolate Films, *Radiation Physics and Chemistry*, 72, 35-40.

Lecerf, J.M., Shirley, T.L., Zhu, Q., KazansteV, A., Amersdofer, P., Housman, D.E., Messer, A. and Huston, J.S. (2001) Human Single-Chain Fv Intrabodies Counteract *In-Situ* Huntington Aggregation in Cellular Models of Huntington's Disease. *Proceedings of the National Academy of Science USA*, 98, 4764-4769.

Lowy, R.J., Vavrina, G.A. & LaBarre, D.D. (2001) Comparison of Gamma and Neutron Radiation Inactivation of Influenza A Virus, *Antiviral Research*, 52, 261-273.

Lowy, R.J., Vavrina, G.A. and LaBarre, D.D. (2001) Comparison of Gamma and Neutron Radiation Inactivation of Influenza A Virus. *Antiviral Research*, 52, 261-273.

MacBeath, G. & Schreiber, S.L. (2000) Printing Proteins as Microarrays for High-Throughput Function Determination, *Science*, 289, 1760-1763.

MacClune, K., Fountain, G., Kargel, J.S. & MacAyeal, D.R. (2003) Glaciers of the McMurdo Dry Valleys: Terrestrial Analog for Martian Polar Sublimation, *Journal of Geophysical Research*, 108, 2-11.

Mahaffy, P.R., Beaty, D.W., Anderson, M., Aveni, G., Bada, J., Clemett, S., Des Marais, D., Douglas, S., Dworkin, J., Kern, R., Papanastassiou, D., Palluconi, F., Simmonds, J. Steele, A., Waite, H., and Zent, A. (2004). Science Priorities Related to the Organic Contamination of Martian Landers. Unpublished white paper, 32 p, posted Nov., 2004 by the Mars Exploration Program Analysis Group (MEPAG) at <http://mepag.jpl.nasa.gov/reports/index.html>.

Malin, M.C. & Edgett, K.S. (2000) Sedimentary rocks of early Mars. *Science*, 290, 1927-1937.

Malin, M.C., Edgett, K.S., Posiolova, L.V., McColley, S.M. & Dobreá, E.Z.N. (2006) Present-Day Impact Cratering Rate and Contemporary Gully Activity on Mars, *Science*, 314, 1573-1577.

McCullom, T.M. & Hynek, B.M. (2005) A volcanic environment for bedrock diagenesis at Meridiani Planum on Mars, *Nature*, 438, 1129-1131.

Mileikowsky, C., Cucinotta, F.A., Wilson, J.W., Gladman, B., Horneck, G., Lindegren, L., Melosh, H.J., Rickman, H., Valtonen, M. & Zheng, J.Q. (2000) Natural transfer of viable microbes in space. Part 1: From Mars to Earth and Earth to Mars. *Icarus*, 145, 391-427.

Mitchell, A., Holland, A., Vora, K. & Ghantasala, M. K. (2004) Integration of Microfluidic Channels and Optical Waveguides using low-cost Polymer Microfabrication Techniques, *IEEE, Biophotonics / Optical Interconnects and VLSI Photonics / WBM Microcavities, Digest of the LEOS.*, 12-13.

Mobile Science Laboratory Mission 2009, Landed Science Payload, Proposal Information Package, (2004) NASA. NOTE: Cited as "MSL PIP, 2004".

Moon, S. & Song, K.B. (2001) Effect of Gamma-Irradiation on the Molecular Properties of Ovalbumin and Ovomuroid and Protection by Ascorbic Acid, *Food Chemistry*, 74, 479-483.

Morris, S.C. (2003) *Life's Solution: Inevitable Humans in a Lonely Universe*, Cambridge University Press, Cambridge, UK, ISBN 978-0521827041.

Orry, A. J. W.; Janes, R. W.; Sarra, R.; Hanlon, M. R.; Wallace, B. A. (2001) Synchrotron radiation circular dichroism spectroscopy: vacuum ultraviolet irradiation does not damage protein integrity, *Journal of Synchrotron Radiation*, 8, 1027-1029.

Pang, G.T., Clancy, R.L., O'Reilly, S.E. & Cripps, A.W. (1992) A Novel Particulate Influenza Vaccine Induces Long-Term and Broad-Based Immunity in Mice After Oral Immunisation, *Journal of Virology*, 66, 1162-1170.

Parnell, J., Cullen, D., Sims, M., Bowden, S., Cockell, C., Court, R., Ehrenfreund, P., Gaubert, F., Grant, B., Parro, V., Rohmer, M., Sephton, M., Stan-Lotter, H., Steele, A., Toporski, J., & Vago, J. (2006) Searching for Life on Mars: Selection of Molecular Targets for the ESA Aurora ExoMars Mission, *In Press*.

Parnell, J., Lee, P., Cockell, C.S. & Osinski, G.R. (2004) Microbial Colonization In Impact Generated Hydrothermal Sulphate Deposits, Haughton Impact Structure, And Implications For Sulphates On Mars, *International Journal of Astrobiology*, 0, 1-10.

Peterson, R.C. & Wang, R. (2006) Crystal molds on Mars: Melting of a possible new mineral species to create Martian chaotic terrain, *Geology*, 34, 957-960

Petrov, V. (2004) Problems and conception of ensuring radiation safety during Mars missions. *Adv. Space Res.*, 34, 1451–1454.

Puchala, M. & Schuessler, H. (1993) Oxygen Effect in the Radiolysis of Proteins, *International Journal of Radiation Biology*, 64, 149-156.

Rowe-Taitt, C.A., Hazzard, J.W., Hoffman, K.E., Cras, J.J., Golden, J.P. and Ligler, F.S. (2000) Simultaneous Detection of Six Biohazardous Reagents Using a Planar Waveguide Array Biosensor. *Biosensors & Bioelectronics*, 15, 579-589.

Schuessler, H. & Schilling, K. (1984) Oxygen effect in the Radiolysis of Proteins, *International Journal of Radiation Biology*, 45, 267-281.

Schweitzer, M.H., Wittmeyer, J., Avci, R. & Pincus, S. (2005) Experimental Support for an Immunological Approach to the Search for Life on Other Planets, *Astrobiology*, 5, 30-47.

Sharma, A. & Khanna, R. (1998) Pattern Formation in Unstable Thin Liquid Films, *Physical Review Letters*, 81, 3463 – 3466.

Simoneit, B.R.T., Summons, R.E. & Jahnke, L.L. (1998) Biomarkers as tracers for life on early Earth and Mars, *Origins of Life and Evolution of the Biosphere*, 28, 475-483.

Sims, M.R., Cullen, D.C., Bannister, N.P., Grant, W.D., Henry, O., Jones, R., McKnight, D., Thompson, D.P. & Wilson, P.K. (2005) The Specific Molecular Identification of Life Experiment (SMILE), *Planetary and Space Science*, 53, 781–791.

Singh, A., Singh, H. & Henderson, J.S. (1990) Radioprotection by Ascorbic Acid, Desferal, and Mercaptoethylamine, *Methods in Enzymology*, 186, 686-696.

Singh, S.P., Cohen, D., Dytlewski, N., Houldsworth, J. & Lavin, M.F. (1990) Neutron and Gamma-Irradiation of Bacteriophage M13 DNA: Use of Standard Neutron Irradiation Facility (SNIF), *Journal of Radiation Research*, 68, 1-9.

Squyres, S. W., Grotzinger, J. P., Arvidson, R. E., Bell III, J. F., Calvin, W., Christensen, P. R., Clark, B. C., Crisp, J. A., Farrand, W. H., Herkenhoff, K. E., Johnson, J. R., Klingelhofer, G., Knoll, A.H., McLennan, S.M., McSween, H.Y., Morris, R.V., Rice, J.W., Rieder, R., Soderblom, L.A. (2004) In situ evidence for an ancient aqueous environment at Meridiani Planum, Mars, *Science*, 306, 1709-1704.

Steele, A. 2005, Private Communication, Geophysical Laboratory, Carnegie Institution of Washington D.C., USA.

Steele, A., Maule, J., Toporski, J., Monaco, L., Spearing, S., Avci, R., Schweitzer, M. & Wainwright, N. (2004) Modular Assays for Solar System Exploration, *Mars Astrobiology Science and Technology Workshop, 8-10 September 2004*, Carnegie Institution of Washington, Washington, DC.

Stevens, C.O., Sauberlich, H.E. & Bergstrom, G.R. (1967) Radiation-Produced Aggregation and Inactivation in Egg White Lysozyme, *The Journal of Biological Chemistry*, 242, 1821-1826.

Thompson, D.P., Wilson, P.K., Sims, M.R., Cullen, D.C., Bannister, N.P., Holt, J.M., Parker, D.J., and Smith, M.D. (2006) Preliminary Investigation of the Effect of Proton and Helium Ion Radiation on Fluorescent Dyes for Astrobiology Applications. *Analytical Chemistry*, 78, 2738 – 2743.

- Vago, J.L., Gardini, B., Kminek, G., et al. (2003) ESA's new mission to search for signs of Life on Mars : ExoMars and its Pasteur scientific payload, EGS-AGU-EUG Joint Assembly (meeting report).
- Van Der Voort, P. & Vansant, E.F. (1996) Silylation of the silica surface: A review, *Journal of Liquid Chromatography and Related Technologies*, 19, 2723-2752.
- White, L.A., Freeman, C.Y., Hall, H.E. & Forrester, B.D. (1990) Inactivation and Stability of Viral Diagnostic Reagents Treated by Gamma Radiation, *Biologicals*, 18, 271-280.
- White, L.A., Freeman, C.Y., Hall, H.E. & Forrester, B.D. (1990) Inactivation and Stability of Viral Diagnostic Reagents Treated by Gamma Radiation, *Progress in Nucleic Acid Research and Molecular Biology*, 35, 96-125.
- Westall, F., Steele, A., Toporski, J. Walsh, M., Allen, C., Guidry, S., Gibson, E., Mckay, D., Chafetz, H., (2000). Polymeric substances and biofilms as biomarkers in terrestrial materials: Implications for extraterrestrial samples. *Journal of Geophysics Research Planets*, 105, 24, 511-24, 527.
- Westall, F., Brack, A., Barbier, B., Bertrand, M., Chabin, A. (2002). Early Earth and early life: an extreme environment and extremophiles - application to the search for life on Mars. *Proceedings of the Second European Workshop on Exo/Astrobiology Graz, Austria, 16-19 September 2002*, ESA SP-518, 131-136.
- Whitesides, G.A. (2006) The Origin and Future of Microfluidics, *Nature*, 442, 368-373.
- Wilson, J., Badavi, F., Cucinotta, F. et al. (1995) *HZETRN: Description of a Free-Space Ion and Nucleon Transport and Shielding Computer Program*, NASA TP-3495.
- Wolff, S.P., Garner, A. & Dean, R.T. (1986) Free Radicals, Lipids and Protein Degradation, *Trends in Biochemical Sciences*, 11, 27-31.
- Woods, R.J. & Pickaev, A.K. (1994) *Applied Radiation Chemistry*, New York, Plenum Press.
- Yang, J., Kim, J., Matsushashi, S. & Kume, T (1996) Changes in Biochemical Properties of Ovomuroid by Radiation, *Radiation in Physics and Chemistry*, 48, 731-735.
- Yamamoto, O. (1977) *Protein Cross-Linking: Biochemical and Molecular Aspects*, New York, Plenum Press.

Yamaguchi, H., Uchihori, Y., Yasuda, N., Takada, M., Kitamura, H., (2005) *Radiation Research*, 46, 333-341.

A Appendix A: Initial development of microarray spotting equipment and immunoassay readout protocols

A.1 Configuring a robotic system for microarray spotting

The most successful technology for the automated creation of microarrays is contact pin printing, using robotically controlled micro-machined pins to deposit controlled nanolitre volumes of liquid onto a surface (Affara, 2003, Macbeath & Schreiber, 2000). This approach was adopted for this work because it was desirable to use standard microarray spotting equipment and a robot capable of carrying out the printing was available at Cranfield University and could be adapted to this function with only minor modifications. Other potential approaches to microarray production include ink-jet printing, but since a suitable ink-jet printer was not readily available in the short term this was not considered further in this work.

In order to create a protein microarray by pin printing, a robotically controlled printing system is required to achieve accurate and precise deposition of microarray spots. At Cranfield University, a suitable robotic system, a SPI GmbH XYZ robot (SPI GmbH, Oppenheim, Germany), shown in Figure A.1, was available for this project. The movement within the SPI GmbH robot is precisely controlled by THK LM Guide Actuators, specifically by two 520mm rails controlling movement in the Y direction, a 420mm rail controlling movement in the X direction and a 200mm rail controlling movement in the Z direction. These actuators are designed to give reproducible sub-micron positional accuracy (<http://www.lmsystem.com>: Accessed 11 January 2005).

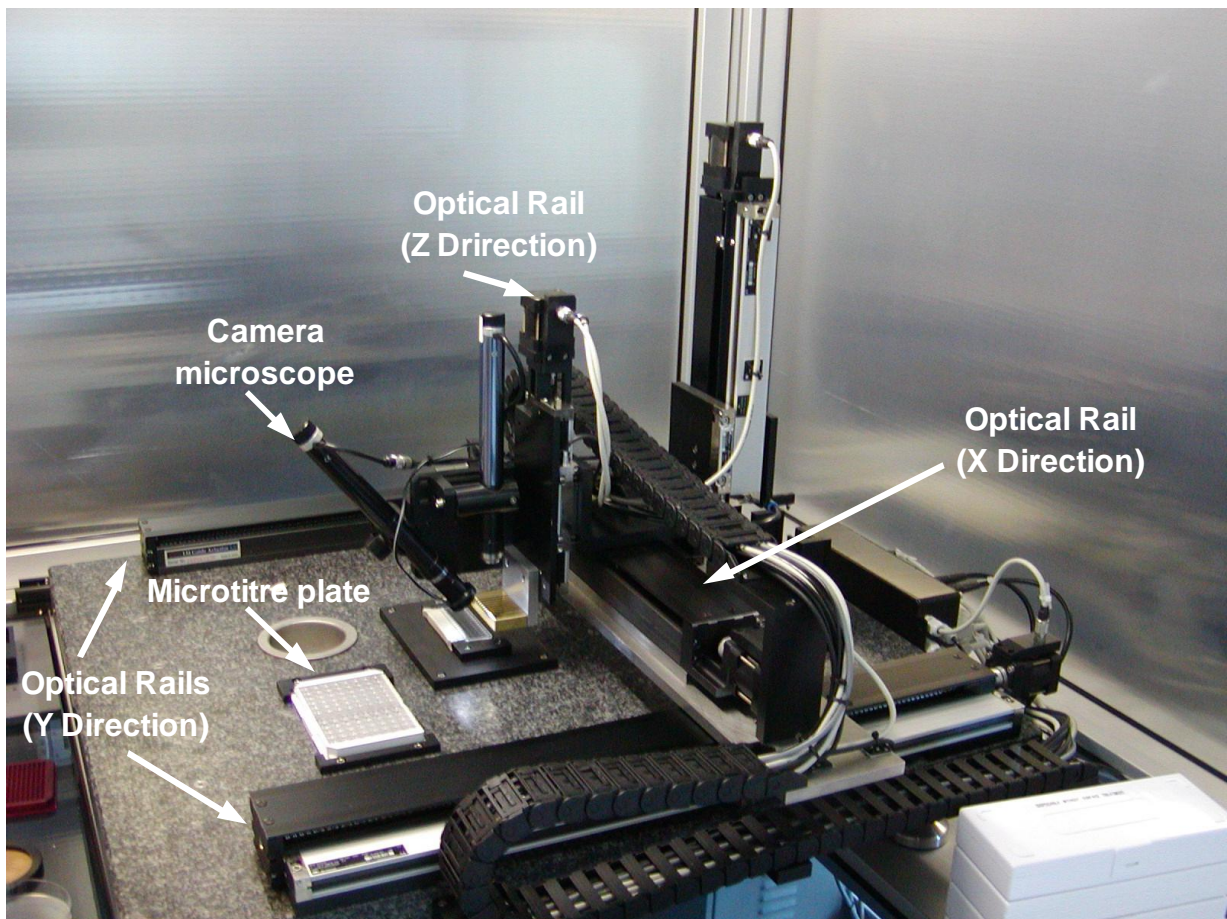


Figure A.1: View of the SPI GmbH robot, showing the guide actuators and other key features.

Movement of the robot along the 3 axes was controlled by the Advanced Robotic Control (ARC) software (version 3.2), which was developed by SPI GmbH and supplied with the robot. This software allows users to create a program consisting of a series of movements and functions in order to make the robot perform a particular task automatically and reproducibly, therefore ensuring that the printing process is highly reproducible. The details of this macro programming process will not be included here, but are described in the ARC Manual (ARC (Advanced Robot Control) Manual 3.2 (2003) SPI GmbH Technologies, Oppenheim, Germany.)

In order to be adapted to the production of microarray spots it was necessary to adapt the SPI GmbH technologies robot by the addition of a printing pin, and specific printhead for use with that spotting pin. In order to meet the mass and volume constraints of the ExoMars Mission, it was desirable that the microarray spots be as small as possible provided that the optical imaging could provide a suitable image of the microarray. This had the consequence that pins producing spots at the smaller size of the range of commercially available equipment, approximately 100 μ m, were desirable. Taking this, the cost and availability of components, and the feasibility of attaching components to the SPI

robot into consideration, ArrayIT™ Stealth™ 32 pin print head and Stealth Micro-spotting Pin SMP3 class of spotting pins (Telechem International, Sunnydale, CA, USA) were selected as the most suitable printing equipment for this project. SMP3 spotting pins were supplied in 3 sizes, with slightly different spot sizes and reservoir capacity. The SMP3B pin, which prints spots approximately 110µm in diameter, was chosen for the initial work, since this was close to the desired 100µm spot size. The smaller SMP3 pin did not have a large enough reservoir for printing large arrays and the larger SMP3XB pin produces spots of 130µm diameter, which was slightly larger than the SMP3B spots. The print head was attached onto the robot arm with a customised mounting block, as shown in Figure A.2.

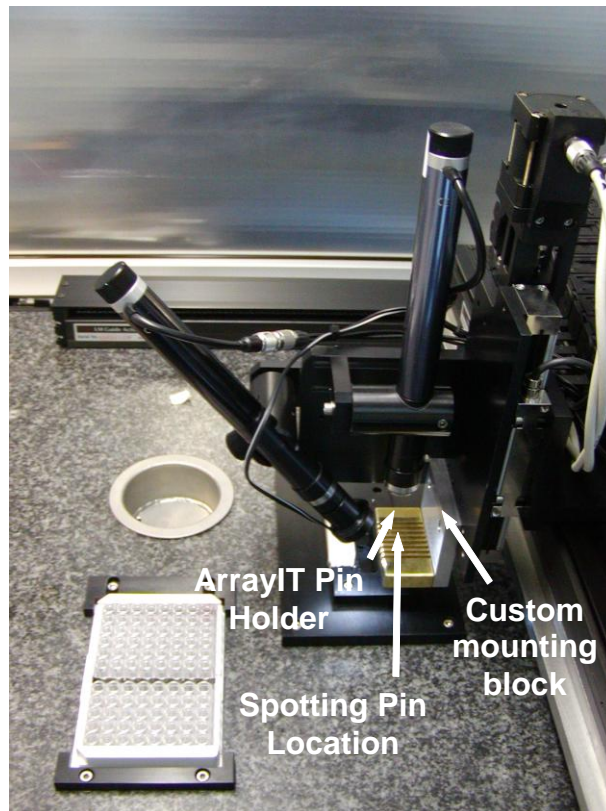


Figure A.2: SPI GmbH Technologies robot after addition of the Stealth™ print matrix

A camera microscope was mounted on the spotting robot and focussed on the spotting pin, such that it showed both the pin and an area of the surface underneath the pin. This camera microscope was fitted with a ring of white LEDs around the objective lens to provide better illumination of the pin and surface (see Figure A.1). The camera microscope images were displayed in real-time in the spotting robot software (described below). This real-time imaging was critical when using the robot for spotting microarrays, as the light source was required to allow manual alignment of the spotting pin with reference coordinates each time.

SMP3B Stealth Pins have a machined “slot-like” reservoir in their tips with a capacity of 0.6µl, and nominally deposit 600pl in each spot, so they can print up to 510 spots of 110µm diameter per loading (www.arrayit.com). They are designed to capillary fill when immersed in a reservoir of solution, for example in this work was a microtitre plate well, and then, provided the properties of the pin surface and printing solution are suitable, a small volume of liquid is held over the end of the pin by surface tension. Normally this is achieved by using the same controlled printing buffer for all print runs. A typical printing buffer consists of a standard biological buffer e.g. PBS or HEPES mixed with 30% volume glycerol to prevent evaporation of the spotting buffer during any reaction with the printing surface e.g. for covalent attachment of a protein or antibody to a functionalised surface. Printing buffers may also contain stabilising agents and other preservatives, but none were used during this work. When the spotting pin is brought into contact with a solid surface, assuming the properties of the pin surface, spotting buffer and printing surface are suitable, the liquid volume suspended from the bottom of the spotting pin is deposited onto the surface and replaced by liquid from a reservoir as the pin is raised away from the solid surface. This is shown in Figure A.3. There are a number of conditions under which this does not happen, and these will be described later in this chapter.

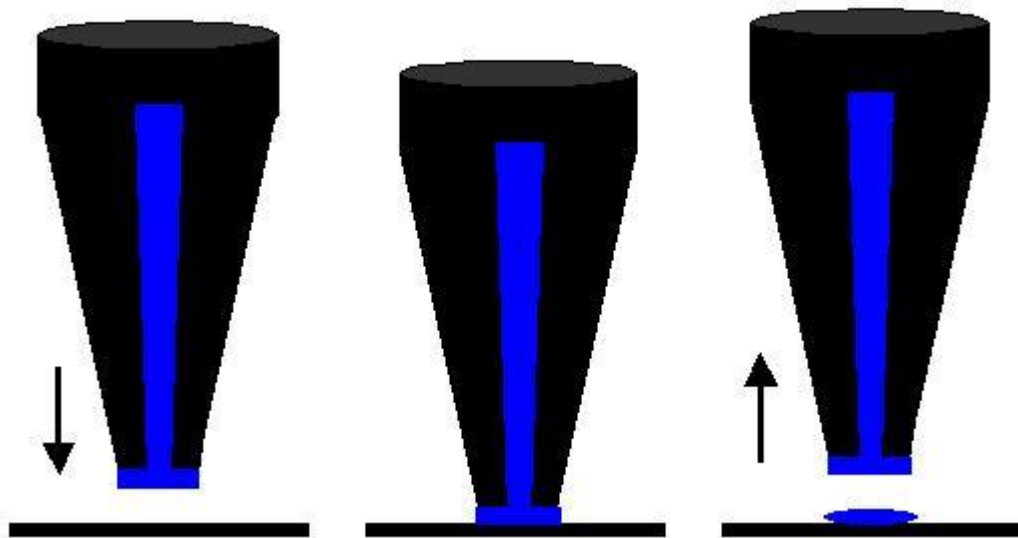


Figure A.3: Function of Stealth™ print pins (taken from www.arrayit.com)

A.2 Initial contact pin printing protocol demonstrations - overview

This section describes a series of experiments which were carried out in order to validate the contact pin printing process and methods of confirming successful pin printing and

readout of different reagents, such that these procedures were established prior to using the pin printing system to prepare protein or antibody microarrays for immunoassays.

After modification of the spotting robot for microarray pin printing, the next objective was to demonstrate successful pin printing of microarray spots using a solution that would make it easy to visualise the spots. For convenience, the solution used in the first experiment was a conveniently available fluorescent dye (Rhodamine G) in deionised water containing 1% surfactant. This dye was selected because it was conveniently available and is visible both by eye and fluorescently. The initial dye concentration was not controlled since this was not a quantitative test; the solution used was an uncontrolled high concentration of dye which make the solution a dark red colour.

A method of imaging fluorescent microarray spots was also a key objective of this section of work. In order to ensure that fluorescent spots could be imaged on the fluorescent microscope at Cranfield University, a BSA-fluorescein conjugate was selected as an inexpensive reagent suitable for fluorescent imaging involving protein interactions. This protein was initially pin printed from a standard buffer solution resulting in a high concentration of protein dried down on the surface, largely to test the imaging of the fluorescent protein, and then immobilised onto a hydrophobic surface by physical adsorption and washed thoroughly to show that a very thin layer of fluorescent material could be detected.

These experiments confirmed that the pin printing process and readout method was suitable for preliminary assays in a microarray format. The experiments are described in detail below.

A.2.1 Initial contact pin printing – materials and methods

As an initial demonstration of the spotting procedure, the robot was programmed to deposit an array of spots consisting of five rows each containing twenty spots. Each spot in a row was separated by 100 μ m (centre to centre), and each row was separated by 500 μ m (centre to centre). An uncontrolled highly concentrated solution of rhodamine G in RO water containing 1% surfactant (a domestic washing-up liquid) was used as a printing solution, since rhodamine G could be seen by eye, would behave similarly to other fluorescent dyes and could be visualised fluorescently if required. The concentration of the

solution was not critical at this stage, since the main objective of this initial experiment was to demonstrate printing of a dye solution.

As discussed in section 2.3.1, the final SMILE instrument is to be based on microfluidic devices. For this initial printing demonstration, The microfluidic devices used were fabricated by a laser cutting a biocompatible double-sided tape (Product code AR8939, ArCare, Adhesives Research, Dunmow UK). This tape was selected because it is designed to be compatible with biological assays and would allow the easy assembly of prototype microfluidic devices in future experiments, and provided a reference location where the microarray spots were printed in this experiment. The laser cut microfluidic structure was mounted on a glass microscope slide, and this slide was placed under the spotting robot for pin-printing (see Figure A.4). The pattern printed was a 20 x 5 array of spots with a horizontal spacing of 200 μ m and a vertical spacing of 250 μ m. Images of the spots were then taken under an optical microscope (Zeiss, Oppenheim, Germany), using a Peltier cooled CCD digital camera (Zeiss, Oppenheim, Germany).

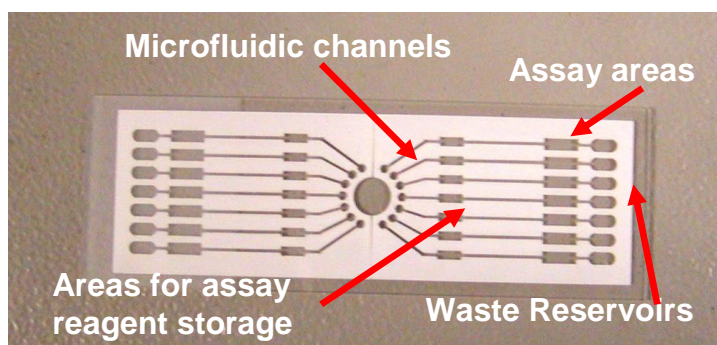


Figure A.4: Microfluidic structure on a standard microscope slide for test printing of microarray spots

A.2.2 Initial contact pin printing - results and discussion

Figure A.5 shows examples of the spots produced in this experiment. The end of the SMP3B pin is designed to produce approximately circular spots with a diameter of 110 μ m. A sample section of an array of spots produced using this solution is shown in Figure A.5 A. The dark area towards the bottom of the picture is the edge of the assay area of the microfluidic channel that the spots were deposited in to. Figure A.5 shows that the spots produced in this experiment are essentially circular, with some small variation in the size and shape of the spots. It is also clear particularly from Figure A.5 B that there are a series of rings within the spot, which is typical of a drying effect that might be expected from an aqueous solution (e.g. Deegan *et al.*, 1997). This result indicates that pin-printing from water-based solutions may not produce uniform spots. Standard microarray printing methods deposit proteins on functionalised surfaces to allow covalent immobilisation and

use buffers containing 10% to 30% glycerol, to prevent evaporation of the solution during this reaction. Drying effects such as those seen in Figure A.5 are therefore unlikely to occur in the flight instrument.

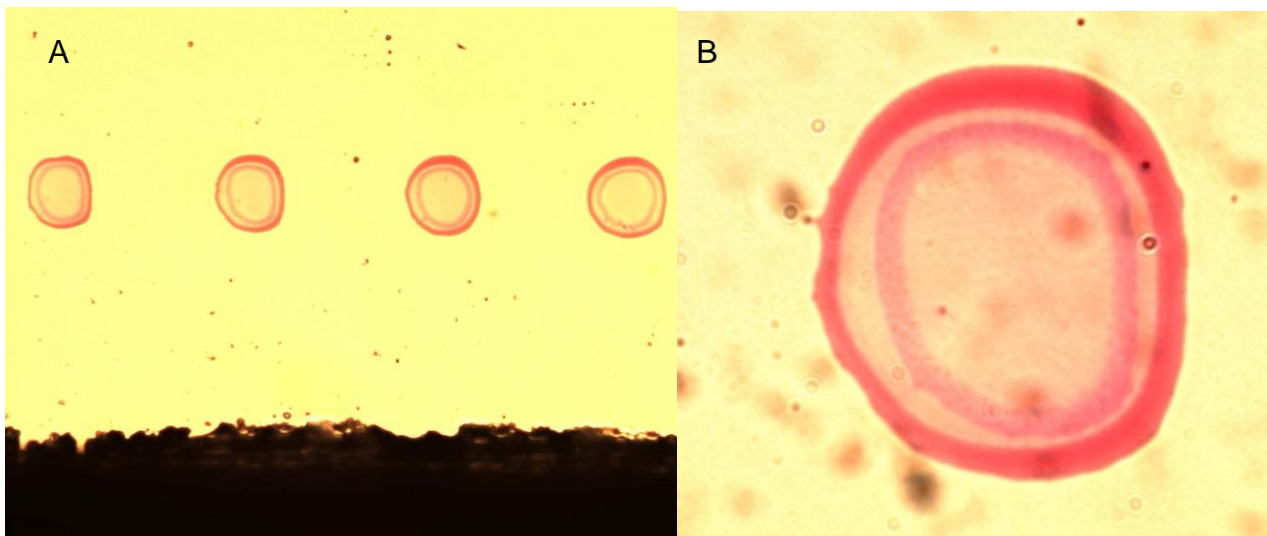


Figure A.5: Highly concentrated of rhodamine Dye in PBS microarray printed onto a glass surface within a microfluidic channel. Image taken on a ZEISS CCD camera at A) 10x magnification B) 40x Magnification (images not to scale).

The final assay system proposed for SMILE was to utilise fluorescently labelled antibodies or capture reagents in a microarray format within a microfluidic channel such as that shown in Figure A.4 (Sims *et al.*, 2005). This experiment established a basic printing protocol and imaging system for printing microarray spots using fluorescent dyes in water-based solutions. This is a first step towards developing an antibody assay in a microarray spot format within a microfluidic structure. The next step was to extend this printing protocol to the deposition of proteins in buffer solutions, and to establish a message for fluorescent imaging of the spots. Establishing a fluorescent imaging method would provide input into the design of a bespoke imaging system which would allow a breadboard version of the flight instrument to be assembled.

A.2.3 Development of protocols for printing proteins in solution and fluorescent imaging – materials and methods

The next step in the assay development was to verify that proteins in solution could be used with the microarray pin printing system and to confirm a fluorescent readout method. Since a protocol for drying down reagents in solution have been demonstrated in section A.2.2, a similar system was used in this experiment to print a fluorescently labelled protein in buffer solution. A $1\text{mg}\cdot\text{ml}^{-1}$ concentration solution of BSA-fluorescein (Sigma-Aldrich, Poole, UK) in 10mM PBS pH 7.4 (PBS tablets, Sigma-Aldrich, Poole, UK), was printed onto

glass microscope slides and allowed to dry down. The pattern printed was a 20 x 5 array of spots with a horizontal spacing of 200 μm and a vertical spacing of 250 μm , as for the previous experiment (see section A.2.1). The spot array was then imaged under an optical fluorescent microscope (Zeiss, Oppenheim, Germany) using a Peltier cooled CCD digital camera (Zeiss, Oppenheim, Germany).

A.2.4 Development of protocols for printing proteins in solution and fluorescent - results and discussion

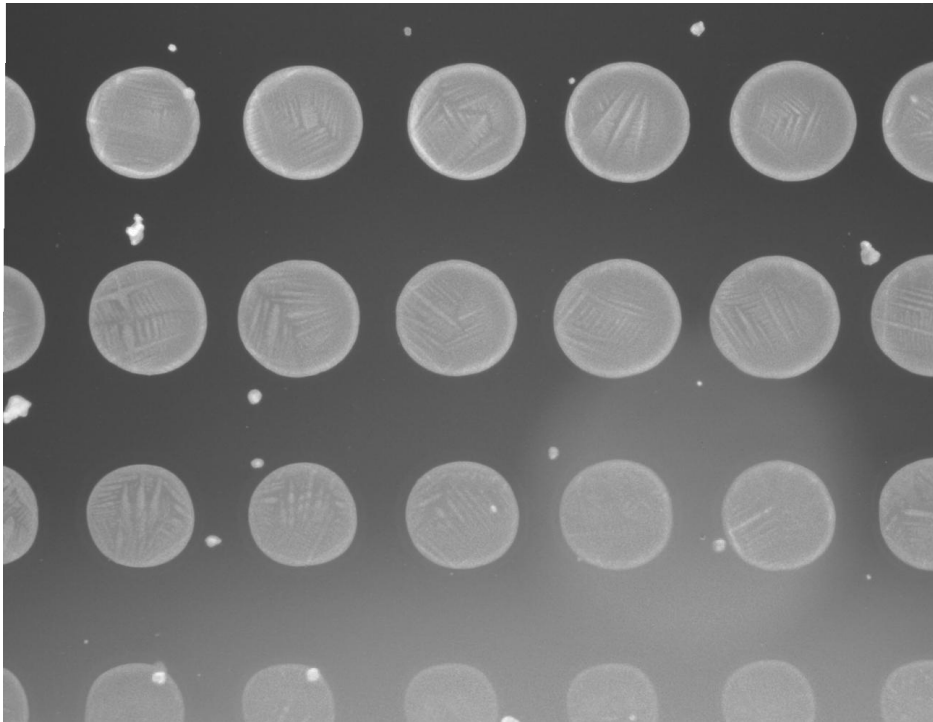


Figure A.6: 1mg.ml⁻¹ BSA-Fluorescein microarray spots printed onto a glass microscope slide. Image taken with a Zeiss CCD camera with a 10000ms exposure at 10x magnification (image not to scale)

Figure A.6 shows the spots of BSA-Fluorescein conjugate produced in this experiment. The spots are all present, indicating that printing in the standard PBS buffer was successful.. The spacing of the spots appears to be less in Figure A.6 than in Figure A.5, but this may be due to the spotted solution spreading further over the surface in this experiment, creating larger spots. By visual inspection, the spots in Figure A.6 appear all to be similar both in terms of size and structure i.e. they all have a ring feature around their edges and linear structures within the central area of the spot.

Image analysis, scale bar

In addition to what appears to be a drying effect around the outside of the spots (Deegan *et al.*,1997), as was observed with the rhodamine B spots above, there appears to be structure within the spots. These features are assumed to be crystals of phosphate buffer

salts produced as the water in the spotting solution evaporated. As discussed in section 2.3.1, and A.2.5, in the final microarray spotting format the reagent in the spots would be attached to the printing surface in a monolayer and any remaining printing solution would not be allowed to dry out, so these drying effects would not be expected.

In order to confirm that buffer salt precipitates could be removed by washing, and determine whether it was possible to visualise a monolayer of immobilised material on the slide surface, the protocol was modified in the next experiment.

A.2.5 Immobilisation of BSA-fluorescein by physical absorption in order to create an approximation of a monolayer of fluorescent microarray spots – materials and methods

In the previous experiment it has been shown that spots of fluorescently labelled protein could be imaged using a fluorescent microscope. In the final SMILE instrument the fluorescent material on the microarray spots would be present in a monolayer, since it would arise from a layer of bound antibody. In section A.2.4, the fluorescent image was created from a relatively large amount of dried down protein material. In order to determine whether a monolayer of fluorescently labelled material could be visualised, an array of $1\text{mg}\cdot\text{ml}^{-1}$ BSA – Fluorescein conjugate (Sigma-Aldrich, Poole, UK) in 10mM PBS pH 7.4 was printed onto a polystyrene surface (a plastic petri dish), using the same printing program as in section A.2.4. In contrast to a glass microscope slide, polystyrene would allow the protein to bind to the surface by physical adsorption rather than drying down. This would be a stronger bond and vigorous washing would remove excess material from the surface leaving only a monolayer. After printing the array was incubated in a humidity chamber for 2 hours and then thoroughly washed by agitation in a beaker of RO water and left to dry for 2 hours, to try to remove any dried down BSA-fluorescein and therefore produce a monolayer of adsorbed protein on the surface. This array was then imaged on a fluorescent optical microscope with a cooled CCD camera (Zeiss, Oppenheim, Germany).

A.2.6 Creating a monolayer of fluorescent microarray spots – results

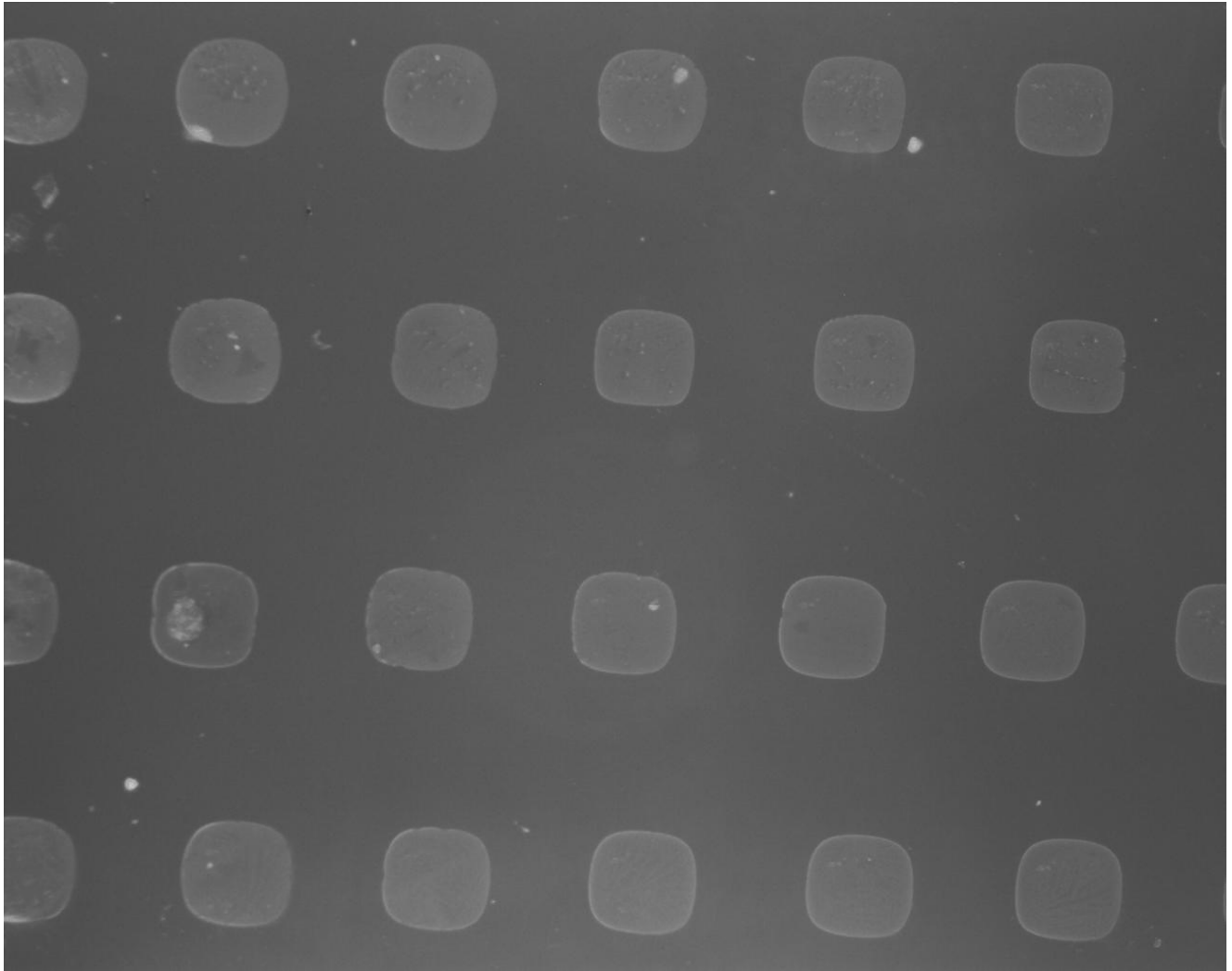


Figure A.7: 1mg.ml⁻¹ BSA-Fluorescein microarray spots printed onto a polystyrene substrate and washed thoroughly with deionised water. Image taken with a Zeiss CCD camera with a 10000ms exposure at 10x magnification.

Figure A.7 shows a 10,000ms exposure image of the array of washed BSA-fluorescein spots on the polystyrene Petri dish, taken with the Zeiss optical fluorescent microscope. All of the spots appear to be present and have a broadly uniform appearance. In Figure A.7, in contrast to Figure A.5 and Figure A.6, the spots appear to be square. This is likely to be because the end of the sporting pin is square, and in contrast to the hydrophilic glass microscope slide, the hydrophobic surface of the polystyrene Petri dish prevented the liquid forming circular spots. The intensity of the spots appears to be significantly lower than in the previous experiment (Figure A.6). Both images were taken under the same conditions and with the same exposure time, so the reason for this is likely to be that the washing procedure did remove a large amount dried down material, leaving only a very small amount of material, approximating a monolayer, of physically adsorbed protein on the surface.

There are some particulates and inclusions present within and outside the spots. However, the crystalline structures within the spots observed in the previous experiment are no longer present, indicating that washing the microscope slide in RO water immediately after incubation in a humidity chamber either prevented crystallisation of buffer salts on the surface or away any crystals that were formed. In either case it prevented crystals remaining on the surface after washing. The remaining particulates in the spots could be removed by passing all the solutions through a 0.2µm particle filter.

The columns of spots appear to be slightly offset from one another. This was thought to be due to slight movement of the relatively low mass polystyrene material during the printing process, as when the robot changed speed or direction suddenly this could cause movement of the polystyrene.

Having now reached the point of developing a confirmed microarray printing and readout system through preliminary experiments, these techniques were used and adapted to develop an antibody based assay in this microarray format.

A.3 Demonstration of binding immunoassay in microarray format with fluorescent readout

Since an image of a very thin layer of fluorescently labelled material on a surface had been produced, an experiment to use this to carry out a binding immunoassay experiment in a microarray format was carried out with the BSA-atrazine system described previously (see section 3.1.1.4). In order to use this assay system with a fluorescent readout, a fluorescein-labelled anti-human kappa light chain secondary antibody (Sigma-Aldrich, Poole, UK) was used to replace the HRP labelled anti-human kappa light chain secondary antibody used in section 3.1.1.4.

A.3.1 Initial microarray format binding immunoassay materials and methods

The protocol used for this assay was as follows:

- An array of 1µg.ml⁻¹ BSA-atrazine conjugate (Haptogen, Aberdeen, UK) in 10mM PBS pH 7.4 was spotted onto a polystyrene Petri dish
- The polystyrene Petri dish was then placed in a humidity chamber, consisting of a sealed plastic container lined with a moist paper towel, for 2 hours.
- The polystyrene Petri dish was immersed in a beaker of blocking solution (0.1g.ml⁻¹ skimmed milk powder (Marvel) in 10mM PBS pH 7.4) for 2 hours.

- The polystyrene Petri dish was then removed from the blocking solution and the assay area washed twice with 1ml of 10mM PBS pH 7.4 and once with RO water, by pipetting these solutions over the assay area at an acute downwards angle.
- 20 μ l of 0.2 μ g.ml⁻¹ fluorescein-labelled anti-human kappa light chain in 10mM PBS pH 7.4 was pooled over the array areas of the slide and incubated for 2 hours in the humidity chamber.
- The assay area was then washed three times with 1ml of 10mM PBS-0.1% TWEEN 20 and once with RO water as described above, then dried with a nitrogen gas stream from a compressed nitrogen gas source for 1 minute, and stored until analysis.

A.3.2 Initial microarray format binding immunoassay results and discussion

Figure A.8 shows the results of this experiment in the form of a 10,000ms exposure image taken under the Zeiss florescent microscope. It is clear that the array spots are visible, which indicates that all of the key steps in the assay are working – printing, adsorption of the dye, binding of the anti-atrazine scAb and binding of the secondary antibody. The background is also relatively low, indicating that the blocking and washing system is effective. However, the spots all appear to be non-uniform in fluorescent intensity, and in fact many features are present in all of the spots. This indicates that there was a problem with the printing process, possibly contamination on the spotting pin which could have been introduced the pin had been allowed to dry after printing the protein solution. There is also some evidence of particulates and some non-specific binding around the lower spots in this image. This could have been introduced by the printing process, or spreading of the pin printing solution to areas outside the microarray spots during incubation in the humidity chamber.

This experiment showed that an immunoassay can be carried out in a microarray format with a fluorescent readout. While there are still some problems with non-specific binding and particulates, this proof of concept experiment has shown that the approach was valid and generated enough data to design a test rig which would be more representative of the flight model of the SMILE instrument. Also, at this time in the project additional funding was available which allowed the test rig equipment to be purchased and used to further develop the microarray immunoassay. The design and assembly of this test rig is described in section 3.1.2.

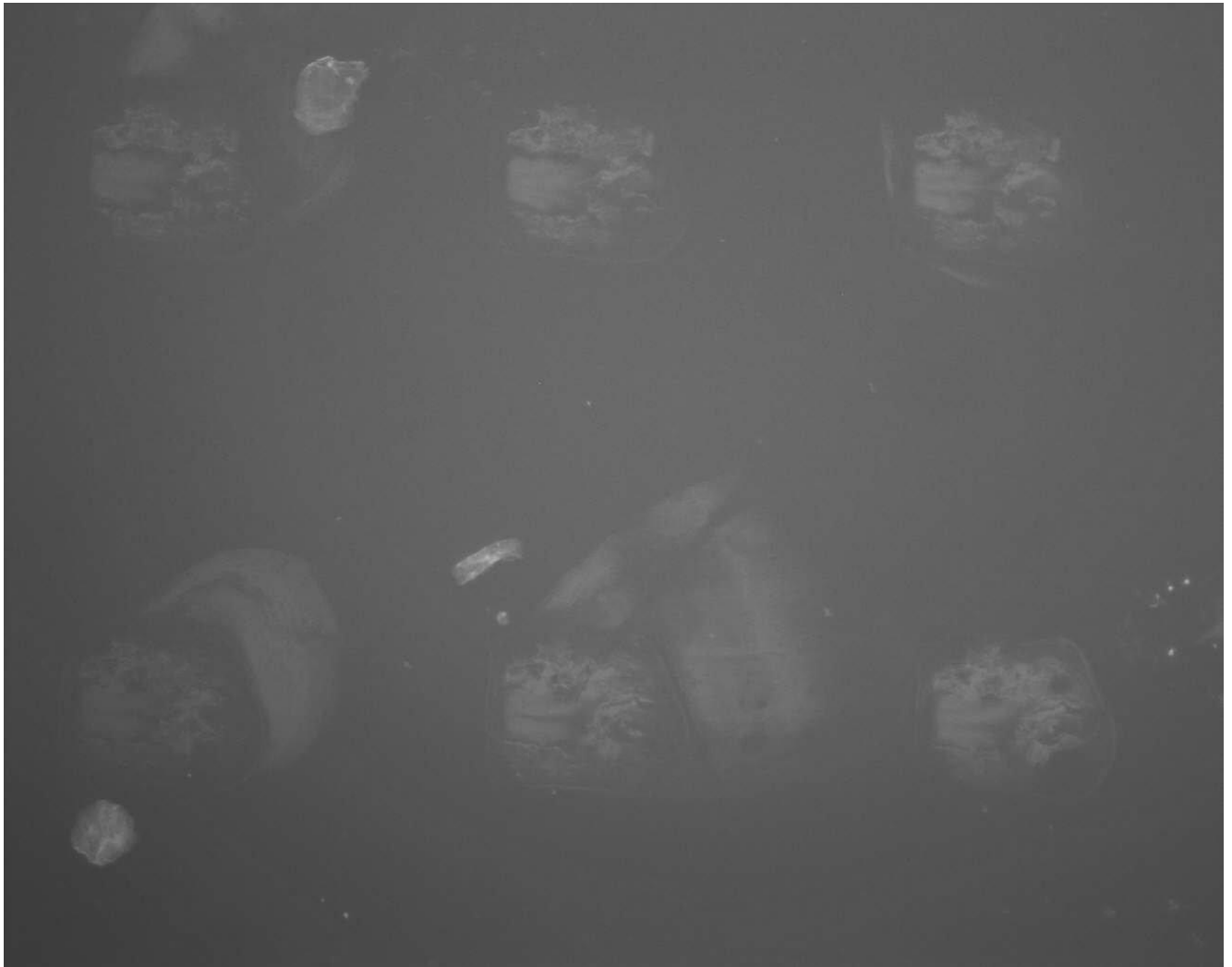


Figure A.8: immunoassay carried out on spots of atrazine-BSA physically adsorbed onto glass microscope slides